University of Szeged
Faculty of Pharmacy
Institute of Pharmaceutical Technology and Regulatory Affairs
Head: Prof. Dr. Ildikó Csóka, PhD

PhD Thesis

Development and Characterization of Lysozyme Pellets Prepared by Extrusion and Spheronization Method

by

Yousif Hamed Elneil Yousif Ibrahim
Pharmacist

Supervisors
Dr. Géza Regdon jr., PhD

Dr. Tamás Sovány, PhD

Szeged
2021

LIST OF PUBLICATIONS AND CONFERENCE PROCEEDINGS

List of Publications Related to the Thesis

1. **Ibrahim, Yousif H-E. Y.**; Regdon jr., Géza; Hamedelniel, Elnazeer I; Sovány, Tamás. Review of recently used techniques and materials to improve the efficiency of orally administered proteins/peptides, DARU J. Pharm. Sci. 28 (2020) 403-416. https://doi.org/10.1007/s40199-019-00316-w. **Indep. citations: 17 Q2 IF (2020): 3,117**
2. **Ibrahim, Yousif H-E. Y.**; Regdon jr., Géza; Kristó, Katalin; Kelemen, András; Adam, Mohamed E.; Hamedelniel, Elnazeer I.; Sovány, Tamás. Design and characterization of chitosan/citrate films as carrier for oral macromolecule delivery, Eur. J. Pharm. Sci. 146 (2020) 105270. https://doi.org/10.1016/j.ejps.2020.105270.

   Indep. citations: 3 Q1 IF (2020): 4,384
3. **Ibrahim, Yousif, H-E. Y.**; Wobuoma, Patience; Kristó, Katalin; Lajkó, Ferenc; Klivényi, Gábor; Jancsik, Béla; Regdon jr., Géza; Pintye-Hódi, Klára; Sovány, Tamás. Effect of processing conditions and material attributes on the design space of lysozyme pellets prepared by extrusion/spheronization, J. Drug Deliv. Sci. Technol. (2021) accepted for publication **Q2 IF (2020): 3,981**

List of Publications not Related to the Thesis

1. Hamedelniel, Elnazeer I.; Omer, Hagir M.; Balla, Qussai I.; **Ibrahim, Yousif H-E. Y.**; Osman, Fakhr Aldeen Y.; Abdelmonem, M. Abdellah. Formulation and evaluation of Grewia tenax fruits as effervescent tablets for treatment of iron deficiency anemia, Int. J. Develop. Res. 10 (2020) 34084-34090.
2. Vlad, Robert-A.; Sovany, Tamas; Kristó, Katalin; **Ibrahim, Yousif H-E. Y.**; Ciurba, Adriana; Aigner, Zoltan; Muntean, Daniela; Regdon jr., Geza. Structural and thermal analysis of cannabidiol orodispersible formulations, Pharmacia, 69 (2021) 426–433. https://doi.org/10.31925/farmacia.2021.3.5.

List of Conference Proceedings

1. **Ibrahim, Yousif H-E. Y.**; Regdon jr, Géza; Sovány, Tamás. Design, development and characterization of chitosan film as effective oral-macromolecule delivery system using new multifunctional plasticizer. 12th Central European Symposium on Pharmaceutical Technology and Regulatory Affairs, 20-22 September 2018, Szeged, Hungary, Book of Abstracts (Acta Pharmaceutica Hungarica 88(3)) pp. 148-148. Paper: P4/11.
2. **Ibrahim, Yousif H-E. Y.**; Sovány, Tamás; Regdon jr., Géza. Characterization of chitosan/citrate films as a suitable oral-macromolecule carrier. I. Ph.D. Symposium at the University of Szeged - Medical and Pharmaceutical Sciences, November 2018, Szeged, Hungary.
3. **Ibrahim, Yousif H-E. Y.**; Sovány, Tamás; Regdon jr., Géza. Design and characterization of chitosan/citrate films as suitable multifunctional coating for oral-macromolecule delivery. I. Symposium of Young Researchers on Pharmaceutical Technology, Biotechnology and Regulatory Science, 31 January 2019, Szeged, Hungary pp. 15-15.
4. **Ibrahim, Yousif H-E. Y.**; Sovány, Tamás; Regdon jr., Géza. Effect of plasticizer type/quantity on the thermal behavior of acetic acid and citric acid-based chitosan films. 2nd Journal of Thermal Analysis and Calorimetry Conference, 18-21 June 2019, Budapest, Hungary Book of Abstracts (Akadémiai Kiadó), (2019) p. 653.
5. Kristó, Katalin; **Ibrahim, Yousif H-E. Y.**; Regdon jr., Géza; Sovány, Tamás. A tervezési tér optimálása lizozim tartamú pelletek előállítása során. Gyógyszertechnológiai és Ipari Gyógyszerészeti Konferencia 2019, 26-28 September 2019, Siófok, Hungary, Book of Abstracts p. 35.
6. Sovány, Tamás; **Ibrahim, Yousif H-E. Y.**; Kristó, Katalin; Regdon jr., Géza. Effect of material attributes on the design space of lysozyme containing pellets. 8th BBBB International Conference on Pharmaceutical Sciences, 14-16 October 2019, Cesme, Turkey, Abstract Book
7. **Ibrahim, Yousif H-E. Y.**; Kristó, Katalin; Regdon jr., Géza; Sovány, Tamás. Effect of processing conditions and material attributes on the design space of lysozyme pellets prepared by extrusion/spheronization. II. Symposium of Young Researchers on Pharmaceutical Technology, Biotechnology and Regulatory Sciences, 23-24 January

2020, Szeged, Hungary, Book of Abstracts pp. 39. https://doi.org/10.14232/syrptbrs.2020.op34.

8. **Ibrahim, Yousif H-E. Y.**; Kristó, Katalin; Regdon jr., Géza; Sovány, Tamás. Effect of plasticizer type and quantity on the properties of oral chitosan films. EUGLOH Annual Student Research Conference, University of Szeged, 28-30 September 2020, Hungary.
9. **Ibrahim, Yousif H-E. Y.**; Kristó, Katalin; Regdon jr.; Géza; Sovány, Tamás. Development and optimization of the coating processes of lysozyme loaded pellets for oral delivery, III. Symposium of Young Researchers on Pharmaceutical Technology, Biotechnology and Regulatory Sciences. 20-22 January 2021, Szeged, Hungary, Book of Abstracts pp. 48. https://doi.org/10.14232/syrptbrs.2021.op36.

TABLE OF CONTENTS

LIST OF ABBREVIATIONS

AA	Acetic Acid
API	Active Pharmaceutical Ingredient
C-1, C-2, C-3	First, Second and Third Compositions
CA	Citric Acid
CM	Crystalline Mannitol
DSC	Differential Scanning Calorimetry
FDA	Food and Drug Administration
G	Glycerol
GIT	Gastrointestinal Tract
LP	Lipopolysaccharide
MCC	Microcrystalline Cellulose
MFFT	Minimum Film Forming Temperature
PAT	Process Analytical Technology
PE	Permeation Enhancer
PEG	Polyethylene Glycol
PG	Propylene Glycol
PI	Protease Inhibitor
QbD	Quality by Design
RH	Relative Humidity
SDM	Spray-Dried Mannitol
SFE	Surface Free Energy
TGA	Thermal Gravimetric Analysis
TJs	Tight Junctions
TP	Therapeutic Protein

1. INTRODUCTION

Orally administered medications are more preferable than those administered by other routes as a result of good patient compliance and formulation adjustability [1]. Oral multiparticulate delivery systems such as pellets consist of multiple discrete small units, each exhibiting the required properties. They offer better pharmaceutical and biopharmaceutical advantages compared with traditional single-unit dosage forms [2, 3]. These include lower gastrointestinal tract (GIT) irritation due to the decreased local concentration [4] as a result of more even and predictable distribution and transportation in the GIT regardless of the nutritional state [5, 6], flexibility by mixing units with different release behaviors [7], low risk of dose dumping as each unit represents a standalone delivery system [8, 9], spherical shape enabling the coating/subcoating process to be performed efficiently and hence setting the release design, which results in improvement of drug dissolution and increased bioavailability with low inter- and intra-subject variations [10–12]. In addition, the incorporation of mucoadhesive polymers could add extra innovative properties to multiparticulate delivery systems, some of which include precise site-specific delivery, long residence time in the absorptive tissues and hence improved bioavailability of the loaded drug [13]. Generally, the release of the incorporated drug depends on its content and the properties of the carrier used [14]. Therefore, they may offer a promising alternative for the delivery of therapeutic proteins (TPs), which are currently administered mainly parenterally. TPs have high potency and specificity in controlling, treating and preventing numerous pathological conditions, such as diabetes, infectious and inflammatory diseases [15]. However, their oral administration still represents a challenging goal because of many production and delivery obstacles. Briefly, the large and complex structure, as well as fragile nature act as barriers to their successful formulation into stable solid dosage forms [16, 17], whereas poor oral absorption, susceptibility to pH change and breakdown by proteases represent pharmacokinetic barrier [18]. Accordingly, safe and efficient protease inhibitors (PIs), permeation enhancers (PEs) and conformation stabilizers are key excipients of a suitable carrier system [19–21], while the intensive investigation of the material characteristics and the effect of different processing parameters on the targeted product profile could be helpful tools in identifying the optimal design space of their production.

2. AIMS

The main aim of this study was the development and optimization of a system for lysozyme delivery, based on pellets prepared by extrusion/spheronization. The main optimization parameters were preserving the biological activity during and after production and acquiring adequate sphericity and hardness for the subsequent coating processes.

The identification of the optimal design space was based on the following hypotheses:

I. the optimal design space of pelletization and the thermomechanical stress on lysozyme are potentially affected by the material attributes,

II. the knowledge of the distribution of relative humidity (RH%) and temperature (T) helps to optimize the processing parameters.

Therefore, wetting was performed in a high-shear granulator constructed with a specially designed chamber to monitor the change of RH% and T under different processing conditions. Firstly, the experiments were conducted according to 2^3 full factorial design with a central point at different mechanical stresses to determine the optimum design space and to study the impact of the material attributes on the design space.

III. chitosan citrate may represent a novel well-shielding multifunctional protein carrier system, as it provides a long residence time in the targeted absorptive tissues and concurrently offers PI and PE effects in a localized pattern, by ensuring an optimal acidic microenvironment unfavorable for peptidases and increasing calcium iron chelation and hence opening the tight junctions (TJs), e.g. the gates of absorption, and therefore it results the in improvement of overall therapeutic performance.

Citric acid (CA)-based chitosan films were designed and thoroughly investigated in comparison to acetic acid (AA)-based films as a reference, and the optimal film composition was selected to be suitable as a functional subcoating layer.

3. LITERATURE SURVEY

3.1. Pelletization and Pellets

Pelletization is an agglomeration procedure that converts the homogenized powders of a drug and excipients into relatively high density, free-flowing spherical or semi-spherical units of narrow size distribution called pellets, having a dimension of 500-1500 μm [22–24]. Pelletization techniques are mainly categorized into four basic groups: agitation method (balling), compaction (compression and extrusion/spheronization), layering (powder, solution and suspension) and globulation including spray-drying and spray-congealing [25–27]. Other alternative methods include high shear pelletization, wet spherical agglomeration, spherical crystallization, melt pelletization, cryopelletization and freeze pelletization [28].

Among the production methods, the extrusion and spheronization method is used extensively and is widely considered as a potential future method due to its ability to produce denser spheres with higher drug-loading capacity while retaining their small size. Moreover, the flexible tuning of both the composition and process settings helps to meet the required quality, and hence the process is considered pharmaceutically more efficient than other pelletization methods [29–32]. On the other hand, the main disadvantage is its multistep nature, which is relatively complicated and time-consuming [33].

Microcrystalline cellulose (MCC) is the most commonly used polymer as pellet former acting as an excellent binder with high internal porosity, due to its high capacity to strongly retain water molecules [34–36]. Usually, water is used as a granulating liquid to wet the drug-MCC powder mixture during kneading in higher quantity than usual in conventional granulation [37]. The suitable quantity of water should be carefully determined, as over-wetting affects the quality of the extrudate as well as both the shape and mechanical properties of the particles [38, 39]. Nevertheless, the quantity of the required granulating liquid is less than normal in the case of formulations containing polyols such as mannitol or sorbitol [40]. Generally, the impeller torque value oscillation of the high shear granulator represents an efficient way to determine the end point of wet kneading [41].

Mannitol is a polyol, which could be used with MCC for various purposes, such as a diluent or pore-forming agent, thereby improving the release performance of the loaded-drug [42, 43]. Moreover, mannitol has been reported to stabilize proteins against aggregation during high shear granulation through stabilizing their conformation [44, 45].

3.2. Pellet Coating

To achieve a better therapeutic effect, pellets are usually coated to control the release of the incorporated drug or to target the release to a specific GI absorptive site (e.g. enteric coating and colon targeting delivery systems) [46–48]. The coated particles are then filled into hard gelatin capsules or compressed into tablets as a final dosage form [49]. Recently, targeted drug delivery to the colon has received increased attention from pharmaceutical technologists, since both local and systemic effects of drugs, particularly proteins and peptides, may be achieved [50]. Furthermore, colon targeted drug delivery guarantees maximum release in the colonic region with less fluctuation in drug concentration at the absorptive site [51]. For this purpose, mostly acrylic polymers (e.g., Eudragit®) are used as pH-sensitive polymers. The release of the active pharmaceutical ingredient (API) occurs close to the colon in the pH range of 6.5 to 7.5 [52–54].

Generally, the enteric coating of pellets is performed to protect the stomach from the toxic effect of the drug, or to shield the acid-unstable drug from gastric acidity [55]. Most of the coating polymers are applied as aqueous or organic solutions/dispersions, and the aqueous ones are more preferred for many reasons, e.g. non-toxicity, no need to recover and non-explosiveness [56].

3.3. Challenges of Oral Protein Delivery

The flourishing in biotechnology leads to the development of numerous macromolecular drugs which have found a place in controlling and treating various diseases, such as certain infections, malignant tumors and immunological disorders [57–59]. More than a hundred TPs are available commercially, and more than 50 have been approved by the Food and Drug Administration (FDA) for commercialization [60, 61]. They represent attractive drug candidates due to their specificity, exceptional efficacy and low toxicity, which are basically attributed to their complex structures, but concurrently poses the main challenge for their development as oral delivery systems [62–64].

3.3.1. Pharmaceutical Processing Challenges

The formulation of stable oral delivery systems for these biopharmaceuticals represents a challenging goal to pharmaceutical technologists because they possess a fragile nature, making them more vulnerable to misfolding, aggregation and denaturation, which results in lost or

diminished biological activity [65]. This instability should be carefully evaluated and managed, especially for the processes involving high mechanical shear stress with an elevated moisture content [15, 66]. Accordingly, the incorporation of a protein stabilizer in the formulation is a useful approach to stabilize proteins during their processing and storage [67]. In addition, the implementation of process analytical technology (PAT) could be a crucial tool.

3.3.2. Oral Administration Challenges

The main obstacle for orally administered TPs is low bioavailability attributed to the undesirable bio- and physiochemical properties, such as large molecular weight or inactivation by gastrointestinal secretions and first pass effect, which results in low penetration and pre-systemic degradation [68–71]. The lumen of the small intestines contains various proteolytic enzymes secreted by the pancreas, mucosal cells and the border of the epithelial cells. Moreover, the enzymes produced by the microflora in the colon should be taken into consideration [72–74].

Orally administered drugs penetrate across the membranes through the following pathways: paracellularly, transcellularly and through the microfold. Paracellular absorption is the main pathway for the absorption of proteins, but it is tightly closed by non-static TJs along the intestines. However, some penetration enhancers have the ability to loosen the proteins of the TJs [75–78]. The epithelial mucosal layer also acts as a rigid coat to the intestinal lumen [79]. It has different thickness and turnover values regarding the anatomical position [80], possesses a negative charge and lipophilic nature [81], and thus acts as a physical barrier [82].

Based on the above-mentioned barriers, most researchers recommend the incorporation of PIs and PEs in a suitable delivery system, i.e. a multifunctional delivery system. The utilization of mucoadhesive polymers also represents a rational approach to further improve the performance of the orally administered systems [17, 83–86]. However, the concurrent administration of TPs with PIs and PEs should be carefully designed, as these agents can interfere with dietary proteins and may cause non-specific absorption or damage the integrity of the mucosal layer. In addition, the effectiveness of these agents is not similar along the GIT due to the variation of numerous parameters, such as pH, proteolytic activity or membrane thickness [87–90]. Accordingly, a less damaging, rational and safe method would be the transient opening of TJs by an effective concentration of PIs and PEs applied in localized delivery systems, such as mucoadhesive systems [91, 92].

3.4. Mucoadhesive Delivery Systems

Mucoadhesion is the adherence of a polymeric carrier to the mucosal layer of the epithelium, which enables the polymer to tightly stick to the biological substrate for a substantial period of time [93–95] as a result of multiple steps of interactions with the mucosal surfaces [96, 97]. It includes GIT, oral cavity, nasal, ocular, pulmonary, vaginal and rectal drug delivery systems [98, 99]. They are considered as attractive carrier systems for either local or systemic delivery of poorly absorbed drugs, such as proteins [87, 100]. Additionally, they may isolate proteins/peptides from the degrading environment [101–103] and promote the absorption of incorporated drugs [104–106]. Moreover, they may control the release of the incorporated molecules through their gel-forming property and ensure the concurrent release of the drug and the EI and PE in a localized pattern [107, 108]. Accordingly, mucoadhesive carrier systems reduce the possible toxicity of EI and PE while improving the overall therapeutic performance of the dosage form.

4. MATERIALS AND METHODS

4.1. Materials

Lysozyme, also known as muramidase, was used as a model protein. It is a harmless natural antimicrobial enzyme protein obtained from plants, animals and microorganisms as a single chain polypeptide with a globular shape consisting of 129 amino acids with an approximate molecular weight of 14.3 kDa [109–112]. The diversity in the source renders lysozyme the most affordable and cost-effective protein for the investigations [113]. Hen-egg white is a common source used in the studies of lysozyme [114]. Two brands of the hen egg-white-derived enzyme, with greatly different stabilities were involved into the study. Lysoch-40000 (Handary SA, Brussels, Belgium) described as "lyso-1" may be stored under ambient conditions up to 24 months while (CAT. HY-B2237/CS-7671, MedChemExpress, Hungary) described as "lyso-2" should be stored frozen (-20°C). According to our hypothesis, the poorer thermal stability may negatively affect enzymatic activity, but with careful design, it is still possible to produce pellets of the required quality. Scanning electron micrographs (Fig. 1a, b) showed no considerable differences in the size or morphology of lyso-1 and lyso-2.

The antimicrobial activity of lysozyme is attributed to the destruction and lysation of the cell wall of Gram-positive bacteria and some fungi [115–117] through the hydrolysis of β-1,4-linkage of *N*-acetyl-*D*-glucosamine and *N*-acetylmuramic acid residue of the peptidoglycan of the bacterial cell walls [118]. Recent studies confirmed its activity against some Gram-negative bacteria, including *Pseudomonas aeruginosa* [119]. In addition, lysozyme has a great potential in the treatment of diseases of inflammatory origin [120] by reducing the lipopolysaccharide (LPS)-induced inflammatory responses, and some studies suggested the alleviation of the inflammation by suppressing the inflammatory cytokine levels in both serum and organs [121, 122]. Moreover, some researchers reported anti-inflammatory action at the gene expression level [123].

Spray-dried mannitol (SDM) (Pearlitol SD-200, Roquette Pharma, France) and crystalline mannitol (CM) (Hungaropharma Ltd., Hungary) were utilized as conformation stabilizers against thermal shocks caused by the raised mechanical stress or during the drying of the protein formulation [124–126]. The CM has big columnar/tabular crystals with sharp edges, and wide particle size distribution (Fig. 1c), while SDM has spherical particles with more narrower size

distribution (Fig. 1d), which may be considered as aggregates of columnar microcrystals. Further difference that while CM is pure β form, SDM is a mixture of α and β forms, which exerted smaller elasticity in compression studies. Microcrystalline cellulose (MCC, Avicel pH 101, FMC Biopolymer, Philadelphia, USA) was used as pellet former and drug carrier.

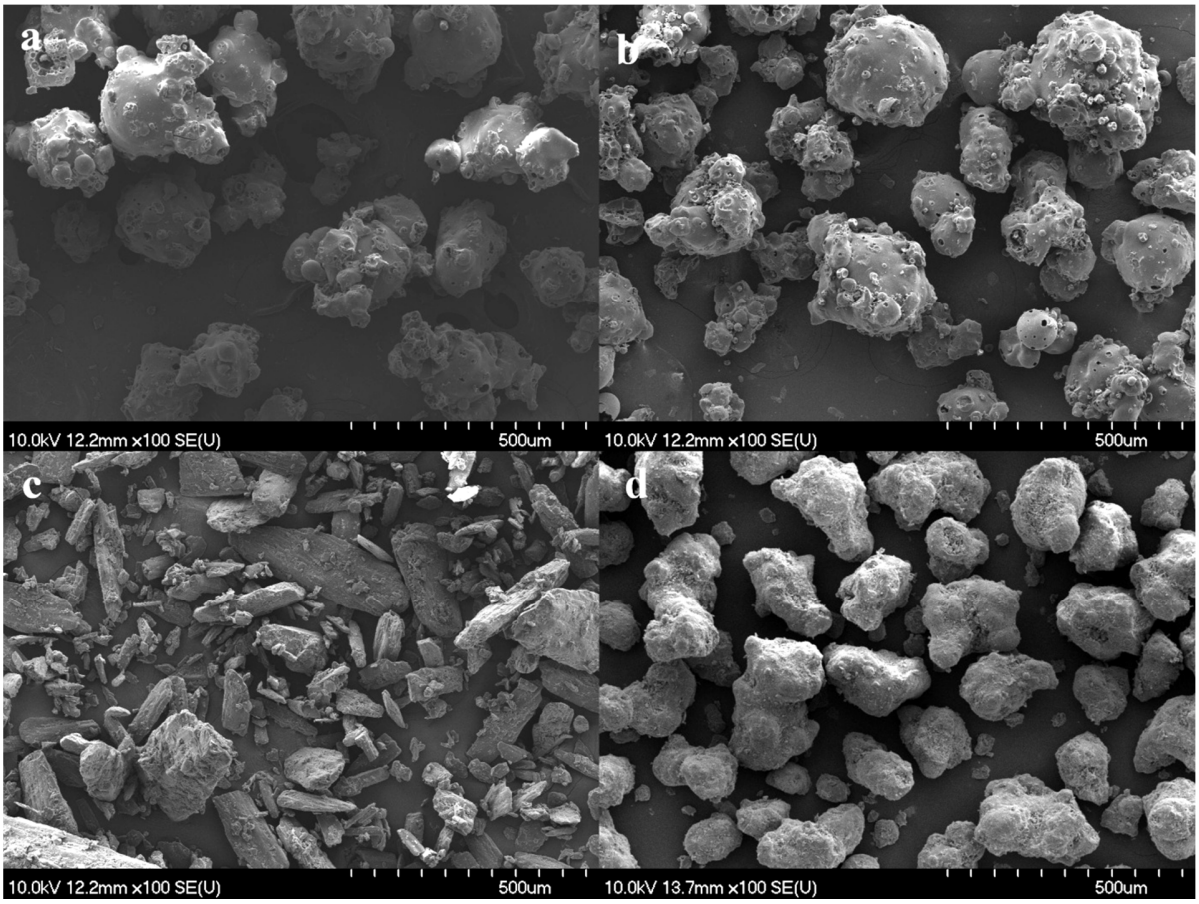

Figure 1. Scanning electron micrographs of lyso-1 (a), lyso-2 (b), CM (c) and SDM (d)

Lyophilized *Micrococcus lysodeikticus* (Sigma-Aldrich, USA) was used as a model Gram-positive bacterium to investigate the biological activity of the prepared pellets.

Chitosan 80/1000 (Heppe Medical Chitosan GmbH., Germany) was applied as a functional subcoating polymer. Acetic acid (AA) 99.8% (Sigma-Aldrich, Germany) and citric acid monohydrate (CA) (Molar Chemicals Kft, Hungary) were primarily used as solubility enhancers for chitosan. Glycerol (G), propylene glycol (PG) (Hungopharma Ltd., Hungary), and polyethylene glycol 400 (PEG-400) (Sigma-Aldrich, Germany) were used as plasticizers. Mucin 75-95% (Roth, Germany) was used as a substrate for the mucoadhesivity investigation and

diiodomethane (VWR Prolabo, USA) was used as a non-polar liquid for the surface free energy (SFE) investigation.

Chitosan is a linear biopolymer composed of randomly distributed ß (1, 4) - linked *D*-glucosamine and *N*-acetyl-*D*-glucosamine obtained by partial deacetylation of chitin [127–129]. Its unique properties such as biocompatibility, biodegradability, non-toxicity and low immunogenicity make chitosan the second most abundant natural polymer in the world [130, 131], and due to its weak alkaline nature, chitosan is solubilized by aqueous acidic media and produces highly viscous solutions suitable for the preparation of free films and coatings [132]. In addition, it possesses superior mucoadhesivity due to the presence of reactive hydroxyl and amino groups [133], which enable ionic interaction with sialic acid residues of the mucosa [134]. Thus, it could be involved in opening TJs and assisting the penetration of macromolecular drugs [135, 136]. The reversible opening of TJs has been approved and is regarded as the safest approach to penetration enhancement [137, 138]. Furthermore, its incorporation may enable the controlled release of the incorporated macromolecule, EI and PE [139]. Accordingly, chitosan is considered to be an effective positively charged and harmless PE along the intestinal lumen [137, 138, 140].

In addition, the incorporation of CA instead of AA will tailor the properties of chitosan, as CA can be used as plasticizing agent. Moreover, CA has been described to increase the absorption of proteins by various mechanisms, e.g. by effective suppression of luminal proteases [141] and permeation enhancement by calcium chelation, which results in the opening of TJs [142–144]. Accordingly, it could be a logical approach when multiparticulates are suitably subcoated by a multifunctional layer to improve bioavailability by the different ways discussed above. However, it is necessary to thoroughly investigate CA-based chitosan solutions/films by involving different plasticizers and screening out the one with preferable criteria for coating.

4.2. Methods

4.2.1. Pelletization

4.2.1.1. Design of Experiments

The experiments were performed according to 2^3 full factorial design with a central point. The impeller speed (x_1), liquid addition rate (x_2) and extrusion speed (x_3) were studied as independent factors, while the optimization parameters were enzyme activity (y_1), pellet hardness (y_2), moisture content (y_3), roundness (y_4) and aspect ratio (y_5). The effect of factors and their interactions on the optimization parameters were evaluated statistically by using Statistica v. 13.5. Software (Tibco Statistica Inc, CA, USA).

4.2.1.2. Homogenization

100 g of powder mixtures composed of Lyso-1 or Lyso-2, CM or SDM and MCC in a ratio of 1:4:5, respectively, were homogenized in a Turbula mixer (Willy A. Bachofen Maschinenfabrik, Switzerland) for 10 minutes. The composition of the homogenized powder mixtures is shown in Table 1.

Table 1. Composition of the mixtures

Excipients	C1 (g)	C2 (g)	C3 (g)
Lyso-1	10	10	-
Lyso-2	-	-	10
CM	40	-	40
SDM	-	40	-
MCC	50	50	50

Lyso-1: lyophilized lysozyme, Lyso-2: spray-dried lysozyme, C 1, C 2 and C 3: first, second and third composition, respectively

4.2.1.3. Estimation of Water Quantity

The exact quantity of the granulating liquid is critical since the liquid quantity will affect the quality of the extrudate as well as the hardness and sphericity of the particles [145, 146]. Accordingly, the Enslin number was estimated, which is a simple measurement and is equal to the quantity of water absorbed by 1 g of the powder mixture (ml/g). The equipment is simple and consists of a G4 glass filter and a pipette with 0.01 accuracy. 0.5 g of each homogenized powder mixture was dispersed as a monolayer over a filter paper placed horizontally at the bottom of the glass filter, and the maximum water uptake was determined; the experiment was performed three times and the average was taken.

4.2.1.4. Wet Granulation

The homogenized mixtures of the powder samples were wetted and kneaded in a ProCepT 4M8 high shear granulator (ProCepT nv. Zelzate, Belgium) at different impeller speeds (x_1) and liquid addition rates (x_2). The impeller and the chopper were located vertically; the processing parameters are illustrated below in Table 2. 60 ml of purified water was added at different rates (-1, 0 and +1 level), followed by 60s wet massing time. Wet granulation and kneading were performed in a specially designed Teflon granulation chamber (Opulus Ltd., Hungary) equipped with three immersed PyroDiff® sensors (channel 1, 2 and 3) located at different heights from the bottom of the chamber and at different distances from the chamber wall, as demonstrated in Figure 2. They were directly connected to a computer via an interface and four calibrated PyroButton-TH® sensors equipped on the chamber wall at different positions (at the bottom, 42 mm, 65 mm and 87 mm from the bottom). The sensors were programmed to continuously measure the change in temperature and relative humidity (RH) in every 2 seconds during granulation, at the temperature and humidity resolution of 0.06°C and 0.04% RH, respectively, in addition to the infrared temperature sensor of the high-shear granulator. The obtained wetted masses were preserved in tightly closed containers until extrusion/spheronization.

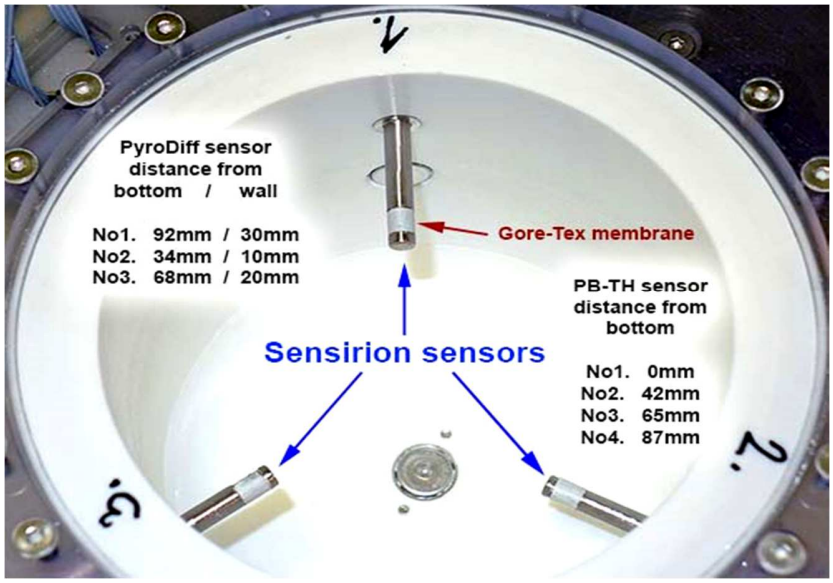

Figure 2. Kneading chamber showing the configuration of immersed (PyroDiff®) and PyroButton-TH® sensors

Table 2. Processing parameters of the kneading, extrusion and spheronization

Kneading	**Process-1**		**Process-2**		**Process-3**		**Process-4**		**Process-5**
Impeller speed (x_1)	500 (-1)		500 (-1)		1500 (+1)		1500 (+1)		1000 (0)
Liquid addition rate ml/min (x_2)	5 (-1)		10 (+1)		5 (-1)		10 (+1)		7.5 (0)
Purified H_2O (ml)	60		60		60		60		60
Chopper speed	500		500		500		500		500
Extr./spheron.	**Process-1**		**Process-2**		**Process-3**		**Process-4**		**Process-5**
Extrusion speed (x_3)	70 (-1)	120(+1)	70 (-1)	120(+1)	70 (-1)	120(+1)	70 (-1)	120(+1)	95 (0)
Spher. speed (rpm)	2000	2000	2000	2000	2000	2000	2000	2000	2000
Spher. time (minute)	1	1	1	1	1	1	1	1	1
Spher. amount (g)	17	17	17	17	17	17	17	17	17
Sample code	**LysC-11**	**LysC-12**	**LysC-21**	**LysC-22**	**LysC-31**	**LysC-32**	**LysC-41**	**LysC-42**	**LysC-c**

***C**: referring to the composition; 1, 2 and 3 for the first (C1), second (C2) and third (C3) composition, respectively

4.2.1.5. Extrusion and Spheronization

The kneaded wet masses were extruded with a single-screw extruder (Caleva Process Solutions Ltd., UK), which was equipped with an axial screen of 4-mm thickness and had 16 dies with a diameter of 1 mm. The extruder was equipped with a laboratory-developed water-cooling jacket to maintain the temperature constant during extrusion. Extrusion was performed at different extrusion rates (x_3) (70, 95 and 120 rpm) and at a constant feeding rate. The obtained extrudates were preserved in moisture-retentive containers to prevent water loss.

The extruded samples were spheronized with a Caleva MBS spheronizer (Caleva Process Solutions Ltd., UK). 17 g of each extruded sample was spheronized at a speed of 2000 rpm for 1 min (according to the preformulation study). The obtained spheroids were dried for 24 hours under ambient conditions (22±1°C, 31±2% RH).

4.2.1.6. Measurement of Pellet Activity

The biological activity (y_1) of the prepared pellets was measured via the degradation of lyophilized *Micrococcus lysodeikticus* by using a Genesys 10 S UV-VIS Spectrometer (ThermoScientific, MA, USA). 70 mg of lyophilized bacteria was suspended in 100 ml of phosphate buffer (pH 6.24); the basic absorption at 450 nm was around 0.7. The absorption of the bacterial suspension was measured for 5 minutes before each test to reduce the error arising from bacterial sedimentation. 100 mg of pellet or 10 mg of crude lysozyme was dissolved in 25 ml of phosphate buffer. 0.1 ml of pellet/or crude lysozyme solution was added to 2.5 ml of bacterial suspension and shaken for 20 seconds in a quartz cuvette, then the change in bacterial

absorption was measured for 5 minutes. Pellet activity was calculated from the percentage degradation of the bacterial cells relative to crude lysozyme activity as a reference by SigmaPlot Software (version 12).

4.2.1.7. Hardness and Deformation

Deformation force (y_2) and behavior was investigated with a custom-made texture analyzer. The equipment and its software were developed at the University of Szeged, Institute of Pharmaceutical Technology and Regulatory Affairs. The equipment consists of a sample holder at the base and a probe moving vertically at a constant speed of 20 mm/min. The test was conducted in the force range of 0-50 Newtons. The deformation characteristics and breakage force of pellets (n=20 for each sample) were obtained and the average and SD were calculated.

4.2.1.8. Moisture Content

The moisture content (y_3) of the prepared pellets was measured by using a Mettler-Toledo HR73 (Mettler-Toledo Hungary Ltd., Hungary) halogen moisture analyzer. The moisture content of approximately 0.5 g of each sample was measured in triplicate at a drying temperature of 105°C until a constant weight was obtained.

4.2.1.9. Size and Shape Study

The size and shape (y_4 and y_5) of the prepared samples were investigated by using a system consisting of a stereomicroscope and a ring light with a cold light source (Carl Zeiss, Oberkochen, Germany). The images were analyzed with Leica Quantimet 500 C image analysis software (Leica Microsystems, Wetzlar, Germany), and the area, length, breadth, perimeter, convex perimeter, roundness and aspect ratio of 100 pellets were measured or calculated. The roundness and aspect ratio are the most common shape parameters used to characterize the shape of pellets and are calculated by the applied Leica Q500MC software using the following equations:

$$\text{Roundness} = Perimeter^2/(4*\pi*Area*1.064) \quad (1)$$

$$\text{Aspect ratio} = d_{max}/d_{min} \quad (2)$$

where *Perimeter* is the total length of boundary of the feature, *Area* is calculated from the total number of detected pixels within the feature, while d_{max} and d_{min} are the longest and shortest Feret diameter measured.

4.2.1.10. Scanning Electron Microscopy

The morphology and size of the raw materials were investigated by Scanning Electron Microscope (SEM) (Hitachi 4700, Hitachi Ltd., Tokyo, Japan). The samples were coated with a conductive gold thin layer by a sputter coating unit (Polaron E5100, VG Microtech, UK), images were taken at an accelerating voltage of 10.0 kV, the used air pressure was 1.3– 13 mPa during the analyses. The particle size was determined using Image J 1.47 t (National Institute of Health, Bethesda, MD, USA) software.

4.2.2. Design of Chitosan Films

4.2.2.1. Preparation Method

Chitosan films were prepared with the solvent casting method, by dissolving the polymer (2 w/v%) in aqueous AA solution (2 v/v%) as prescribed by *Liu et al.* [147] as a reference, and with the use of CA (2.5, 3, 3.5, 4, 5 and 7 w/v%). Plasticizers were added to AA, CA 2.5% and CA 7%-based solutions in approx. five to ten times excess (5 w/v% and 10 w/v%) compared to the polymer, to significantly modify the surface characteristics, which could be crucial when the films are applied as subcoating. The exact compositions of the prepared solutions/films are shown below in Table 3, while the molar ratios can be found in Annex 5 Table S1.

Table 3. Composition of prepared citric acid (CA)- and acetic acid (AA)-based solutions/films

Plasticizer	w/v%	Chitosan w/v%	CA w/v%	CA w/v%	CA w/v%	CA w/v%	CA w/v%	CA w/v%	AA v/v%
-	0	2	2.5	3	3.5	4	5	7	2
G	5	2	2.5	-	-	-	-	7	2
	10	2	2.5	-	-	-	-	7	2
PG	5	2	2.5	-	-	-	-	7	2
	10	2	2.5	-	-	-	-	7	2
PEG-400	5	2	2.5	-	-	-	-	7	2
	10	2	2.5	-	-	-	-	7	2

A magnetic stirrer was used to obtain 100 mL of homogeneous solutions. Heating to 50–58°C for two hours was required to dissolve chitosan if a low amount of CA (2.5 and 3 w/v%) was applied, as the pH of these solutions was around pH 4, whereas for AA and CA (3.5–7 w/v%) based solutions (pH of ~2.75) heating was not required. After the whole polymer was dissolved, the obtained solutions were left to stand for 3 h to enable the entrapped air bubbles to evolve. A portion (~ 25 mL) of each solution was taken to test the minimum film forming temperature (MFFT), while the remaining amount was cast into gasket rings (19.635 cm^2 x 0.5 cm) as 10 g/ring. The cast solutions were dried under ambient conditions (25.5 ± 1°C and 28 ± 1 RH%) for 48 h, the dried films were carefully released from the plates and preserved in tightly closed containers for further investigations.

4.2.2.2. Investigation of Minimum Film Forming Temperature

Minimum Film Forming Temperature (MFFT) was investigated with a Rhopoint MFFT-60 Bar tester (Rhopoint, UK) in the temperature range of 15–60 ºC. After temperature equilibrium had been established, a cube applicator was used to make 5 parallel films of 75 µm thickness over the temperature bar. The hinged Perspex cover was returned down to provide atmospheric and thermal equilibrium whilst enabling the visual inspection of the applied films. The films (n = 5) were then let completely dry, and the result was recorded manually by inspecting the cracked regions on the applied film forms on the graduating scale of the equipment.

4.2.2.3. Infrared Spectroscopy

The infrared spectra of the films and raw materials were obtained by using an Avatar 330 (ThermoScientific, USA) Fourier transform infrared (FT-IR) apparatus coupled with a Zn/Se HATR (horizontal attenuated total reflectance) accessory. Each film was directly placed on an ethanol-cleaned crystal of the equipment; the scanning was run in the wavelength range of 600–4000 cm^{-1}, the spectra were collected from 128 scans to obtain smooth spectra, at the spectral resolution of 4 cm^{-1} and applying CO_2 and H_2O corrections.

4.2.2.4. Film Thickness

The thickness of the films was measured at 10 randomly selected points on each film (n = 10) by using a screw micrometer (Mitutoyo Co. Ltd, Japan) with sensitivity of 0.001 mm, and the means and SDs were calculated.

4.2.2.5. Hardness and Mucoadhesion Investigations

The hardness of films and mucoadhesive forces were investigated with the same equipment described in Section (4.2.1.7), but with a different assembly of the moving probe and sample holder. For the hardness test, a needle-like probe with a half-sphere end was fixed at the top movable part of the assembly and set to move downward at a controllable speed toward the tested film, which was tightly fixed on the sample holder, enabling the moving probe to pass through the fixed film until the film cracked. This test was repeated ten times for each film (n = 10), and the means and SDs were calculated.

On the other hand, for mucoadhesivity a rod-like probe with an outer diameter of 9 mm represented the sample holder. A double-faced adhesive tape was used to fix the polymer film with an equivalent area on its surface. At the bottom of the equipment, a circular flat disc with an outer diameter of 35 mm was fixed, on which a few drops of freshly prepared 1 mg/ml mucin solution were spread. The equipment was adjusted to move downward to press the film with 50 ± 1 N force for 30 s to mucin. The probe then moved upwards, which resulted in the drop-down of the force curve until the fixed film started to detach from mucin, which is represented as a sharp peak on the force-time curve, as shown in (Fig. 9), where the peak maximum represents mucoadhesivity. This test was repeated five times (n = 5), and the means and SDs were calculated.

4.2.2.6. Calculation of Surface Free Energy

The measurement of SFE allows the evaluation of the wetting behavior and the applicability of the tested polymer for the coating process as the SFE of a mucoadhesive polymer should be adequate to enable wetting with the mucosal surface [148]. SFEs were calculated indirectly from the means of the contact angles (Θ) of two liquids [149] with known surface tension, dispersive and polar components by using the optical contact angle measuring apparatus (OCA20, DataPhysics Instrument GmbH, Germany), via the application of the sessile drop method. Distilled water (γ_{tot} = 72.8 mN/m, γ_d = 21.8 mN/m, γ_p = 51.0 mN/m) and diiodomethane (γ_{tot} = 50.8 mN/m, γ_d = 50.8 mN/m, γ_p = 0 mN/m) were used as polar and non-polar reagents, respectively. One drop of each liquid (10 µL of distilled water and 5 µL of diiodomethane) was applied via a motor-driven micro-syringe on the prepared thin, plain and smooth film of chitosan and the angles were measured automatically for 30 s. The starting (0 s) and equilibrium (30 s)

contact angles (n = 10 of each liquid) were recorded, and the means and SDs were calculated separately. The results were introduced into OCA-20, SFE-calculating-program by introducing the means and SDs of first and equilibrium contact angles in every combination by applying the method of Wu. (Eq. 3):

$$(1+\cos\Theta)\cdot\gamma = \frac{4\left(\gamma_s^{\,d}\cdot\gamma_l^{\,d}\right)}{\gamma_s^{\,d}+\gamma_l^{\,d}} + \frac{\left(\gamma_s^{\,p}\cdot\gamma_l^{\,p}\right)}{\gamma_s^{\,p}+\gamma_l^{\,p}} \quad (3)$$

where Θ is the contact angle, γ_l is the liquid surface tension, γ_s is the solid surface energy, and the superscripts indicate their polar (γ_p) and dispersive components (γ_d). As the surface free energy of the film is the sum of the dispersive part and the polar part, the polarity (percent of hydrophilic groups formed during film formation) of the prepared films can be calculated by the following formula (Eq. 4):

Polarity % = (Polar part/ Surface energy) x 100 (4)

4.2.2.7. Thermal Analysis

Thermal gravimetric analysis (TGA) and differential scanning calorimetry (DSC) were carried out by using TG/DSC1 equipment (Mettler-Toledo Inc., Switzerland). The samples were heated from 25 to 500°C in a non-hermetically sealed 40 µl aluminium pan. Heating was at a constant rate of 10°C·min^{-1}. The mass of the samples was 10±2 mg, and the measurements were performed in nitrogen atmosphere at a rate of 70 ml·min^{-1}.

4.2.2.8. Statistical Analysis

The gathered data were analyzed according to a factorial ANOVA method by using Tibco Statistica v13.1 (Tibo Sofware Inc, OK, USA) software.

5. RESULTS AND DISCUSSION

5.1. Determination of the Design Space

5.1.1. Investigation of the Change in T and RH%

The variation of the recorded values was attributed to the location of the sensor and its distance from the impeller rotational axis, as illustrated above (Fig. 2), and the detected local temperatures may be considerably higher than the general temperature recorded by the granulator's own built-in sensor. The variation of T and RH% with the various experimental settings can be found in (Annex 3.)

As expected, at a lower (-1) level of impeller speed, the internal chamber temperature was relatively low and constant throughout the wet kneading period, which is advantageous for processing thermolabile molecules. Under these conditions, the liquid addition rate has less impact on the temperature value, as demonstrated in Figure 3.

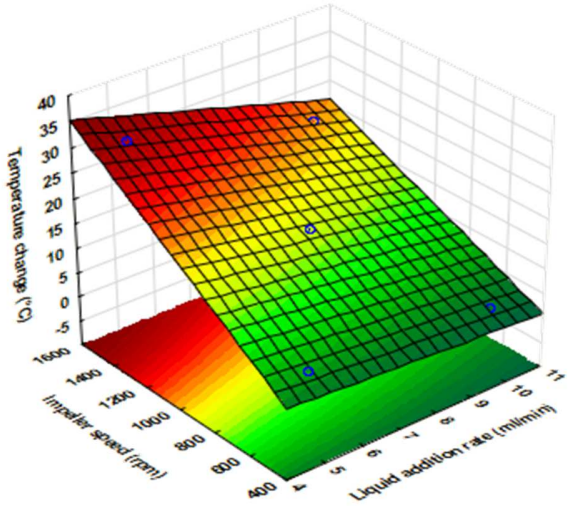

Figure 3. Temperature change in the kneading phase

When operating at a higher (+1) level of impeller speed (processes 3 and 4), the liquid addition rate exhibited more considerable influence on the temperature distribution inside the chamber, although it was only partially able to compensate for the temperature elevation which was induced by mechanical friction between the kneaded mass, impeller and chamber wall. Overall, the temperature change mostly depends on impeller speed and exhibited a linear relation with the investigated parameters (Eq. 5).

$y_{\Delta T}$= *15.409+**10.643x_1**-3.176x_2-1.633x_1x_2* (5)

R^2= 0.99836 Adj R^2= 0.99344 MS Residual= 0.828245

In contrast, the variation of system RH did not follow the expectations since the increasing liquid addition rate resulted in a reduced increment of RH. This unexpected phenomenon may be due to the insufficient equilibration time of MC% on the solid-air interface. The highest increment in the system RH% values was recorded in the central point (Fig. 4). The low adj. R^2 and the high curvature coefficient of the corresponding Equation 6. indicates poor model quality, which may be due to a strong nonlinear relationship between the tested factors and RH%.

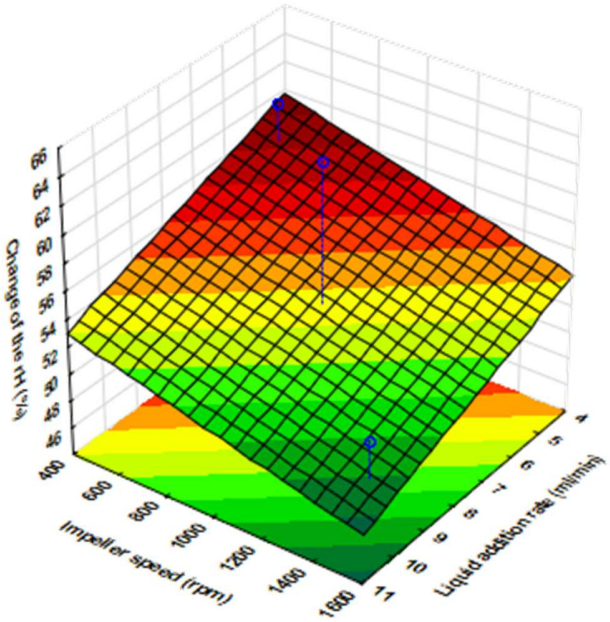

Figure 4. Relative humidity change in the kneading phase

$y_{RH\%}$=*53.6158-2.3742x_1-2.2925x_2* (6)

R^2= 0.80017 Adj R^2=0.20067 MS Residual=31.4534 Curvature=10.148

The increasing impeller speed also decreases the general increment in the system RH%, which may indicate that more intensive mixing promotes the uniform distribution of moisture, which increases the amount of the surface adsorbed fraction. Nevertheless, at a lower impeller speed, RH% was comparable in the entire granulation chamber, but the increasing impeller speed resulted in greater RH% variation with a rapid increase in RH% values throughout the granulation chamber (Figs. S3 and S4 in Annex 3). This may be due to the increased evaporation

rate in the elevated temperature regions, which is supported by the similar distribution of temperature and RH% values (Figs. S2 and S4 in Annex 3).

The results confirmed the original hypothesis that there are differences in the distribution of T and RH% inside the granulation chamber, which may result in the formation of hot spots, which represent the critically degrading microenvironment for sensitive drugs. Nevertheless, it should be noted that despite the similar tendencies, generally better enzyme activities were recorded when granulation was carried out in a glass chamber (92.67% vs. 58.98% of enzyme activity). This phenomenon may be explained by the different thermal conductivity of Teflon and glass (0.25 W/mK vs. 0.96-1.05 W/mK, respectively), which is resulted in a more uniform heat distribution in the glass chamber.

5.1.2. Investigation of the Impact of Material Attributes

Despite the considerable variation in T and RH% distribution, the detected maximum temperatures (Fig. 5) are good indicators of material behavior during the kneading phase. It is clearly visible that at low shear rates (processes 1 and 2) there is no difference in the recorded temperature. In contrast, at high levels of impeller speed and low levels of liquid addition, C2 exhibited considerably lower maximum temperature compared to C1 and C3. *Schaefer and Mathiesen* reported that the increase in T in high shear granulation is mainly attributed to the conversion of the mechanical energy input into the heat of friction within the moist mass [150]. Therefore, the lower temperature elevation upon high mechanical attrition may be due to the better deformation properties of SDM over CM.

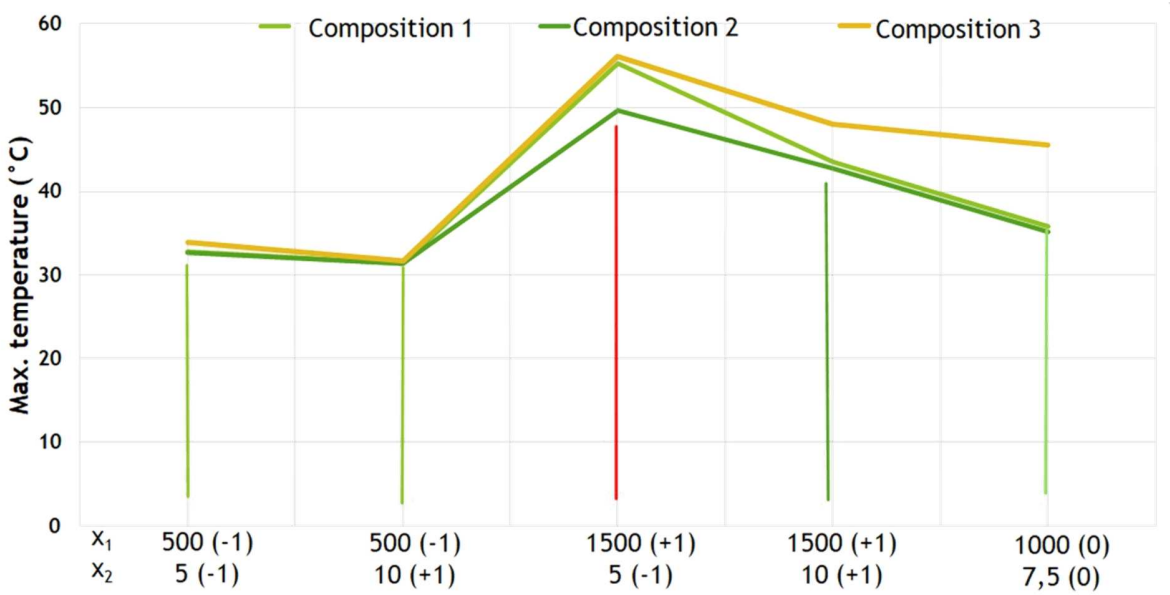

Figure 5. Maximum recorded temperature under different processing conditions for the various compositions (C1, C2 and C3)

The T excess arising in the case of C1 may be compensated by the cooling effect of an increased liquid addition rate as long as it is related only to the presence of CM. However, if CM is combined with lyso-2 in C3, the further increasing friction results in much higher T than a composite containing lyso-1 (C1 and C2), despite the increased liquid addition rate. In conclusion, in spite of the general physicochemical similarities and the similar liquid uptake pattern (0.6 ml/g) of the SD and C form of raw materials, the material attributes showed obvious differences in thermal behavior upon the applied mechanical stress, especially at higher shear rates. This finding is supported by *Hulse et al.,* who reported that despite the similarity in the thermal behavior of CM and its different forms such as SDM, a full characterization is required as a preformulation step because these polymorphs are dissimilar in their physical properties [151]. Overall, the method of raw material production (i.e. conventional crystallization or spray-drying) has an effect on the thermomechanical response upon exposure to higher mechanical stress and may considerably influence the critical quality attributes of the final product (Tables 4-6).

Table 4. Physical properties and biological activity of C-1-pellets

Sample	Activity% (y_{11})	Hardness (N) (y_{21})	MC% (y_{31})	Roundness (y_{41})	Aspect ratio (y_{51})
Lys1-11	95.92	15.55 ±1.67	0.93 ±0.02	1.13 ±1.13	1.14 ±1.10
Lys1-12	92.75	13.03 ±1.10	0.51 ±0.03	1.11 ±0.08	1.13 ±0.06
Lys1-21	88.56	13.00 ±1.17	0.62 ±0.02	1.17 ±0.10	1.18 ±0.10
Lys1-22	111.56	11.60 ±1.24	0.44 ±0.01	1.15 ±0.10	1.16 ±0.10
Lys1-31	90.68	14.64 ±1.54	0.59 ±0.02	1.15 ±0.07	1.16 ±0.07
Lys1-32	76.46	12.50 ±1.55	0.41 ±0.03	1.14 ±0.07	1.15 ±0.06
Lys1-41	96.30	14.00 ±1.05	0.63 ±0.02	1.14 ±0.09	1.14 ±0.06
Lys1-42	85.93	13.60 ±1.41	0.40 ±0.01	1.1 5 ±0.12	1.14 ±0.07
Lys1-C	88.99	14.04 ±1.05	0.77 ±0.02	1.13 ±0.10	1.13 ±0.05

Table 5. Physical properties and biological activity of C-2-pellets

Sample	Activity% (y_{12})	Hardness (N) (y_{22})	MC% (y_{32})	Roundness (y_{42})	Aspect ratio (y_{52})
Lys2-11	89.84	13.01 ±1.50	1.00 ±0.03	1.12 ±0.06	1.17 ±0.07
Lys2-12	109.96	12.33 ±1.21	0.47 ±0.02	1.12 ±0.06	1.17 ±0.08
Lys2-21	89.43	11.12 ±1.57	1.10 ±0.02	1.10 ±0.04	1.15 ±0.07
Lys2-22	97.30	10.20 ±1.53	0.82 ±0.02	1.11 ±0.06	1.17 ±0.08
Lys2-31	88.49	16.10 ±2.50	0.56 ±0.01	1.17 ±0.22	1.20 ±0.12
Lys2-32	91.91	14.44 ±2.53	0.40 ±0.01	1.16 ±0.14	1.22 ±0.10
Lys2-41	102.50	15.13 ±2.40	0.59 ±0.02	1.14 ±0.10	1.17 ±0.08
Lys2-42	103.08	13.21 ±1.50	0.42 ±0.01	1.16 ±0.16	1.20 ±0.10
Lys2-C	84.15	14.76 ±1.63	0.79 ±0.03	1.15 ±0.10	1.21 ±0.10

Table 6. Physical properties and biological activity of C-3-pellets

Sample	Activity% (y_{13})	Hardness(N) (y_{23})	MC% (y_{33})	Roundness (y_{43})	Aspect ratio (y_{53})
Lys3-11	79.00	15.23 ±1.64	0.93 ±0.03	1.17 ±0.13	1.18 ±0.11
Lys3-12	76.47	13.35 ±2.02	0.55 ±0.02	1.17 ±0.10	1.16 ±0.07
Lys3-21	84.81	15.26 ±2.10	0.94 ±0.04	1.17 ±0.13	1.17 ±0.10
Lys3-22	74.51	13.28 ±1.58	0.65 ±0.02	1.16 ±0.10	1.17 ±0.10
Lys3-31	87.18	15.95 ±2.61	0.67 ±0.05	1.16 ±0.08	1.24 ±0.10
Lys3-32	77.66	14.21 ±2.26	0.59 ±0.03	1.20 ±0.16	1.28 ±0.14
Lys3-41	92.79	12.83 ±2.18	0.97 ±0.03	1.21 ±0.14	1.22 ±0.12
Lys3-42	79.17	11.01 ±1.32	0.72 ±0.07	1.22 ±0.11	1.20 ±0.10
Lys3-C	66.67	13.77 ±1.48	0.83 ±0.03	1.24 ±0.20	1.23 ±0.10

5.1.3. Biological Activity

The statistically obtained equations describing the relationship between factors x_1, x_2 and x_3, and enzyme activity (y_1) are listed below. The statistically significant factor coefficients are shown in bold. The second subscript number of the optimization parameters (y) refers to the composition (C1, C2 or C3). The coefficients of the variables and their interactions showed the change in the optimization parameters when the variable value increased from 0 to +1 level. In

order to get a good fit by increasing the $_{adj}R^2$ values, some unnecessary elements were omitted from the equations.

$$y_{11}=92.267-0.597x_1+3.314x_2-4.926x_3+3.749x_1x_2-5.550x_1x_3-2.786x_1x_2x_3 \quad (7)$$

$$_{adj}R^2=0.9814 \quad MS_{Residual}=1.667 \quad Curv.\ coeff.=-3.282$$

$$y_{12}=96.56\mathbf{+4.00x_1+1.51x_2-1.89x_1x_2-3.00x_1x_3+4.78x_2x_3+1.18x_1x_2x_3} \quad (8)$$

$$_{adj}R^2=0.9995 \quad MS_{Residual}=0.0369 \quad Curv.\ coeff.=\mathbf{-12.41}$$

$$y_{13}=81.45-4.50x_1+1.37x_2+2.75x_3-1.49x_1x_2-1.29x_1x_3+0.46x_1x_2x_3 \quad (9)$$

$$_{adj}R^2=0.9771 \quad MS_{Residual}=1.3337 \quad Curv.\ coeff.=-14.78$$

The average enzyme activity was relatively high (92.267% and 96.56%) for C1 and C2 (Eqs. 7 and 8, respectively). However, while there were no statistically significant coefficients for C1, for C2 the increment of both impeller speed and liquid addition rate significantly ($p<0.05$) increased the enzyme activity (Eq. 8). A further difference is that in the case of C1, the increasing liquid addition rate has a clearly positive effect (coefficients b_2 and b_{12}) on enzyme activity by compensating for the temperature excess caused by higher friction. In contrast, for C2 the negative value of coefficient b_{12} indicates the negative effect of the high dosing rate when low shear rates are applied. This supports the previous conclusion made by *Sovány et al.* that the over-wetting of the enzyme increases its sensitivity to thermo-mechanical stress [15, 59]. The higher biological activity of C2 and the considerably lower enzyme activity of C3 support the argument concerning the impact of critical material attributes, especially the deformability of particles, on the quality of the macromolecular product. Consequently, the variation in the properties of formulation excipients or a macromolecular drug results in different biological activities and different thermal behaviors in response to elevated mechanical stress, and the differences in factor coefficients and interactions indicate that it will also have a considerable impact on the design space.

5.1.4. Mechanical Properties and Moisture Content

All the prepared samples showed fairly good breaking force (10.20 to 16.10 N), making them suitable for the subsequent coating process, which requires the granules to be hard enough to withstand the mechanical attrition encountered during the coating process.

$$y_{21}=13.49+0.195x_1-0.440x_2-0.808x_3+0.555x_1x_2+0.173x_1x_3+0.358x_2x_3 \quad (10)$$

$$_{adj}R^2=0.9654 \quad MS_{Residual}=0.0481 \; Curv.\ coeff.=0.5500$$

$$y_{22}=13.19\mathbf{+1.528x_1-0.778x_2-0.648x_3+0.228x_1x_2-0.248x_1x_3-0.063x_2x_3} \quad (11)$$

$$_{adj}R^2=0.9999 \quad MS_{Residual}=0.0001 \; Curv.\ coeff.=\mathbf{1.568}$$

$$y_{23}=13.89\mathbf{-0.390x_1-0.795x_2-0.928x_3-0.785x_1x_2+0.038x_1x_3}-0.023x_2x_3 \quad (12)$$

$$_{adj}R^2=0.999 MS_{Residual}=0.0005 \; Curv.\ coeff.=\mathbf{-0.1200}$$

Despite the considerably high values of the coefficients, none of the factors showed statistical significance in the case of C1 (Eq. 10). In contrast, their effects on C2 and C3 were significant (Eqs. 11 and 12). Increasing the impeller speed increases the hardness of C1 and C2 while decreasing the breaking force of C3, which indicates that increasing friction has a negative influence on the bonding ability of mechanically resistant particles. The increment of both the liquid addition rate (x_2) and extrusion speed (x_3) decreases hardness in all cases, which may be related to the less uniform distribution of water and particle density, which considerably influences the internal texture of the pellets. The deformation of the pellets starts with a viscoelastic deformation to the increasing load. No visible change in the shape of the pellets may be observed during this stage. In the next phase, plastic deformation of the pellets results in complete crushing of the pellets (Fig. 6). In some cases, a multi-stage deformation process was observed (Fig. 6b), where the first peak indicates the presence of microfractures due to small inconsistencies or structural defects in the pellet texture without visible deformations or breakage of the pellets. Therefore, peak C, which is equal to the crushing strength, was considered as pellet hardness in all cases.

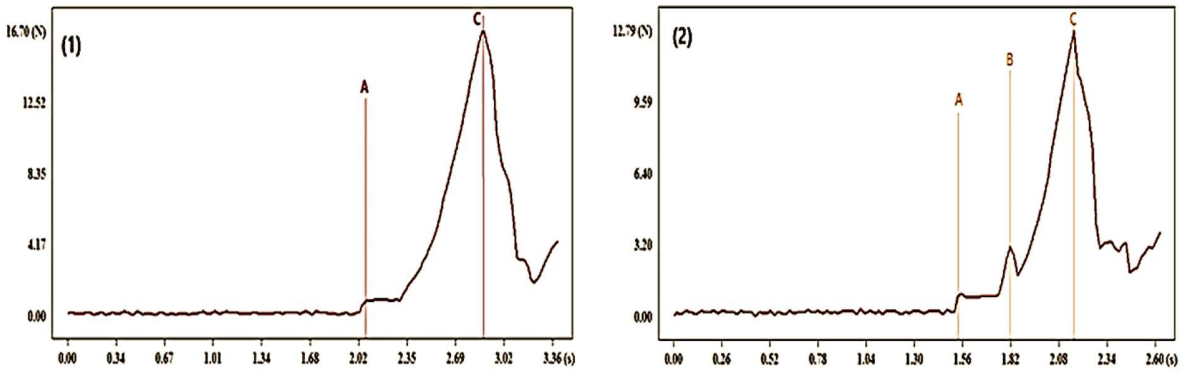

Figure 6. Typical pellet deformation curves, A and B: viscoelastic stages of deformation and C: the final plastic deformation step

The results revealed that the observed differences in the stability, polymorphs or mechanical properties of the raw materials did not affect the water uptake pattern of the various compositions (0.6 ml/g). Therefore, the physical interactions upon liquid (water) addition and mixing were almost similar for all formulations (C1-C3) processed under the same experimental conditions and confirmed by the comparable moisture content of the formulations processed under the same conditions. In case of C1 and C2, a weaker model quality was observed, which may be related to the higher values of curvature coefficients of these compositions, which indicates certain nonlinearity of the effect of the factors. Due to the weaker fit, the resulting models should be evaluated with cautions. The most considerable effect was exerted by the extruder speed (x_3), but it was found significant only for C1 (Eq. 11). The results indicate higher extrusion rates may repulse water from the wet mass and so decrease the final MC of the pellets.

$$y_{31}=0.566-0.059x_1-0.044x_2\mathbf{-0.126x_3}+0.051x_1x_2-0.036x_1x_2x_3 \quad (13)$$
$$_{adj}R^2=0.8544 \quad MS_{Residual}=0.0045 \; Curv.\ coeff.=0.2038$$

$$y_{32}=0.670-0.178x_1+0.063x_2-0.143x_3-0.050x_1x_2+0.060x_1x_3-0.033x_1x_2x_3 \quad (14)$$
$$_{adj}R^2=0.8899 \quad MS_{Residual}=0.0072 \; Curv.\ coeff.=0.1200$$

$$y_{33}=0.753-0.015x_1+0.068x_2-0.125x_3+0.040x_{1x2}+0.043x_1x_3-0.033x_1x_2x_3 \quad (15)$$
$$_{adj}R^2=0.9688 \quad MS_{Residual}=0.0008 \; Curv.\ coeff.=0.0775$$

According to the literature, *Colley et al.* reported that increasing the moisture content of pellets is accompanied by increasing their breaking force up to a certain moisture content, and then further moisture will reduce their breaking hardness [152]. However, the increase in the moisture content in a formulation containing macromolecules is problematic because it reduces long-term stability and adversely affects biological activity [153]. Generally, the moisture content of all the prepared samples was good (max. 1.1%) and could be maintained under appropriate packaging and storage conditions.

5.1.5. Roundness and Aspect Ratio

The preformulation study showed a maximum spheronization time of one minute, therefore it was kept constant for all the prepared samples as a result of the incorporation of higher amounts of polyols, which are hygroscopic and have a tendency to develop electrostatic charges, therefore increasing the spheronization time will lead to the sticking of the pellets [154, 155]. The

roundness of all the produced samples of C1 and C2 was good (<1.2), while C3 showed slightly higher values (≤ 1.28).

As known, the closer roundness is to 1, the closer the sample shape is to circular, thus allowing pellets to be coated effectively. According to the literature, the sphericity of pellets is markedly affected by the quantity of the granulating liquid and the duration of spheronization time [156]. The liquid addition rate had a significant effect on pellet roundness for C1 and C2 (Eqs. 16 and 17). Interestingly, the increasing liquid addition rate increased the roundness of C1 and C3, while decreasing the roundness of C2. This could be attributed to the different material characteristics, especially to the different deformation characteristics of SDM. The fact that impeller speed affected roundness significantly only for C2 and the significance of the curvature coefficient of the same composition indicate that the uniformity of liquid distribution had a significant impact on the sphericity of C2. Impeller speed also had a significant effect on the AR of C2 and C3 (Eqs. 20 and 21), it was directly proportional to AR, and the interaction of the tested factors was not significant.

$$y_{41}=1.143+\mathbf{0.010x_2}-0.005x_3-\mathbf{0.010x_1x_2}+0.005x_1x_3 \quad (16)$$

$$_{adj}R^2=0.8252 \quad MS_{Residual}=0.00005 \quad Curv.\ coeff.=-0.013$$

$$y_{42}=1.135+\mathbf{0.023x_1-0.008x_2+0.005x_2x_3}+0.003x_1x_2x_3 \quad (17)$$

$$_{adj}R^2=0.9733 \quad MS_{Residual}=0.00002 \quad Curv.\ coeff.=\mathbf{0.015}$$

$$y_{43}=1.183+0.015x_1+0.005x_2+0.005x_3+0.010x_1x_2+0.008x_1x_3-0.005x_2x_3 \quad (18)$$

$$_{adj}R^2=0.9419 \quad MS_{Residual}=0.00005 \quad Curv.\ coeff.=0.058$$

$$y_{51}=1.15+0.005x_2-0.005x_3-0.013x_1x_2+0.003x_1x_3+0.003x_1x_2x_3 \quad (19)$$

$$_{adj}R^2=0.9072 \quad MS_{Residual}=0.00003 \quad Curv.\ coeff.=-0.0200$$

$$y_{52}=1.181+\mathbf{0.016x_1}-0.009x_2+0.009x_3-0.004x_1x_2+0.004x_1x_3+0.004x_2x_3 \quad (20)$$

$$_{adj}R^2=0.9774 \quad MS_{Residual}=0.00001 \quad Curv.\ coeff.=0.0275$$

$$y_{53}=1.203+\mathbf{0.033x_1}-0.013x_2-0.013x_1x_2-0.005x_2x_3-0.001x_1x_2x_3 \quad (21)$$

$$_{adj}R^2=0.9376 \quad MS_{Residual}=0.0001 \quad Curv.\ coeff.=0.0275$$

5.1.6. Evaluation of the Changes on the Process Design Space

It is clear from the results of the previous chapters that the different compositions showed considerable differences in the response to changes in process parameters, which greatly influenced the size and position of the process design space (DS) in the modelled knowledge space. The DS was determined according to the recommendations of the Appendix 2 of the ICH Q8 guideline, using the following acceptance criteria in case of various CQAs: enzyme activity >75%, pellet hardness >15 N, moisture content <1%, aspect ratio <1.2, roundness <1.2. The contour plots of CQAs (Fig. S5-S49, Annex 3) and the scheme of the determination of the DS (Fig S50, Annex 3) can be found in the supplementary material, while Figure 7. shows the position of DS of different compositions at different extruder speeds.

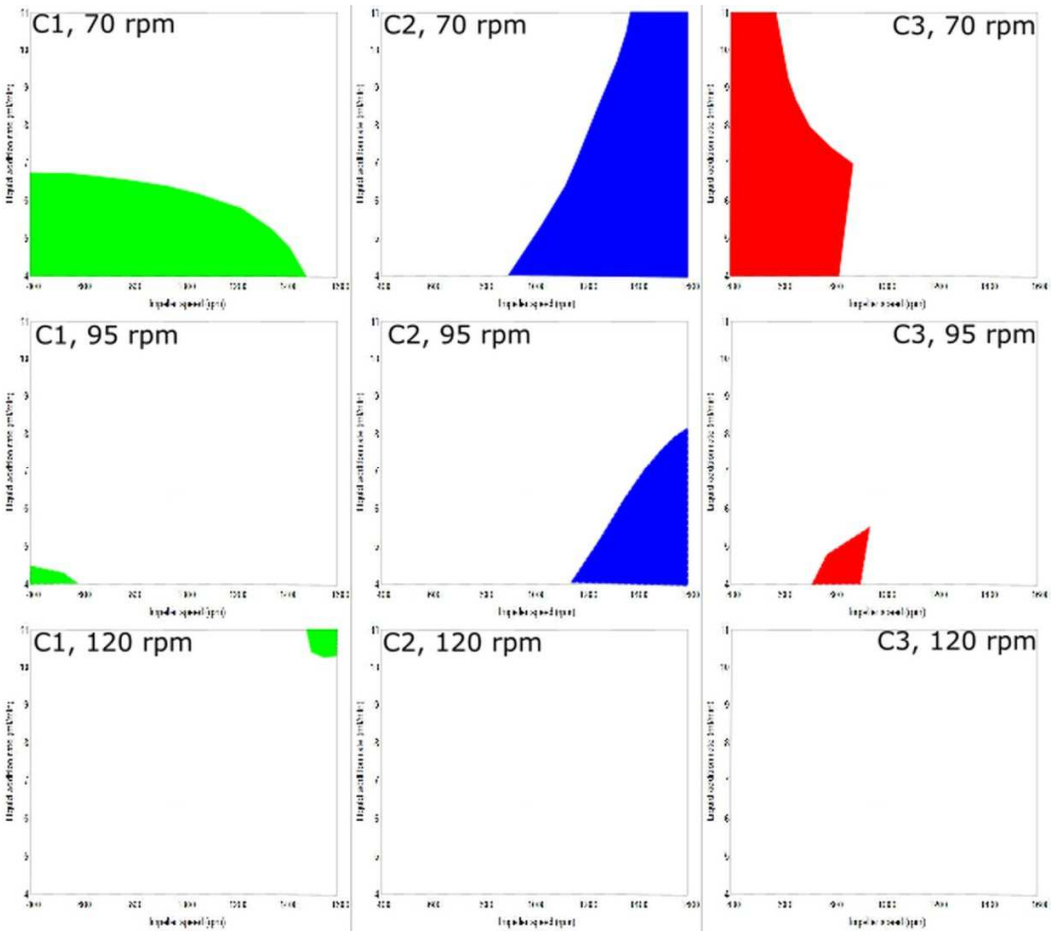

Figure 7. Design space of the kneading process in case of various compositions and extruder speeds

The results showed that the enzymatic activity and the moisture content were the less limiting factors, and the DS was mostly determined by the overlapping portions of the acceptance areas of hardness and shape parameters. Since increasing the extruder speed generally reduced the hardness and worsened shape parameters, this resulted in a decrease in the size of the DS of all compositions. The results showed that DS only partially overlap in the case of different formulations. A liquid feed rate of 4-5 ml/min and an impeller speed of 1100-1300 rpm and an extruder speed of 70 rpm can be used as controls for samples C1 and C2, while for sample C3 a liquid feed rate of 4-5 ml/min and 750-800 rpm impeller speed can be used at an extruder speed of 70-95 rpm.

5.2. Characterization of Chitosan Solutions/Films

5.2.1. Properties of Chitosan-Based Solutions

The pH of the obtained AA-based solutions varied in the range of 2.75 ± 0.25, and all the solutions were transparent and comparable with those made with CA. The addition of plasticizers slightly increased the pH, but the pH of G 10% solution was comparable with the plasticizer-free reference solution. The pH values of the obtained CA 2.5%-based solutions were in a relatively higher pH range of 4.12-5.37, which explains why heating was necessary to dissolve the polymer. Nevertheless, the visual appearance of the solutions and the films with and without different plasticizers was comparable with that of the AA-based ones. To eliminate the problems of elevated pH, a series of CA-based solutions was made in the range of 2.5–7 w/v%. The pH of the solutions was decreased from 4.25 to 2.58 with the increment of CA concentration, which was comparable with the pH of AA-based solutions and enabled the dissolution of the polymer without heating.

5.2.2. Physical Properties of the Prepared Films

MFFT was less than 15 ºC for all the investigated compositions, as shown below in Table 7. All the films applied on the temperature bar were dried as smooth, transparent and continuous films, i.e. no cracking or other failures were observed, which confirms the applicability of the compositions for the coating/subcoating of protein-containing solid dosage forms, since the low

MFFT allows a flawless coating process to be performed under gentle temperature conditions (between 30–45 ºC), which may generally decrease the risk of the temperature-induced misfolding of the processed polymers. Furthermore, the low MFFT enabled the drying of the cast films under ambient conditions.

Table 7. Physical properties of the various chitosan solutions/films

AA (v/v%)	CA (w/v%)	Plasticizer	Plasticizer content (w/v%)	MFFT (°C)	Thickness (mm)	Hardness (N)	Mucoadhesion (N)	MC (w/w%)
2	-	-	0	<15	0.07 ± 0.02	44.63 ± 3.40	42.30 ± 3.60	01.20 ± 1.70
2	-	G	5	<15	0.21 ± 0.04	2.39 ± 0.90	9.00 ± 4.62	13.83 ± 3.64
2	-		10	<15	0.32 ± 0.10	2.91 ± 1.10	8.34 ± 1.63	11.15 ± 0.54
2	-	PG	5	< 15	0.33 ± 0.01	6.66 ± 0.71	19.49 ± 3.20	06.41 ± 2.34
2	-		10	< 15	0.13 ± 0.02	6.81 ± 0.72	10.37 ± 2.27	07.80 ± 1.90
2	-	PEG 400	5	< 15	0.21 ± 0.01	20.88 ± 1.70	13.68 ± 3.40	7.92 ± 2.71
2	-		10	< 15	0.43 ± 0.03	18.48 ± 1.70	8.69 ± 2.89	13.27 ± 3.96
-	2.5	-	0	< 15	0.13 ± 0.01	36.01 ± 3.70	47.57 ± 3.03	0.75 ± 1. 26
-	3	-	0	< 15	0.15 ± 0.10	35.65 ± 3.36	35.41 ± 2.22	0.86 ± 2.54
-	3.5	-	0	< 15	0.14 ± 0.01	48.52 ± 0.50	42.68 ± 3.10	1.14 ± 3.34
-	4	-	0	< 15	0.16 ± 0.04	32.83 ± 4.78	41.10 ± 2.93	1.99 ± 2.82
-	5	-	0	< 15	0.23 ± 0.02	39.20 ± 5.40	30.32 ± 1.84	1.05 ± 2.46
-	7	-	0	< 15	0.27 ± 0.02	8.40 ± 1.98	25.65 ± 3.90	9.15 ± 3.84
-	2.5	G	5	< 15	0.17 ± 0.02	1.04 ± 0.27	14.52 ± 1.28	0.86 ± 3.43
-	2.5		10	< 15	0.20 ± 0.01	1.93 ± 0.89	13.71 ± 0.46	1.14 ± 3.03
-	2.5	PG	5	< 15	0.21 ± 0.01	1.39 ± 0.43	13.77 ± 1.78	1.99 ± 2.50
-	2.5		10	< 15	0.22 ± 0.01	4.95 ± 0.68	9.91 ± 2.18	1.05 ± 0.92
-	2.5	PEG 400	5	< 15	0.26 ± 0.02	8.12 ± 3.95	8.67 ± 2.10	2.15 ± 1.56
-	2.5		10	< 15	0.34 ± 0.01	6..22 ± 1.92	7.86 ± 3.86	2.75 ± 2.01
-	7	G	5	< 15	0.10 ± 0.01	0.58 ± 0.64	11.07 ± 2.76	11.83 ± 4.52
-	7		10	< 15	0.14 ± 0.01	0.64 ± 0.64	13.24 ± 1.10	17.36 ± 3.67
-	7	PG	5	< 15	0.16 ± 0.01	1.33 ± 0.14	15.80 ± 0.84	8.33 ± 1.80
-	7		10	< 15	0.18 ± 0.01	1.27 ± 0.25	12.20 ± 1.22	10.46 ± 2.67
-	7	PEG 400	5	< 15	0.23 ± 0.02	2.75 ± 1.10	18.13 ± 2.57	4.55 ± 0.73
-	7		10	< 15	0.33 ± 0.02	6.22 ± 1.80	16.79 ± 1.35	3.25 ± 2.22

The thicknesses of the prepared films are shown in Table 7. Plasticizer-free AA-based chitosan films showed the least thickness (0.07 mm), in accordance with the literature [157]. The thickness of CA-based chitosan films was minimum the double and proved to be directly proportional to the CA concentration (0.13–0.27 mm), indicating a dilatation in the polymer backbone as a result of cross-linking by CA. A similar direct relation between lactic acid quantity and the thickness of the chitosan film was also reported by *Bujang et al.* [158].

The addition of a plasticizer also increases film thickness up to a certain limit, in the order of G<PG<<PEG-400 in all cases (Table 7). The increment in film thickness upon the addition of the plasticizer is attributed to a good distribution of these plasticizers within the chitosan backbone. The significantly ($p < 0.001$) greater thickness obtained with PEG-400 may be due to the higher molecular weight and longer chain length of this plasticizer, which resulted in greater distance between chitosan chains and in higher water retention capacity. Generally, the film thickness of chitosan films may be manipulated and optimized by the amount of the plasticizer and the amount of chitosan itself, as also shown by *Nady and Kandil* [159]. The results also support that differences in film thickness may also contribute to the difference in the moisture content (MC) of the various samples as a weak positive correlation was revealed between these two parameters. The MC of plasticizer-free chitosan films showed no significant difference and ranged from approximately 1% up to 5% CA content. However, after a certain threshold, MC increases and may reach 9.15%, as recorded for the CA 7%-based film. This may also be explained by the cross-linking between CA and chitosan, which may result in the entrapment of water molecules within the polymer backbone. The addition of plasticizers significantly ($p < 0.0001$) increased MC in all the cases because of physical interactions enabling the solvent to be entrapped within the polymer skeleton and also due to their hygroscopic and moisture retentive behavior. From this aspect, G exhibited significantly higher MC ($p < 0.01$) than PG or PEG, which may be connected to the presence of unbounded OH groups. It is also notable that MC showed considerable pH dependency since the CA 2.5%-based samples exhibited significantly lower MC ($p < 0.0001$) than others, which may be due to a lower degree of ionization.

Plasticizer-free films made with CA in different quantities (2.5, 3, 3.5, 4 and 5 w/v%) showed a high breaking force in the range of 32.83–48.52 N, which was comparable with AA-based chitosan films. Nevertheless, a dramatic increase was observed in the time of elongation (Fig. 8) due to a viscoelastic change in the texture of the films, found to be proportional to the amount

of CA. However, when CA reaches 7 w/v%, a sharp reduction of hardness may be observed with a marked increase in elasticity.

In conclusion, CA may be a good plasticizer for chitosan and the ideal mechanical property may be achieved when it is used in the 3.5–5 w/v% range. Earlier, *Wan et al.* [160] prepared CA-based hydroxy propyl-methylcellulose (HPMC) and CA-based sodium carboxymethylcellulose (NaCMC) films containing theophylline, and they concluded that the films made with 10% of CA were brittle and CA should be over 30% to obtain a good plasticizing effect. On the other hand, *Shi et al.* stated that CA used in a concentration of 5 wt% increases the tensile strength of polyvinyl alcohol/starch films, and above this concentration (5–30 wt%) the excess of CA acts as a plasticizer and hence reduces tensile strength [161].

In the present study CA exerts a plasticizing effect above 3 w/v% but results in a significant decrease of hardness only above 7 w/v%, which equals 150% and 350% CA content compared to the polymer, respectively, which is higher compared to the above. Nevertheless, the different behavior may be attributed to the weak alkaline nature of chitosan, forming stronger interactions and requiring much more CA than needed by HPMC, NaCMC and polyvinyl alcohol/starch. Independently of the original hardness, the addition of plasticizers significantly ($p < 0.0001$) decreased the hardness of all investigated films (Table 7), in the order of PEG-400<<PG<G. Nevertheless, despite the significant decrease in hardness, a notable viscoelastic deformation was observed, which resulted in an increase of the required time of elongation. A comparable finding for chitosan/G was obtained by *Zaini et al.* [162].

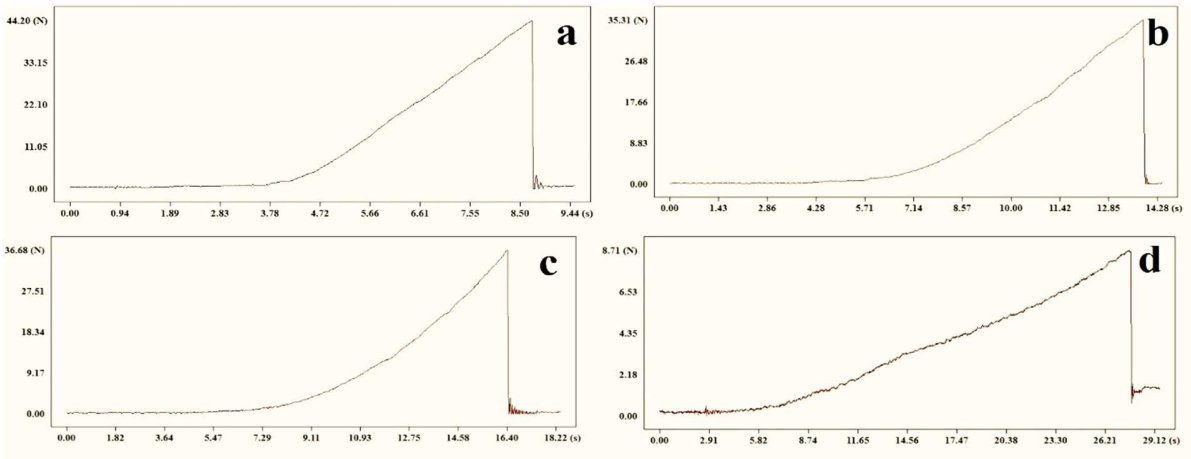

Figure 8. Breaking curves of CA 2.5% (a), CA 4% (b), CA 5% (c) and CA 7% (d) based chitosan films

As regards the hardness of films made with PEG-400, it was significantly ($p<0.0001$) better compared to the other plasticizers. However, it is notable that the addition of PEG-400 affected hardness inversely compared to PG or G, and a further decrease in hardness was observed when the added quantity of PEG-400 was increased. In contrast, the increasing amount of PG and G resulted in a slight but not significant increase in hardness.

Regarding mucoadhesion, the plasticizer-free AA-based chitosan films exhibited a high force of detachment (42.30 N) (Table 7), whereas plasticizer-free CA 2.5 w/v%-based films showed even higher values (47.57 N), possibly due to the lower degree of ionization, which enables the formation of strong ionic interactions between the unionized amino groups of chitosan and the sialic acid parts of mucin molecules [163, 164]. In contrast, the increment of CA content or the addition of a plasticizer significantly ($p<0.0001$) reduced mucoadhesive force (Fig. 9). This could be attributed to the interactions between chitosan and the plasticizers, which decrease the number of free functional groups, or to the covering of the pores on the film surface and retarding the wetting process. Compared to the other films, CA 3.5, 4 and 5 w/v%-based films are the most applicable depending on their tensile strength and mucoadhesion in these concentration ranges, as CA showed an ideal plasticizing effect as well as a good cross-linking effect on the chitosan molecule.

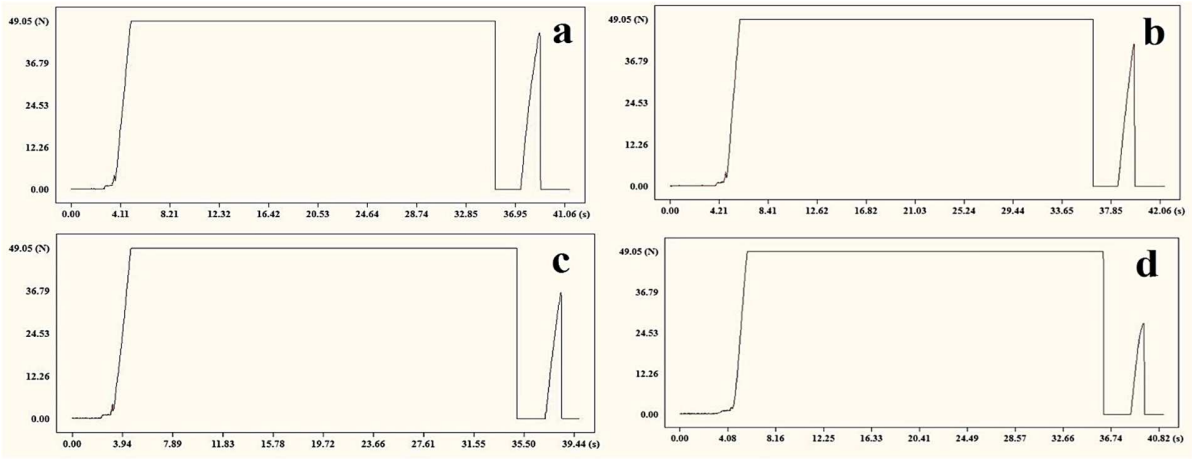

Figure 9. Mucoadhesion curves of CA 2.5% (a), CA 4% (b), CA 5% (c) and CA 7%-based chitosan films

The obtained SFEs of the prepared films are shown below in Table 8. The plasticizer-free AA-based film exhibited moderate SFE (~27 mN/m), while CA-based films showed significantly higher SFE around 40 mN/m without any considerable difference regarding the CA

content. The polarity of CA-based films was also higher than that of the AA-based ones. However, the increasing CA content significantly decreased polarity, which may be related to the pH of the solution. The addition of PEG-400 increased SFE as well as polarity, in both 5 and 10 w/v% concentrations, which may be due to the presence of polar oxygen in the PEG backbone, which will be present on the film surface after the cross-linking of the chitosan chains, or in a manner enabling the polymer to dissolve in a relatively high amount of CA, resulting in ester formation and at the same time saving some polar functional groups (OH groups) on the surfaces when the films get dry.

Table 8. SFE (γ^{total}), its dispersive (γ^{d}) and polar (γ^{p}) components and polarity of the prepared films

AA (w/v%)	CA (w/v%)	Plasticizer	Plasticizer content (w/v%)	γ^{total} (mN/m)	γ^{d} (mN/m)	γ^{p} (mN/m)	Polarity (%)
2	-	-	0	26.58 ± 2.25	14.82 ± 0.65	11.80 ± 2.15	44.40
2	-	G	5	15.55 ± 1.94	9.22 ± 0.78	6.33 ± 1.80	40.71
2	-		10	13.21 ± 1.85	8.21 ± 0.78	5.00 ± 1.70	37.85
2	-	PG	5	14.95 ± 2.12	8.12 ± 0.94	7.33 ± 1.90	49.03
2	-		10	15.75 ± 1.84	12.39 ± 0.86	3.40 ± 1.38	21.61
2	-	PEG 400	5	44.71 ± 2.74	22.38 ± 0.90	22.20 ± 2.60	49.65
2	-		10	47.30 ± 3.00	25.66 ± 1.50	22.10 ± 2.56	46.72
-	2.5	-	0	41.50 ± 1.90	18.33 ± 0.90	23.13 ± 1.70	55.73
-	3	-	0	44.31 ± 1.65	24.44 ± 0.70	19.87 ± 1.50	44.84
-	3.5	-	0	37.97 ± 1.80	17.12 ± 0.68	20.90 ± 1.63	55.04
-	4	-	0	43.34 ± 1.72	17.12 ± 0.74	20.76 ± 1.55	48.00
-	5	-	0	42.54 ± 1.71	23.98 ± 0.86	18.31 ± 1.50	43.04
-	7	-	0	39.40 ± 2.65	22.80 ± 2.01	16.59 ± 1.64	41.40
-	2.5	G	5	29.60 ± 2.02	16.54 ± 1.33	13.05 ± 1.50	44.10
-	2.5		10	27.23 ± 2.72	16.69 ± 2.01	10.54 ± 1.70	38.71
-	2.5	PG	5	47.66 ± 1.84	29.38 ± 1.12	18.30 ± 1.50	38.40
-	2.5		10	36.85 ± 1.80	19.15 ± 0.90	17.82 ± 1.54	48.40
-	2.5	PEG 400	5	57.40 ± 1.73	35.73 ± 1.00	21.70 ± 1.42	37.80
-	2.5		10	54.14 ± 1.60	35.16 ± 0.82	19.00 ± 1.33	35.10
-	7	G	5	40.10 ± 1.85	27.58 ± 1.27	12.50 ± 1.64	31.20
-	7		10	38.57 ± 1.52	24.98 ± 0.72	13.60 ± 1.33	35.30
-	7	PG	5	37.30 ± 2.04	26.78 ± 1.58	10.25 ± 1.31	27.50
-	7		10	36.63 ± 1.72	26.84 ± 1.15	9.80 ± 1.25	26.80
-	7	PEG 400	5	65.77 ± 2.11	34.37 ± 1.55	31.40 ± 1.43	47.74
-	7		10	68.11 ± 1.81	36.77 ± 1.23	31.35 ± 1.32	46.03

On the other hand, films made with the addition of G and PG demonstrated a strong decrease in both SFE and polarity. This may be attributed to the inclusion of the polar groups of these

plasticizers with the carboxyl group of the acid, or involvement in hydrogen bonding with chitosan and hydrocarbon backbone on the surface decreases polarity, surface porosity and therefore reduces wettability. All of these events also participate in the reduction of the mucoadhesivity of these films. As wetting is the first step of the mucoadhesion process, *Casariego et al.* reported that the addition of a hydrophilic plasticizer such as glycerol and sorbitol reduces the wettability and adhesion coefficient of chitosan films [165].

5.2.3. Investigation of the Chemical Structure and Interactions

The FT-IR spectrum of chitosan is shown in Figure 10, which reveals the fundamental absorption bands. The stretching vibrations of the OH and NH groups of chitosan are shown by a broad band between 3800–3400 cm^{-1} and 3300– 3000 cm^{-1}, respectively. The peak around 2870 cm^{-1} belongs to the symmetric stretching of the $–CH_3$ group in the acetyl side chain, while that of 2715 cm^{-1} to the symmetric $-CH_2$ stretching in the ring. The strong absorption band at 1660 cm^{-1} belongs to the C=O stretching of the acetylated carbonamide group. The absorption bands around 1592 cm^{-1}, at 1423 cm^{-1} and 1377 cm^{-1} belong to the presence of N–H, C–H and O–H bending vibrations, respectively. The peak at 1170 cm^{-1} is attributed to the asymmetric stretching of the (C–O–C) bridge. Chitosan was dissolved in AA 2 v/v% due to the ionization of the non-acetylated amide groups, as shown by the right shift of the N–H stretching and the left shift of the N–H bending absorption bands. The appearance of a new band at 1750 cm^{-1} indicates the esterification and hydrogen bonding of some hydroxyl groups, similarly to the right shift of the broad O–H stretching peak at 3600–3000 cm^{-1} and the left shift of the OH bending. The addition of plasticizers resulted in no considerable change in the texture, but some signs of weak hydrogen bonds were noticed in the order of G>PEG-400>PG, which may be due to the number of free hydroxyl groups on the plasticizers.

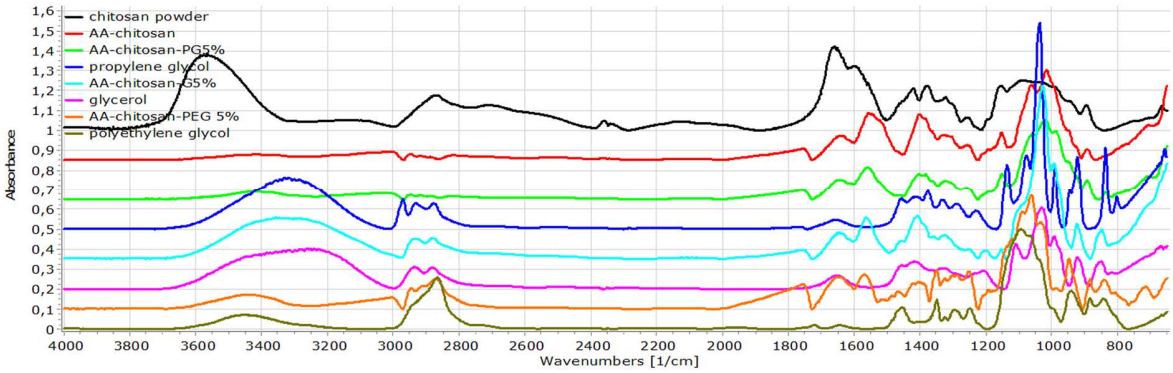

Figure 10. FT-IR spectra of raw materials and AA-based films

The FT-IR spectra of CA-based chitosan films made with varying amounts of CA (Fig. 11) indicate the presence of strong H-bonds between the –OH groups of the polymer and the carboxyl groups of the acid with a right shift of the –OH stretching peak between 3600–3300 cm^{-1}. The more intensive right shift of the N–H stretching signal between 3300–3000 cm^{-1}, the stronger left shift of the NH bending at 1590 cm^{-1} and the increasing intensity of the new broad peak at 2000 cm^{-1} indicate the stronger ionization of the amino groups with increasing CA content.

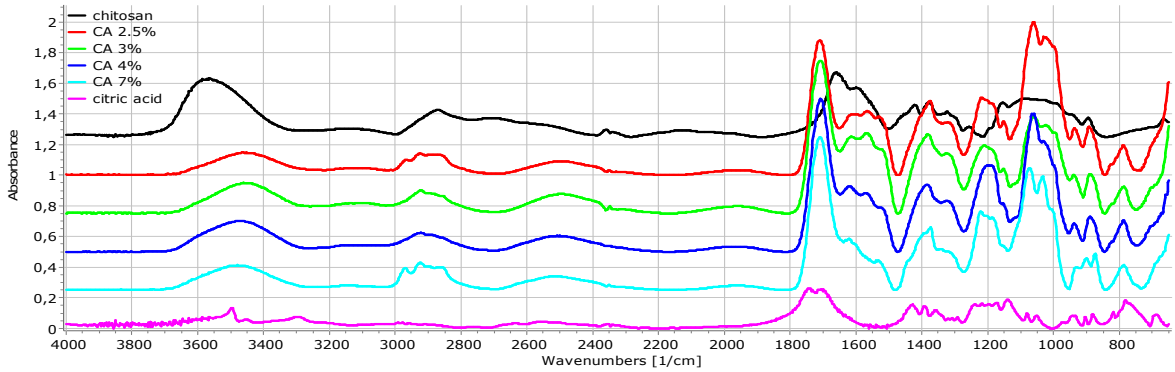

Figure 11. FT-IR spectra for 2.5, 3, 4, and 7 w/v% CA-based chitosan films

In all the shown film spectra, the presence of the peak around 1400 cm^{-1} was due to carboxylate anion absorption ($–COO^-$), indicating citrate salt formation. According to *Llanos et al.*, the peak around 1588 cm^{-1} is due to the protonation of amine group NH^{+3} and its intensity can be used to estimate the degree of protonation [166], while according to *Lusiana et al.*, the appearance of a peak around 1580–1590 cm^{-1} indicates the modification of the amine groups in chitosan from primary amine to secondary amine upon the addition of acid [167]. However, according to our knowledge, the secondary amine did not show N–H absorption in this range. On the other hand, *He et al.* reported a characteristic peak around 1588 cm^{-1} due to the N–H

bending vibration of primary amine -NH_2 [168], which opinion corresponds with our point of view.

When chitosan was dissolved in CA (Figs. 12 and 13), the addition of plasticizers also resulted in the formation of weak H bonds, but in this case in the order of PG>G>PEG-400, which also confirms the differences in the texture formation and interactions of AA- and CA-based films. However, no considerable difference was observed between CA 2.5% and CA 7% films in this manner, which indicates that polymer-plasticizer interactions may be related mostly to the bonding of -OH groups, and therefore the increasing ionization grade of chitosan does not considerably affect the strength of these interactions.

Generally, it can be concluded that the addition of polyhydroxy alcohols such as G, PG and PEG-400 will result in the formation of weak H bonds with the hydroxyl groups of chitosan, and the white opalescent color of chitosan/PEG-400-based films was only due to physical interactions and may not be connected with more intensive chemical change [169].

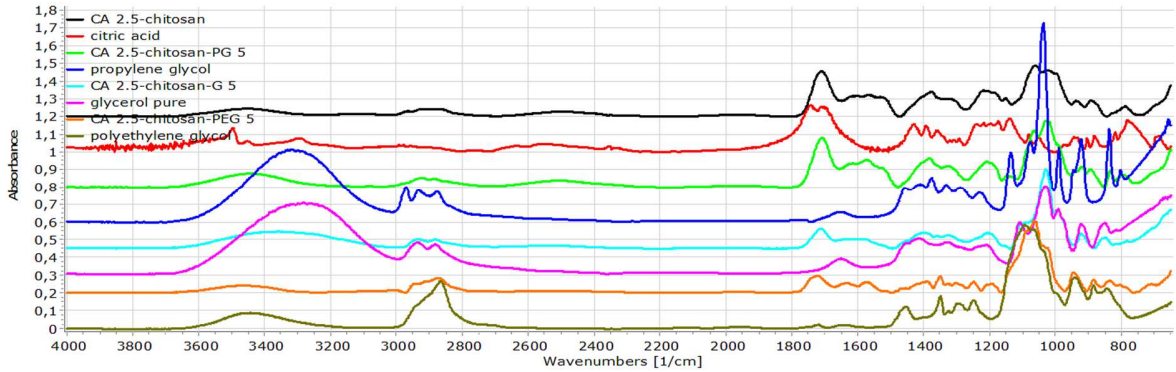

Figure 12. FT-IR spectra of raw materials and CA 2.5%w/v-based chitosan films

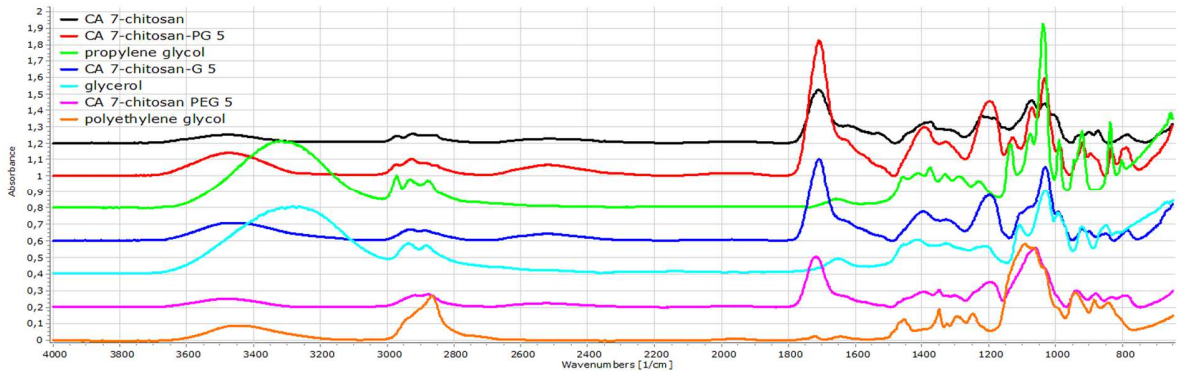

Figure 13. FT-IR spectra of raw materials and CA 7%w/v-based chitosan films

5.2.4. Thermal Stability

The TG-DSC curves of CA (2.5%)-based chitosan films made with/without 5% G, PG and PEG-400 are shown in Figure 14. The CA-based films showed minimal moisture content compared to the others made with plasticizers which possess a hygroscopic nature. The melting point of CA shifted to a higher temperature (from 168 to 182.8°C), as illustrated by the endothermic peak (-90.1 Jg^{-1}) because of cross-linking with the polymer. Obviously, films made with PG had the lowest thermal stability overall compared to those made with G and PEG-400. The latter showed the thermally most stable composite, which is attributed to the stability of PEG-400. Clearly, this composite showed the least weight loss upon heating and the highest decomposition temperature of 426.2°C with an enthalpy of 95 Jg^{-1}. Generally, PEG-based films are the best composites as regards long-term stability.

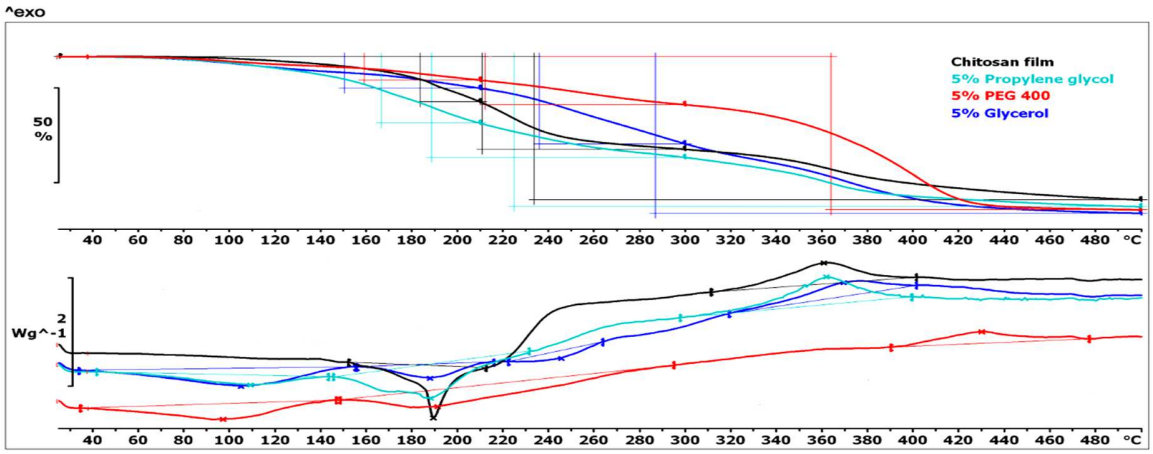

Figure 14. TG/DSC curves of 2.5 w/v% CA-based chitosan films made with/without 5w/v% of plasticizers

Overall, it can be stated that CA is an ideal dissolution aid and plasticizer for chitosan-based films. CA-based films, without additional plasticizer, may be chosen to formulate oral mucoadhesive films for macromolecule delivery due to their high mucoadhesivity, while the values of hardness and SFE are relatively adequate to ensure good mechanical properties and good wetting, which enables the films to tightly adhere to the mucosal surface.

However, if the film is utilized as the subcoating of an intestinosolvent coat, the PEG plasticized film seems to be best solution due to its greater hardness and higher surface free energy, which will enable better spreading and adhesion of the intestinosolvent coat on the substrate surface, with the additional advantage of increased thermal stability.

6. SUMMARY

The present study covered the investigation of the effects of material characteristics on the design space of the production of lysozyme-containing pellets and the development of chitosan-based films suitable for their subsequent coating process.

The results revealed that material attributes had considerable effects on the process design space. Accordingly, the investigation of the critical material attributes during the early stage of the development is essential both for APIs and excipients since they have a potential impact on the process temperature, and therefore on the biological activity of biopharmaceuticals. Nevertheless, despite their different deformability, both CM and SDM elicited a considerable conformation stabilizing property against high shear-stress and allowed only reversible modification in the lysozyme structure, which was confirmed by the fact that the protein regained its active conformation and activity after a few days.

The specially designed granulation chamber represented a novel tool of process analytical technology (PAT) and quality by design (QbD). It allowed the precise monitoring of the changes in temperature and RH% during high shear kneading, helping to optimize process parameters for the requirements of macromolecular or other thermolabile drugs.

The results also confirmed the importance of the chamber wall material, since the granulation chamber made from Teflon demonstrated a lower temperature upon elevated mechanical attritions than a glass-constructed chamber because of their different thermal conductivity. Therefore, this parameter should also be taken into account, since it may influence the temperature distribution inside the chamber.

In the second phase of the study, CA-based chitosan solutions/films were intensively characterized, and their applicability as a multifunctional subcoating polymer as well as their suitability as oral films with respect to AA-based films as a reference were successfully done. It was proven that CA-based chitosan films may be successfully prepared with the direct dissolution of the polymer in CA solution, and the obtained films exhibited properties comparable to AA-based ones. Nevertheless, CA-based films offer possibility to tailor

mucoadhesivity of chitosan and synergistically intensification of the penetration enhancing and protease inhibiting effects.

The MFFT and SFE of chitosan citrate films, which are essential for optimizing the coating process but had never been reported in the literature before, were also investigated. Both AA- and CA-based films showed MFFT less than 15°C, which ensures the required integrity of the coat even at low drying temperatures. The slightly higher SFE of CA-based formulations enables better tunability to achieve the required properties of the subcoating layer. The increasing CA content decreases hardness but increases elasticity, which was directly proportional to the CA quantity. CA 3.5-5% w/v-based chitosan solutions (without additional plasticizer) represent novel solutions for the coating process or for developing novel oral mucoadhesive films for macromolecule delivery as at these concentrations they showed an excellent cross-linking, plasticizing effect, MFFT, film thickness, higher force of both deformation and mucoadhesion and suitable moisture content, thus simplifying the formulation, and they seem to be satisfactory to make an acidic microenvironment sufficient to inhibit the peptidases.

The addition of high amounts of various additional plasticizers, e.g. G, PG and PEG, dramatically reduces hardness, wettability and mucoadhesivity for both CA- and AA-based films while enhancing elasticity; therefore, these films can be utilized as coats for site-specific drug delivery or even for food preservation. Furthermore, high-dose plasticizers were effective in modifying the SFE of the films, which may be essential to optimize film properties if they are used for the coating/subcoating of various substrates. Moreover, the size of SFE does not seem to be related to wettability in the presence of G, PG and PEG for either AA- or CA-based films, as the variation in SFE just minimally affects mucoadhesivity, which mainly depends on the wetting process. Overall, CA-based chitosan films plasticized by PEG-400 represent the best choice for the subcoating process because of their higher tensile strength, SFE and thermal stability.

PRACTICAL USEFULNESS

The experimental work of this study has allowed the following conclusions:

Factorial design is highly essential for the design and the investigation of critical processing factors and for the good understanding of the effect of material characteristics and their impacts on the critical product quality (CPQ).

The extrusion/spheronization method of pelletization is a very good technique for the development of lysozyme-loaded pellets because of a wide range of flexibly adjustable process parameters.

Various forms of mannitol (CM and SDM) are suitable enzyme stabilizers despite the different deformability patterns.

The specially designed granulation chamber is a novel tool for precisely monitoring the temperature and RH at different locations within the chamber and for correlating the effect of applied mechanical attritions and generated temperature with the product properties.

The high shear granulator is an ideal granulation method to preserve the homogeneity of the mixtures, thus reducing batch-to-batch variation.

CA-based chitosan solutions/films cross-linked with different plasticizers produce solutions/films with properties such as mucoadhesivity and SFE. This enables the utilization of these solutions/films for various pharmaceutical applications in the development of oral mucoadhesive films, or the development of multifunctional subcoating/coating for the delivery of poorly absorbable drugs.

Financial Support

This study was financially supported by Omdurman Islamic University (OIU) in cooperation with the Higher Ministry of Education and Scientific Research, Sudan.

REFERENCES

[1] C. Zhang, J. Tang, D. Liu, X. Li, L. Cheng, X. Tang, , Int. J. Pharm. 503 (2016) 41–55. https://doi.org/10.1016/j.ijpharm.2016.02.045.

[2] E. Kaffash, A. Badiee, A. Akhgari, N. Akhavan Rezayat, M. Abbaspour, F. Saremnejad, J. Drug Deliv. Sci. Technol. 53 (2019) 101177. https://doi.org/10.1016/j.jddst.2019.101177.

[3] D.M. Gaber, N. Nafee, O.Y. Abdallah, Int. J. Pharm. 488 (2015) 86–94. https://doi.org/10.1016/j.ijpharm.2015.04.021.

[4] K. Nikowitz, P. Kása, K. Pintye-Hódi, G. Regdon jr., Powder Technol. 205 (2011) 155–159. https://doi.org/10.1016/j.powtec.2010.09.006.

[5] C. Schmidt, R. Bodmeier, Int. J. Pharm. 216 (2001) 9–16.

[6] T.P. Pagariya, S.B. Patil, Colloids Surf. B Biointerfaces. 102 (2013) 171–177. https://doi.org/10.1016/j.colsurfb.2012.08.035.

[7] A. Dashevsky, A. Mohamad, Int. J. Pharm. 318 (2006) 124–131. https://doi.org/10.1016/j.ijpharm.2006.03.022.

[8] M.C. García, M. Martinelli, N.E. Ponce, L.M. Sanmarco, M.P. Aoki, R.H. Manzo, A.F. Jimenez-Kairuz, Eur. J. Pharm. Sci. 120 (2018) 107–122. https://doi.org/10.1016/j.ejps.2018.04.034.

[9] S. Pál, S. Nagy, T. Bozó, B. Kocsis, A. Dévay, Eur. J. Pharm. Sci. 49 (2013) 258–264. https://doi.org/10.1016/j.ejps.2013.03.006.

[10] S. Muley, T. Nandgude, S. Poddar, Asian J. Pharm. Sci. 11 (2016) 684–699. https://doi.org/10.1016/j.ajps.2016.08.001.

[11] S. Bhaskaran, P.K. Lakshmi, Int J Pharm Tech Res. 2 (2010) 2429–2433.

[12] N.R. Trivedi, M.G. Rajan, J.R. Johnson, A.J. Shukla, Crit. Rev. Ther. Drug Carr. Syst. 24 (2007).

[13] S. Komati, S. Swain, M.E.B. Rao, B.R. Jena, V. Dasi, Adv. Pharm. Bull. 9 (2019) 521–538. https://doi.org/10.15171/apb.2019.062.

[14] N. Dey, S. Majumdar, M. Rao, Trop. J. Pharm. Res. 7 (2008) 1067–1075. https://doi.org/10.4314/tjpr.v7i3.14692.

[15] T. Sovány, K. Csordás, A. Kelemen, G. Regdon jr., K. Pintye-Hódi, Chem. Eng. Res. Des. 106 (2016) 92–100. https://doi.org/10.1016/j.cherd.2015.11.022.

[16] Y. Han, Z. Gao, L. Chen, L. Kang, W. Huang, M. Jin, Q. Wang, Y.H. Bae, Acta Pharm. Sin. B. 9 (2019) 902–922. https://doi.org/10.1016/j.apsb.2019.01.004.

[17] Y.H.-E.Y. Ibrahim, G. Regdon jr., E.I. Hamedelniel, T. Sovány, DARU J. Pharm. Sci. 28 (2020) 403–416. https://doi.org/10.1007/s40199-019-00316-w.

[18] S.K. Dubey, S. Parab, N. Dabholkar, M. Agrawal, G. Singhvi, A. Alexander, R.A. Bapat, P. Kesharwani, Drug Discov. Today. (2021) S1359644621000015. https://doi.org/10.1016/j.drudis.2021.01.001.

[19] U. Bhutani, T. Basu, S. Majumdar, Eur. J. Pharm. Biopharm. 162 (2021) 23–42. https://doi.org/10.1016/j.ejpb.2021.02.008.

[20] T.-H. Kim, A. Tunsirikongkon, J.-K. Lee, W.S. Jang, S.-E. Lee, J.-S. Park, Drug Metab. Pharmacokinet. 32 (2017) S47. https://doi.org/10.1016/j.dmpk.2016.10.198.
[21] E.Y. Chi, S. Krishnan, T.W. Randolph, J.F. Carpenter, Pharm. Res. 20 (2003) 1325–1336.
[22] L. Palugan, M. Cerea, L. Zema, A. Gazzaniga, A. Maroni, J. Drug Deliv. Sci. Technol. 25 (2015) 1–15. https://doi.org/10.1016/j.jddst.2014.12.003.
[23] M. Hirjau, A.C. Nicoara, V. Hirjau, D. Lupuleasa, Farma. 4 (2011) 4.
[24] É. Bölcskei, G. Regdon jr., T. Sovány, P. Kleinebudde, K. Pintye-Hódi, Chem. Eng. Res. Des. 90 (2012) 651–657. https://doi.org/10.1016/j.cherd.2011.09.005.
[25] J. Mandić, M. Luštrik, F. Vrečer, M. Gašperlin, A. Zvonar Pobirk, Int. J. Pharm. 566 (2019) 89–100. https://doi.org/10.1016/j.ijpharm.2019.05.055.
[26] C.R.S. Siow, P.W.S. Heng, L.W. Chan, AAPS PharmSciTech. 19 (2018) 845–857.
[27] V. YADAV, S. SATHESHKUMAR, Indian Journal of Novel Drug Delivery, Indian J. Nov. Drug Deliv. 11 (2019) 1–12.
[28] N. Jadhav, P. Irny, A. Mokashi, P. Souche, A. Paradkar, Drug Deliv. Lett. 2 (2012) 132–145. https://doi.org/10.2174/2210304x11202020132.
[29] R. Gandhi, C. Lal Kaul, R. Panchagnula, Pharm. Sci. Technol. Today. 2 (1999) 160–170. https://doi.org/10.1016/S1461-5347(99)00136-4.
[30] D.F. Erkoboni, D. Parikh, Drugs Pharm. Sci. 81 (1997) 333–368.
[31] D.H. Alshora, M.A. Ibrahim, E. Ezzeldin, M. Iqbal, J. Drug Deliv. Sci. Technol. 59 (2020) 101902. https://doi.org/10.1016/j.jddst.2020.101902.
[32] C.L.S. Lau, Q. Yu, V.Y. Lister, S.L. Rough, D.I. Wilson, M. Zhang, Chem. Eng. Res. Des. 92 (2014) 2413–2424.
[33] Y. Huang, Z. Huang, M. Wu, Y. Liu, C. Ma, X. Zhang, Z. Zhao, X. Bai, H. Liu, L. Wang, X. Pan, C. Wu, Drug Dev. Res. 80 (2019) 958–969. https://doi.org/10.1002/ddr.21575.
[34] M. Elsakhawy, M. Hassan, Carbohydr. Polym. 67 (2007) 1–10. https://doi.org/10.1016/j.carbpol.2006.04.009.
[35] G. Thoorens, F. Krier, B. Leclercq, B. Carlin, B. Evrard, Int. J. Pharm. 473 (2014) 64–72. https://doi.org/10.1016/j.ijpharm.2014.06.055.
[36] G. Tomer, H. Patel, F. Podczeck, J.M. Newton, Eur. J. Pharm. Sci. 12 (2001) 321–325.
[37] G. Zoubari, R. Ali, A. Dashevskiy, J. Drug Deliv. Sci. Technol. 49 (2019) 1–5. https://doi.org/10.1016/j.jddst.2018.10.030.
[38] J.A.C. Elbers, H.W. Bakkenes, J.G. Fokkens, Drug Dev. Ind. Pharm. 18 (1992) 501–517. https://doi.org/10.3109/03639049209043708.
[39] Q.-B. Ding, P. Ainsworth, G. Tucker, H. Marson, J. Food Eng. 66 (2005) 283–289. https://doi.org/10.1016/j.jfoodeng.2004.03.019.
[40] A. Goyanes, C. Souto, R. Martínez-Pacheco, Pharm. Dev. Technol. 15 (2010) 626–635. https://doi.org/10.3109/10837450903419653.
[41] M.A. Ibrahim, G.M. Zayed, F.M. Alsharif, W.A. Abdelhafez, Saudi Pharm. J. 27 (2019) 182–190. https://doi.org/10.1016/j.jsps.2018.10.002.
[42] A. Jaipal, M.M. Pandey, S.Y. Charde, P.P. Raut, K.V. Prasanth, R.G. Prasad, Saudi Pharm. J. 23 (2015) 315–326. https://doi.org/10.1016/j.jsps.2014.11.012.

[43] S. Zhang, H. Yan, P. Yu, Y. Xia, W. Zhang, J. Liu, Eur. J. Pharm. Sci. 93 (2016) 341–350. https://doi.org/10.1016/j.ejps.2016.08.040.
[44] S. Singh, J. Singh, AAPS PharmSciTech. 4 (2003) 101–109.
[45] S.A. Abbas, V.K. Sharma, T.W. Patapoff, D.S. Kalonia, Opposite Pharm. Res. 29 (2012) 683–694. https://doi.org/10.1007/s11095-011-0593-4.
[46] D. Caccavo, G. Lamberti, M.M. Cafaro, A.A. Barba, J. Kazlauske, A. Larsson, Br. J. Pharmacol. 174 (2017) 1797–1809. https://doi.org/10.1111/bph.13776.
[47] S. Amidon, J.E. Brown, V.S. Dave, AAPS PharmSciTech. 16 (2015) 731–741. https://doi.org/10.1208/s12249-015-0350-9.
[48] E.V. López, A. Luzardo Álvarez, J. Blanco Méndez, F.J. Otero Espinar, J. Drug Deliv. Sci. Technol. 42 (2017) 273–283. https://doi.org/10.1016/j.jddst.2017.03.031.
[49] N. Al-Hashimi, N. Begg, R. Alany, H. Hassanin, A. Elshaer, Pharmaceutics. 10 (2018) 176. https://doi.org/10.3390/pharmaceutics10040176.
[50] S. Pandey, S.M.V. Swamy, A. Gupta, A. Koli, S. Patel, F. Maulvi, B. Vyas, J. Microencapsul. 35 (2018) 259–271. https://doi.org/10.1080/02652048.2018.1465138.
[51] N. Desai, M. Momin, Drug Deliv. Transl. Res. (2020). https://doi.org/10.1007/s13346-020-00756-x.
[52] V. Kaur, A.K. Goyal, G. Ghosh, S. Chandra Si, G. Rath, Heliyon. 6 (2020) e03125. https://doi.org/10.1016/j.heliyon.2019.e03125.
[53] L.A. Soares, E. Crema, Acta Sci. Health Sci. 42 (2020) e48422. https://doi.org/10.4025/actascihealthsci.v42i1.48422.
[54] A. Kumari, A. Jain, P. Hurkat, A. Tiwari, S.K. Jain, Drug Dev. Ind. Pharm. 44 (2018) 902–913. https://doi.org/10.1080/03639045.2017.1420079.
[55] C. Cui, J. Sun, X. Wang, Z. Yu, Y. Shi, Factors Contributing to Drug Release Dose-Response. 18 (2020) 155932582090898. https://doi.org/10.1177/1559325820908980.
[56] T. Rongthong, S. Sungthongjeen, F. Siepmann, J. Siepmann, T. Pongjanyakul, Eur. J. Pharm. Biopharm. 148 (2020) 126–133. https://doi.org/10.1016/j.ejpb.2020.01.011.
[57] R.K. Keservani, A.K. Sharma, U. Jarouliya, Ars Pharm. 56(3) (2015) 165-177
[58] L.N. Hassani, A. Lewis, J. Richard, OnDrugDelivery. 59 (2015) 12–17.
[59] T. Sovány, Z. Tislér, K. Kristó, A. Kelemen, G. Regdon jr., Eur. J. Pharm. Biopharm. 106 (2016) 79–87. https://doi.org/10.1016/j.ejpb.2016.05.009.
[60] P. Batista, P.M. Castro, A.R. Madureira, B. Sarmento, M. Pintado, Peptides. 101 (2018) 112–123.
[61] M. Philippart, J. Schmidt, B. Bittner, Drug Res. 66 (2015) 113–120. https://doi.org/10.1055/s-0035-1559654.
[62] S. Mitragotri, P.A. Burke, R. Langer, Nat. Rev. Drug Discov. 13 (2014) 655–672.
[63] S. Sadeghi, W.K. Lee, S.N. Kong, A. Shetty, C.L. Drum, Pharmacol. Res. 158 (2020) 104685. https://doi.org/10.1016/j.phrs.2020.104685.
[64] D.J. Brayden, T.A. Hill, D.P. Fairlie, S. Maher, R.J. Mrsny, Adv. Drug Deliv. Rev. (2020) S0169409X20300405. https://doi.org/10.1016/j.addr.2020.05.007.

[65] Y. Zhang, H. Zhang, D. Ghosh, R.O. Williams, Int. J. Pharm. 587 (2020) 119491. https://doi.org/10.1016/j.ijpharm.2020.119491.
[66] K. Kristó, O. Kovács, A. Kelemen, F. Lajkó, G. Klivényi, B. Jancsik, K. Pintye-Hódi, G. Regdon jr., Eur. J. Pharm. Sci. 95 (2016) 62–71. https://doi.org/10.1016/j.ejps.2016.08.051.
[67] L. Satish, S. Millan, H. Sahoo, J. Mol. Liq. 278 (2019) 329–334. https://doi.org/10.1016/j.molliq.2019.01.052.
[68] T.D. Brown, K.A. Whitehead, S. Mitragotri, Nat. Rev. Mater. 5 (2020) 127–148. https://doi.org/10.1038/s41578-019-0156-6.
[69] A. Misra, Elsevier, 2010.
[70] L.N. Thwala, V. Préat, N.S. Csaba, Expert Opin. Drug Deliv. 14 (2017) 23–36. https://doi.org/10.1080/17425247.2016.1206074.
[71] M. Werle, A. Makhlof, H. Takeuchi, Recent Pat. Drug Deliv. Formul. 3 (2009) 94–104. https://doi.org/10.2174/187221109788452221.
[72] H.J. Lee, Arch. Pharm. Res. 25 (2002) 572.
[73] T. Hetal, P. Bindesh, T. Sneha, AHealth (N. Y.). 4 (2010) 033.
[74] V.K. Pawar, J.G. Meher, Y. Singh, M. Chaurasia, B.S. Reddy, M.K. Chourasia, J. Controlled Release. 196 (2014) 168–183.
[75] N.N. Salama, N.D. Eddington, A. Fasano, Tight junction modulation and its relationship to drug delivery, in: Tight Junctions, Springer, 2006: pp. 206–219.
[76] S.H. Bakhru, S. Furtado, A.P. Morello, E. Mathiowitz, Adv. Drug Deliv. Rev. 65 (2013) 811–821.
[77] R.L. DiMarco, D.R. Hunt, R.E. Dewi, S.C. Heilshorn, Biomaterials. 129 (2017) 152–162.
[78] K.R. Groschwitz, S.P. Hogan, J. Allergy Clin. Immunol. 124 (2009) 3–20.
[79] S. MS I, N.D. Derle, R. Bhamber, J. Appl. Pharm. Sci. 2 (2012) 34–39.
[80] A. Lechanteur, J. das Neves, B. Sarmento, Adv. Drug Deliv. Rev. 124 (2018) 50–63.
[81] M. Boegh, H.M. Nielsen, Basic Clin. Pharmacol. Toxicol. 116 (2015) 179–186.
[82] L. Wright, T.J. Barnes, C.A. Prestidge, Int. J. Pharm. 585 (2020) 119488. https://doi.org/10.1016/j.ijpharm.2020.119488.
[83] H. Cheng, X. Zhang, L. Qin, Y. Huo, Z. Cui, C. Liu, Y. Sun, J. Guan, S. Mao, J. Controlled Release. 321 (2020) 641–653. https://doi.org/10.1016/j.jconrel.2020.02.034.
[84] P.-Y. Lin, E.-Y. Chuang, Y.-H. Chiu, H.-L. Chen, K.-J. Lin, J.-H. Juang, C.-H. Chiang, F.-L. Mi, H.-W. Sung, J. Controlled Release. 259 (2017) 168–175. https://doi.org/10.1016/j.jconrel.2016.12.018.
[85] J. Ndayishimiye, A. Popat, M. Blaskovich, J.R. Falconer, J. Controlled Release. 324 (2020) 728–749. https://doi.org/10.1016/j.jconrel.2020.05.002.
[86] A. Yamamoto, H. Ukai, M. Morishita, H. Katsumi, Pharmacol. Ther. 211 (2020) 107537. https://doi.org/10.1016/j.pharmthera.2020.107537.
[87] K. Park, I.C. Kwon, K. Park, React. Funct. Polym. 71 (2011) 280–287. https://doi.org/10.1016/j.reactfunctpolym.2010.10.002.

[88] A. Alexander, M. Ajazuddin, M. Swarna, M. Sharma, D.K. Tripathi, Stamford J. Pharm. Sci. 4 (2011) 91–95.
[89] F. McCartney, J.P. Gleeson, D.J. Brayden, Tissue Barriers. 4 (2016) e1176822.
[90] S. Maher, J. Heade, F. McCartney, S. Waters, S.B. Bleiel, D.J. Brayden, Int. J. Pharm. 539 (2018) 11–22. https://doi.org/10.1016/j.ijpharm.2018.01.008.
[91] B.J. Aungst, Intestinal permeation enhancers, J. Pharm. Sci. 89 (2000) 429–442.
[92] K. Whitehead, N. Karr, S. Mitragotri, Pharm. Res. 25 (2008) 1782–1788.
[93] D.M. Rajaram, S.D. Laxman, Syst. Rev. Pharm. 8 (2016) 31–38. https://doi.org/10.5530/srp.2017.1.7.
[94] K.C. Ugoeze, Bioadhesive Polymers for Drug Delivery Applications, in: K.L. Mittal, I.S. Bakshi, J.K. Narang (Eds.), Bioadhesives Drug Deliv., 1st ed., Wiley, 2020: pp. 29–56. https://doi.org/10.1002/9781119640240.ch2.
[95] S. Roy, K. Pal, A. Anis, K. Pramanik, B. Prabhakar, Des. Monomers Polym. 12 (2009) 483–495.
[96] E. Russo, F. Selmin, S. Baldassari, C.G.M. Gennari, G. Caviglioli, F. Cilurzo, P. Minghetti, B. Parodi, J. Drug Deliv. Sci. Technol. 32 (2016) 113–125. https://doi.org/10.1016/j.jddst.2015.06.016.
[97] L. Vijapur, S. Sreenivas, S. Patil, P. Vijapur, P. Patwari, Int. Res. J. Pharm. 3 (2012) 51–57.
[98] G.C. Rajput, F.D. Majmudar, J.K. Patel, K.N. Patel, R.S. Thakor, B.P. Patel, N.B. Rajgor, Int J Pharm Biol Res. 1 (2010) 30–41.
[99] A. Sosnik, J. das Neves, B. Sarmento, Prog. Polym. Sci. 39 (2014) 2030–2075. https://doi.org/10.1016/j.progpolymsci.2014.07.010.
[100] A. Rohani Shirvan, A. Bashari, N. Hemmatinejad, Eur. Polym. J. 119 (2019) 541–550. https://doi.org/10.1016/j.eurpolymj.2019.07.010.
[101] B.M. Boddupalli, Z.N. Mohammed, R.A. Nath, D. Banji, J. Adv. Pharm. Technol. Res. 1 (2010) 381.
[102] F.C. Carvalho, M.L. Bruschi, R.C. Evangelista, M.P.D. Gremião, Braz. J. Pharm. Sci. 46 (2010) 1–17.
[103] B. Phanindra, B.K. Moorthy, M. Muthukumaran, Int. J. Pharm. Med. Biol. Sci. 2 (2013) 68-84.
[104] M. Zhang, S. Asghar, X. Jin, Z. Hu, Q. Ping, Z. Chen, F. Shao, Y. Xiao, TInt. J. Biol. Macromol. 138 (2019) 636–647. https://doi.org/10.1016/j.ijbiomac.2019.07.114.
[105] A. Jain, P. Hurkat, A. Jain, A. Jain, A. Jain, S.K. Jain, Thiolated polymers: pharmaceutical tool in nasal drug delivery of proteins and peptides, Int. J. Pept. Res. Ther. 25 (2019) 15–26.
[106] S. Kitiyodom, S. Kaewmalun, N. Nittayasut, K. Suktham, S. Surassmo, K. Namdee, C. Rodkhum, N. Pirarat, T. Yata, Shellfish Immunol. 86 (2019) 635–640. https://doi.org/10.1016/j.fsi.2018.12.005.
[107] E.-S. Khafagy, M. Morishita, Y. Onuki, K. Takayama, Adv. Drug Deliv. Rev. 59 (2007) 1521–1546.

[108] T.Q. Phan, P.H.L. Tran, T.T.D. Tran, DARU J. Pharm. Sci. (2020). https://doi.org/10.1007/s40199-020-00360-x.
[109] S. Sarkar, K. Gulati, A. Mishra, K.M. Poluri, Int. J. Biol. Macromol. 151 (2020) 467–482. https://doi.org/10.1016/j.ijbiomac.2020.02.179.
[110] Z. Wang, Z. Meng, M. Xue, H. Zhang, K.J. Shea, L. Kang, Microchem. J. 157 (2020) 105073. https://doi.org/10.1016/j.microc.2020.105073.
[111] T. Wu, C. Wu, S. Fu, L. Wang, C. Yuan, S. Chen, Y. Hu, Carbohydr. Polym. 155 (2017) 192–200.
[112] V.L. Hughey, E.A. Johnson, Appl. Environ. Microbiol. 53 (1987) 2165–2170.
[113] M. Bilej, Mucosal immunity in invertebrates, in: Mucosal Immunol., Elsevier, 2015: pp. 135–144.
[114] Y.-F. Guan, S.-Y. Lai, C.-S. Lin, S.-Y. Suen, M.-Y. Wang, Food Chem. 286 (2019) 483–490. https://doi.org/10.1016/j.foodchem.2019.02.023.
[115] K. Düring, P. Porsch, A. Mahn, O. Brinkmann, W. Gieffers, FEBS Lett. 449 (1999) 93–100. https://doi.org/10.1016/S0014-5793(99)00405-6.
[116] T. Yada, K. Muto, T. Azuma, K. Ikuta, Comp. Biochem. Physiol. Part C Toxicol. Pharmacol. 139 (2004) 57–63. https://doi.org/10.1016/j.cca.2004.09.003.
[117] S. Nakamura, A. Kato, K. Kobayashi, J. Agric. Food Chem. 39 (1991) 647–650.
[118] G.G. Syngai, G. Ahmed, Lysozyme: A Natural Antimicrobial Enzyme of Interest in Food Applications, in: Enzym. Food Biotechnol., Elsevier, 2019: pp. 169–179.
[119] R. Epaud, C. Delestrain, T.E. Weaver, H.T. Akinbi, Respir. Med. Res. 76 (2019) 22–27. https://doi.org/10.1016/j.resmer.2019.07.005.
[120] U. Glamočlija, M. Mehić, A. Šukalo, A.T. Avdić, J.D. Jaganjac, Bosn. J. Basic Med. Sci. 20 (2020) 281.
[121] A. Tagashira, K. Nishi, T. Sugahara, Cytotechnology. 71 (2019) 497–506. https://doi.org/10.1007/s10616-019-00296-4.
[122] A. Tagashira, K. Nishi, S. Matsumoto, T. Sugahara, Cytotechnology. 70 (2018) 929–938. https://doi.org/10.1007/s10616-017-0184-2.
[123] A. Bergamo, M. Gerdol, A. Pallavicini, S. Greco, I. Schepens, R. Hamelin, F. Armand, P.J. Dyson, G. Sava, Int. J. Mol. Sci. 20 (2019) 5502. https://doi.org/10.3390/ijms20215502.
[124] S. Belluzo, V. Boeris, B. Farruggia, G. Picó, Int. J. Biol. Macromol. 49 (2011) 936–941. https://doi.org/10.1016/j.ijbiomac.2011.08.012.
[125] S.J. Prestrelski, N. Tedeschi, T. Arakawa, J.F. Carpenter, Biophys. J. 65 (1993) 661–671.
[126] S. Wang, X. Zhang, G. Wu, Z. Tian, F. Qian, Int. J. Pharm. 530 (2017) 173–186. https://doi.org/10.1016/j.ijpharm.2017.07.057.
[127] S. Liu, L. Li, Polymer. 141 (2018) 124–131. https://doi.org/10.1016/j.polymer.2018.03.012.
[128] P. Li, J. Zhao, Y. Chen, B. Cheng, Z. Yu, Y. Zhao, X. Yan, Z. Tong, S. Jin, Carbohydr. Polym. 157 (2017) 1383–1392. https://doi.org/10.1016/j.carbpol.2016.11.016.

[129] A. Shah, I. Hussain, G. Murtaza, Int. J. Biol. Macromol. 116 (2018) 520–529. https://doi.org/10.1016/j.ijbiomac.2018.05.057.
[130] J. Rotta, R.Á. Ozório, A.M. Kehrwald, G.M. de Oliveira Barra, R.D. de Melo Castanho Amboni, P.L.M. Barreto, Mater. Sci. Eng. C. 29 (2009) 619–623. https://doi.org/10.1016/j.msec.2008.10.032.
[131] J. Cao, J. You, L. Zhang, J. Zhou, Carbohydr. Polym. 185 (2018) 138–144. https://doi.org/10.1016/j.carbpol.2018.01.010.
[132] N. Rahmouni, W. Tahri, H.M. Sbihi, I.A. Nehdi, J. Desbrieres, S. Besbes-Hentati, Int. J. Biol. Macromol. 113 (2018) 623–630. https://doi.org/10.1016/j.ijbiomac.2018.02.121.
[133] M. Agarwal, M.K. Agarwal, N. Shrivastav, S. Pandey, P. Gaur, Int. J. Life-Sci. Sci. Res. 4 (2018) 1721–1728. https://doi.org/10.21276/ijlssr.2018.4.2.18.
[134] B. Phanindra, B.K. Moorthy, M. Muthukumaran, Int. J. Pharm. Med. Biol. Sci. 2 (2013) 68-84.
[135] J. Hombach, A. Bernkop-Schnürch, Int. J. Pharm. 376 (2009) 104–109. https://doi.org/10.1016/j.ijpharm.2009.04.027.
[136] M. Thanou, J.C. Verhoef, H.E. Junginger, Adv. Drug Deliv. Rev. 52 (2001) 117–126. https://doi.org/10.1016/S0169-409X(01)00231-9.
[137] B. Fan, Y. Xing, Y. Zheng, C. Sun, G. Liang, Drug Deliv. 23 (2016) 238–247.
[138] K. Sonaje, K.-J. Lin, M.T. Tseng, S.-P. Wey, F.-Y. Su, E.-Y. Chuang, C.-W. Hsu, C.-T. Chen, H.-W. Sung, Biomaterials. 32 (2011) 8712–8721.
[139] W.-Z. Jiang, Y. Cai, H.-Y. Li, Powder Technol. 312 (2017) 124–132. https://doi.org/10.1016/j.powtec.2017.02.021.
[140] M. Nur, T. Vasiljevic, Int. J. Biol. Macromol. 103 (2017) 889–901.
[141] T.A.S. Aguirre, D. Teijeiro-Osorio, M. Rosa, I.S. Coulter, M.J. Alonso, D.J. Brayden, Adv. Drug Deliv. Rev. 106 (2016) 223–241. https://doi.org/10.1016/j.addr.2016.02.004.
[142] M.C. Bonferoni, G. Sandri, S. Rossi, F. Ferrari, S. Gibin, C. Caramella, Eur. J. Pharm. Sci. 33 (2008) 166–176. https://doi.org/10.1016/j.ejps.2007.11.004.
[143] S.H. Welling, F. Hubálek, J. Jacobsen, D.J. Brayden, U.L. Rahbek, S.T. Buckley, Eur. J. Pharm. Biopharm. 86 (2014) 544–551. https://doi.org/10.1016/j.ejpb.2013.12.017.
[144] S. Devendra, K.S. Pankaj, V.S.S. Udai, World J Pharma Pharm Sci. 2 (2013) 17998.
[145] J.A.C. Elbers, H.W. Bakkenes, J.G. Fokkens, Drug Dev. Ind. Pharm. 18 (1992) 501–517. https://doi.org/10.3109/03639049209043708.
[146] Q.-B. Ding, P. Ainsworth, G. Tucker, H. Marson, J. Food Eng. 66 (2005) 283–289. https://doi.org/10.1016/j.jfoodeng.2004.03.019.
[147] M. Liu, Y. Zhou, Y. Zhang, C. Yu, S. Cao, Food Hydrocoll. 33 (2013) 186–191.
[148] G.P. Andrews, T.P. Laverty, D.S. Jones, Eur. J. Pharm. Biopharm. 71 (2009) 505–518. https://doi.org/10.1016/j.ejpb.2008.09.028.
[149] J.M. Schuster, C.E. Schvezov, M.R. Rosenberger, Procedia Mater. Sci. 8 (2015) 732–741. https://doi.org/10.1016/j.mspro.2015.04.130.
[150] T. Schæfer, C. Mathiesen, Int. J. Pharm. 139 (1996) 125–138. https://doi.org/10.1016/0378-5173(96)04549-8.

[151] W.L. Hulse, R.T. Forbes, M.C. Bonner, M. Getrost, Drug Dev. Ind. Pharm. 35 (2009) 712–718. https://doi.org/10.1080/03639040802516491.
[152] Z. Colley, O. O. Fasina, D. Bransby, Y. Y. Lee, Trans. ASABE. 49 (2006) 1845–1851. https://doi.org/10.13031/2013.22271.
[153] Y.-F. Maa, P.-A. Nguyen, J.D. Andya, N. Dasovich, T.D. Sweeney, S.J. Shire, C.C. Hsu, Pharm. Res. 15 (1998) 768–775.
[154] L. Gu, C.V. Liew, P.W.S. Heng, Drug Dev. Ind. Pharm. 30 (2004) 111–123. https://doi.org/10.1081/DDC-120028706.
[155] C. Vecchio, G. Bruni, A. Gazzaniga, Research Papers: Preparation of Indobufen Pellets by Using Centrifugal Rotary Fluidized Bed Equipment Without Starting Seeds, Drug Dev. Ind. Pharm. 20 (1994) 1943–1956. https://doi.org/10.3109/03639049409049329.
[156] K. Lövgren, P.J. Lundberg, Drug Dev. Ind. Pharm. 15 (1989) 2375–2392.
[157] S. Bhuvaneshwari, D. Sruthi, V. Sivasubramanian, K. Niranjana, J. Sugunabai, Ijera. 1 (2011) 292–299.
[158] A. Bujang, S.N. Adila, N.E. Suyatma, Physical properties of chitosan films as affected by concentration of lactic acid and glycerol, in: 2013 4th Int. Conf. Biol. Environ. Chem. IPCBEE, 2013: pp. p27-31.
[159] N. Nady, S.H. Kandil, Membranes. 8 (2018) 2.
[160] L.S.C. Wan, P.W.S. Heng, C.G.H. Chia, J. Microencapsul. 10 (1993) 11–23. https://doi.org/10.3109/02652049309015308.
[161] R. Shi, J. Bi, Z. Zhang, A. Zhu, D. Chen, X. Zhou, L. Zhang, W. Tian, Carbohydr. Polym. 74 (2008) 763–770. https://doi.org/10.1016/j.carbpol.2008.04.045.
[162] K. Ziani, J. Oses, V. Coma, J.I. Maté, LWT - Food Sci. Technol. 41 (2008) 2159–2165. https://doi.org/10.1016/j.lwt.2007.11.023.
[163] I. Bravo-Osuna, C. Vauthier, A. Farabollini, G.F. Palmieri, G. Ponchel, Biomaterials. 28 (2007) 2233–2243. https://doi.org/10.1016/j.biomaterials.2007.01.005.
[164] N.A. Peppas, Y. Huang, Adv. Drug Deliv. Rev. 56 (2004) 1675–1687. https://doi.org/10.1016/j.addr.2004.03.001.
[165] A. Casariego, B.W.S. Souza, A.A. Vicente, J.A. Teixeira, L. Cruz, R. Díaz, CFood Hydrocoll. 22 (2008) 1452–1459. https://doi.org/10.1016/j.foodhyd.2007.09.010.
[166] J.H.R. Llanos, L.C. de O. Vercik, A. Vercik, J. Biomater. Nanobiotechnology. 06 (2015) 276–291. https://doi.org/10.4236/jbnb.2015.64026.
[167] R.A. Lusiana, D. Siswanta, M. Mudasir, Indones. J. Chem. 16 (2018) 144. https://doi.org/10.22146/ijc.21157.
[168] Q. He, Q. Ao, Y. Gong, X. Zhang, J. Mater. Sci. Mater. Med. 22 (2011) 2791–2802. https://doi.org/10.1007/s10856-011-4444-y.
[169] K.N. Turhan, F. Sahbaz, A. Güner, J. Food Sci. 66 (2001) 59–62.

ACKNOWLEDGEMENTS

First of all, I would like to express my sincere gratitude and thanks to my supervisors, **Dr. Géza Regdon jr., Dr. Tamás Sovány** and **Dr. Katalin Kristó** for their guidance, encouragement, continuous support and excellent facilities during my Ph.D. study and preparation of this dissertation.

My warmest thanks to **Prof. Dr. Ildikó Csóka,** Head of the Institute of Pharmaceutical Technology and Regulatory Affairs, for her continuous support and valuable advice.

I express my kindest thanks to **Prof. Dr. Ferenc Fülöp,** previous Head of the Doctoral School of Pharmaceutical Sciences, for providing me with the opportunity of acceptance, and my thanks are extended to **Prof. Dr. Judit Hohmann,** current Head of the Doctoral School**,** for her help and support. Also, I would like to thank **Prof. Dr. István Zupkó**, Dean of the Faculty of Pharmacy, for his support.

Sincerest thanks to **Opulus Company Ltd**. Szeged for providing me with an innovative granulation chamber instrumented with the calibrated PyroDiff and PyroButton sensors, which were helpful during my study.

My sincere thanks and gratefulness to all my **co-authors** for their collaboration in this work. And my kindest thanks to all the Department members for their assistance. Finally, limitless thanks to my **parents** and **my friends** who encouraged and supported me during this study, and deepest gratitude to my **wife Aisha Ibrahim** for her moral support.

ANNEXES

Annex 1.

Ibrahim, Yousif H-E. Y.; Regdon jr., Géza; Hamedelniel, Elnazeer I; Sovány, Tamás. Review of recently used techniques and materials to improve the efficiency of orally administered proteins/peptides, DARU J. Pharm. Sci. 28 (2020) 403-416. https://doi.org/10.1007/s40199-019-00316-w.

Annex 2.

Ibrahim, Yousif H-E.Y.; Wobuoma, Patience; Kristó, Katalin; Lajkó, Ferenc; Klivényi, Gábor; Jancsik, Béla; Regdon jr., Géza; Pintye-Hódi, Klára; Sovány, Tamás Effect of Processing Conditions and Material Attributes on the Design Space of Lysozyme Pellets Prepared by Extrusion/Spheronization Journal of Drug Delivery Science and Technology

Annex 3.

Supplementary Material for Ibrahim, Yousif H-E.Y.; Wobuoma, Patience; Kristó, Katalin; Lajkó, Ferenc; Klivényi, Gábor; Jancsik, Béla; Regdon jr., Géza; Pintye-Hódi, Klára; Sovány, Tamás Effect of Processing Conditions and Material Attributes on the Design Space of Lysozyme Pellets Prepared by Extrusion/Spheronization

Annex 4.

Ibrahim, Yousif H-E. Y.; Regdon jr., Géza; Kristó, Katalin; Kelemen, András; Adam, Mohamed E.; Hamedelniel, Elnazeer I.; Sovány, Tamás. Design and characterization of chitosan/citrate films as carrier for oral macromolecule delivery, Eur. J. Pharm. Sci. 146 (2020) 105270. https://doi.org/10.1016/j.ejps.2020.105270.

Annex 5.

Supplementary Material for Ibrahim, Yousif H-E. Y.; Regdon jr., Géza; Kristó, Katalin; Kelemen, András; Adam, Mohamed E.; Hamedelniel, Elnazeer I.; Sovány, Tamás. Design and characterization of chitosan/citrate films as carrier for oral macromolecule delivery

ANNEX - 1

DARU Journal of Pharmaceutical Sciences (2020) 28:403–416
https://doi.org/10.1007/s40199-019-00316-w

REVIEW ARTICLE

Review of recently used techniques and materials to improve the efficiency of orally administered proteins/peptides

Yousif H-E. Y. Ibrahim[1,2] · Géza Regdon Jr[1] · Elnazeer I. Hamedelniel[2] · Tamás Sovány[1]

Received: 1 July 2019 / Accepted: 13 November 2019 / Published online: 6 December 2019

Abstract

Objectives The main objective of present review is to explore and evaluate the effectiveness of recently developed methods to improve the bioavailability of orally administered biopharmaceutical drugs.

Methods A systematic search of sciencedirect, tandfonline and Google Scholar databases based on various sets of keywords was performed. All results were evaluated based on their abstracts, and irrelevant studies were neglected during further evaluation.

Results At present, biopharmaceuticals are used as injectable therapies as they are not absorbed adequately from the different routes of drug administration, particularly the oral one. Their insufficient absorption is attributed to their high molecular weight, degradation by proteolytic enzymes, high hydrophilicity and rigidity of the absorptive tissues. From industrial aspect incorporation of enzyme inhibitors (EIs) and permeation enhancers (PEs) and mucoadhesive polymers into conventional dosage forms may be the easiest way of formulation of orally administered macromolecular drugs, but the effectiveness of protection and absorption enhancement here is the most questionable. Conjugation may be problematic from regulatory aspect. Encapsulation into lipid-based vesicles sufficiently protects the incorporated macromolecule and improves intestinal uptake but have considerable stability issues. In contrast, polymeric nanocarriers may provide good stability but provides lower internalization efficacy in comparison with the lipid-based carriers.

Conclusion It can be concluded that the combination of the advantages of mucoadhesive polymeric and lid-based carriers in hybrid lipid/polymer nanoparticles may result in improved absorption and might represent a potential means for the oral administration of therapeutic proteins in the near future.

Keywords Biopharmaceuticals · Enzyme inhibitors · Permeation enhancers · Mucoadhesive

Introduction

Various diseases like diabetes, malignant tumors and some types of infections have been managed by peptides and proteins. In addition, peptides and peptidomimetics can serve as immunomodulating agents [1]. They produce their response either by antigenic properties or by stimulating the immune system as an agonist. Some intensively investigated peptides, such as cyclosporine, tuftsin, muramyl dipeptide (MDP) and thymic peptide analogues have already been used as therapeutic peptides [2]. Host defense peptides (HDPs) were accepted on a large scale as immune system stimulators and modulators, their effects include wound healing and the induction of both intra- and extracellular bactericidal effect through phagocytosis [3]. Consequently, biopharmaceuticals, including hormones, enzymes and immunomodulators, play an important role through the controlling of various functions, therefore they are useful in clinical practice to treat or prevent human disorders pathophysiological processes [4]. These days various macromolecules are intensively examined and more than thirty have been accepted by the Food and Drug Administration (FDA) for commercialization [5].

The design, formulation and peroral administration of therapeutically active biomolecules have represented a difficulty as well as a target for several years, and until now only a few biopharmaceuticals (insulin derivatives, interferon alpha,

✉ Tamás Sovány
t.sovany@pharm.u-szeged.hu

[1] Institute of Pharmaceutical Technology and Regulatory Affairs, University of Szeged, Eötvös u. 6, Szeged H-6720, Hungary

[2] Pharmaceutics Department, Omdurman Islamic University, Omdurman, Sudan

calcitonin, growth hormone, etc.) are known to be in clinical development [6, 7], and even less macromolecule is commercialized currently for oral administration (Table 1).

As a class, biopharmaceutical drugs, such as proteins and peptides, have the advantages of higher potency and specificity compared to small molecular drugs. These advantages are related to their rigid and complex structure, which at the same time represents the greatest obstacle in designing and formulating an oral delivery system of these macromolecules [8]. Accordingly, in the past significant interest was focused on the delivery of oral macromolecules in the hope of controlling different diseases and achieving better patient compliance by employing advanced pharmaceutical biotechnology for production and development [9]. Recently, the formulation of polymers with mucoadhesive properties as intestinal patches containing safe surfactant, as an oral insulin delivery system, has been one of the most studied techniques [10]. Biocompatible and biodegradable polymeric nanocarriers and lipid based nanoparticles have also come forth as promising oral delivery platforms for these biopharmaceuticals, as these systems give protection against proteases as well as control the release of proteins [11, 12]. The increasing importance of proteins/peptides can be explained as a result of three main developments: evolution in the analytical methods, which has promoted the discovery of a huge number of peptides and hormones applicable as biopharmaceuticals; good knowledge about the role of these molecules in the regulation of human pathophysiology; and the development of biotechnology and genetic engineering, which enables the production of biomolecules in a bulk quantities [13].

Barriers to oral absorption

Any orally administered drug will face many barriers while passing along the gastrointestinal tract (GIT) before reaching the targeted absorptive capillaries at the absorption site of the sub-epithelial tissue. The most frequently encountered barriers are stomach acidity and the intestinal milieu, the tight junctions (TJs), which prevent the paracellular way, the external cells of the GIT and finally the subepithelial tissues [14]. The epithelium layer of the intestinal tract is a group of consolidated cells which act as a cover for the GIT and as mucosal immunological defense against the invading pathogens and harmful chemicals. The most common absorptive areas throughout the intestine are the microvilli covered apical surfaces of enterocytes, which are negatively charged. The distance between microvilli is around 25 nm, thus they prevent the passage of larger molecules [15]. Therefore, these cells act as a physical-, whereas the degrading enzymes represent a biochemical barrier. Therefore the understanding of the these barrier mechanisms and finding the way to overcome the limitations of macromolecule transportation are essential to develop effective oral protein/peptide delivery systems [16, 17].

The crossing of the cell barrier is possible via various ways; passively through diffusion, crossing the hydrophobic TJs or transepithelial cells, transcellularly via facilitated transport and by carrier-mediated transport (Fig. 1) [18]. Moreover, the absorption of both some biomolecules and some drugs may vary along the various parts of the GIT due to variation in the pH values, surface areas, activity of proteases and permeability of the absorptive site. Therefore, the determination of the proper region of the GIT for the chosen peptide/protein will be the primary step in the design and development of an oral dosage form with improved bioavailability [19].

Table 1 Macromolecules commercialized for oral administration

Trade name	Drug	Company
Leftose	Lysozyme	Wellchem
Linzess	Linaclotide	Allergan
Trulance	Plecanatide	Synergy Pharmaceuticals

Intestinal digestive environment

The greatest difficulty encountered in the case of orally administered bioactive macromolecules is the lumen of the small intestine, where there is high concentration of proteolytic enzymes secreted by the pancreas and by mucosal cells. Another main enzymatic obstacle is the border of the epithelial cells, which contains around fifteen degrading enzymes with high selectivity for the breakdown of the macromolecular biomolecules [20]. In addition, the colon contains various enzymes produced by the local microflora, which should also be taken into account [21]. Generally, the degradation of administered biomolecules depends on numerous mechanisms adopted by these enzymes, and the overall result is that the byproducts of macromolecule degradation, such as short peptide chains and amino acids, have no ability to produce the required effect [22].

Tight junction (TJ)

As mentioned above, drugs may penetrate across the membranes through the following pathways: paracellular pathway, transcellular pathway and through transport via microfold cells. Recently, some researchers have investigated the applicability of the absorption of drug entities from the small intestines via receptor-mediated, clathrin-mediated and even caveolae-mediated endocytosis. Most drugs are transported transcellularly, but for hydrophilic molecules (like proteins and peptides) paracellular absorption is the main pathway. However, this gate is tightly closed by tight junctions (TJs) [23, 24]. TJ proteins are associated with higher paracellular permeability, which is highly explicit throughout the small

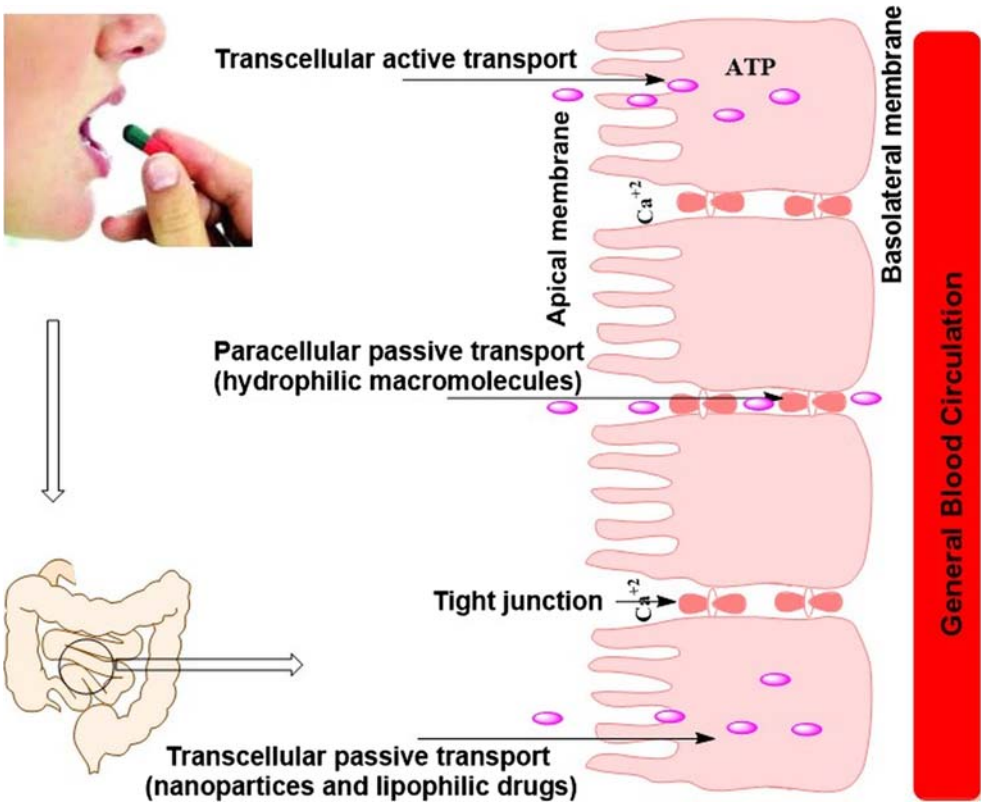

Fig. 1 General pathways of absorption across the small intestines

intestines [25]. TJs contain four types of unique transmembrane proteins: occludin, claudins, junctional adhesion molecules (JAMs) and tricellulin [26]. TJs are not static protein structures, they serve as penetration regulators of the molecules across the intestinal epithelium. Some penetration enhancers have the ability to loosen the TJs and thus facilitate the paracellular absorption of drug molecules [27].

Mucous barrier

The mucosa is covered by the mixture of mucins, ions and proteins; therefore, it is a rigid layer which acts as a coat to the intestinal lumen and is bound to the surface by a glycoprotein structure (about 500-nm thick). The primary role of the mucosal layer is the regulation of pH at the lumen surface and thus results in the formation of an acidic microenvironment [28]. The mucosal layer has different thickness and turnover values regarding the anatomical position, pathophysiological status and interaction with the external environment [29]. Generally, the mucous layer acts as a physical barrier as a result of its negative charges and lipophilic nature, whereas the general hydrophilicity of mucus also acts as an interactive barrier, which retards the movement of the molecules within and through the mucus. The dynamic behavior of the mucosal layer is due to its continuous secretion and sloughing from the surface of the mucosal membrane, therefore mucus represents a rigid gel barrier to drug delivery [30].

Formulation aids and techniques for improving bioavailability

Due to limiting factors such as large molecular weight, hydrophilic nature, inactivation due to stomach secretions and intestinal proteases, first pass effect, and tendency to aggregation, the bioavailability of orally administered proteins/peptides is usually recorded less than 1% [31]. Numerous approaches have been taken by researchers to improve the oral delivery of therapeutic proteins, like insulin. The most studied strategies include the use of permeation improvers, protease inhibitors, mucoadhesive polymers, polymeric nanoparticles, liposomal encapsulation, modification of the structure and microsphere encapsulation [7, 24].

Permeation enhancers approach (PEs)

The use of permeation enhancers represents the most common approach of protein delivery, their use can modulate the characteristics of the absorptive epithelium and may facilitate both transcellular or paracellular absorption. Therefore, it is an applicable strategy to enhance the bioavailability of administered macromolecules [32]. These agents were first investigated twenty years ago to enhance the absorption of pharmacologically active molecules with poor bioavailability due to their low permeability as well as in an attempt to develop non-injectable systems for insulin delivery [33]. The enhancing effect through the

paracellular pathway is due to the opening of TJs, whereas the transcellular pathway ensues from the increased permeability of the plasma membrane. Both pathways may be possible for one enhancer, but the number of enhancers that increase transcellular membrane permeability is 10 times higher than the number of those increasing paracellular absorption [34]. Calcium chelators act by stirring the cells through calcium depletion, which results in loosening the attachments of the TJs. In contrast, surfactants work through the disruption of the barrier function of the epithelium [35]. The less damaging paracellular pathway by a transient opening of TJs seems to be more rational and safer when compared to the disruption of the cell membrane structure. Nevertheless, the successful improvement of oral bioavailability in vivo necessitates the concurrent delivery of the drug and efficient concentrations of the absorption promoter to the intended absorption site [36]. It is also notable that the effectiveness of absorption enhancers is not the same along the GI tract due to the variations of numerous parameters, such as membrane thickness, morphology of the cells, proteolytic activity, lipid composition and fundamental protein interactions [37]. Moreover, despite the effective promotion of the oral absorption of poorly absorbable molecules, the use of PEs should be evaluated carefully as they can cause non-specific absorption and they must be avoided in the case of patients suffering from irritable bowel disease, celiac disease and inflammatory bowel disease [38]. Therefore, PEs offer the greatest potential when incorporated in localized delivery systems, like hydrogels and intestinal patches, to avoid non-specific absorption [39].

The general classes of PEs are demonstrated below in Table 2.

Besides the promotion of the transport of small drug molecules, sodium salicylate and EDTA have also demonstrated an improved oral bioavailability of insulin in dogs and rabbits [50]. They increase the paracellular transport of drug entities through affecting the permeability of TJs by chelating the membrane-bound calcium ions [51]. Medium chain fatty acids (as shown in Table 1) and gel-forming polymer media for example, octreotide may be also utilized to improve the efficiency of orally administered macromolecules [33]. Chitosan is a positively charged polymer commonly considered as an effective and harmless penetration enhancer for therapeutic macromolecules along the intestinal lumen via a reversible integrity modulation of epithelial TJs in a concentration dependent manner [52–54]. Phenyl piperazine at a concentration of 0.1%*w*/w has also been considered as a safe and effective transepithelial permeation enhancer amongst fifty-one studied promoters from eleven discrete chemical categories [39]. Sodium dodecyl sulfate (SDS) has also been reported as an effective, potent and safe absorption enhancer in oral formulations, as neither the change the epithelial surface, nor toxic luminal absorption has been reported [55]. Bile salts may serve as effective aids in drug formulation since they may improve absorption through both transcellular and intercellular paths. An investigation has shown the enhancement of heparin absorption by either the chemical conjugation of heparin or physical mixing with bile acids [55–57].

Enzyme inhibitors (EIs) approach

One of the key issues to achieve appropriate oral activity is to protect the therapeutic peptides against luminal breakdown caused by the presence of various proteases. The inhibition of these proteolytic enzymes is achieved mainly by two mechanisms: local modulation of the pH away from the optimum ranges of peptidases or binding to target enzymes and limiting their activity [58]. In recent studies the use of numerous trypsin and α-chymotrypsin inhibitors have been investigated, such as soybean trypsin inhibitor, camostat mesylate, pancreatic inhibitor, amastatin, bestatin, aprotinin, boroleucine, bestatin, and aminopeptidase inhibitors, such as puromycin, to control the effect of these enzymes [16, 59]. The coadministration of oral insulin and EIs resulted in an improved hypoglycemic effect, which may be explained either by protecting insulin from the degradation activity of proteases or enhancing the absorption of insulin, or both at the same time [60]. Similarly, the concurrent administration of insulin microcrystals with protease inhibitor resulted in improved bioavailability also in the case of pulmonary delivery, and the absorption

Table 2 Classification of permeation enhancers [33, 40–49]

Class	Example	Mechanism and pathway
Surfactants	polysorbates, poloxamer 407, Tween 80, labrasol, sodium dodecyl sulphate, lauryl methyl glucamide	inhibiting the effect of P-glycoprotein and modulating TJs, transcellular and paracellular pathways
Chitosan derivatives	Di- and tri-methyl chitosan, carboxymethyl chitosan	Strong mucoadhesion, opening tight junctions, maily paracellular pathway
Multicarboxylic acids	Citric acid, ethylenediaminetetraacetic acid (EDTA)	Chelating the calcium ions at the absorptive tissues and loosening the TJs, mainly paracellular pathway
Bile acid salts	Sodium cholate, glycocholate, taurocholate and deoxycholate	Enhancing lymphatic uptake or modulating TJs, both transcellular and paracellular pathways
Fatty acids and fatty alcohols	Stearic acid, octanoic acid, palmityl alcohol	

enhancement was the highest with soybean trypsin inhibitor among all the tested inhibitors [61]. Duck and chicken ovomucoids (DkOVM and CkOVM) have been reported as a unique class of protease inhibitors. Dissolution stability investigations showed that the percentage of insulin remaining for absorption increased dramatically against the action of proteases (trypsin and chymotrypsin) when administered with CkOVM and DkOVM [62].

As it was mentioned above, another technique to inhibit enzyme activity is to modify the pH at the targeted absorption site as the activity of proteases is extremely sensitive to pH change; intestinal proteases are active at a relatively elevated pH, thus lowering the pH at this site may decrease the activity of the enzymes present [63]. A pH modulator like citric acid (CA) can be utilized to suppress lumen peptidases, and it has been reported to be a helpful excipient for the oral delivery of some peptides, as the proteolytic action is particularly elevated in the upper part of the intestines [58]. Nevertheless, safety issues should be taken into consideration for formulations that contain any kind of protease inhibitors as these agents may interact with dietary proteins or rupture the integrity of the mucosal surfaceand cause upregulated enzyme secretion after long-term treatment [64, 65]. Moreover, the use of enzyme inhibitors may increase the amount of the intact drug at the absorption site but will not help passing through biological membranes. Therefore, the combination of the various approaches may be essential to have an appropriate therapeutic effect. In a recent study, enteric-coated capsules have been developed for oral insulin delivery, consisting of a greasy mixture of omega-3 fatty acids, containing insulin, EI such as aprotinin and chelating agent or bile acid salt as PE acid. This formulation has passed Phase II-a of clinical trials and is progressing into Phase II-b [66].

Bioadhesive polymer approach

Bioadhesion is a circumstance resulting from the attractive forces generated between a polymer and the surface of biological substrates, which enables the polymer to tightly stick to the biological substrate for various periods of time, depending on the nature of the forces participating [67]. As regards the phenomenon of mucoadhesion, two phases can be distinguished: the adhesion phase between the polymer and the mucosa, which enables the polymer to diffuse and dilate, and the integration phase as a result of the development of different adhesion forces (Fig. 2) [67, 68].

To date, six hypotheses have been proposed to express the phenomena behind the two stages of mucoadhesion, which are:

(a) The electronic theory is based on the transfer of electrons amongst the polymer backbone and the substrate, leading to the development of binding forces.
(b) The wetting theory proposes the higher affinity of the surrounding liquid to substrate surface to the surrounding liquid medium resulting in case of lower angle of contact.
(c) The cohesive theory describes that bioadhesion phenomena are basically attributed to the interactions arising between similar molecules.
(d) The adsorption theory expects the existence of molecular attraction based on van der Waals or H-bonding between the surfaces of the biological substrate and the polymer.
(e) The diffusion hypothesis supposes the formation of a networked structure as a result of the polymer backbone spreading on the mucosal surface along the adherent interface.
(f) The mechanical hypothesis describes the adhesion developing between the substrate and the polymer as a result of the interlinking of the polymer's structure with the microholes present on the biological surface [69].

The effectiveness of various drugs may be improved by applying mucoadhesive delivery systems, which stay in direct contact with the targeted mucosal surface, hence they release the incorporated macromolecule directly to the absorptive tissues, thus enhancing the delivery efficiency, and they can be used either for local or systemic effects. Therefore, mucoadhesive polymeric systems are attractive carriers for protein delivery as their properties may be tuned as a result of various changes in their network structure or swelling behavior as a response to various surrounding triggers, e.g. the change of pH, electric field, temperature, light or ionic strength [59]. In addition, they may isolate protein/peptide from the degradation effect of the low gastric pH as well as of proteolytic enzymes [70–72]. Moreover, they control the release of incorporated molecules from the delivery system and provide the concurrent release of the drug and the enzyme inhibitor. Furthermore, they also localize the effect of enzyme inhibitors as well as make the drug closer to the absorption site for a sufficient time [73]. This effectiveness was confirmed in recent studies, where mucoadhesive devices containing a mixture of polymers with mucoadhesive character were developed. These enteric coated devices were entirely coated with water impermeable backing layer except on one side, where the device will adhere to the intestinal mucosal membrane, making the release of incorporated macromolecules possible in a unidirectional pattern. These devices provide protection from luminal proteases; therefore, they prevent the loaded drug from enzymatic degradation. Moreover, the investigations showed that the developed devices are safe and can tolerate the shear stress of peristalsis due to strong mucoadhesion, and were reported as an efficient alternative to insulin injection in controlling diabetes [74, 75].

There are numerous available and commonly used mucoadhesive polymers including chitosan, carbopol,

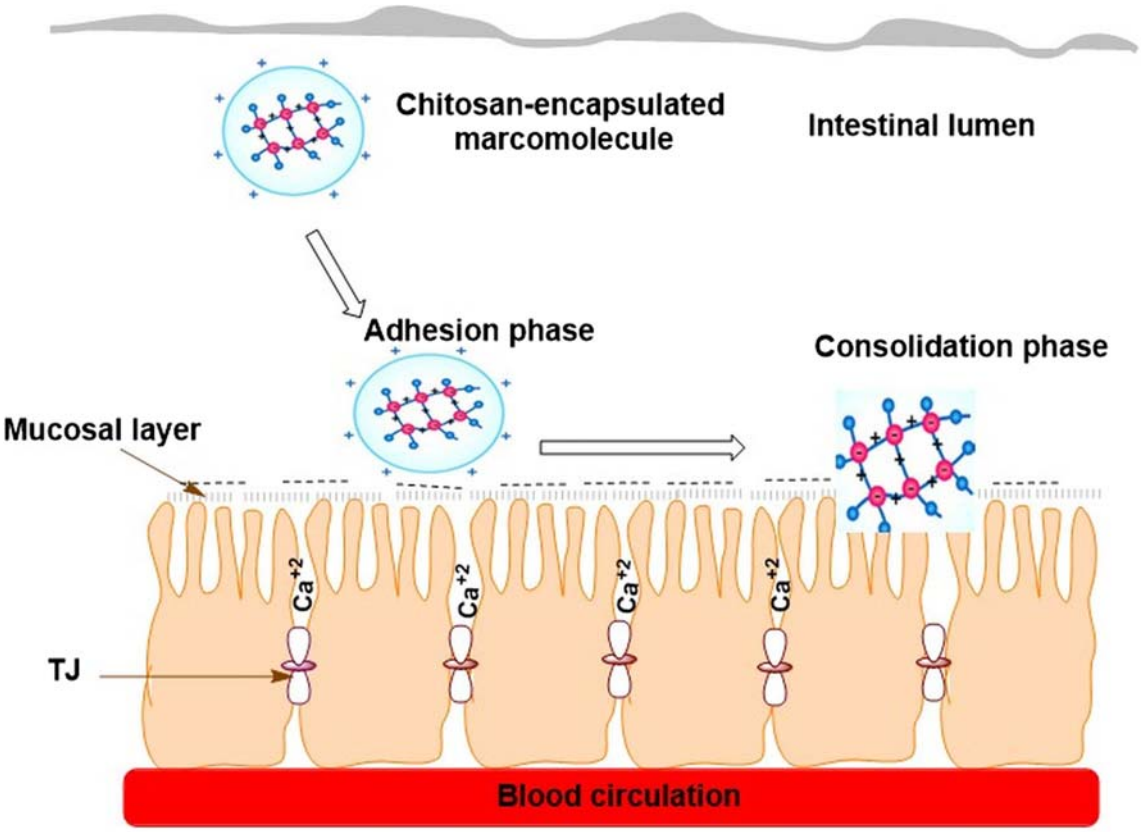

Fig. 2 The attachment and consolidation stages of a positively charged mucoadhesive polymer

cellulose derivatives and alginate. Nevertheless, the selection of the polymer type and its molecular mass should be done very carefully before utilizing it in the formulation, as the release of the peptide may be retarded because of steric hindrance if polymers with a higher molecular weight are used [76]. Most of the polymers which exhibit the strongest interaction with mucins are hydrophilic and positively charged under the pH conditions of the GIT. Chitosan (poly [ß-(1–4)-2-amino-2-deoxy-D-glucopyranose]), a positively charged polymer derived by the partial deacetylation of chitin [77], was described to form a strong matrix with mucus glycoprotein, enabling it to release insulin and significantly controlling the plasma glucose levels in normal rats for 24 h [78]. In addition, chitosan can sustain drug release, extend the duration of drug treatment time and concurrently enhance the mucoadhesive force of drug particles to the mucosal membrane at the absorption site [79].

Chitosan and its derivatives have been utilized by many researchers for protein/peptide delivery particularly because, besides their mucoadhesive properties, they are recognized as effective and safe absorption enhancers, which considerably improves their capacity for the delivery of hydrophilic macromolecules through the (nasal and peroral) mucosa [80]. The mechanism of permeation enhancement is attributed to the free positive charges, enabling strong adhesion with the absorptive substrate and leading to the modulation of the TJ proteins [81]. As it was discussed above, the interaction between the mucosal membrane (mucin) and polymers is mostly based on non-covalent bonds, but some polymers are also able to form covalent bonds [82]. This novel class of mucoadhesive polymers, often called multifunctional polymers, have recently replaced conventional polymers on the market thanks to their distinctive attributes, such as considerably improved mucoadhesive characteristics and similarly improved permeation enhancing effects [83]. These novel polymers (like poly (acrylic acid)–homocysteine, chitosan–iminothiolane, chitosan–thioglycolic acid, poly (acrylic acid)–cysteine, chitosan–thioethylamidine, alginate–cysteine, poly (methacrylic acid)–cysteine and sodium carboxymethylcellulose–cysteine) have been produced by thiomerization. This improves their water uptake, which – along with intra- and interchain disulfide linkages – improves viscosity, strengthens cohesiveness and mucoadhesion, which are in turn responsible for the prolonged residence of the polymeric system at mucosal surfaces [84, 85]. The newly developed preactivated polysulfonate thiomers also showed a distinct improvement in the paracellular transport of both low and high molecular weight hydrophilic penetration markers along the monolayer cells of Caco-2 of newly enucleated rat gut; therefore thiolated polymers are recommended as potential

carriers, particularly for orally administered macromolecules [86].

Prodrug approach

Prodrugs are inactive forms of therapeutic molecules produced via the chemical modification of the original molecule, which turns into the active form of the molecule during administration, commonly by the effect of enzymatic reactions or other possible reactions inside the body [7]. The primary goals of the prodrug approach can be outlined as follows: targeted release, ameliorating absorption or membrane permeability and decreasing metabolism or side effects [87]. The generation of prodrugs from proteins/peptides appears to be an attractive approach concerning the improvement and optimization of their delivery because all the basic objectives of this approach may be fulfilled with the modification of the structure of biopharmaceuticals [88]. These hydrophilic molecules require a certain increase in lipophilicity to penetrate the epithelial cell membrane and thus to cross the cells [89]. Chemical alteration on a reactive amino acid like lysine and cysteine or other amino acids will not only give rise to sustained absorption and reduce the amount of drug required to produce the therapeutic effect but will also improve stability as well as decrease immunogenicity [90, 91], and based on the size of the conjugated molecule renal ultrafiltration may be decreased due to the increased molecular size of the polypeptide [92]. The nature of the conjugated molecule may be varied in a wide range such as direct modification by the use of acetylation, C-amidation, N-pyroglutamate conjugation, PEGylation (PEG) or glycosylation [93], or via the sugar part of the glycoprotein [13]. Other strategies used for prodrug formation include d-amino acid substitution, olefenic substitution, carboxyl reduction, dehydro-amino acid substitution, retro inversion modification and thiomethylene modification [94]. Substantial success was achieved in producing protein prodrugs, but due to the structural complexity of proteins, this tool was unsatisfactory when attempting to modify most proteins, and successful modification also faced the problem of overall low yield [95].

Mimetic peptides approach

Parallel peptides are peptides with abnormal arrangement of synthesized amino acids or incorporation of different new linking bonds between those amino acids. The inclusion of these chemical changes provides the preservation of peptides against peptidases, which have high specificity towards normal peptides, but the main drawback of this approach is the change or loss of the biological activity which should be retained as the initial one [96].

Fatty acids-conjugation (lipidation) approach

Lipidation is the chemical alteration of a hydrophilic biomolecule, made by the addition of a lipophilic entity mainly via the acylation reaction to improve both the delivery and the pharmacological efficiency of macromolecular drugs by influencing membrane transport, metabolic stability and bioavailability [97]. The covalent modification of proteins can be done with various lipophilic substances, including isoprenoids, lipid acids and fats. Accordingly, the lipidation process has a great role in tailoring as well as in localizing proteins [98]. Large numbers of proteins, including many proteins utilized in the therapy of human diseases, are modified by covalently linking fatty acids and/or isoprenoid groups, which play a basic role in regulating their structure and function. Palmitate and myristate are the two fatty acids most commonly linked to proteins [99]. Reversible lipidation represents an effective way to retain the basic biological activity of the lipidized molecule. Lately, a reversible lipidation method has been accomplished to guarantee the re-formation of the therapeutic peptide from its lipidized form subsequent to oral absorption [89].

Cell penetration peptide (CPP) conjugation approach

CPP is a peptide with a high penetration capacity across the absorptive cell membranes, thus a conjugation of the CPP to macromolecular drugs like proteins will improve their kinetics. Furthermore, a macromolecule and CPP can be administered as a simple mixture [100]. At present, various non-injection routes including nasal, pulmonary and oral routes have been developed by utilizing a conjugate of CPP with antidiabetic peptide for controlling blood glucose level. Most of such research reported that after a suitable CPP conjugation with antidiabetic peptide hypoglycemic activity could be retained. Furthermore, they show better stability and resistance to proteolytic degradation [101].

Protein-polymer conjugation

In comparison with lipidation, the covalent conjugation of proteins with various polymers offers the advantage of the wider range of the targetable side chains, which results in altered solubility, lipophilicity, targetability, crystallinity and taste. Consequently, pharmaceutical and biotechnological companies are conducting numerous studies and testing new techniques to find the ideal modification [97]. Short chains of both chitosan and polyethylene glycol (PEG) represent the most utilized conjugates because they overcome the issue of low solubility and improve the formulation stability in the GIT [102]. Lee et al. developed a conjugate of insulin and low molecular weight chitosan (LMWC) in an attempt to enhance the oral delivery of insulin. The conjugates were found to have

good ability to manage the plasma glucose level for several hours in diabetic rat models, and they are considered as a potential future technique for improving the efficacy of orally administered therapeutic peptides and proteins [103]. Moreover, a conjugate of insulin and low relative molecular mass protamine as CPP has been incorporated into mucoadhesive nanoparticles (MNPs), and the composite showed an effective delivery of insulin following oral application. MNPs were found to render the loaded conjugates in direct contact with the intestinal absorptive tissues. As a result of their high permeation, it is possible for the released conjugates to be absorbed without digestion, and hence higher bioavailability of insulin in diabetic rats has been obtained [104].

Lipid-based drug delivery system (LBDDS) approach

Lipid excipients are commonly involved in a formulation to increase the absorption of drug molecules along the intestines by different mechanisms, including limiting intestinally mediated proteolysis, increasing membrane permeability and enhancing intestinal lymphatic uptake [105]. Therefore an emerging interest was observed concerning LBDDSs over the past two decades despite the pharmaceutical difficulties entailed by these candidates [106]. Lipid-based carrier systems as drug vehicles are composed of physiological lipids and offer several advantages, including high biocompatibility and controlled release based on the nature of natural lipids, no susceptibility to erosion phenomena compared to polymeric systems, easy and simple manufacturing by compressing or moulding, and slow water uptake after administration, which may offer a less damaging environment for the loaded proteins [107]. Thus, they have most of the advantages without the risks and regulatory concerns involved in the direct conjugation of proteins with lipids.

Liposomal encapsulation approach

Liposomes are defined as microscopic vesicles with a spherical shape, consisting of two compartments, an inner aqueous sinus surrounded by one or multiple homocentric lipid bilayers. The liposomal membrane consists of reasonably biocompatible, biodegradable and non-immunogenic natural and/or synthetic lipids usually stabilized with cholesterol, which also extends the circulating time [108, 109]. The versatile nature of liposomes enables lipophilic drugs to be incorporated within the lipid bilayers, while lipophobic molecules like proteins may be solubilized inside the internal aqueous core [110]. Therefore liposomal carriers were utilized for the successful encapsulation of various therapeutic molecules like tropicamide, artemether, paclitaxel, acyclovir, cyclosporine, dithranol and chloroquine diphosphate [111]. In addition, they represent excellent carriers for the delivery of protein antigens as they may be functionalized to mimic pathogens, which may induce the immune system due to their enhanced uptake by antigen presenting cells through various mechanisms, and the increased exposure of liposome encapsulated antigens to the lymphocytes of the immune system [112]. In recent years, several liposome-based vaccines have been designed to deliver oral antibodies to target several diseases caused by viruses and bacteria, such as *Salmonella enteritidis* and influenza-A viral vaccines. Thus, liposomes have shown high capacities to deliver various antigens, such as peptides/proteins and DNA [113].

Compared to various lipid carries, liposomes have high capacity to enclose and protect labile molecules against the hazardous GIT environment which would result in denaturation, and they may also increase absorption into enterocytes via the stimulation of their chylomicron production, thus promoting drug transport [114]. Protein drugs of interest may be both enclosed inside the liposomes or chemically attached to the outer surface of the vesicles. The simple enclosure of a macromolecule can be attained by the incubation of a macromolecular drug alongside the vesicles at or somewhat below the transformation temperature of the constituting lipids, whereas triggered (active) loading of biopharmaceuticals can be achieved by the gentle swirling of liposomes in the presence of a buffered alcoholic solution of the proteins at elevated temperature for a specified period of time [115].

Despite their numerous advantages, liposomes pose considerable issues regarding physical, chemical and biological stability, and these issues should be investigated and evaluated thoroughly in the course of research, during and after preparation to achieve a good background stability profile. Similarly, the development of general guidelines for the stability testing of liposomes would also be necessary [116]. The chemical stability of lipids against hydrolysis or in the case of unsaturated lipid chains also against oxidation is a point of concern, especially during the storage period. Therefore, it is recommended to store liposomes frozen or in a lyophilized powder form, but in this case the re-check of their size distribution, drug load and morphology before use is essential [117]. Furthermore, the development of liposomal protein delivery systems has to face other challenges as well, such as low protein loading efficiency, especially when using a small vesicle size (range of 50~150 nm), or the instability of the encapsulated protein during preparation, particularly under harsh processing conditions or when using organic solvents [118]. Overall, numerous issues such as the presence of organic solvent residues, physical and chemical instabilities, sterilization and pyrogen control (when designed as injectable), variation in size distribution, difficulties in batch to batch reproducibility and shortened half-life due to pancreatic lipase and bile salts should be overcome during the formulation of liposomes. This explains why only a limited number of liposome-based drug formulations for oral delivery may be found on the market today [119, 120]. A further issue is that liposomes

designed to tolerate the harsh GI environment may exhibit decreased permeability across GIT epithelia, which constitute the main barrier to absorption [121]. However, the rational design approach to attain therapeutic goals might represent the rate-determining step in the development of more advanced liposome-based oral therapeutics in the future [122].

Solid lipid nanoparticles (SLNs)

To overcome the previously discussed drawbacks of liposomes, two different research groups have developed SLNs loaded with insulin for application via the oral route [123, 124]. SLNs are nanosized lipid carriers with particle sizes of 50–1000 nm, which remain solid at ambient and body temperatures. SLNs usually contain physiological lipids, for example, glyceride mixtures and steroids. They are stabilized by biocompatible surfactants and represent an alternative to liposomes and other nanoparticles [35, 125]. These loaded SLN formulations exhibited good efficiency to improve the gastrointestinal absorption of insulin, which was confirmed by the plasma sugar level of the tested rats, which was lower than that of the rats receiving oral insulin solution and unloaded SLNs (control) for one day. Accordingly, loaded SLNs showed a partial protection of insulin against luminal proteases, therefore they are considered as stable carriers to deliver oral insulin with good results of controlling plasma glucose level [123, 124].

SLNs are increasingly used as the protective delivery systems of labile drugs as well as to control/sustain the release of incorporated molecules due to their low toxicity and superior physical stability compared to other lipid-based carrier systems [126]. In addition, SLNs may have excellent reproducibility even with the use of various organic solvent-free methods. Besides their relatively easy manufacturing, SLNs may positively affect drug uptake through various ways, such as enhancing the extent of solubility, hindering drug precipitation upon dilution, suppressing efflux transporters, increasing both membrane permeability and lymphatic uptake. Nevertheless, despite the numerous advantages, the low loading efficiency, particularly for hydrophilic drugs, and the possible expulsion of drugs after polymeric transition during storage still pose considerable problems to scientists [127, 128]. In spite of these drawbacks, their flexibility in preparation and the simplicity of large-scale production may encourage the widespread use of SLNs [129].

Further enhancement of the orally administered medicinal proteins may be accomplished if the lipid-based nanocarriers are conjugated with polymers. In a recent study, poly lactic-co-glycolic acid (PLGA)–lipid lipospheres were developed, which consisted of a PLGA lipophilic interior and a self-assembled lipophilic layer at the interface. These lipospheres demonstrated high crossing efficiency along the microfold cells (an in vivo model), resulting in the efficient improvement of the intestinal absorption for the loaded protein molecules over regular polymeric nanoparticles [130]. Another research group recently developed and formulated low molecular weight (LMW) chitosan-lipid nanoparticle composites to deliver siRNA into the cytoplasm. The formulation gave promising results as it takes benefit of the mucoadhesive and permeation-enhancing properties of chitosan as well as utilizes the hydrophobic reservoir capacity of the hydrophobic core of the hybrid particles [131].

Polymeric nanoparticles approach

From the pharmaceutical aspect, both polymeric micro- and nanoparticles are of emerging interest since they show better stability and therefore better preservation capacity against the degrading effect of the GI environment compared to the carriers of fatty origin, such as liposomes [132]. The effectiveness of protein drugs may be improved successfully with both micro- and nanoencapsulation [133] via protection from hydrolysis and proteolytic enzymes and the improvement of their absorption, in addition to their mucoadhesive properties and permeation enhancing characteristics [134]. However, it was observed that while microparticles are absorbed only through the microfold cells, nanoparticles may also utilize the same pathway and are also able to penetrate cell membranes, therefore the quantity of nanosized carriers penetrating through the intestinal membrane is higher compared to microspheres [134]. The penetration and absorption enhancement properties may be further improved by tailoring its surface characteristics to adjust mucoadhesion property, lymphatic and cellular uptake and site-specific absorption. Nanoparticles are derived mainly from the most common polymers, like poly (lactic-co-glycolic acid) PLGA, poly lactic acid (PLA) and poly sebacic acid (PSA). These polymers perform their mucoadhesivity through different possible methods of interactions, such as covalent and non-covalent bonding or the involvement of both [135]. From this aspect, especially chitosan and its derivatives showed high safety, biocompatibility, biodegradability and represent multifunctional polymers since besides their extremely good mucoadhesive properties, their penetration enhancing effect was also reported [133]. Because of this multifunctionality, chitosan NPs are promising drug delivery carriers suitable for a wide group of drugs, including labile drugs and macromolecules [136, 137]. The combination of various polymers and the utilization of oppositely charged polyelectrolytes like chitosan, polyacrylic acid, alginate, polyalkylamine hydrochloride in the formulation of layer by layer (LBL) coated nanoparticles may also offer further improvement and show a great impact on both macromolecular drug stability and the oral absorbability of protein from the GIT [138]. All in all, mucoadhesive polymer nanoparticles were successfully used for the delivery of the extracellular products (ECPs) of *Vibrio*

anguillarum to deliver oral vaccination in turbots [139], where it was confirmed that the process of insulin uptake seemed to be a joint process of both insulin crossing the intestinal cells and the uptake of the insulin loaded nanoparticles by aggregated lymphoid nodules. However, Yao et al. showed the main limitations of nanoparticulate carrier systems are usually associated with limited loading efficiency and particle agglomeration due to thermodynamic instability [140], which was also observed by Gao et al., who found that the efficiency of loading was only 57.8 ± 2.54% for the turbot vaccination [139].

Self-assembling bubbles carrier approach

Besides the previously discussed approaches, recent studies by the research group of Chuang E-Y introduced a very innovative bubble carrier system as delivery vehicle for the oral delivery of insulin, with possible application as a technique for the oral application of other medicinal macromolecules [141]. This self-assembling bubble carrier composed of pentetic acid, carbonate, surface active agent and insulin was enclosed in oral capsules and enterically coated to bypass gastric acidity. Once the formulation reaches the lower part of GIT fluids, it breaks down and releases acid and bicarbonate, which react quickly and produce carbon dioxide, which acts as a transporter for the involved insulin. The obvious elevation in plasma insulin level accompanied with a decrease in plasma glucose level was noticed in diabetic rats. Accordingly, self-assembling bubble carriers represent an effective and safe method suitable to deliver other biologically active macromolecules [55].

Conclusion

The oral delivery of biopharmaceuticals is a challenging research area as a result of many difficulties, for example, the rigid physical barriers of absorptive tissues for these high molecular mass, hydrophilic drugs, and the degradation by gastric juice and intestinal metabolizing enzymes, all together acting as pharmacokinetic barriers and are responsible for the absorption of a tiny amount of the orally administered dose. Accordingly, the first step in the formulation requires comprehensive knowledge about these barriers. For this reason, most attempts focused on overcoming the enzymatic barrier within the lumen and on improving the permeation of macromolecules.

This review reveals the versatility of methods and involved excipients to overcome the bioavailability problem. From industrial aspect, the combination of mucoadhesive polymers, EIs and PEs in a conventional dosage form appears to be the most applicable approach, as the concurrent release of these excipients may form appropriate microenvironment to obviate the protease barrier and achieve facilitated absorption of the loaded macromolecules. Especially if the effect is localized on the absorption site by the mucoadhesivity of the carrier which increases the chance for absorption. However, the incorporation of these agents may be critical and hence careful screening is required. Nevertheless, some molecules such as phenyl piperazine (0.1%*w*/w), SDS, chitosan and its derivatives were investigated recently and regarded as potential enhancers with reliable safety. The use of multifunctional excipients such as CA to inhibit enzymatic activity by the careful modification of the pH in which peptidases are more active at the targeted absorption site as well as to facilitate paracellular absorption by modulating the permeability of TJs due to the chelating of membrane-bound calcium may further increase the safety of the carrier.

PEGylation by attaching one or more PEG series was developed to increase the circulating time and hide the linked macromolecule from the enzymatic attack, but PEGylation and other prodrug models may conflict with the general regulatory rules and may require more intensive testing of the produced conjugate.

The utilization of lipid-based nanocarriers (e.g. liposomes or SLNs) for the delivery of macromolecules seems to be an efficient technique for oral administration as it provides protection and internalization through the stimulation of intestinal lipoprotein transporters and the possibility to encapsulate hydrophilic and hydrophobic molecules at the same time. On the other hand, the difficulty to reproduce in the same manner, physical and chemical instability during storage, low loading capacity and degradation by pancreatic lipase represent the main limitations and may restrict their utilization as oral macromolecule carriers. From the aspect of reproducibility, SLNs are better than liposomes. However, due to the lack of the hydrophilic interior, they provide poor drug loading capacity for hydrophilic macromolecules and hence, the expulsion of hydrophilic drugs was observed during storage, which considerably decreases the shelf-life of these products.

From the aspect of stability and loading capacity, mucoadhesive polymeric micro/nanocarriers may offer better solution compared to lipid nanocarriers, due to their more hydrophilic structure. However, despite their protecting effect against both luminal and mucosal secretions and enzymes their effectiveness in enhancement of therapeutic effect may be limited due to their lower internalization efficiency. Nevertheless, among them, chitosan micro/nanoparticles proved to be prospective drug delivery carriers as they offer many advantages, including safety, biocompatibility, biodegradability, micro/nanosized nature and the ability to open reversibly TJs, which may facilitate drug uptake through the cell membrane, while their mucoadhesive property increases the residence time at the site of absorption.

Accordingly, it can be concluded that formulation of hybridlipid/polymeric micro/nanoparticles would be the most

appropriate carrier systems for the oral delivery of therapeutic macromolecules as it may provide appropriate loading capacity and stability with improved internalization capacity.

Acknowledgements Open access funding provided by University of Szeged (SZTE). This research was supported by the EU-funded Hungarian grant EFOP-3.6.1-16-2016-00008. The Figures were constructed by ChemBioDraw Ultra 14.0 software.

Compliance with ethical standards

Conflict of interest The authors declare that they have no conflict of interest.

References

1. Keservani RK, Sharma AK, Jarouliya U. Protein and peptide in drug targeting and its therapeutic approach. Ars Pharmaceutica (Internet). 2015;56:165–77.
2. Dutta RC. Peptide immunomodulators versus infection; an analysis. Immunol Lett. 2002;83:153–61.
3. Mansour SC, Pena OM, Hancock REW. Host defense peptides: front-line immunomodulators. Trends Immunol. 2014;35:443–50.
4. Kwon K-C, Daniell H. Oral delivery of protein drugs bioencapsulated in plant cells. Mol Ther. 2016;24:1342–50.
5. Batista P, Castro PM, Madureira AR, Sarmento B, Pintado M. Recent insights in the use of nanocarriers for the oral delivery of bioactive proteins and peptides. Peptides. 2018;101:112–23.
6. Semalty A, Semalty M, Singh R, Saraf S, Saraf S. Properties and formulation of oral drug delivery systems of protein and peptides. Indian J Pharm Sci. 2007;69:741.
7. Muheem A, Shakeel F, Jahangir MA, Anwar M, Mallick N, Jain GK, Warsi MH, Ahmad FJ. A review on the strategies for oral delivery of proteins and peptides and their clinical perspectives. Saudi Pharm J. 2016;24:413–28.
8. Mitragotri S, Burke PA, Langer R. Overcoming the challenges in administering biopharmaceuticals: formulation and delivery strategies. Nat Rev Drug Discov. 2014;13:655–72.
9. Agrawal GR, Wakte P, Shelke S. Formulation, physicochemical characterization and in vitro evaluation of human insulin-loaded microspheres as potential oral carrier. Prog Biomater. 2017;6:125–36.
10. Toorisaka E, Watanabe K, Ono H, Hirata M, Kamiya N, Goto M. Intestinal patches with an immobilized solid-in-oil formulation for oral protein delivery. Acta Biomater. 2012;8:653–8.
11. Santalices I, Gonella A, Torres D, Alonso MJ. Advances on the formulation of proteins using nanotechnologies. J Drug Delivery Sci Technol. 2017;42:155–80.
12. Truong-Le V, Lovalenti PM, Abdul-Fattah AM. Stabilization challenges and formulation strategies associated with oral biologic drug delivery systems. Adv Drug Deliv Rev. 2015;93:95–108.
13. Shaji J, Patole V. Protein and peptide drug delivery: oral approaches. Indian J Pharm Sci. 2008;70:269.
14. Lundquist P, Artursson P. Oral absorption of peptides and nanoparticles across the human intestine: opportunities, limitations and studies in human tissues. Adv Drug Deliv Rev. 2016;106:256–76.
15. Wong CY, Al-Salami H, Dass CR. Potential of insulin nanoparticle formulations for oral delivery and diabetes treatment. J Control Release. 2017;264:247–75.
16. Renukuntla J, Vadlapudi AD, Patel A, Boddu SHS, Mitra AK. Approaches for enhancing oral bioavailability of peptides and proteins. Int J Pharm. 2013;447:75–93.
17. Solaro R, Chiellini F, Battisti A. Targeted delivery of protein drugs by nanocarriers. Materials. 2010;3:1928–80.
18. Mahato RI, Narang AS, Thoma L, Miller DD. Emerging trends in oral delivery of peptide and protein drugs. Crit Rev Ther Drug Carrier Syst. 2003;20:153–214.
19. Kompella UB, Lee VHL. Delivery systems for penetration enhancement of peptide and protein drugs: design considerations. Adv Drug Deliv Rev. 2001;46:211–45.
20. Lee HJ. Protein drug oral delivery: the recent progress. Arch Pharm Res. 2002;25:572–84.
21. Hetal T, Bindesh P, Sneha T. A review on oral Techniques for oral bioavailability. Int J Pharm Sci Rev Res. 2010;4:033. Available from: https://pdfs.semanticscholar.org/0dd6/cc180bdabeab5bc627dcbbff2567735f494f.pdf
22. Pawar VK, Meher JG, Singh Y, Chaurasia M, Surendar Reddy B, Chourasia MK. Targeting of gastrointestinal tract for amended delivery of protein/peptide therapeutics: strategies and industrial perspectives. J Control Release. 2014;196:168–83.
23. Salama N, Eddington N, Fasano A. Tight junction modulation and its relationship to drug delivery. Adv Drug Deliv Rev. 2006;58:15–28.
24. Bakhru SH, Furtado S, Morello AP, Mathiowitz E. Oral delivery of proteins by biodegradable nanoparticles. Adv Drug Deliv Rev. 2013;65:811–21.
25. DiMarco RL, Hunt DR, Dewi RE, Heilshorn SC. Improvement of paracellular transport in the Caco-2 drug screening model using protein-engineered substrates. Biomaterials. 2017;129:152–62.
26. Groschwitz KR, Hogan SP. Intestinal barrier function: molecular regulation and disease pathogenesis. J Allergy Clin Immunol. 2009;124:3–20.
27. Lemmer HJ, Hamman JH. Paracellular drug absorption enhancement through tight junction modulation. Expert Opin Drug Deliv. 2013;10:103–14.
28. Shaikh. Permeability enhancement techniques for poorly permeable drugs: a review. J Appl Pharmaceut Sci. 2012;02(06):34–9. [cited 2018 Apr 21]; Available from: http://www.japsonline.com/abstract.php?article_id=543
29. Lechanteur A, das Neves J, Sarmento B. The role of mucus in cell-based models used to screen mucosal drug delivery. Adv Drug Delivery Rev. 2018;124:50–63.
30. Boegh M, Nielsen HM. Mucus as a barrier to drug delivery - understanding and mimicking the barrier properties. Basic Clin Pharmacol Toxicol. 2015;116:179–86.
31. Patel G, Misra A. Oral delivery of proteins and peptides. In: Misra A, editor. Challenges in delivery of therapeutic genomics and proteomics [Internet]. London: Elsevier; 2011. p. 481–529. [cited 2018 Apr 22] Available from: http://linkinghub.elsevier.com/retrieve/pii/B9780123849649000104.
32. Ismail R, Csóka I. Novel strategies in the oral delivery of antidiabetic peptide drugs – insulin, GLP 1 and its analogs. Eur J Pharm Biopharm. 2017;115:257–67.
33. Aungst BJ. Absorption enhancers: applications and advances. AAPS J. 2012;14:10–8.
34. Maher S, Mrsny RJ, Brayden DJ. Intestinal permeation enhancers for oral peptide delivery. Adv Drug Deliv Rev. 2016;106:277–319.

35. Ozer S, Kerimoglu O, Ugurlu T. Nanocarriers: novel approaches to oral delivery of insulin. Clin Experimental Health Sci. 2017;7:115–22.
36. Aungst BJ. Intestinal permeation enhancers. J Pharm Sci. 2000;89:429–42.
37. Alexander A, Ajazuddin M, Swarna M, Sharma M, Tripathi D. Polymers and permeation enhancers: specialized components of mucoadhesives. Stamford J Pharmaceut Sci [Internet]. 2011;4(1):91–5. [cited 2018 Apr 22]; Available from: http://www.banglajol.info/index.php/SJPS/article/view/8878
38. McCartney F, Gleeson JP, Brayden DJ. Safety concerns over the use of intestinal permeation enhancers: a mini-review. Tissue Barriers. 2016;4:e1176822.
39. Whitehead K, Karr N, Mitragotri S. Safe and effective permeation enhancers for oral drug delivery. Pharm Res. 2008;25:1782–8.
40. Singh D, Sharma PK, Sara UVS. Enhancement of intestinal absorption of poorly absorbed drugs by using various permeation enhancers: an overview. World J Pharm Pharmaceut Sci. 2013;2(1):179–98.
41. Wong SM, Kellaway IW, Murdan S. Enhancement of the dissolution rate and oral absorption of a poorly water soluble drug by formation of surfactant-containing microparticles. Int J Pharm. 2006;317:61–8.
42. Al-Ali AAA, Steffansen B, Holm R, Nielsen CU. Nonionic surfactants increase digoxin absorption in Caco-2 and MDCKII MDR1 cells: impact on P-glycoprotein inhibition, barrier function, and repeated cellular exposure. Int J Pharm. 2018;551:270–80.
43. Sangsen Y, Wiwattanawongsa K, Likhitwitayawuid K, Sritularak B, Graidist P, Wiwattanapatapee R. Influence of surfactants in self-microemulsifying formulations on enhancing oral bioavailability of oxyresveratrol: studies in Caco-2 cells and in vivo. Int J Pharm. 2016;498:294–303.
44. Thanou M, Verhoef JC, Junginger HE. Oral drug absorption enhancement by chitosan and its derivatives. Adv Drug Deliv Rev. 2001;52:117–26.
45. van der Merwe SM, Verhoef JC, Verheijden JHM, Kotzé AF, Junginger HE. Trimethylated chitosan as polymeric absorption enhancer for improved peroral delivery of peptide drugs. Eur J Pharm Biopharm. 2004;58:225–35.
46. Sadeghi A, Dorkoosh F, Avadi M, Weinhold M, Bayat A, Delie F, Gurny R, Larijani B, Rafiee-Tehrani M, Junginger HE. Permeation enhancer effect of chitosan and chitosan derivatives: comparison of formulations as soluble polymers and nanoparticulate systems on insulin absorption in Caco-2 cells. Eur J Pharm Biopharm. 2008;70:270–8.
47. Zhang Z, Gao F, Jiang S, Chen L, Liu Z, Yu H, Li Y. Bile salts enhance the intestinal absorption of lipophilic drug loaded lipid nanocarriers: mechanism and effect in rats. Int J Pharm. 2013;452:374–81.
48. Niu M, Tan Y, Guan P, Hovgaard L, Lu Y, Qi J, Lian R, Li X, Wu W. Enhanced oral absorption of insulin-loaded liposomes containing bile salts: a mechanistic study. Int J Pharm. 2014;460:119–30.
49. Elmowafy M, Shalaby K, Badran MM, Ali HM, Abdel-Bakky MS, El-Bagory I. Fatty alcohol containing nanostructured lipid carrier (NLC) for progesterone oral delivery: in vitro and ex vivo studies. J Drug Delivery Sci Technol. 2018;45:230–9.
50. Gupta V, Hwang BH, Doshi N, Mitragotri S. A permeation enhancer for increasing transport of therapeutic macromolecules across the intestine. J Control Release. 2013;172:541–9.
51. Hussain A, Arnold JJ, Khan MA, Ahsan F. Absorption enhancers in pulmonary protein delivery. J Control Release. 2004;94:15–24.
52. Sonaje K, Lin K-J, Tseng MT, Wey S-P, Su F-Y, Chuang E-Y, Hsu CW, Chen CT, Sung HW. Effects of chitosan-nanoparticle-mediated tight junction opening on the oral absorption of endotoxins. Biomaterials. 2011;32:8712–21.
53. Fan B, Xing Y, Zheng Y, Sun C, Liang G. pH-responsive thiolated chitosan nanoparticles for oral low-molecular weight heparin delivery: in vitro and in vivo evaluation. Drug Delivery. 2016;23:238–47.
54. Nur M, Vasiljevic T. Can natural polymers assist in delivering insulin orally? Int J Biol Macromol. 2017;103:889–901.
55. Lin P-Y, Chuang E-Y, Chiu Y-H, Chen H-L, Lin K-J, Juang J-H, Chiang CH, Mi FL, Sung HW. Safety and efficacy of self-assembling bubble carriers stabilized with sodium dodecyl sulfate for oral delivery of therapeutic proteins. J Control Release. 2017;259:168–75.
56. Moghimipour E, Ameri A, Handali S. Absorption-enhancing effects of bile salts. Molecules. 2015;20:14451–73.
57. Nurunnabi M, Khatun Z, Revuri V, Nafiujjaman M, Cha S, Cho S, et al. Design and strategies for bile acid mediated therapy and imaging. RSC Adv. 2016;6:73986–4002.
58. Aguirre TAS, Teijeiro-Osorio D, Rosa M, Coulter IS, Alonso MJ, Brayden DJ. Current status of selected oral peptide technologies in advanced preclinical development and in clinical trials. Adv Drug Deliv Rev. 2016;106:223–41.
59. Park K, Kwon IC, Park K. Oral protein delivery: current status and future prospect. React Funct Polym. 2011;71:280–7.
60. Ansari MJ. Role of protease inhibitors in insulin therapy of diabetes: are these beneficial. Bull Environ Pharmacol Life Sci. 2015;4:1–8.
61. Jain AK, Jain SK, Chalasani KB. Non-invasive systemic delivery of proteins (s) and peptide (s). Pharmagene. 2013;1:73–84.
62. Agarwal V, Reddy IK, Khan MA. Polymethyacrylate based microparticulates of insulin for oral delivery: preparation and in vitro dissolution stability in the presence of enzyme inhibitors. Int J Pharm. 2001;225:31–9.
63. Bruno BJ, Miller GD, Lim CS. Basics and recent advances in peptide and protein drug delivery. Ther Deliv. 2013;4:1443–67.
64. Choonara BF, Choonara YE, Kumar P, Bijukumar D, du Toit LC, Pillay V. A review of advanced oral drug delivery technologies facilitating the protection and absorption of protein and peptide molecules. Biotechnol Adv. 2014;32:1269–82.
65. Herrero EP, Alonso MJ, Csaba N. Polymer-based oral peptide nanomedicines. Ther Deliv. 2012;3:657–68.
66. Hassani LN, Lewis A, Richard J. Oral peptide delivery: technology landscape and current status. OnDrugDelivery. 2015;59:12–7.
67. Roy S, Pal K, Anis A, Pramanik K, Prabhakar B. Polymers in mucoadhesive drug-delivery systems: a brief note. Des Monomers Polym. 2009;12:483–95.
68. Saraswathi B, Balaji A, Umashankar MS. Polymers in mucoadhesive drug delivery system-latest updates. Int J Pharm Pharmaceut Sci. 2013;5:423–30.
69. Vijapur LS, Sreenivas SA, Patil SH, Vijapur PV, Patwari PK, Saraswathi. Thiolated chitosan: a novel mucoadhesive polymer: a review. Int Res J Pharam. 2012;3(4):51–7.
70. Carvalho FC, Bruschi ML, Evangelista RC, Gremião MPD. Mucoadhesive drug delivery systems. Braz J Pharmaceut Sci. 2010;46:1–17.
71. Boddupalli BM, Mohammed ZN, Nath RA, Banji D. Mucoadhesive drug delivery system: an overview. J Adv Pharm Technol Res. 2010;1:381.
72. Phanindra B, Moorthy BK, Muthukumaran M. Recent advances in mucoadhesive/bioadhesive drug delivery system: a review. Int J Pharma Med Biol Sci. 2013;2(1):68–84.
73. Khafagy E-S, Morishita M, Onuki Y, Takayama K. Current challenges in non-invasive insulin delivery systems: a comparative review. Adv Drug Deliv Rev. 2007;59:1521–46.
74. Banerjee A, Mitragotri S. Intestinal patch systems for oral drug delivery. Curr Opin Pharmacol. 2017;36:58–65.

75. Banerjee A, Lee J, Mitragotri S. Intestinal mucoadhesive devices for oral delivery of insulin. Bioeng Translational Med. 2016;1:338–46.
76. Swaminathan J, Ehrhardt C. Liposomal delivery of proteins and peptides. Expert Opin Drug Deliv. 2012;9:1489–503.
77. Palazzo C, Trapani G, Ponchel G, Trapani A, Vauthier C. Mucoadhesive properties of low molecular weight chitosan- or glycol chitosan- and corresponding thiomer-coated poly (isobutylcyanoacrylate) core-shell nanoparticles. Eur J Pharm Biopharm. 2017;117:315–23.
78. Fonte P, Araújo F, Reis S, Sarmento B. Oral insulin delivery: how far are we? J Diabetes Sci Technol. 2013;7:520–31.
79. Jiang W-Z, Cai Y, Li H-Y. Chitosan-based spray-dried mucoadhesive microspheres for sustained oromucosal drug delivery. Powder Technol. 2017;312:124–32.
80. Khan S, Parvez N, Sharma PK. Novel natural mucoadhesive polymers. 2015;4:374-388.
81. Sreenivas SA, Pai KV. Thiolated chitosans: novel polymers for mucoadhesive drug delivery–a review. Trop J Pharm Res. 2008;7:1077–88.
82. Bernkop-Schnürch A, Steininger S. Synthesis and characterisation of mucoadhesive thiolated polymers. Int J Pharm. 2000;194:239–47.
83. Laffleur F, Psenner J, Suchaoin W. Permeation enhancement via thiolation: in vitro and ex vivo evaluation of hyaluronic acid-cysteine ethyl ester. J Pharm Sci. 2015;104:2153–60.
84. Kumar R, Sinha VR. Thiomer: a potential carrier for therapeutic delivery. React Funct Polym. 2013;73:1156–66.
85. Mythri G, Kavitha K, Kumar MR, Singh S. Novel mucoadhesive polymers–a review. 2011;01(08):37-42
86. Mahmood A, Bonengel S, Laffleur F, Ijaz M, Leonaviciute G, Bernkop-Schnürch A. An in-vitro exploration of permeation enhancement by novel polysulfonate thiomers. Int J Pharm. 2015;496:304–13.
87. Abet V, Filace F, Recio J, Alvarez-Builla J, Burgos C. Prodrug approach: an overview of recent cases. Eur J Med Chem. 2017;127:810–27.
88. Jitendra PK, Bansal S, Banik A. Noninvasive routes of proteins and peptides drug delivery. Indian J Pharm Sci. 2011;73:367.
89. Morishita M, Peppas NA. Is the oral route possible for peptide and protein drug delivery? Drug Discov Today. 2006;11:905–10.
90. Pérez Y, Urista C, Martínez J, Nava M, Rodríguez F. Functionalized polymers for enhance oral bioavailability of sensitive molecules. Polymers. 2016;8:214.
91. Grigoletto A, Maso K, Mero A, Rosato A, Schiavon O, Pasut G. Drug and protein delivery by polymer conjugation. J Drug Delivery Sci Technol. 2016;32:132–41.
92. Veronese FM. Peptide and protein PEGylation: a review of problems and solutions. Biomaterials. 2001;22:405–17.
93. Goodwin D, Simerska P, Toth I. Peptides as therapeutics with enhanced bioactivity. Curr Med Chem. 2012;19:4451–61.
94. Ratnaparkhi MP, Chaudhari SP, Pandya VA. Peptides and proteins in pharmaceuticals. Int J Curr Pharm Res. 2011;3:1–9.
95. Castro PM, Fonte P, Sousa F, Madureira AR, Sarmento B, Pintado ME. Oral films as breakthrough tools for oral delivery of proteins/peptides. J Control Release. 2015;211:63–73.
96. Yin N, Brimble MA, Harris PWR, Wen J. Enhancing the oral bioavailability of peptide drugs by using chemical modification and other approaches. Med Chem. 2014;4:763–9.
97. Mahajan A, Rawat AS, Bhatt N, Chauhan MK. Structural modification of proteins and peptides. Indian J Pharm Educ Res. 2014;48:34–47.
98. Nadolski MJ, Linder ME. Protein lipidation: function and mechanism of palmitoylation. FEBS J. 2007;274:5202–10.
99. Resh MD. Targeting protein lipidation in disease. Trends Mol Med. 2012;18:206–14.
100. Kristensen M, Nielsen HM. Cell-penetrating peptides as carriers for oral delivery of biopharmaceuticals. Basic Clin Pharmacol Toxicol. 2016;118:99–106.
101. Rehmani S, Dixon JE. Oral delivery of anti-diabetes therapeutics using cell penetrating and transcytosing peptide strategies. Peptides. 2018;100:24–35.
102. Buckley ST, Hubálek F, Rahbek UL. Chemically modified peptides and proteins - critical considerations for oral delivery. Tissue Barriers. 2016;4:e1156805.
103. Lee E, Lee J, Jon S. A novel approach to oral delivery of insulin by conjugating with low molecular weight chitosan. Bioconjug Chem. 2010;21:1720–3.
104. Sheng J, He H, Han L, Qin J, Chen S, Ru G, Li R, Yang P, Wang J, Yang VC. Enhancing insulin oral absorption by using mucoadhesive nanoparticles loaded with LMWP-linked insulin conjugates. J Control Release. 2016;233:181–90.
105. Niu Z, Conejos-Sánchez I, Griffin BT, O'Driscoll CM, Alonso MJ. Lipid-based nanocarriers for oral peptide delivery. Adv Drug Deliv Rev. 2016;106:337–54.
106. Mu H, Holm R, Müllertz A. Lipid-based formulations for oral administration of poorly water-soluble drugs. Int J Pharm. 2013;453:215–24.
107. Rawat M, Singh D, Saraf S, Saraf S. Lipid carriers: a versatile delivery vehicle for proteins and peptides. Yakugaku Zasshi. 2008;128:269–80.
108. Basu MK. Liposomes in drug targeting. Biotechnol Genet Eng Rev. 1994;12:383–408.
109. Laouini A, Jaafar-Maalej C, Limayem-Blouza I, Sfar S, Charcosset C, Fessi H. Preparation, characterization and applications of liposomes: state of the art. J Colloid Sci Biotechnol. 2012;1:147–68.
110. Martins S, Sarmento B, Ferreira DC, Souto EB. Lipid-based colloidal carriers for peptide and protein delivery–liposomes versus lipid nanoparticles. Int J Nanomedicine. 2007;2:595.
111. Kalepu S, Sunilkumar KT, Betha S, Mohanvarma M. Liposomal drug delivery system—a comprehensive review. Int J Drug Dev Res. 2013;5:62–75.
112. Leserman L. Liposomes as protein carriers in immunology. J Liposome Res. 2004;14:175–89.
113. Vela Ramirez JE, Sharpe LA, Peppas NA. Current state and challenges in developing oral vaccines. Adv Drug Deliv Rev. 2017;114:116–31.
114. Ahn H, Park J-H. Liposomal delivery systems for intestinal lymphatic drug transport. Biomaterials Res. 2016;20:36. [cited 2018 Apr 23];20. Available from: http://biomaterialsres.biomedcentral.com/articles/10.1186/s40824-016-0083-1
115. Pisal DS, Kosloski MP, Balu-Iyer SV. Delivery of therapeutic proteins. J Pharm Sci. 2010;99:2557–75.
116. Yadav A, Murthy MS, Shete AS, Sakhare S. Stability aspects of liposomes. Indian J Pharmaceut Educ Res. 2011;45:402–13.
117. Ulrich AS. Biophysical aspects of using liposomes as delivery vehicles. Biosci Rep. 2002;22:129–50.
118. Xu X, Costa A, Burgess DJ. Protein encapsulation in unilamellar liposomes: high encapsulation efficiency and a novel technique to assess lipid-protein interaction. Pharm Res. 2012;29:1919–31.
119. Chin J, Foyez Mahmud KA, Kim SE, Park K, Byun Y. Insight of current technologies for oral delivery of proteins and peptides. Drug Discov Today Technol. 2012;9:e105–12.
120. Sipai ABM, Vandana Y, Mamatha Y, Prasanth VV. Liposomes: an overview. J Pharm Sci Innov. 2012;1:13–21.
121. Wu W, Lu Y, Qi J. Oral delivery of liposomes. Future Science; 2015.
122. Lila ASA, Ishida T. Liposomal delivery systems: design optimization and current applications. Biol Pharm Bull. 2017;40:1–10.

123. Sarmento B, Martins S, Ferreira D, Souto EB. Oral insulin delivery by means of solid lipid nanoparticles. Int J Nanomedicine. 2007;2:743.
124. Ansari MJ, MdK A, Jamil S, Al-Shdefat R, Ali BE, Ahmad MM, et al. Enhanced oral bioavailability of insulin-loaded solid lipid nanoparticles: pharmacokinetic bioavailability of insulin-loaded solid lipid nanoparticles in diabetic rats. Drug Delivery. 2015;23:1972–9.
125. Kim H, Kim Y, Lee J. Liposomal formulations for enhanced lymphatic drug delivery. Asian J Pharm Sci. 2013;8:96–103.
126. Cai S, Yang Q, Bagby TR, Forrest ML. Lymphatic drug delivery using engineered liposomes and solid lipid nanoparticles. Adv Drug Deliv Rev. 2011;63:901–8.
127. Jawahar N, Meyyanathan SN, Reddy G, Sood S. Solid lipid nanoparticles for oral delivery of poorly soluble drugs. J Pharm Sci Res. 2012;4:1848.
128. Ganesan P, Narayanasamy D. Lipid nanoparticles: different preparation techniques, characterization, hurdles, and strategies for the production of solid lipid nanoparticles and nanostructured lipid carriers for oral drug delivery. Sustain Chem Pharm. 2017;6:37–56.
129. Yassin AEB, Albekairy A, Alkatheri A, Sharma RK. Anticancer-loaded solid lipid nanoparticles: high potential advancement in chemotherapy. Dig J Nanomater Biostruct. 2013;8:905–16.
130. Ma T, Wang L, Wang D, Ma G, Wang S. PLGA–lipid liposphere as a promising platform for oral delivery of proteins. Colloids Surf B: Biointerfaces. 2014;117:512–9.
131. Tezgel Ö, Szarpak-Jankowska A, Arnould A, Auzély-Velty R, Texier I. Chitosan-lipid nanoparticles (CS-LNPs): application to siRNA delivery. J Colloid Interface Sci. 2018;510:45–56.
132. des Rieux A, Fievez V, Garinot M, Schneider Y-J, Préat V. Nanoparticles as potential oral delivery systems of proteins and vaccines: a mechanistic approach. J Control Release. 2006;116:1–27.
133. De Kruif JK, Varum F, Bravo R, Kuentz M. A systematic study on manufacturing of prilled microgels into lipids for oral protein delivery. J Pharm Sci. 2015;104:3351–65.
134. Yun Y, Cho YW, Park K. Nanoparticles for oral delivery: targeted nanoparticles with peptidic ligands for oral protein delivery. Adv Drug Deliv Rev. 2013;65:822–32.
135. Ensign LM, Cone R, Hanes J. Oral drug delivery with polymeric nanoparticles: the gastrointestinal mucus barriers. Adv Drug Deliv Rev. 2012;64:557–70.
136. Tiyaboonchai W. Chitosan nanoparticles: a promising system for drug delivery. Naresuan Univ J. 2013;11:51–66.
137. Chen M-C, Mi F-L, Liao Z-X, Hsiao C-W, Sonaje K, Chung M-F, Hsu LW, Sung HW. Recent advances in chitosan-based nanoparticles for oral delivery of macromolecules. Adv Drug Deliv Rev. 2013;65:865–79.
138. Liu L, Yao W, Rao Y, Lu X, Gao J. pH-responsive carriers for oral drug delivery: challenges and opportunities of current platforms. Drug Delivery. 2017;24:569–81.
139. Gao P, Xia G, Bao Z, Feng C, Cheng X, Kong M, Liu Y, Chen X. Chitosan based nanoparticles as protein carriers for efficient oral antigen delivery. Int J Biol Macromol. 2016;91:716–23.
140. Yao X, Bunt C, Cornish J, Quek S-Y, Wen J. Oral delivery of lactoferrin: a review. Int J Pept Res Ther. 2013;19:125–34.
141. Chuang E-Y, Lin K-J, Lin P-Y, Chen H-L, Wey S-P, Mi F-L, Hsiao HC, Chen CT, Sung HW. Self-assembling bubble carriers for oral protein delivery. Biomaterials. 2015;64:115–24.

ANNEX - 2

Journal of Drug Delivery Science and Technology

Effect of Processing Conditions and Material Attributes on the Design Space of Lysozyme Pellets Prepared by Extrusion/Spheronization

--Manuscript Draft--

Manuscript Number:	JDDST-D-21-00228R2
Article Type:	Research Paper
Keywords:	lysozyme; polyol; extrusion/spheronization; Quality by Design; design space; material attributes
Corresponding Author:	Tamás Sovány, Ph.D. University of Szeged: Szegedi Tudomanyegyetem Szeged, HUNGARY
First Author:	Yousif H-E.Y. Ibrahim
Order of Authors:	Yousif H-E.Y. Ibrahim
	Patience Wobuoma
	Katalin Kristó
	Ferenc Lajkó
	Gábor Klivényi
	Béla Jancsik
	Géza Regdon jr.
	Klára Pintye-Hódi
	Tamás Sovány, Ph.D.
Abstract:	The present work aimed to investigate the impact of the critical material attributes on the design space of the production of lysozyme pellets with suitable biological and physical properties for the subsequent coating process. The effect of two brands of both lysozyme and conformation stabilizing mannitol on the behavior of the composition in an extrusion/spheronization process was studied, while the experiments were designed according to 2 3 factorial design. The kneading of the mass was carried out in a high shear granulator equipped with a specially designed granulation chamber (Opulus Ltd, Hungary) constructed with seven built-in sensors for the measurement of temperature and relative humidity (RH). The special chamber is a novel tool for the identification of the critical points during processing a thermolabile drug by providing the online monitoring of critical environmental parameters and could be used to accurately determine the effect of critical process parameters and material attributes. The prepared samples were investigated for their biological and physical properties. It was found that the critical material attributes have a potential effect on the production process and product quality, and highly influence the size of the process design space. Therefore, the screening of the formulation materials is a key factor in macromolecular drug development.
Suggested Reviewers:	Stanko Srcic stanko.srcic@ffa.uni-lj.si
	Romána Zelkó zelrom@gytk.sote.hu
	Rok Dreu rok.dreu@ffa.uni-lj.si
	Peter Kleinebudde kleinebudde@hhu.de
Opposed Reviewers:	
Response to Reviewers:	

Effect of Processing Conditions and Material Attributes on the Design Space of Lysozyme Pellets Prepared by Extrusion/Spheronization

Yousif H-E.Y. Ibrahim[1], Patience Wobuoma[1], Katalin Kristó[1], Ferenc Lajkó[2], Gábor Klivényi[2], Béla Jancsik[3], Géza Regdon jr.[1], Klára Pintye-Hódi[1], Tamás Sovány[1*]

[1]University of Szeged, Institute of Pharmaceutical Technology and Regulatory Affairs, Eötvös u. 6., H-6720, Szeged, Hungary

[2]Opulus Ltd, Fürj utca 92/B, H-6726 Szeged, Hungary

[3]Opulus Ltd, 1951 NW 7th. Avenue, 33136, Miami, FL, USA

*Corresponding author: Tamás Sovány, PhD, University of Szeged, Institute of Pharmaceutical Technology and Regulatory Affairs, Eötvös u. 6., H-6720, Szeged, Hungary, e-mail: sovany.tamas@szte.hu, tel: +36626545576

Abstract

The present work aimed to investigate the impact of the critical material attributes on the design space of the production of lysozyme pellets with suitable biological and physical properties for the subsequent coating process. The effect of two brands of both lysozyme and conformation stabilizing mannitol on the behavior of the composition in an extrusion/spheronization process was studied, while the experiments were designed according to 2^3 factorial design. The kneading of the mass was carried out in a high shear granulator equipped with a specially designed granulation chamber (Opulus Ltd, Hungary) constructed with seven built-in sensors for the measurement of temperature and relative humidity (RH). The special chamber is a novel tool for the identification of the critical points during processing a thermolabile drug by providing the online monitoring of critical environmental parameters and could be used to accurately determine the effect of critical process parameters and material attributes. The prepared samples were investigated for their biological and physical properties. It was found that the critical material attributes have a potential effect on the production process and product quality, and highly influence the size of the process design space. Therefore, the screening of the formulation materials is a key factor in macromolecular drug development.

Keywords: lysozyme, polyol, extrusion/spheronization, Quality by Design, design space, material attributes.

1. Introduction

Flourishing in the biotechnological field has produced numerous macromolecules, such as proteins and peptides, which play a great role in managing and treating various diseases, e.g. autoimmune, neurodegenerative and cancer diseases [1]. Their oral delivery remains an attractive alternative to invasive routes because it offers cost-effectiveness as well as patient convenience and compliance [2,3]. To date, they are administered parenterally due to their low bioavailability from other alternative routes of administration, including the oral route [4]. Egg-white lysozyme occurs in many vertebrates and insects, and this diversity of the source renders it the most affordable enzyme [5]. It is harmless to human cells and effectively lyses or inhibits the growth of several pathogens responsible for food spoilage and food-borne diseases; therefore it has a substantial role as a preservative in the food industry [6]. Lysozyme is commonly known as an antimicrobial agent mainly against Gram-positive bacteria and some fungi. Bactericidal activity was due to an approved membrane disturbing effect on the peptidoglycan layers of the bacterial cell wall [7–9]. Due to presence of an outer membrane consisting of lipopolysaccharide, lysozyme is ineffective against Gram-negative bacteria, and consequently various methods are available to expand the activity, such as conjugation and combination with a permeation enhancing agent [10]. Therefore, its successful formulation in a stable oral solid dosage form may contribute to managing and controlling many diseases caused as a result of food contamination.

Compared to single unit solid dosages, multiparticulate dosages, for example pellets, are acquiring definite priority for many reasons, such as anticipated gastric emptying time, reduced riskiness of dose dumping, spherical shape and hence easiness to coat, adjustable release designs, as well as even and predictable distribution through the gastrointestinal tract (GIT), resulting in enhanced drug dissolution, which leads to increased bioavailability with low inter- and intra-subject variations [11–13]. Accordingly, multiparticulates are the most suitable for the development of an orally ingested solid dosage form to deliver a macromolecular drug.

The pelletization process is an agglomeration procedure that converts the homogenized powders of a drug and excipients into relatively high density, free-flowing spherical or semi-spherical units of narrow size distribution called pellets, with a dimension of 500-1500 μm [14–16]. Among the pellet production methods, the extrusion and spheronization method is used frequently and is widely considered as a potential future method, due to its ability to produce more dense spheres

with higher drug-loading capacity while retaining their small size, and thus the process is considered more efficient than other pelletization methods [17–19]. For pellets to be layered or coated, roundness [20] and aspect ratio [21] are the most investigated parameters to evaluate the suitability of pellets for sub-coating/coating processes as well as for estimating flowability. However, in the case of a macromolecular drug such as lysozyme, the mechanical and thermal stresses encountered during processing into an effective dosage form should be carefully evaluated [22] since these stresses might have a reverse effect on enzyme activity when the moisture content is high, especially during high shear pelletization [23]. Accordingly, the implementation of a specially instrumented chamber for the analysis of temperature and relative humidity and the design of experiment as tools of quality by design could be vital to assessing the risk factors encountered during the pelletization process and represent helpful tools for understanding the effect of different process parameters and material characteristics on the quality of the produced pellets.

Similarly, polyols such as glycerol, propylene glycol, trehalose and mannitol can be used to stabilize lysozyme conformation through their exclusion from the vicinity of macromolecules, and thus the interaction with proteins is unfavourable. Among them, mannitol was found to stabilize lysozyme mainly against aggregation [24,25]. Therefore, mannitol can be used to preserve the lysozyme conformation by preventing the misfolding of the enzyme, and hence the activity during the various processing steps of pelletization might be maintained.

The present study is the continuation of a previous experiment series [1,22], aimed at developing a multiparticulate system for lysozyme delivery. The aim of the present phase of the study is to investigate the impact of the material attributes on the process design space, and furthermore to clarify the impact of mechanical and thermal stress encountered during the various production steps on the enzyme activity of the prepared pellets.

2. Materials and methods

2.1. Materials

Two brands of Egg-white lysozyme (Mw: 14.3 kDa), with different stabilities Lysoch-40000 (Handary SA, Brussels, Belgium) here referred to as “Lyso-1” and a CAT. HY-B2237/CS-7671 (MedChemExpress, Hungary), referred to as “Lyso-2” were used as model proteins. The scanning electron micrographs (Fig 1a, b) showed no considerable differences in the size or morphology of Lyso-1 and Lyso-2, but there are considerable differences between their stability, since Lyso-1

may be stored under ambient conditions up to 24 month, while Lyso-2 should be stored at -20 °C. According to our hypothesis, the poorer thermal stability may negatively affect enzymatic activity, but with careful design, it is still possible to produce pellets of the required quality. Conventional crystalline (Hungaropharma Ltd., Budapest, Hungary) and directly compressible spray-dried (Pearlitol SD-200, Roquette Pharma, France) mannitol (referred to as CM and SDM, respectively) served as conformation stabilizers. The CM have big columnar/tabular crystals with sharp edges, and wide particle size distribution (Fig. 1c), while SDM have spherical particles with more narrower size distribution (Fig. 1d), which may be considered as aggregates of columnar microcrystals. Further difference that while CM is pure β form, SDM is a mixture of α and β forms, which exerted smaller elasticity in compression studies. Microcrystalline cellulose (Avicel pH 101, FMC Biopolymer, Philadelphia, USA; Mw: approx.. 160 kDa) referred to as MCC, was utilized as pellet former and drug carrier, lyophilized *Micrococcus lysodeikticus* (Sigma-Aldrich, USA) was used as standard reagent for lysozyme activity investigation.

2.2. Methods

2.2.1. Design of Experiments

The experimental design was made according to 2^3 full factorial design with one central point. The impeller speed (x_1), liquid addition rate (x_2) and extrusion speed (x_3) were studied as independent factors, while the optimization parameters were: enzyme activity (y_1), pellet hardness (y_2), moisture content (y_3), roundness (y_4) and aspect ratio (y_5). The effect of factors and factor interactions on the optimization parameters was evaluated statistically by using Statistica v. 13.5. software (Tibco Statistica Inc, Palo Alto, CA, USA).

2.2.2. Homogenization

100 g of powder mixtures composed of Lyso-1 or Lyso-2, CM or SDM and MCC in a ratio of 1:4:5, respectively, were homogenized in a Turbula mixer (Willy A. Bachofen Maschinenfabrik, Basel, Switzerland) for 10 minutes. The composition of the homogenized powder mixtures is shown in Table 1.

2.2.3. Estimation of water quantity

The amount of the granulating liquid used to produce a moisturized plastic mass of a powder mixture to be ideal for extrusion/spheronization is critical, since the liquid quantity will affect the quality of the extrudate, as well as the hardness and the sphericity of the particles [26,27]. Therefore, the water quantity required for wet granulation was estimated by determining the Enslin

number, which is a simple measurement and equals the quantity of water absorbed by 1 g of the powder mixture (ml/g). The equipment is simple and consists of a G4 glass filter and a pipette with 0.01 accuracy. 0.5 g of each homogenized powder mixture was dispersed as a monolayer over a filter paper which was placed horizontally at the bottom of the glass filter, and the maximum water uptake was determined. The experiment was performed three times.

2.2.4. Wet granulation

The homogenized mixtures of the powder samples were wetted and kneaded in a ProCepT 4M8 high shear granulator (ProCepT nv. Zelzate, Belgium) at different impeller speeds (x_1) and liquid addition rates (x_2). The impeller and chopper were located vertically; the processing parameters are illustrated in Table 2 below. 60 ml of purified water was added at different rates (-1, 0 and +1 level), followed by 60 s wet massing time. Wet granulation and kneading were performed in a specially designed Teflon granulation chamber (Opulus Ltd., Szeged, Hungary) equipped with three immersed PyroDiff® sensors (channel 1, 2 and 3) located at different heights from the bottom of the chamber and at different distances from the chamber wall, as demonstrated in Figure 2. They were connected directly to a computer via an interface, and four calibrated PyroButton-TH® sensors (ISO 17025) were equipped on the chamber wall at different positions (at the bottom, 42mm, 65mm and 87mm from the bottom). The sensors were programmed to continuously measure the change in temperature and relative humidity (RH) in every 2 seconds during the granulation, at a temperature and humidity resolution of 0.0626 °C and 0.04% RH, respectively. In addition, the infrared temperature sensor of the high shear granulator was set to continuously measure the temperature during granulation. The kneaded wet mixtures were preserved in tightly closed containers until extrusion/spheronization.

2.2.5. Extrusion and spheronization

The kneaded wet masses were extruded with a single-screw extruder (Caleva Process Solutions Ltd., Sturminster Newton, UK), equipped with an axial screen of 4-mm thickness and having 16 dies with a diameter of 1 mm. The extruder was equipped with a laboratory-developed water-cooling jacket to maintain the temperature constant during extrusion. Extrusion was performed at different extrusion rates (x_3) (70, 95 and 120 rpm) and at a constant feeding rate of 5 g/min. The obtained extrudates were preserved in moisture-retentive containers to prevent water loss.

The extruded samples were spheronized with a Caleva MBS spheronizer (Caleva Process Solutions Ltd., Sturminster Newton, UK). 17 g of each extruded sample was spheronized at a speed of 2000 rpm for 1 minute (according to the preformulation study). The obtained pellets were dried for 24 hours under ambient conditions (22°C±1, 31±2 % RH).

2.2.6. Pellet activity investigation

The biological activity (y_1) of the prepared pellets was measured via the degradation of lyophilized *Micrococcus lysodeikticus* by using a Genesys 10 S UV-VIS Spectrometer (ThermoScientific, Waltham, MA, USA). 70 mg of lyophilized bacteria was suspended in 100 ml of phosphate buffer (pH 6.24), the base absorption at 450 nm was around 0.7. The absorption of the bacterial suspension was measured for 5 minutes before each test to reduce the error arising from bacterial sedimentation. 100 mg of pellet or 10 mg of crude lysozyme were dissolved in 25 ml of phosphate buffer. 0.1 ml of pellet/or crude lysozyme solution was added to 2.5 ml of bacterial suspension and shaken for 20 seconds in a quartz cuvette, then the change in bacterial absorption was measured for 5 minutes. Pellet activity was calculated from the percentage degradation of the bacterial cells relative to crude lysozyme activity as a reference.

2.2.7. Hardness and deformation

Deformation force (y_2) and behaviour were investigated with a custom-made texture analyzer; the equipment and its software were developed at the University of Szeged, Institute of Pharmaceutical Technology and Regulatory Affairs. The equipment consists of a sample holder at the base and a probe moving vertically at a speed of 20mm/min. The test was conducted in the force range of 0-50 Newtons. The deformation characteristics and breakage force of pellets (n=20 for each sample) were obtained and the average and SD were calculated.

2.2.8. Moisture content

The moisture content (y_3) of the prepared pellets was measured by using a Mettler-Toledo HR73 (Mettler-Toledo Hungary Ltd., Budapest, Hungary) halogen moisture analyzer. The moisture content of approximately 0.5 g of each sample was measured in triplicate at the drying temperature of 105°C until a constant weight was obtained.

2.2.9. Size and shape study

The size and shape (y_4 and y_5) of the prepared samples were investigated by using a system consisting of a stereomicroscope and a ring light with a cold light source (Carl Zeiss, Oberkochen, Germany). The images were analyzed with Leica Quantimet 500 C image analysis software (Leica Microsystems, Wetzlar, Germany), and the area, length, breadth, perimeter, convex perimeter, roundness and aspect ratio of 100 pellets were measured or calculated. The roundness and aspect ratio are the most common shape parameters used to characterize the shape of pellets and are calculated by the applied Leica Q500MC software using the following equations:

$$\text{Roundness} = Perimeter^2/(4*\pi*Area*1.064) \quad (1)$$

$$\text{Aspect ratio} = d_{max}/d_{min} \quad (2)$$

where *Perimeter* is the total length of boundary of the feature, *Area* is calculated from the total number of detected pixels within the feature, while d_{max} and d_{min} are the longest and shortest Feret diameter measured.

2.2.10. Scanning Electron Microscopy

The morphology and size of the raw materials were investigated by Scanning Electron Microscope (SEM) (Hitachi 4700, Hitachi Ltd., Tokyo, Japan). The samples were coated with a conductive gold thin layer by a sputter coating unit (Polaron E5100, VG Microtech, UK), images were taken at an accelerating voltage of 10.0 kV, the used air pressure was 1.3– 13 mPa during the analyses. The particle size was determined using Image J 1.47 t (National Institute of Health, Bethesda, MD, USA) software.

3. Results and Discussion

3.1. Investigation of the change in temperature and RH% during the kneading phase

In our previous studies [1,22] an unexpected effect of the applied kneading parameters was observed on the enzyme activity of the prepared pellets. One of the key objectives of the present study was to clarify the reason for this effect via the use of a special kneading chamber, which enabled the determination of the variations of temperature and relative humidity at representative points of the chamber. In order to reveal if the chamber wall (Teflon) has any effect on the behaviour of the materials, we repeated the previous experiments obtained in a glass chamber with the same quality of materials (composition C1).

The variation of the recorded values was attributed to the sensor location and its distance from the impeller rotation axis, as illustrated above (Fig. 2), and the detected local temperatures may be considerably higher than the general temperature recorded by the granulator's own built-in sensor [23]. The variation of temperature and humidity with the various experimental settings can be found in the supplementary material.

As expected, at a lower (-1) level of impeller speed, the internal chamber temperature was relatively low and constant throughout the wet kneading period, which is advantageous for processing thermolabile molecules. Under these conditions, the liquid addition rate has less impact on the temperature value, as demonstrated in Figure 3, where the difference between the starting and final temperatures is displayed throughout the various experimental settings.

When operating at a higher (+1) level of impeller speed (process 3 and 4), the liquid addition rate exhibited more considerable influence on the temperature distribution inside the chamber, although it was only partially able to compensate for the temperature increase which was induced by mechanical friction between the kneaded mass, impeller, and chamber wall. Overall, the temperature change mostly depends on impeller speed, and it exhibited a linear relation with the investigated parameters (Eq. 3).

$$y_{\Delta T} = 15.409 + \mathbf{10.643x_1} - 3.176x_2 - 1.633x_1x_2 \quad (3)$$

$R^2 = 0.99836$ Adj $R^2 = 0.99344$ MS Residual = 0.828245

In contrast, the variation of system relative humidity did not follow the expectations since the increasing liquid addition rate resulted in a reduced increment of relative humidity. This unexpected phenomenon may be due to the insufficient equilibration time of the moisture content on the solid-air interface. The highest increment in the system RH% values was recorded in the central point (Fig. 4). The low adj. R^2 and high curvature coefficient of the corresponding Equation 4. indicates poor model quality, which may be due to a strong nonlinear relationships between the tested factors and RH%.

$$y_{RH\%}=53.6158-2.3742x_1-2.2925x_2 \quad (4)$$

R^2= 0.80017 Adj R^2=0.20067 MS Residual=31.4534 Curvature=10.148

The increasing impeller speed also decreases the general increment in the system RH%, which may indicate that more intensive mixing promotes the uniform distribution of moisture, which increases the amount of the surface adsorbed fraction. Nevertheless, at a lower impeller speed, RH% was comparable in the whole granulation chamber, but increasing impeller speed resulted in greater RH% variation with a rapid increase in RH% values throughout the granulation chamber (Figs S3 and S4 in the supplementary material). This may be due to the increased evaporation rate in the regions with elevated temperature, which is supported by the similar distribution of temperature and RH% values (Figs S1 and S3 in the supplementary material).

The results confirmed our original hypothesis that there are differences in the distribution of temperature and relative humidity inside the granulation chamber, which may result in the formation of hot spots, which represent the critically degrading microenvironment for sensitive drugs. Nevertheless, it should be noted that despite the similar tendencies, generally better enzyme activities (See chapter 3.2) were recorded than previously in the glass chamber (92.67% vs. 58.98% (5) of enzyme activity). This phenomenon may be explained by the different thermal conductivity of Teflon and glass (0.25 W/mK vs. 0.96-1.05 W/mK), which will result in less localized thermal elevation and therefore the formation of bigger hot spots in the glass chamber.

3.2. Investigation of the impact of material attributes on pellet quality

Despite the considerable variation in temperature and humidity distribution, the detected maximum temperatures (Fig. 5) are good indicators of material behavior during the kneading phase.

It is clearly visible that at low shear rates (process 1 and 2) there is no difference in the recorded temperature. In contrast, at high levels of impeller speed and low levels of liquid addition, C2 exhibited considerably lower maximum temperature compared to C1 and C3. *Schaefer and Mathiesen* and *Kristó et al.* reported that the increase in temperature in high shear granulation is mainly attributed to the conversion of mechanical energy input into heat of friction within the

moist mass [23,28]. Therefore, the lower temperature elevation upon high mechanical attrition may be due to the better deformation properties of SDM over CM.

The temperature excess arising in the case of C1 may be compensated for by the cooling effect of an increased liquid addition rate while it is related only to the presence of CM. However, if CM is combined with lyso-2 in C3, the further increasing friction results in a much higher temperature than a composite containing SD lyso-1 (C1 and C2), despite the increased liquid addition rate. In conclusion, in spite of the general physicochemical similarities and similar liquid uptake pattern (0.6 ml/g) of the SD and C form of raw materials, the material attributes showed obvious differences in thermal behavior upon the applied mechanical stress, especially at higher shear rates. This finding is supported by *Hulse* et al., who reported that despite the similarity in the thermal behavior of CM and its different forms such as SDM, a full characterization is required as a preformulation step because these polymorphs are dissimilar in their physical properties [29]. Overall, the method of raw material production (i.e. conventional crystallization, or spray drying) has an effect on the thermomechanical response upon exposure to higher mechanical stress and may considerably influence the critical quality attributes of the final product (Tables 3-5).

3.2.1. Biological activity

For a macromolecular drug (such as lysozyme) to be formulated into multiparticulates, biological activity is the most important criterion that should be retained for the finished product, particularly when manufacturing processes operate at high shear rates, usually accompanied with an elevation of temperature and high attrition. Accordingly, biological activity might be diminished as a result of protein folding or denaturation.

The statistically obtained equations describing the relationship between factors x_1, x_2 and x_3, and the optimization parameter (y_1) are listed below. The statistically significant factor coefficients are shown in bold. The second subscript number of the optimization parameters (y) refers to the composition (C1, C2 or C3). The coefficients of the factors (variables) and their interactions show the changes in the optimization parameters when the value of the variable increased from 0 to +1 level. In order to get a good fit by increasing the $_{adj}R^2$ values, some unnecessary elements have been omitted from the equations.

$$y_{11}=92.267-0.597x_1+3.314x_2-4.926x_3+3.749x_1x_2-5.550x_1x_3-2.786x_1x_2x_3 \quad (5)$$

$_{adj}R^2=0.9814 \quad MS_{Residual}=1.667 \quad$ Curv. coeff.=-3.282

$$y_{12}=96.56+\mathbf{4.00x_1+1.51x_2-1.89x_1x_2-3.00x_1x_3+4.78x_2x_3+1.18x_1x_2x_3} \quad (6)$$

$_{adj}R^2=0.9995 \quad MS_{Residual}=0.0369 \quad$ Curv. coeff.=**-12.41**

$$y_{13}=81.45-4.50x_1+1.37x_2+2.75x_3-1.49x_1x_2-1.29x_1x_3+0.46x_1x_2x_3 \quad (7)$$

$_{adj}R^2=0.9771 \quad MS_{Residual}=1.3337 \quad$ Curv. coeff.=-14.78

The average enzyme activity was relatively high (92.267% and 96.56 %) for C1 and C2 (Eqs. 5 and 6, respectively). However, while there were no statistically significant coefficients for C1, for C2 the increment of both impeller speed and liquid addition rate significantly ($p<0.05$) increased the enzyme activity (Eq. 6). A further difference is that in the case of C1 the increasing liquid addition rate clearly has a positive effect (coefficients b_1 and b_{12}) on enzyme activity by the compensation of the temperature excess caused by higher friction. In contrast, for C2 the negative value of coefficient b_{12} indicates the negative effect of a high dosing rate when ow shear rates are applied. This supports our previous conclusion [1,22,23] that the over-wetting of the enzyme increases its sensitivity to thermomechanical stress. The higher biological activity of C2 and the considerably lower enzyme activity of C3 support our argument concerning the impact of the critical material attributes, especially the deformability of particles, on the quality of the macromolecular product. Consequently, the variation in the properties of formulation excipients or a macromolecular drug results in different biological activities and different thermal behaviors in response to the elevated mechanical stress, and the differences in factor coefficients and interactions indicate that it will exert considerable impact on the design space too.

3.2.2 Mechanical properties and moisture content

All the prepared pellet samples showed fairly good breaking force (10.20 to 16.10 Newtons), making them to be qualified for the subsequent coating process, which requires the granules to be hard enough to withstand the mechanical attrition encountered during the coating process.

$$y_{21}=13.49+0.195x_1-0.440x_2-0.808x_3+0.555x_1x_2+0.173x_1x_3+0.358x_2x_3 \quad (8)$$

$_{adj}R^2=0.9654 \quad MS_{Residual}=0.0481 \quad$ Curv. coeff.=0.5500

$y_{22}=13.19+\mathbf{1.528x_1-0.778x_2-0.648x_3+0.228x_1x_2-0.248x_1x_3-0.063x_2x_3}$ (9)

$_{adj}R^2=0.9999$ $MS_{Residual}=0.0001$ Curv. coeff.=**1.568**

$y_{23}=13.89-\mathbf{0.390x_1-0.795x_2-0.928x_3-0.785x_1x_2+0.038x_1x_3}-0.023x_2x_3$ (10)

$_{adj}R^2=0.999$ $MS_{Residual}=0.0005$ Curv. coeff.=**-0.1200**

Despite the considerably high values of the coefficients, none of the factors showed statistical significance in the case of C1 (Eq. 8). In contrast, their effects on C2 and C3 were clearly significant (Eqs. 9 and 10). Increasing the impeller speed increases the hardness of C1 and C2 while decreasing the breaking force of C3, which indicates that increasing friction has a negative influence on the bonding ability of mechanically resistant particles. An increase in both liquid addition rate (x_2) and extrusion speed (x_3) decreases hardness in all cases, which may be related to the less uniform distribution of water and particle density, which considerably influences the internal texture of the pellets. The deformation of the pellets starts with a viscoelastic deformation to the increasing load. No visible change in the shape of the pellets may be observed during this stage. In the next phase, plastic deformation of the pellets results in complete crushing of the pellets (Fig. 6). In some cases, a multi-stage deformation process was observed (Fig. 6b), where the first peak indicates the presence of microfractures due to small inconsistencies or structural defects in the pellet texture without visible deformations or breakage of the pellets. Therefore, peak C, which is equal to the crushing strength, was considered as pellet hardness in all cases.

The results revealed that the observed differences in the stability, polymorphs or mechanical properties of the raw materials did not affect the water uptake pattern of the various compositions (0.6 ml/g). Therefore, the physical interactions upon liquid (water) addition and mixing were almost similar for all formulations (C1-C3) processed under the same experimental conditions and confirmed by the comparable moisture content of the formulations processed under the same conditions. In case of C1 and C2, a weaker model quality was observed, which may be related to the higher values of curvature coefficients of these compositions, which indicates certain nonlinearity of the effect of the factors. Due to the weaker fit, the resulting models should be evaluated with cautions. The most considerable effect was exerted by the extruder speed (x_3), but it was found significant only for C1 (Eq. 11). The results indicate higher extrusion rates may repulse water from the wet mass and so decrease the final MC of the pellets.

$y_{31}=0.566-0.059x_1-0.044x_2-\mathbf{0.126x_3}+0.051x_1x_2-0.036x_1x_2x_3$ (11)

$_{adj}R^2$=0.8544 $MS_{Residual}$=0.0045 Curv. coeff.=0.2038

$$y_{32}=0.670-0.178x_1+0.063x_2-0.143x_3-0.050x_1x_2+0.060x_1x_3-0.033x_1x_2x_3 \quad (12)$$

$_{adj}R^2$=0.8899 $MS_{Residual}$=0.0072 Curv. coeff.=0.1200

$$y_{33}=0.753-0.015x_1+0.068x_2-0.125x_3+0.040x_{1x2}+0.043x_1x_3-0.033x_1x_2x_3 \quad (13)$$

$_{adj}R^2$=0.9688 $MS_{Residual}$=0.0008 Curv. coeff.=0.0775

According to the literature, *Colley* et al. reported that increasing the moisture content of pellets is accompanied by increasing their breaking force up to a certain moisture content, and then further moisture will reduce their breaking hardness [30]. However, the increase in the moisture content in a formulation which contains macromolecules is problematic because it reduces the long-term stability and adversely affects biological activity [31]. Generally, the moisture content of all the prepared samples was good (max.1.1%) and could be maintained by appropriate packaging and storage conditions.

3.2.3. Roundness and aspect ratio

The preformulation study showed that the maximum spheronization time was one minute, therefore it was kept constant for all the prepared samples as a result of the incorporation of a higher amount of polyols, which are hygroscopic and have a tendency to develop electrostatic charges, thus increasing the spheronization time will lead to the sticking of the pellets [32,33].

The roundness of all the produced samples of C1 and C2 was good (<1.2), while C3 showed slightly higher values (≤ 1.28). As known, the closer roundness is to 1, the closer the sample shape is to circular, thereby allowing the pellets to be coated effectively. According to the literature, the sphericity of the pellets is markedly affected by the quantity of the granulating liquid and the duration of spheronization time [34]. The liquid addition rate had a significant effect on pellet roundness for C1 and C2 (Eqs. 14 and 15), but significance should be evaluated with caution in case of C1, due to the poorer model quality. Interestingly, the increasing liquid addition rate increased the roundness of C1 and C3 while decreasing the roundness of C2. This could be attributed to the different material characteristics, especially to the different deformation characteristics of SDM. The fact that the impeller speed affected roundness significantly only for C2 and the significance of the curvature coefficient of the same composition indicate that the uniformity of liquid distribution had a significant impact on the sphericity of C2. Impeller speed

also had a significant effect on the AR of C2 and C3 (Eqs. 18 and 19), it was directly proportional to AR and the interaction of the tested factors was not significant.

$$y_{41}=1.143+\mathbf{0.010x_2}-0.005x_3-\mathbf{0.010x_1x_2}+0.005x_1x_3 \quad (14)$$

$$_{adj}R^2=0.8252 \quad MS_{Residual}=0.00005 \quad \text{Curv. coeff.}=-0.013$$

$$y_{42}=1.135+\mathbf{0.023x_1}-\mathbf{0.008x_2}+\mathbf{0.005x_2x_3}+0.003x_1x_2x_3 \quad (15)$$

$$_{adj}R^2=0.9733 \quad MS_{Residual}=0.00002 \quad \text{Curv. coeff.}=\mathbf{0.015}$$

$$y_{43}=1.183+0.015x_1+0.005x_2+0.005x_3+0.010x_1x_2+0.008x_1x_3-0.005x_2x_3 \quad (16)$$

$$_{adj}R^2=0.9419 \quad MS_{Residual}=0.00005 \quad \text{Curv. coeff.}=0.058$$

$$y_{51}=1.15+0.005x_2-0.005x_3-0.013x_1x_2+0.003x_1x_3+0.003x_1x_2x_3 \quad (17)$$

$$_{adj}R^2=0.9072 \quad MS_{Residual}=0.00003 \quad \text{Curv. coeff.}=-0.0200$$

$$y_{52}=1.181+\mathbf{0.016x_1}-0.009x_2+0.009x_3-0.004x_1x_2+0.004x_1x_3+0.004x_2x_3 \quad (18)$$

$$_{adj}R^2=0.9774 \quad MS_{Residual}=0.00001 \quad \text{Curv. coeff.}=0.0275$$

$$y_{53}=1.203+\mathbf{0.033x_1}-0.013x_2-0.013x_1x_2-0.005x_2x_3-0.001x_1x_2x_3 \quad (19)$$

$$_{adj}R^2=0.9376 \quad MS_{Residual}=0.0001 \quad \text{Curv. coeff.}=0.0275$$

3.3. Evaluation of the changes on the Process Design Space

It is clear from the results of the previous chapter (3.2) that the different compositions showed considerable differences in the response to changes in process parameters, which greatly influenced the size and position of the process design space (DS) in the modeled knowledge space. The DS was determined according to the recommendations of the Appendix 2 of the ICH Q8 guideline, using the following acceptance criteria in case of various CQAs: enzyme activity >75%, pellet hardness >15 N, moisture content <1%, aspect ratio <1.2, roundness <1.2. The contour plots of CQAs (Fig. S5-S49) and the scheme of the determination of the DS (Fig S50) can be found in the supplementary material, while Figure 7. shows the position of DS of different compositions at different extruder speeds.

The results showed that the enzymatic activity and the moisture content were the less limiting factors, and the DS were mostly determined by the overlapping portions of the acceptance areas of hardness and shape parameters. Since increasing of the extruder speed generally reduced the hardness and worsened shape parameters, this resulted in a decrease in the size of the DS of all compositions. The results showed that DS only partially overlap in case of the different formulations. A liquid feed rate of 4-5 ml / min and an impeller speed of 1100-1300 rpm and an extruder speed of 70 rpm can be used as controls for samples C1 and C2, while for sample C3 a liquid feed rate of 4-5 ml / min and 750-800 rpm minutes impeller speed can be used at an extruder speed of 70-95 rpm.

4. Conclusion

The specially designed granulation chamber equipped with seven sensors was a useful tool to precisely monitor the changes in the temperature and RH% during the course of high shear kneading. Therefore, the chamber could be used effectively to produce proteins/peptides and other thermolabile drugs, and to correlate the processing conditions with the product quality of these drugs. The continuous monitoring of the changes in temperature and RH% enables the precise determination of the critical points of differently set processes and hence could be used as a novel tool for both process analytical technology (PAT) and QbD.

This has a particular importance in case of strongly thermolabile drugs such as lysozyme. Nevertheless, despite the predominant concept according to which most technologist researchers think that the effect of mechanical attrition and elevated temperature on the processed macromolecules will end in an inactive product as a result of protein folding or deterioration, present work confirmed that lysozyme could be processed under high-shear conditions. Furthermore, we were able to prove our hypothesis that with careful design, enzyme activity can be maintained as desired even when working with less stable forms of enzyme, such as lyso-2.

It could also be concluded that the investigation of the critical material attributes is essential not only for APIs but also for excipients during the development stage of macromolecular drugs, since they have a major impact on the process temperature, and therefore on biological activity, and other product properties, which became clearer when the mechanical energy input increased. Consequently, the evaluation of the omitted design space is crucial from the aspect of the properties of the formulated materials before the large-scale production of biopharmaceuticals.

Acknowledgements

This research was supported by the EU-funded Hungarian grant EFOP-3.6.1-16-2016-00008.

Declaration of Interest

The authors declare no conflict of interest.

References

[1] T. Sovány, Z. Tislér, K. Kristó, A. Kelemen, G. Regdon, Estimation of design space for an extrusion–spheronization process using response surface methodology and artificial neural network modelling, Eur. J. Pharm. Biopharm. 106 (2016) 79–87. https://doi.org/10.1016/j.ejpb.2016.05.009.

[2] D.J. Brayden, M.-J. Alonso, Oral delivery of peptides: opportunities and issues for translation, Adv. Drug Deliv. Rev. 106 (2016) 193–195. https://doi.org/10.1016/j.addr.2016.10.005.

[3] K. Fuhrmann, G. Fuhrmann, Recent advances in oral delivery of macromolecular drugs and benefits of polymer conjugation, Curr. Opin. Colloid Interface Sci. 31 (2017) 67–74. https://doi.org/10.1016/j.cocis.2017.07.002.

[4] V. Truong-Le, P.M. Lovalenti, A.M. Abdul-Fattah, Stabilization Challenges and Formulation Strategies Associated with Oral Biologic Drug Delivery Systems, Adv. Drug Deliv. Rev. 93 (2015) 95–108. https://doi.org/10.1016/j.addr.2015.08.001.

[5] M. Bilej, Mucosal Immunity in Invertebrates, in: Mucosal Immunol., Elsevier, 2015: pp. 135–144.

[6] V.L. Hughey, E.A. Johnson, Antimicrobial activity of lysozyme against bacteria involved in food spoilage and food-borne disease., Appl Env. Microbiol. 53 (1987) 2165–2170.

[7] K. Düring, P. Porsch, A. Mahn, O. Brinkmann, W. Gieffers, The non-enzymatic microbicidal activity of lysozymes, FEBS Lett. 449 (1999) 93–100. https://doi.org/10.1016/S0014-5793(99)00405-6.

[8] S. Nakamura, A. Kato, K. Kobayashi, New antimicrobial characteristics of lysozyme-dextran conjugate, J. Agric. Food Chem. 39 (1991) 647–650.

[9] T. Yada, K. Muto, T. Azuma, K. Ikuta, Effects of prolactin and growth hormone on plasma levels of lysozyme and ceruloplasmin in rainbow trout, Comp. Biochem. Physiol. Part C Toxicol. Pharmacol. 139 (2004) 57–63. https://doi.org/10.1016/j.cca.2004.09.003.

[10] G.G. Syngai, G. Ahmed, Lysozyme: A Natural Antimicrobial Enzyme of Interest in Food Applications, in: Enzym. Food Biotechnol., Elsevier, 2019: pp. 169–179. https://doi.org/10.1016/B978-0-12-813280-7.00011-6.

[11] S. Bhaskaran, P.K. Lakshmi, Extrusion spheronization—a review, Int J Pharm Tech Res. 2 (2010) 2429–2433.

[12] S. Muley, T. Nandgude, S. Poddar, Extrusion–spheronization a promising pelletization technique: In-depth review, Asian J. Pharm. Sci. 11 (2016) 684–699. https://doi.org/10.1016/j.ajps.2016.08.001.

[13] N.R. Trivedi, M.G. Rajan, J.R. Johnson, A.J. Shukla, Pharmaceutical Approaches to Preparing Pelletized Dosage Forms Using the Extrusion-Spheronization Process, Crit. Rev. Ther. Drug Carr. Syst. 24 (2007) 1–40. https://doi.org/10.1615/critrevtherdrugcarriersyst.v24.i1.10.

[14] É. Bölcskei, G. Regdon, T. Sovány, P. Kleinebudde, K. Pintye-Hódi, Optimization of preparation of matrix pellets containing Eudragit® NE 30D, Chem. Eng. Res. Des. 90 (2012) 651–657. https://doi.org/10.1016/j.cherd.2011.09.005.
[15] M. Hirjau, A.C. Nicoara, V. Hirjau, D. Lupuleasa, Pelletization techniques used in pharmaceutical fields, Farma. 4 (2011) 4.
[16] L. Palugan, M. Cerea, L. Zema, A. Gazzaniga, A. Maroni, Coated pellets for oral colon delivery, J. Drug Deliv. Sci. Technol. 25 (2015) 1–15. https://doi.org/10.1016/j.jddst.2014.12.003.
[17] D.F. Erkoboni, Extrusion-spheronization as a granulation technique, Drugs Pharm. Sci. 81 (1997) 333–368.
[18] R. Gandhi, C. Lal Kaul, R. Panchagnula, Extrusion and spheronization in the development of oral controlled-release dosage forms, Pharm. Sci. Technol. Today. 2 (1999) 160–170. https://doi.org/10.1016/S1461-5347(99)00136-4.
[19] C.L.S. Lau, Q. Yu, V.Y. Lister, S.L. Rough, D.I. Wilson, M. Zhang, The evolution of pellet size and shape during spheronisation of an extruded microcrystalline cellulose paste, Chem. Eng. Res. Des. 92 (2014) 2413–2424.
[20] H. Rezaei, C.J. Lim, A. Lau, S. Sokhansanj, Size, shape and flow characterization of ground wood chip and ground wood pellet particles, Powder Technol. 301 (2016) 737–746. https://doi.org/10.1016/j.powtec.2016.07.016.
[21] M. Eriksson, G. Alderborn, C. Nyström, F. Podczeck, J.M. Newton, Comparison between and evaluation of some methods for the assessment of the sphericity of pellets, Int. J. Pharm. 148 (1997) 149–154.
[22] T. Sovány, K. Csordás, A. Kelemen, G. Regdon, K. Pintye-Hódi, Development of pellets for oral lysozyme delivery by using a quality by design approach, Chem. Eng. Res. Des. 106 (2016) 92–100. https://doi.org/10.1016/j.cherd.2015.11.022.
[23] K. Kristó, O. Kovács, A. Kelemen, F. Lajkó, G. Klivényi, B. Jancsik, K. Pintye-Hódi, G. Regdon, Process analytical technology (PAT) approach to the formulation of thermosensitive protein-loaded pellets: Multi-point monitoring of temperature in a high-shear pelletization, Eur. J. Pharm. Sci. 95 (2016) 62–71. https://doi.org/10.1016/j.ejps.2016.08.051.
[24] S.A. Abbas, V.K. Sharma, T.W. Patapoff, D.S. Kalonia, Opposite Effects of Polyols on Antibody Aggregation: Thermal Versus Mechanical Stresses, Pharm. Res. 29 (2012) 683–694. https://doi.org/10.1007/s11095-011-0593-4.
[25] S. Singh, J. Singh, Effect of polyols on the conformational stability and biological activity of a model protein lysozyme, Aaps Pharmscitech. 4 (2003) 101–109.
[26] Q.-B. Ding, P. Ainsworth, G. Tucker, H. Marson, The effect of extrusion conditions on the physicochemical properties and sensory characteristics of rice-based expanded snacks, J. Food Eng. 66 (2005) 283–289. https://doi.org/10.1016/j.jfoodeng.2004.03.019.
[27] J.A.C. Elbers, H.W. Bakkenes, J.G. Fokkens, Effect of amount and composition of granulation liquid on mixing, extrusion and spheronization, Drug Dev. Ind. Pharm. 18 (1992) 501–517. https://doi.org/10.3109/03639049209043708.
[28] T. Schæfer, C. Mathiesen, Melt pelletization in a high shear mixer. VIII. Effects of binder viscosity, Int. J. Pharm. 139 (1996) 125–138. https://doi.org/10.1016/0378-5173(96)04549-8.
[29] W.L. Hulse, R.T. Forbes, M.C. Bonner, M. Getrost, The characterization and comparison of spray-dried mannitol samples, Drug Dev. Ind. Pharm. 35 (2009) 712–718. https://doi.org/10.1080/03639040802516491.
[30] Z. Colley, O. O. Fasina, D. Bransby, Y. Y. Lee, Moisture Effect on the Physical Characteristics of Switchgrass Pellets, Trans. ASABE. 49 (2006) 1845–1851. https://doi.org/10.13031/2013.22271.

[31] Y.-F. Maa, P.-A. Nguyen, J.D. Andya, N. Dasovich, T.D. Sweeney, S.J. Shire, C.C. Hsu, Effect of spray drying and subsequent processing conditions on residual moisture content and physical/biochemical stability of protein inhalation powders, Pharm. Res. 15 (1998) 768–775.
[32] L. Gu, C.V. Liew, P.W.S. Heng, Wet Spheronization by Rotary Processing—A Multistage Single- Pot Process for Producing Spheroids, Drug Dev. Ind. Pharm. 30 (2004) 111–123. https://doi.org/10.1081/DDC-120028706.
[33] C. Vecchio, G. Bruni, A. Gazzaniga, Research Papers: Preparation of Indobufen Pellets by Using Centrifugal Rotary Fluidized Bed Equipment Without Starting Seeds, Drug Dev. Ind. Pharm. 20 (1994) 1943–1956. https://doi.org/10.3109/03639049409049329.
[34] K. Lövgren, P.J. Lundberg, Determination of sphericity of pellets prepared by extrusion/spheronization and the impact of some process parameters, Drug Dev. Ind. Pharm. 15 (1989) 2375–2392.

List of Figure Legends:

Figure 1. Scanning electron micrographs of lyso-1 (a), lyso-2 (b), CM (c) and SDM (d)

Figure 2. Kneading chamber showing the configuration of immersed (PyroDiff®) and PyroButton-TH® sensors

Figure 3. Temperature change in the kneading phase

Figure 4. Relative humidity change in the kneading phase

Figure 5. Maximum recorded temperature under different processing conditions for the various compositions (C1, C2 and C3)

Figure 6. (1 and 2). Typical pellet deformation curves, A and B: viscoelastic stages of deformation and C the final collapse of the pellet

Figure 7. Design space of the kneading process in case of various compositions and extruder speeds

Graphical Abstract

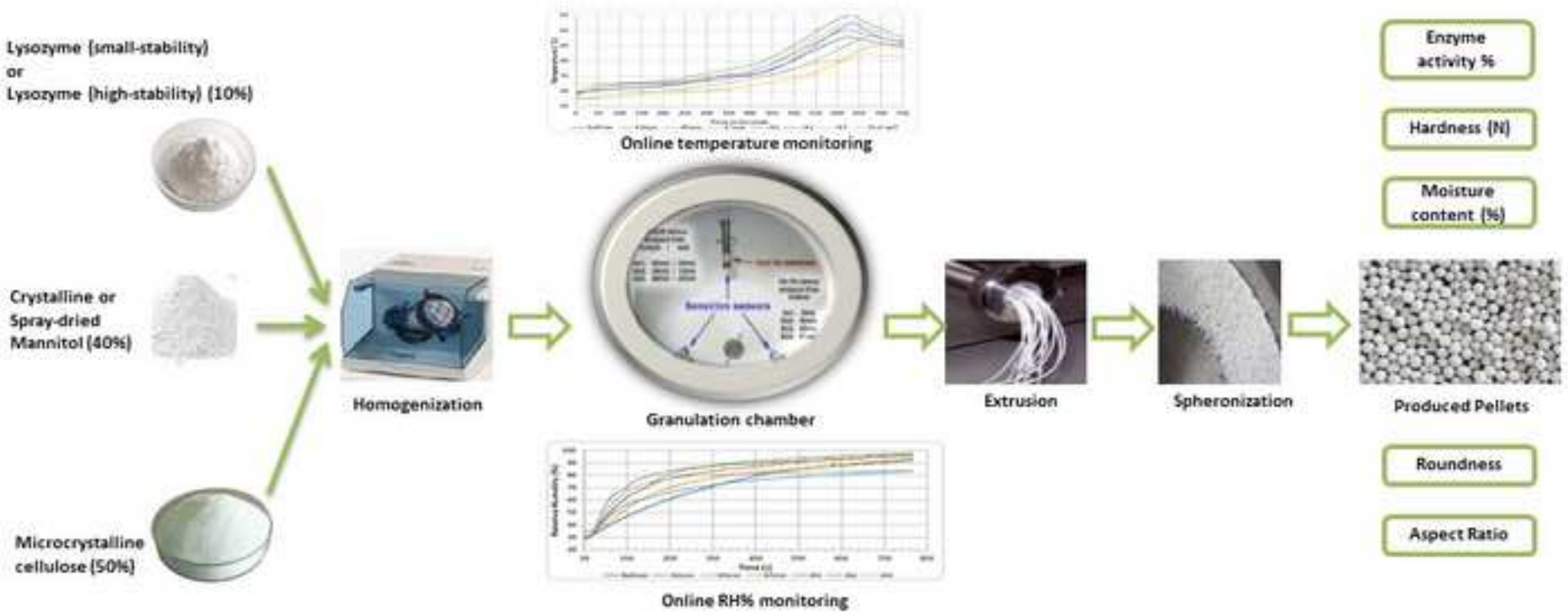

Figure

Click here to access/download;Figure;Fig1.jpg

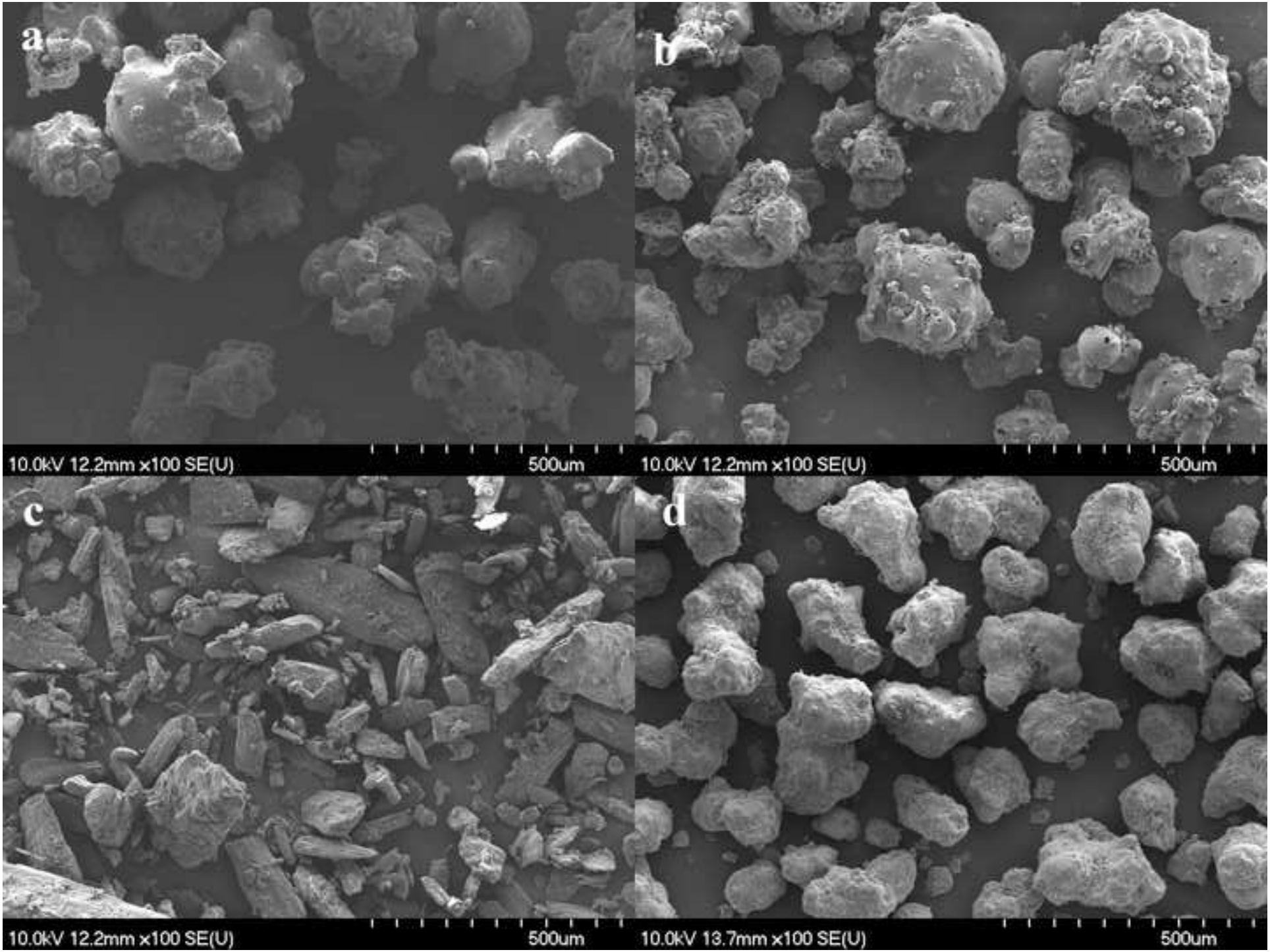

Figure

Click here to access/download;Figure;Fig2.jpg

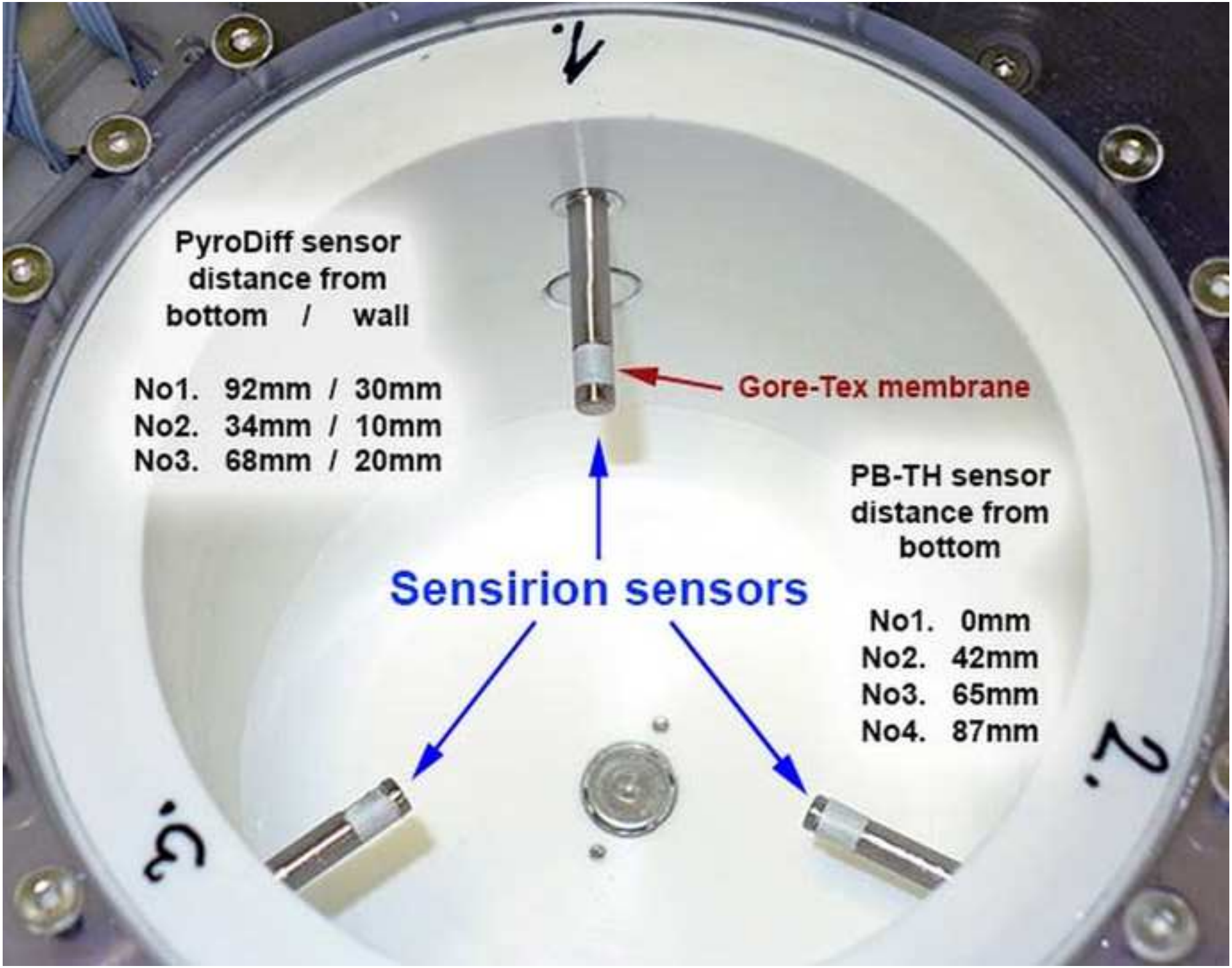

Figure

Click here to access/download;Figure;Fig3.jpg

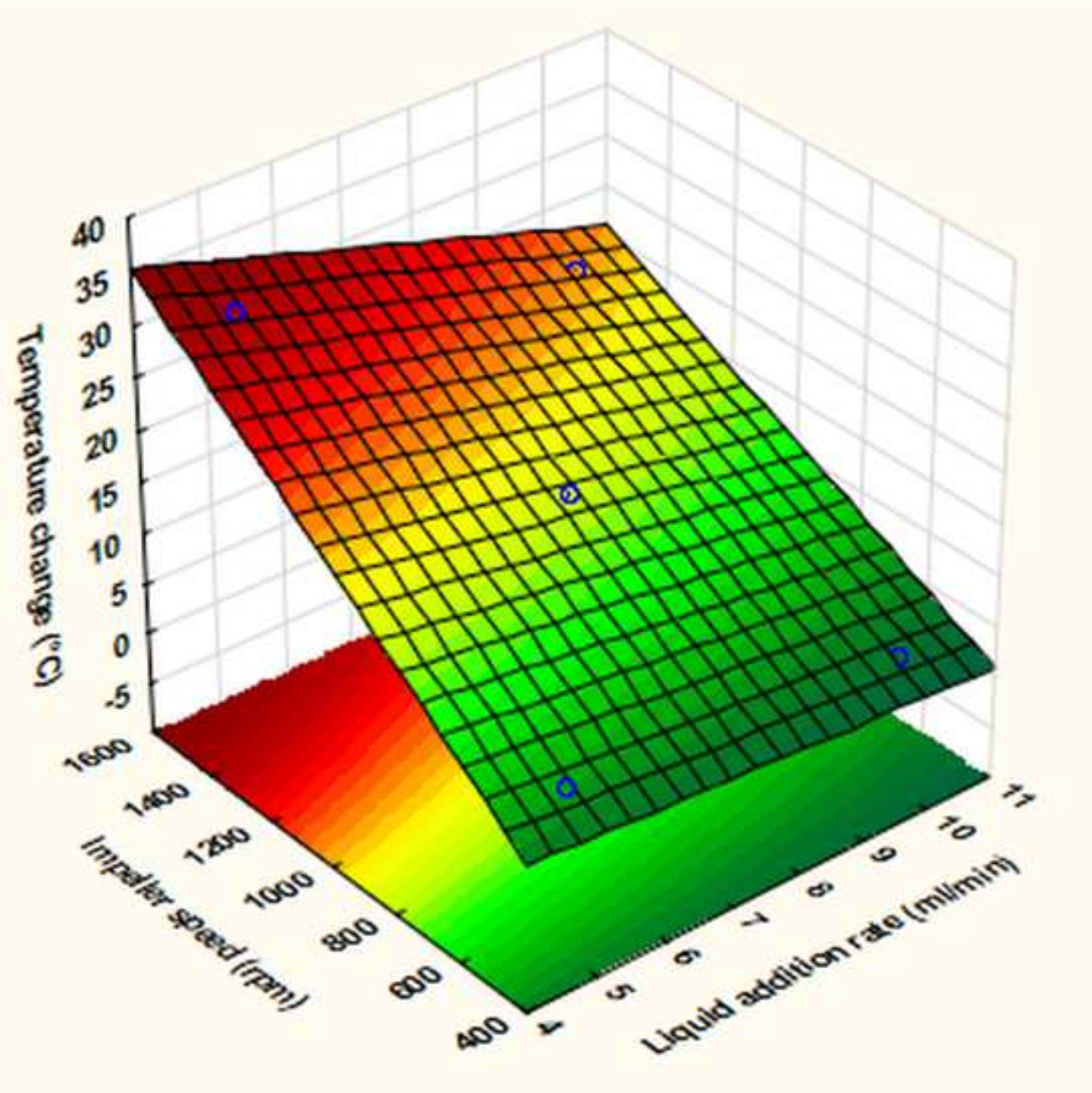

Figure

Click here to access/download;Figure;Fig4.jpg

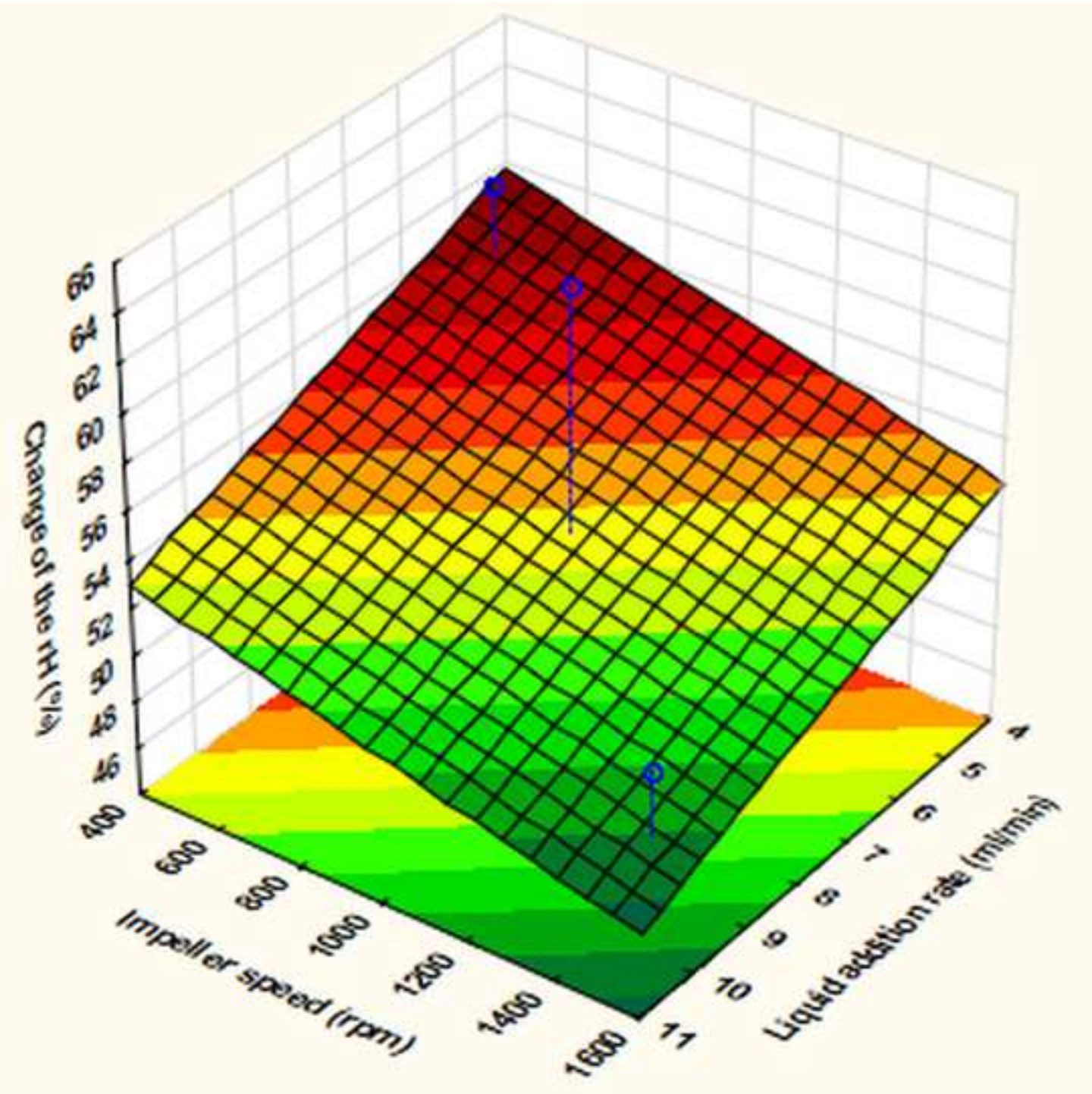

Figure

Click here to access/download;Figure;Fig5.jpg

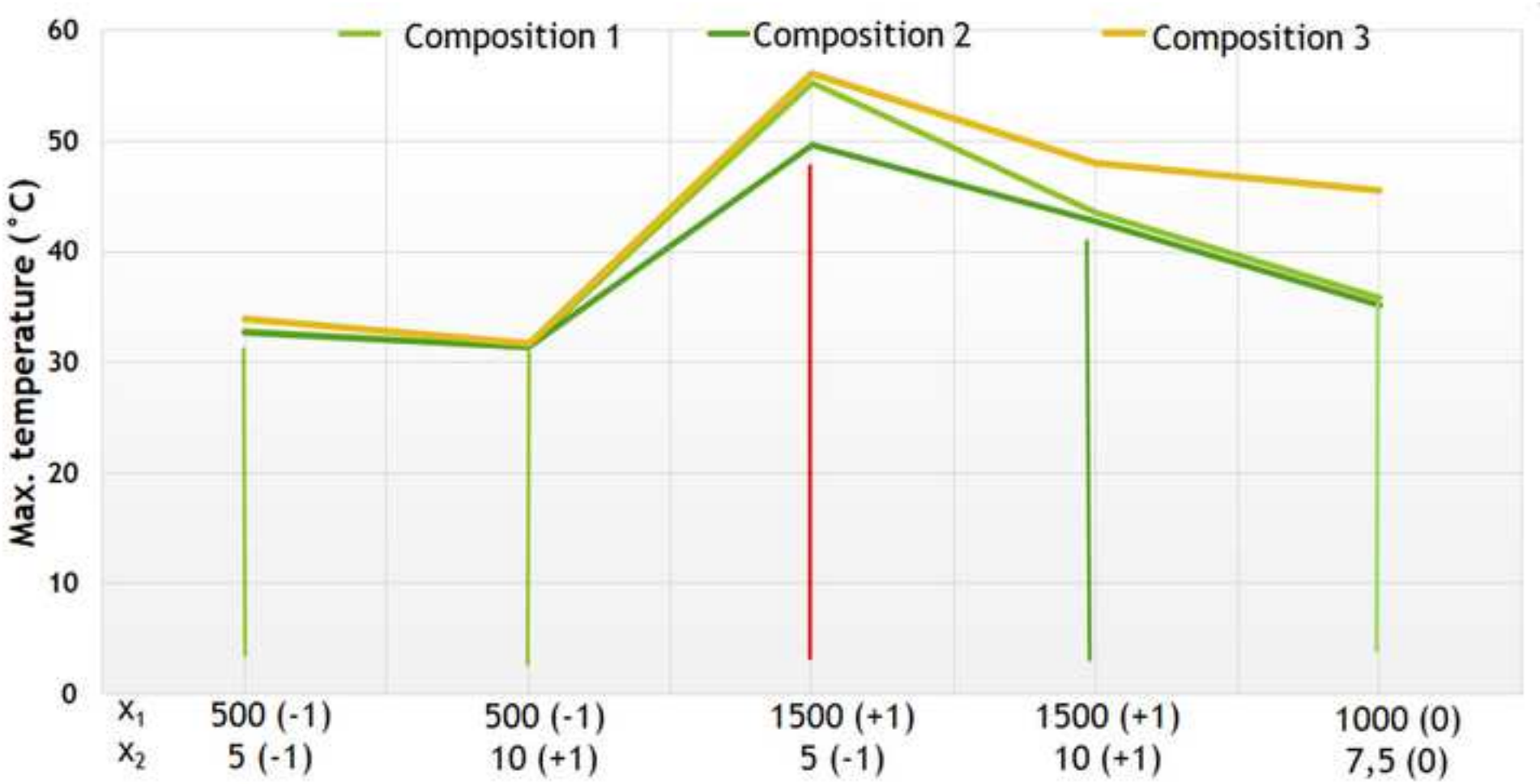

Figure

Click here to access/download;Figure;Fig6.jpg

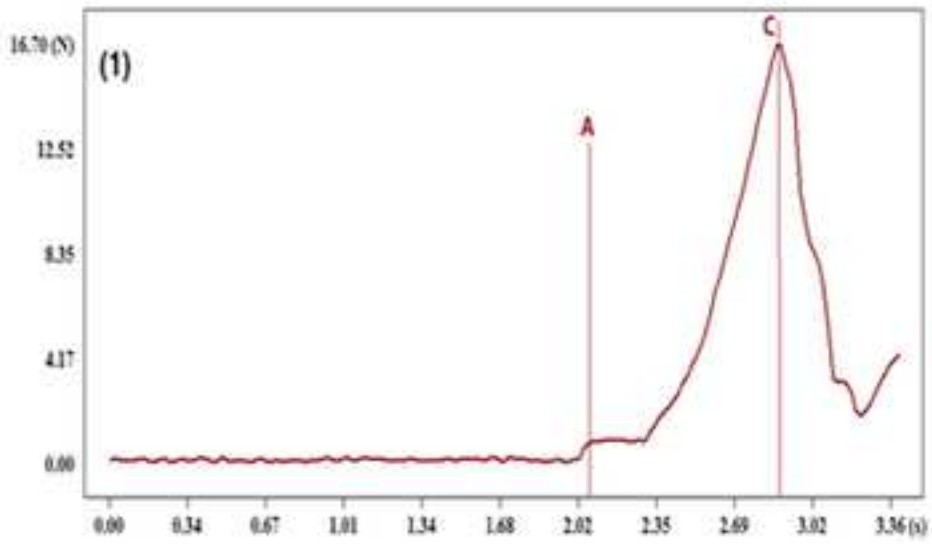

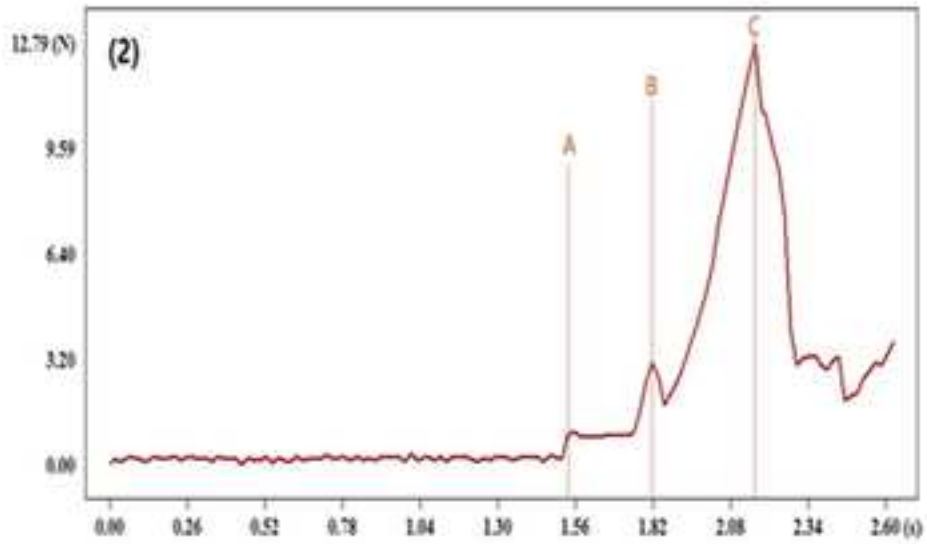

Figure

Click here to access/download;Figure;Fig7-R2.jpg

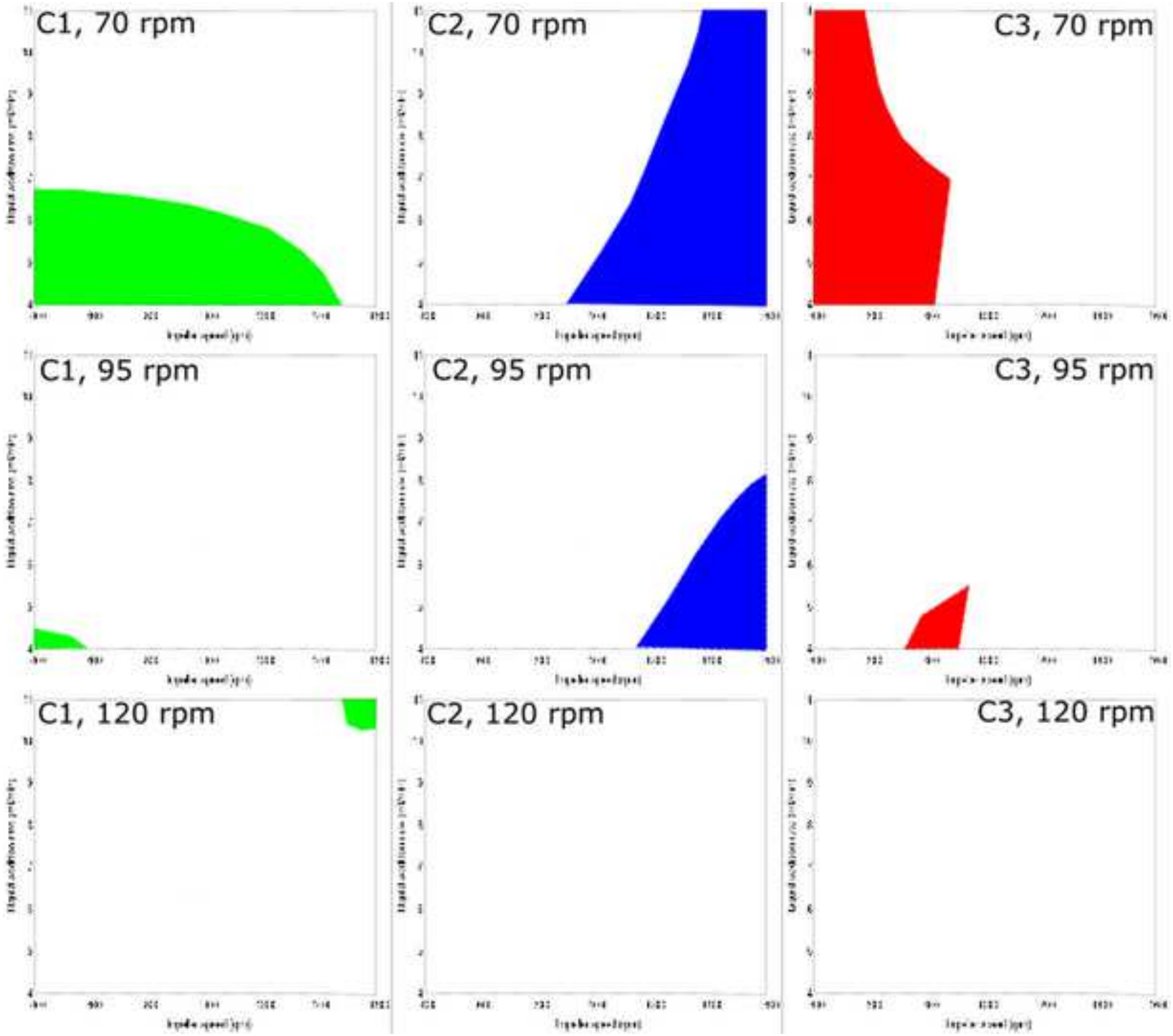

Table 1. Composition of prepared powder mixtures

Excipients	C1 (g)	C2 (g)	C3 (g)
Lyso-1	10	10	-
Lyso-2	-	-	10
CM	40	-	40
SDM	-	40	-
MCC	50	50	50

Table 2. Processing parameters of kneading, extrusion and spheronization

Kneading	**Process-1**		**Process-2**		**Process-3**		**Process-4**		**Process-5**
Impeller speed (rpm) (x_1)	500 (-1)		500 (-1)		1500 (+1)		1500 (+1)		1000 (0)
Liquid addition rate (ml/min) (x_2)	5 (-1)		10 (+1)		5 (-1)		10 (+1)		7.5 (0)
Purified H_2O (ml)	60		60		60		60		60
Chopper speed (rpm)	500		500		500		500		500
Extr./spheron.									
Extrusion speed (x_3)	70 (-1)	120 (+1)	70 (-1)	120 (+1)	70 (-1)	120 (+1)	70 (-1)	120 (+1)	95 (0)
Spher. speed (rpm)	2000	2000	2000	2000	2000	2000	2000	2000	2000
Spher. time (min)	1	1	1	1	1	1	1	1	1
Spher. amount (g)	17	17	17	17	17	17	17	17	17
Sample code	**LysC*-11**	**LysC-12**	**LysC-21**	**LysC-22**	**LysC-31**	**LysC-32**	**LysC-41**	**LysC-42**	**LysC-c**

***C**: referring to the composition; 1, 2 and 3 for the first (C1), second (C2) and third (C3) composition, respectively

Table 3. Physical properties and biological activity of C-1-pellets

Sample	Activity% (y_{11})	Hardness (N) (y_{21})	MC% (y_{31})	Roundness (y_{41})	Aspect ratio (y_{51})
Lys1-11	95.92	15.55 ±1.67	0.93 ±0.02	1.13 ±1.13	1.14 ±1.10
Lys1-12	92.75	13.03 ±1.10	0.51 ±0.03	1.11 ±0.08	1.13 ±0.06
Lys1-21	88.56	13.00 ±1.17	0.62 ±0.02	1.17 ±0.10	1.18 ±0.10
Lys1-22	111.56	11.60 ±1.24	0.44 ±0.01	1.15 ±0.10	1.16 ±0.10
Lys1-31	90.68	14.64 ±1.54	0.59 ±0.02	1.15 ±0.07	1.16 ±0.07
Lys1-32	76.46	12.50 ±1.55	0.41 ±0.03	1.14 ±0.07	1.15 ±0.06
Lys1-41	96.30	14.00 ±1.05	0.63 ±0.02	1.14 ±0.09	1.14 ±0.06
Lys1-42	85.93	13.60 ±1.41	0.40 ±0.01	1.1 5±0.12	1.14 ±0.07
Lys1-C	88.99	14.04 ±1.05	0.77 ±0.02	1.13 ±0.10	1.13 ±0.05

Table 4. Physical properties and biological activity of C-2 -pellets

Sample	Activity% (y_{12})	Hardness (N) (y_{22})	MC% (y_{32})	Roundness (y_{42})	Aspect ratio (y_{52})
Lys2-11	89.84	13.01 ±1.50	1.00 ±0.03	1.12 ±0.06	1.17 ±0.07
Lys2-12	109.96	12.33 ±1.21	0.47 ±0.02	1.12 ±0.06	1.17 ±0.08
Lys2-21	89.43	11.12 ±1.57	1.10 ±0.02	1.10 ±0.04	1.15 ±0.07
Lys2-22	97.30	10.20 ±1.53	0.82 ±0.02	1.11 ±0.06	1.17 ±0.08
Lys2-31	88.49	16.10 ±2.50	0.56 ±0.01	1.17 ±0.22	1.20 ±0.12
Lys2-32	91.91	14.44 ±2.53	0.40 ±0.01	1.16 ±0.14	1.22 ±0.10
Lys2-41	102.50	15.13 ±2.40	0.59 ±0.02	1.14 ±0.10	1.17 ±0.08
Lys2-42	103.08	13.21 ±1.50	0.42 ±0.01	1.16 ±0.16	1.20 ±0.10
Lys2-C	84.15	14.76 ±1.63	0.79 ±0.03	1.15 ±0.10	1.21 ±0.10

Table 5. Physical properties and biological activity of C-3-pellets

Sample	Activity% (y_{13})	Hardness(N) (y_{23})	MC% (y_{33})	Roundness (y_{43})	Aspect ratio (y_{53})
Lys3-11	79.00	15.23 ±1.64	0.93 ±0.03	1.17 ±0.13	1.18 ±0.11
Lys3-12	76.47	13.35 ±2.02	0.55 ±0.02	1.17 ±0.10	1.16 ±0.07
Lys3-21	84.81	15.26 ±2.10	0.94 ±0.04	1.17 ±0.13	1.17 ±0.10
Lys3-22	74.51	13.28 ±1.58	0.65 ±0.02	1.16 ±0.10	1.17 ±0.10
Lys3-31	87.18	15.95 ±2.61	0.67 ±0.05	1.16 ±0.08	1.24 ±0.10
Lys3-32	77.66	14.21 ±2.26	0.59 ±0.03	1.20 ±0.16	1.28 ±0.14
Lys3-41	92.79	12.83 ±2.18	0.97 ±0.03	1.21 ±0.14	1.22 ±0.12
Lys3-42	79.17	11.01 ±1.32	0.72 ±0.07	1.22 ±0.11	1.20 ±0.10
Lys3-C	66.67	13.77 ±1.48	0.83 ±0.03	1.24 ±0.20	1.23 ±0.10

Declaration of interests

☒ The authors declare that they have no known competing financial interests or personal relationships that could have appeared to influence the work reported in this paper.

☐The authors declare the following financial interests/personal relationships which may be considered as potential competing interests:

Yousif H-E.Y. Ibrahim: Investigation, Formal analysis, Writing - original draft; **Patience Wobuoma**: Investigation; **Katalin Kristó**: Formal analysis, Writing – Review and Editing; **Ferenc Lajkó**: Software, Resources; **Gábor Klivényi**: Software, Resources, **Béla Jancsik**: Software, Resources, **Géza Regdon jr.**: Writing – Review and Editing, **Klára Pintye-Hódi**: Conceptualization, Writing – Review and Editing; **Tamás Sovány**: Conceptualization, Methodology, Writing – Review and Editing

ANNEX - 3

Table S1. Recorded temperatures and their differences in the kneading chamber

Parameters		Start			End			Diff		
Impeller speed (rpm)	Liquid addition rate (ml/min)	Ch1 temp	Ch2 temp	Ch3 temp	Ch1 temp	Ch2 temp	Ch3 temp	Ch1 temp	Ch2 temp	Ch3 temp
500	5	24.15	24.27	24.11	29.59	31.36	29.9	5.44	7.09	5.79
500	10	27.49	27.16	27.2	29.98	31.13	29.8	2.49	3.97	2.6
1500	5	23.67	23.58	23.57	53.18	56.09	53.52	29.51	32.51	29.95
1500	10	24.38	24.62	24.54	43.72	47.61	45.33	19.34	22.99	20.79
1000	7.5	25.63	25.42	25.24	40.48	43.32	41.16	14.85	17.9	15.92

Table S2. Recorded relative humidities and their differences in the kneading chamber

Parameters		**Start**			**End**			**Diff**		
Impeller speed(rpm)	Liquid addition rate(ml/min)	Ch1 RH	Ch2 RH	Ch3 RH	Ch1 RH	Ch2 RH	Ch3 RH	Ch1 RH	Ch2 RH	Ch3 RH
500	5	33.93	33.51	34.36	88.23	103.84	92.99	54.3	70.33	58.63
500	10	38.78	40.9	40.2	86.56	97.62	87.89	47.78	56.72	47.69
1500	5	43.13	44.1	42.58	90.8	100.2	91.49	47.67	56.1	48.91
1500	10	40.02	41.54	43.08	87.11	103.46	89.33	47.09	61.92	46.25
1000	7.5	30.74	32.34	32.25	89.68	101.86	95.08	58.94	69.52	62.83

Table 4. maximum recorded temperature for all compositions for the different processes

Process	Chopper (rpm)	Impeller (rpm)	Liquid addition (ml/mi)n	T max. (°C) C 1.	T max. (°C) C 2.	T max. (°C) C 3.
First process	500	500	5	32.80	32.73	33.94
Second process	500	500	10	31.40	31.40	31.75
Third process	500	1500	5	55.30	49.63	56.13
Fourth process	500	1500	10	43.50	42.80	48.00
Fifth process	500	1000	7.5	35.85	35.12	45.50

C1, C2 and C2 referred to the first, second and third composition respectively

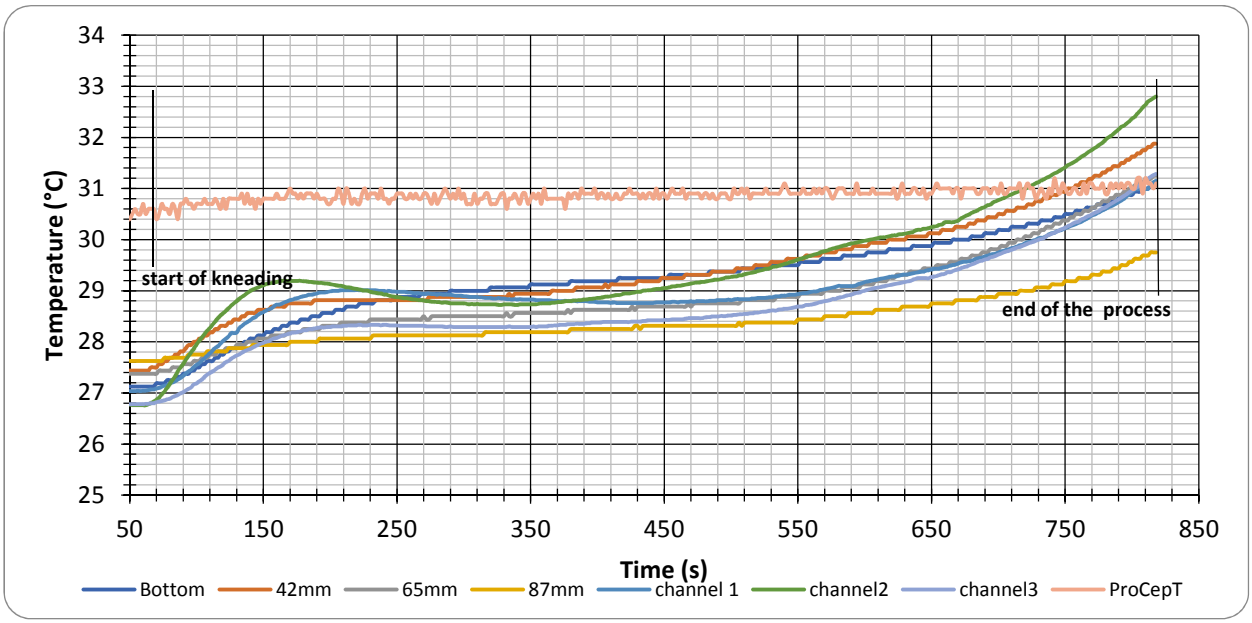

Fig. S1 schematic diagram of temperature versus time for C1- first process

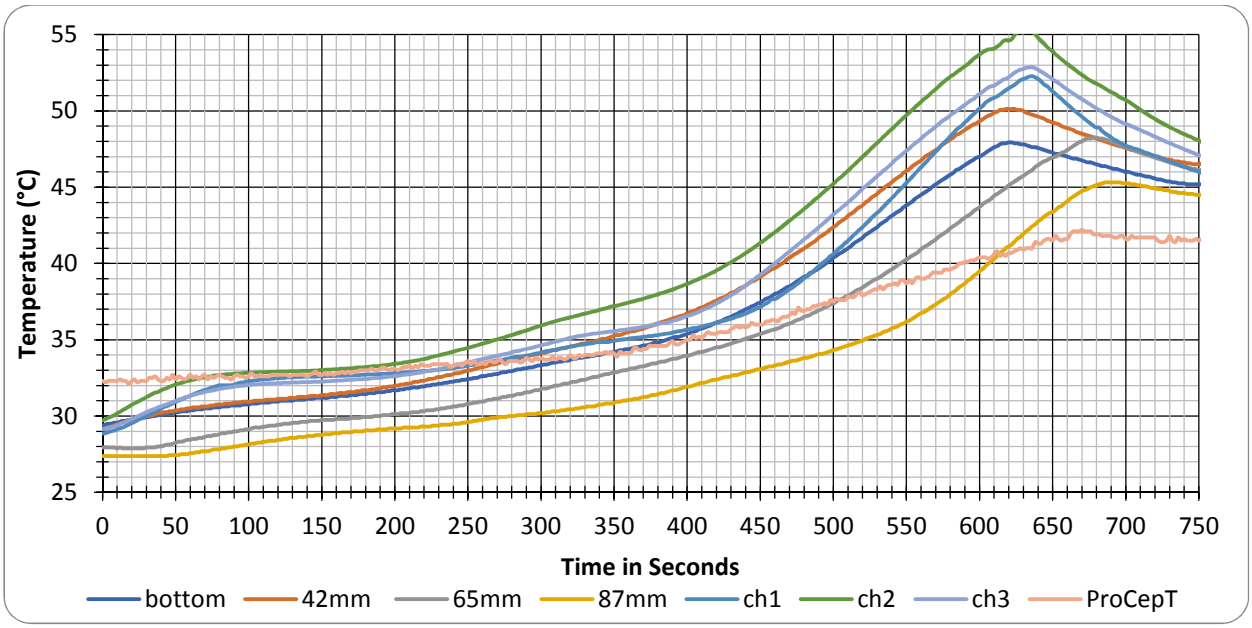

Fig. S2 schematic diagram of recorded temperatures versus time for the C1-third process

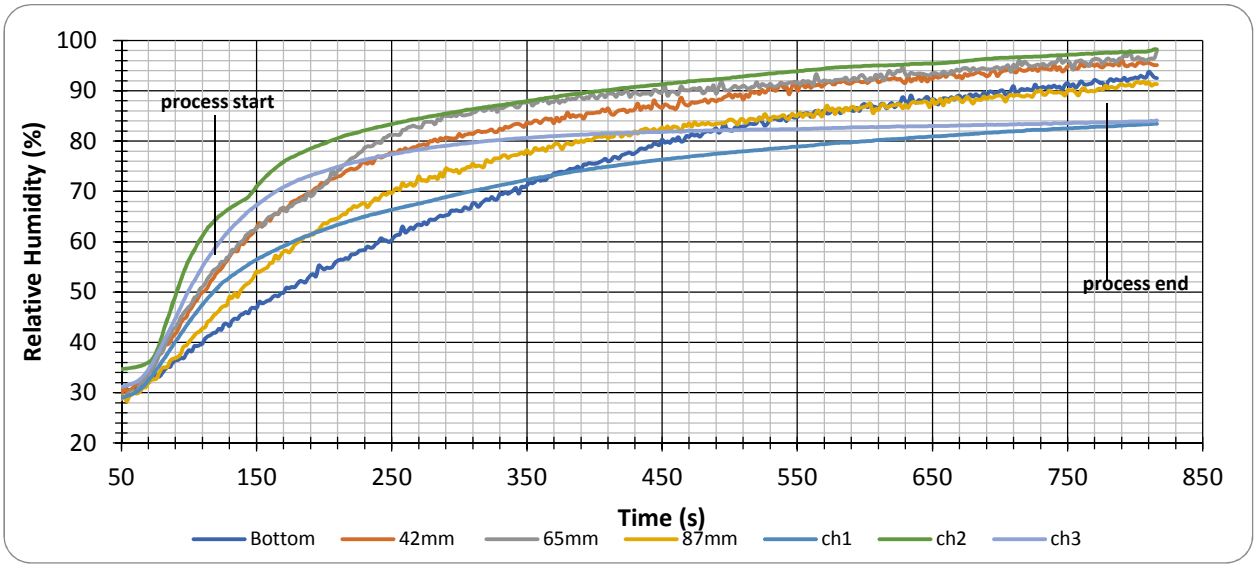

Fig. S3 schematic diagram of relative humidity% versus time for C1- first process

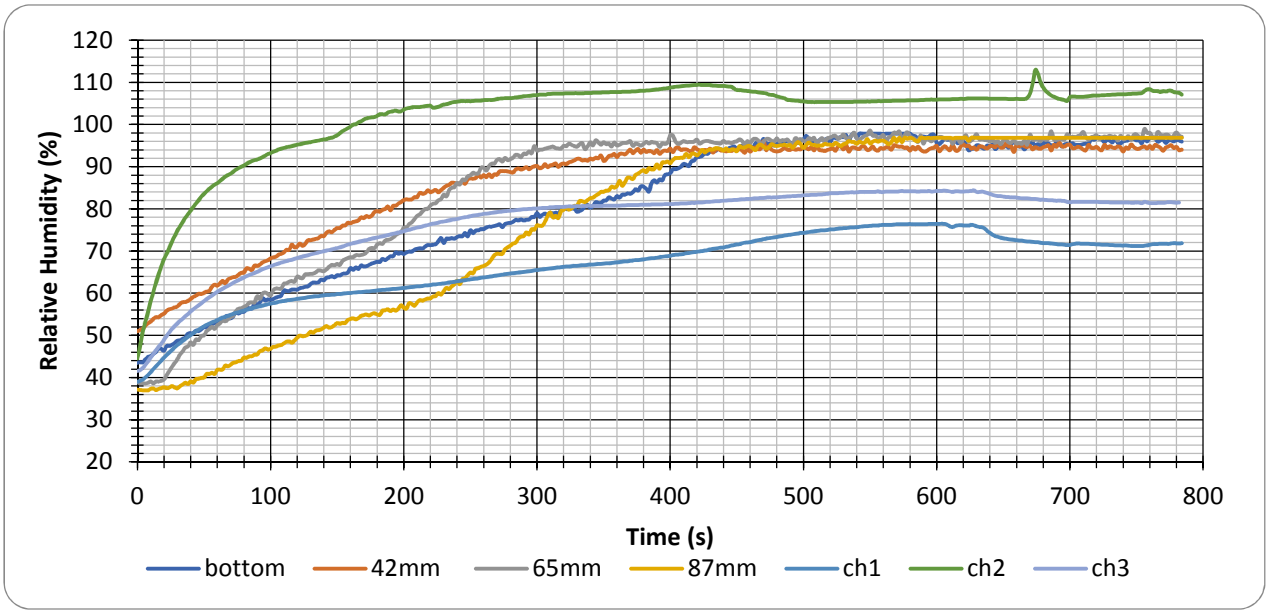

Fig. S4 schematic figure of recorded RH% versus time for the C1-third process

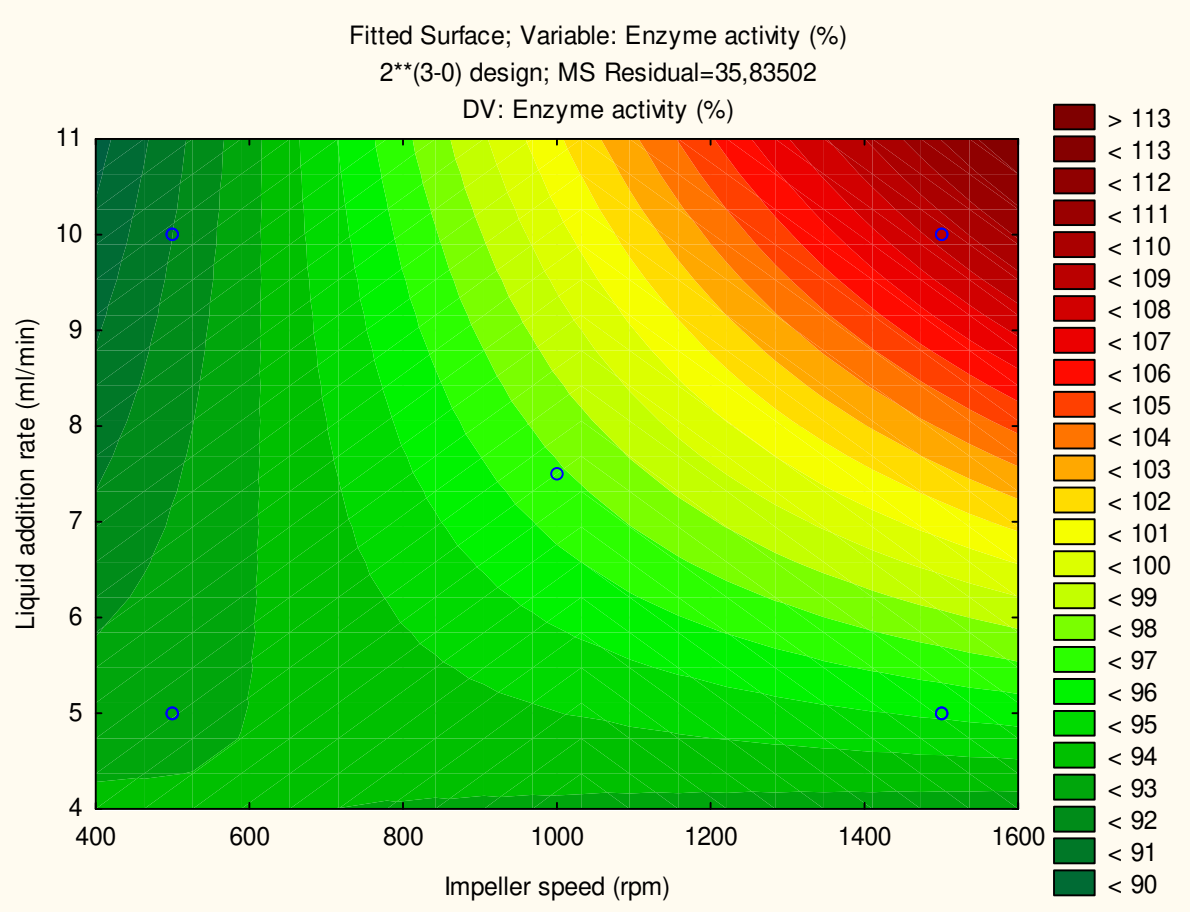

Fig. S5 Contour plot of enzyme activity of C1 at an extruder speed of 70 rpm

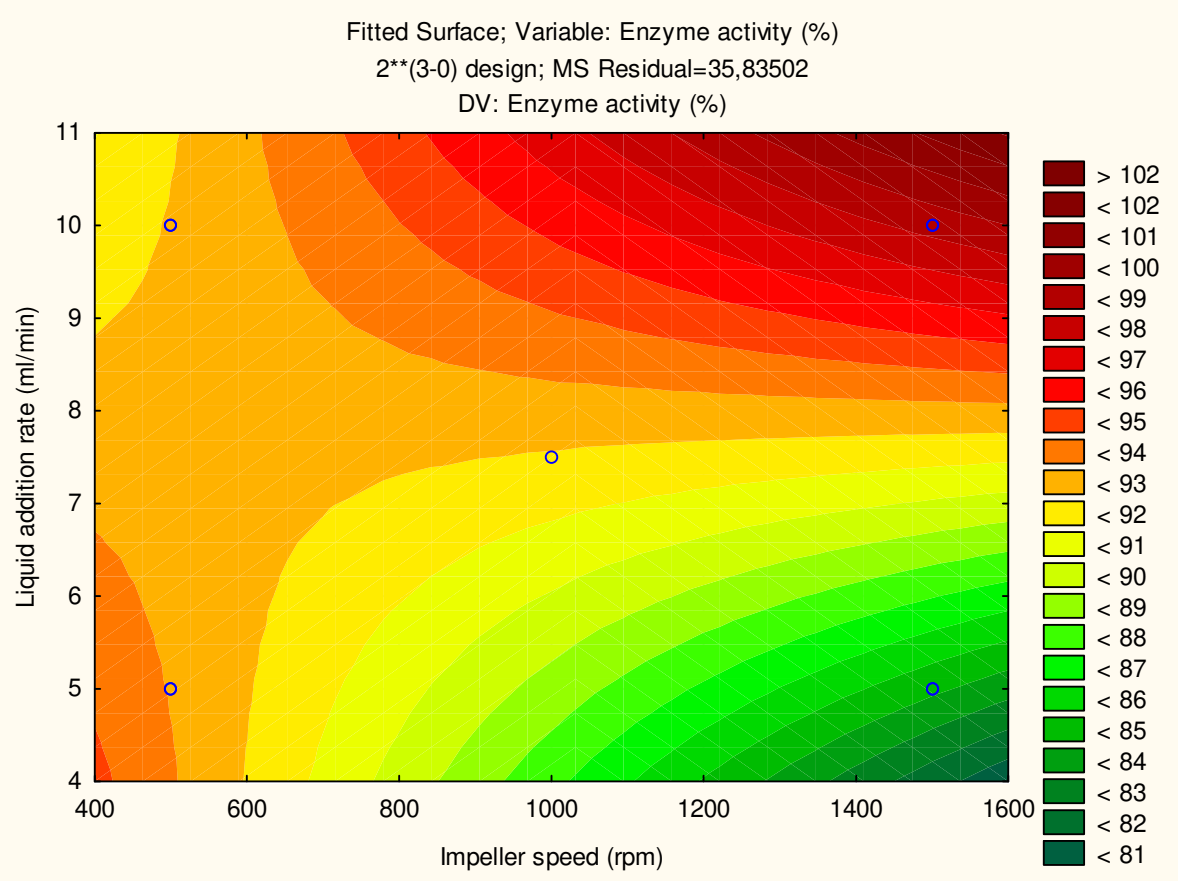

Fig. S6 Contour plot of enzyme activity of C1 at an extruder speed of 95 rpm

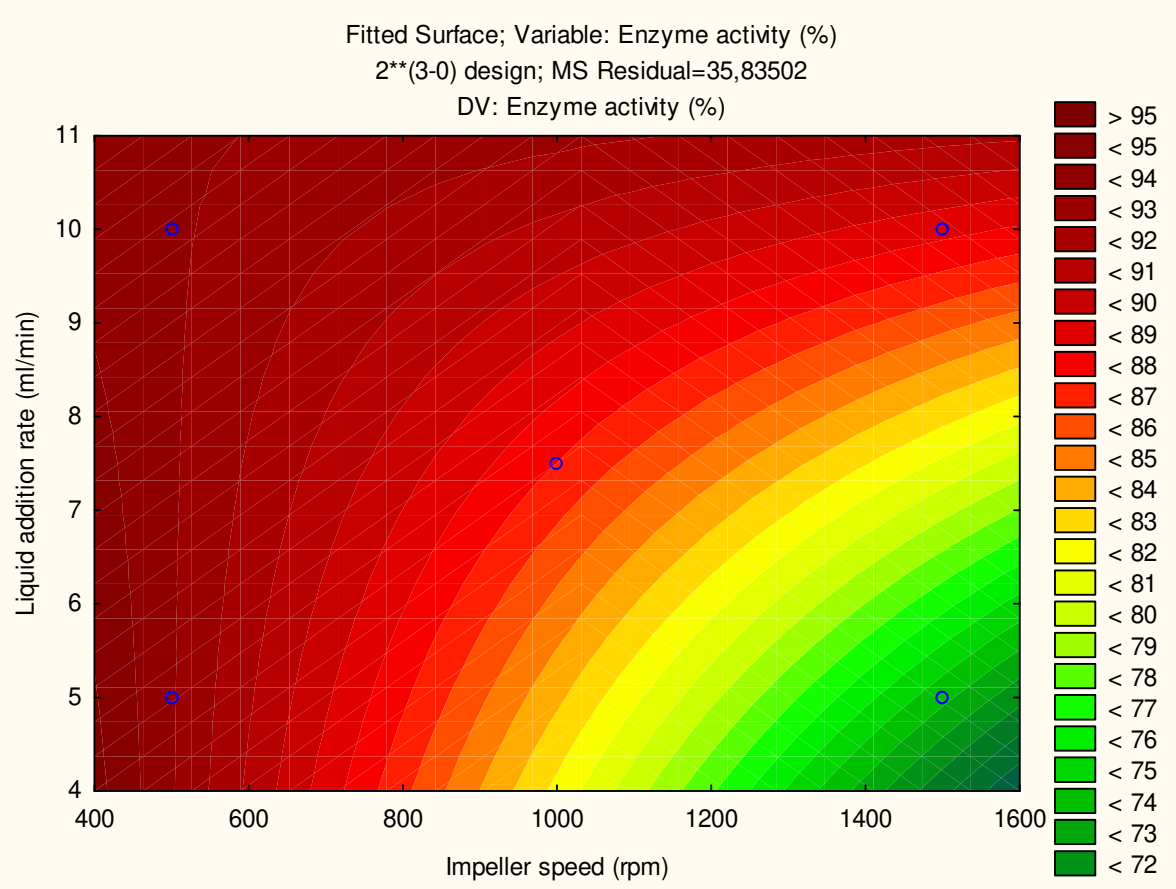

Fig. S7 Contour plot of enzyme activity of C1 at an extruder speed of 120 rpm

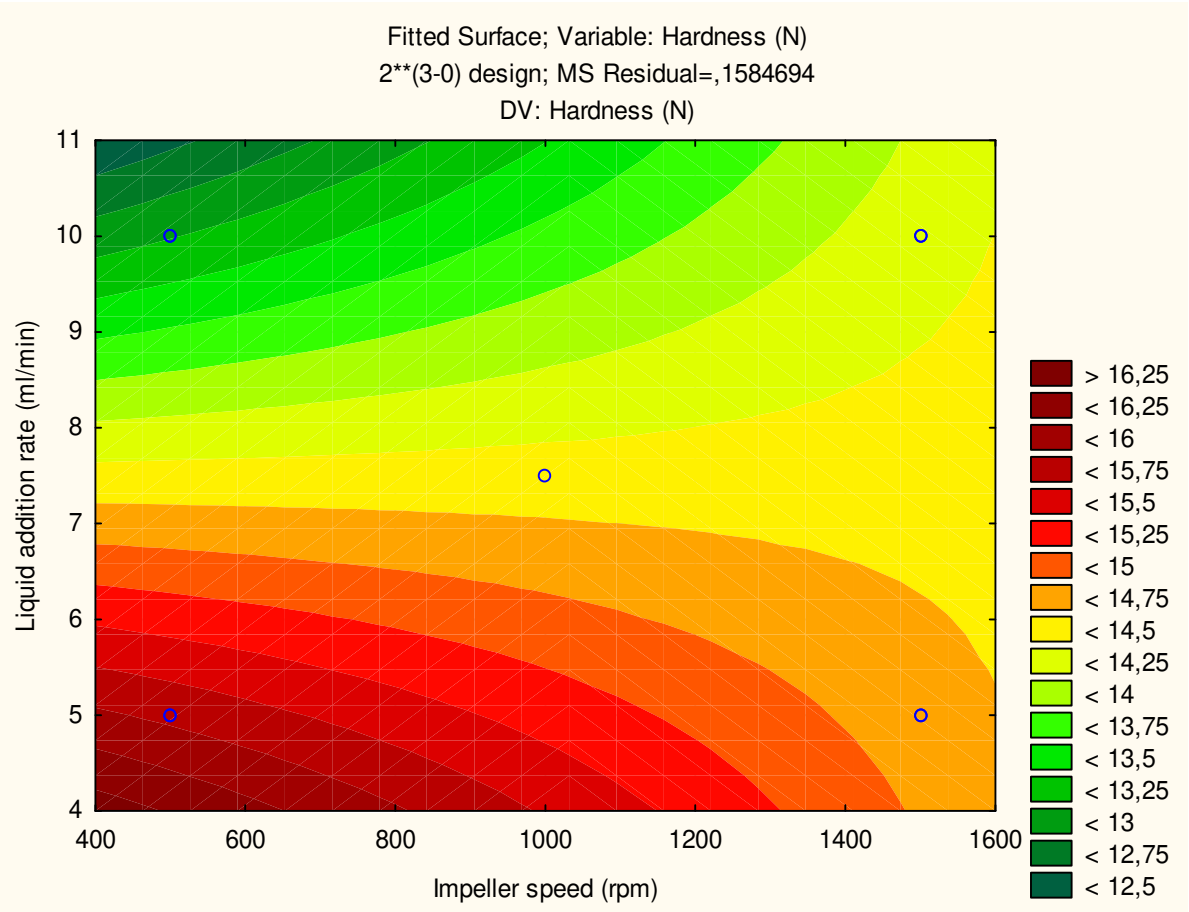

Fig. S8 Contour plot of pellet hardness of C1 at an extruder speed of 70 rpm

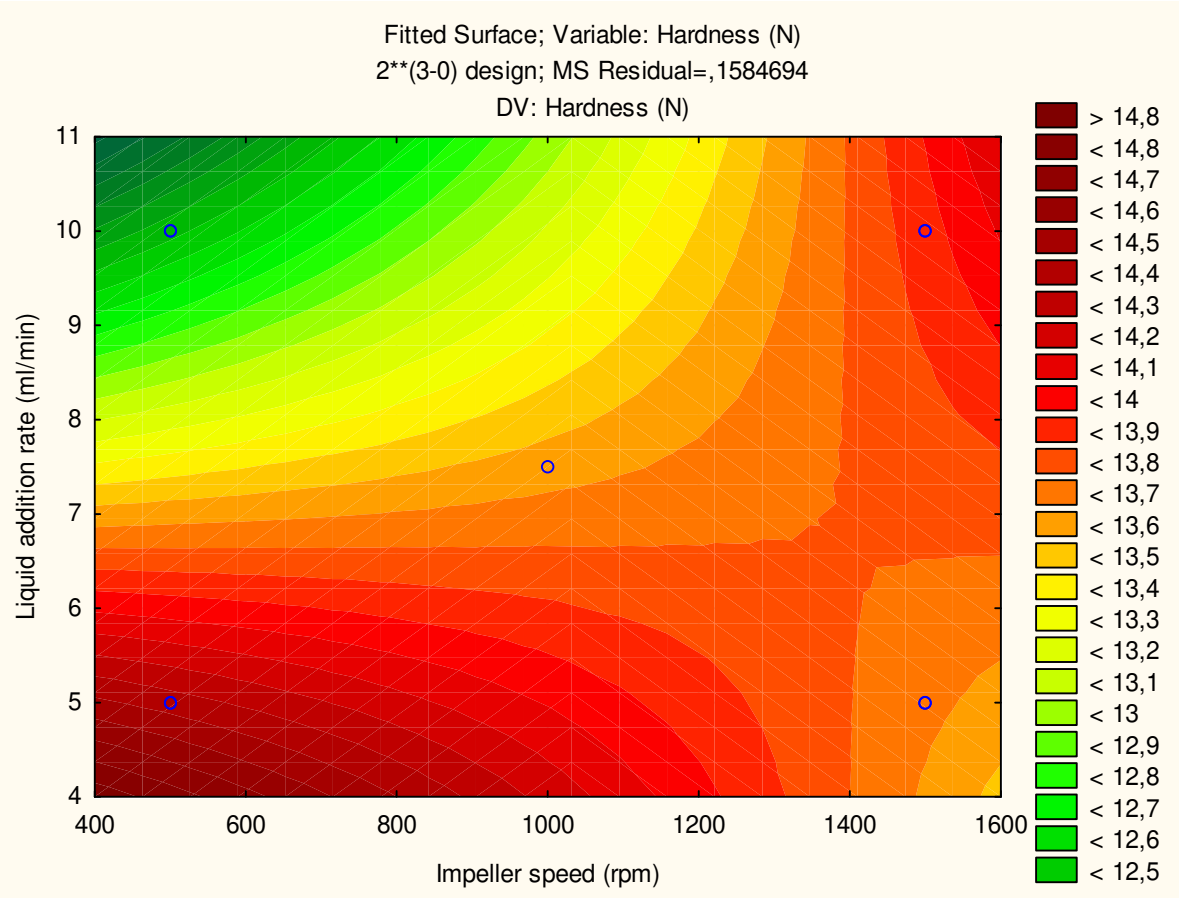

Fig. S9 Contour plot of pellet hardness of C1 at an extruder speed of 95 rpm

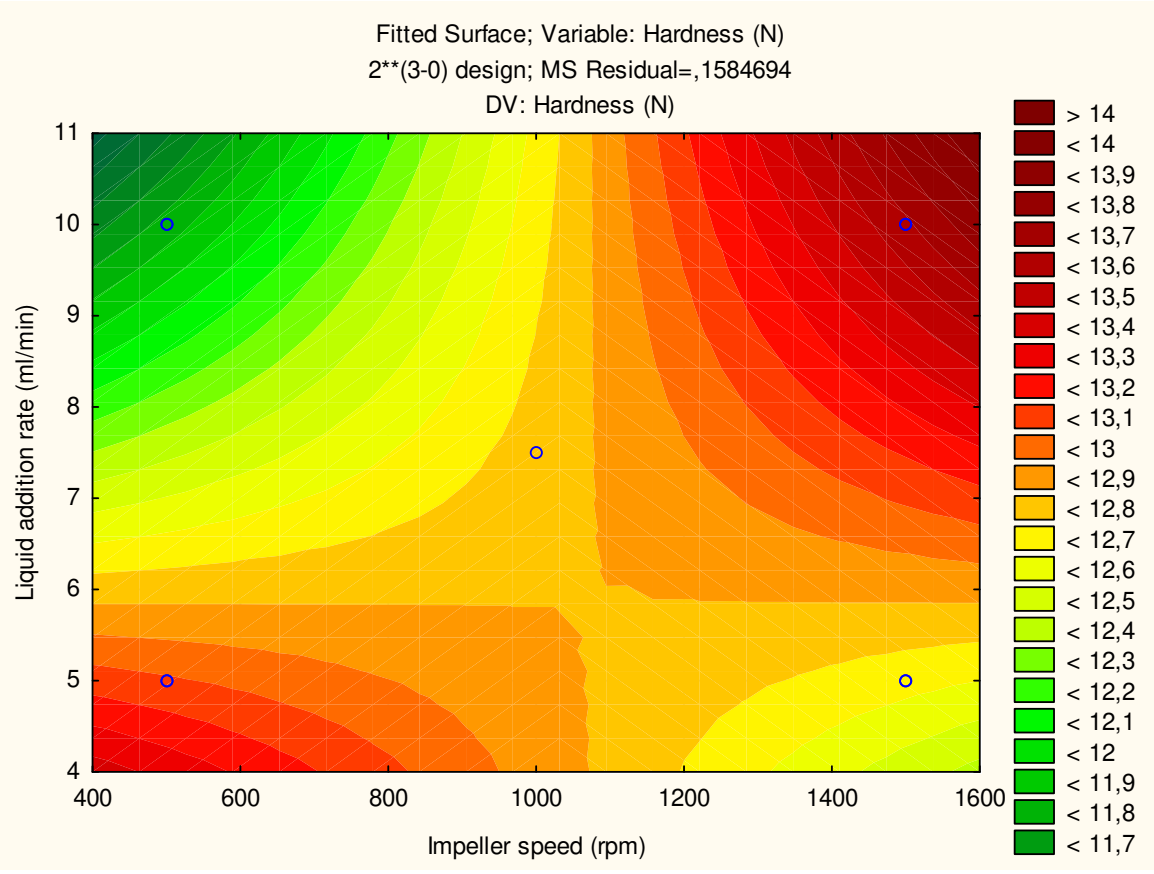

Fig. S10 Contour plot of pellet hardness of C1 at an extruder speed of 120 rpm

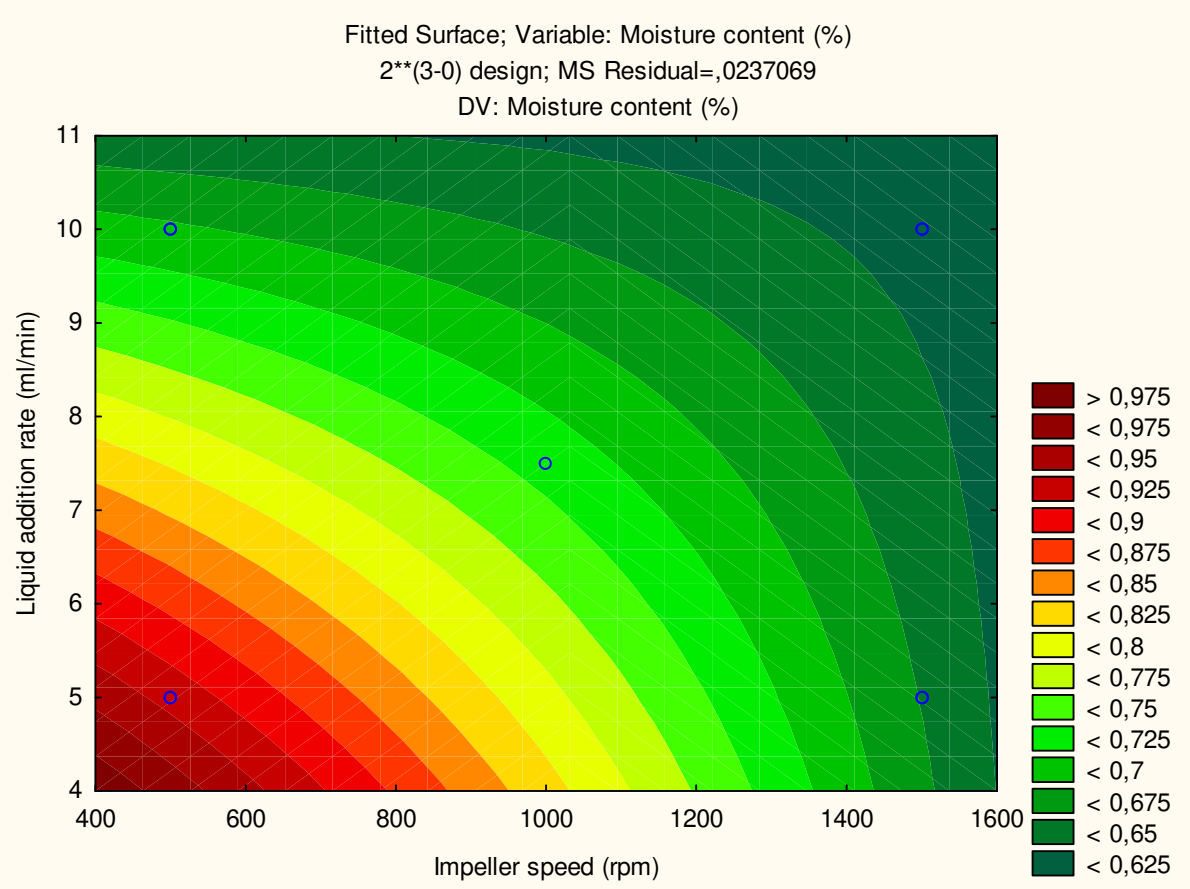

Fig. S11 Contour plot of moisture content of C1 at an extruder speed of 70 rpm

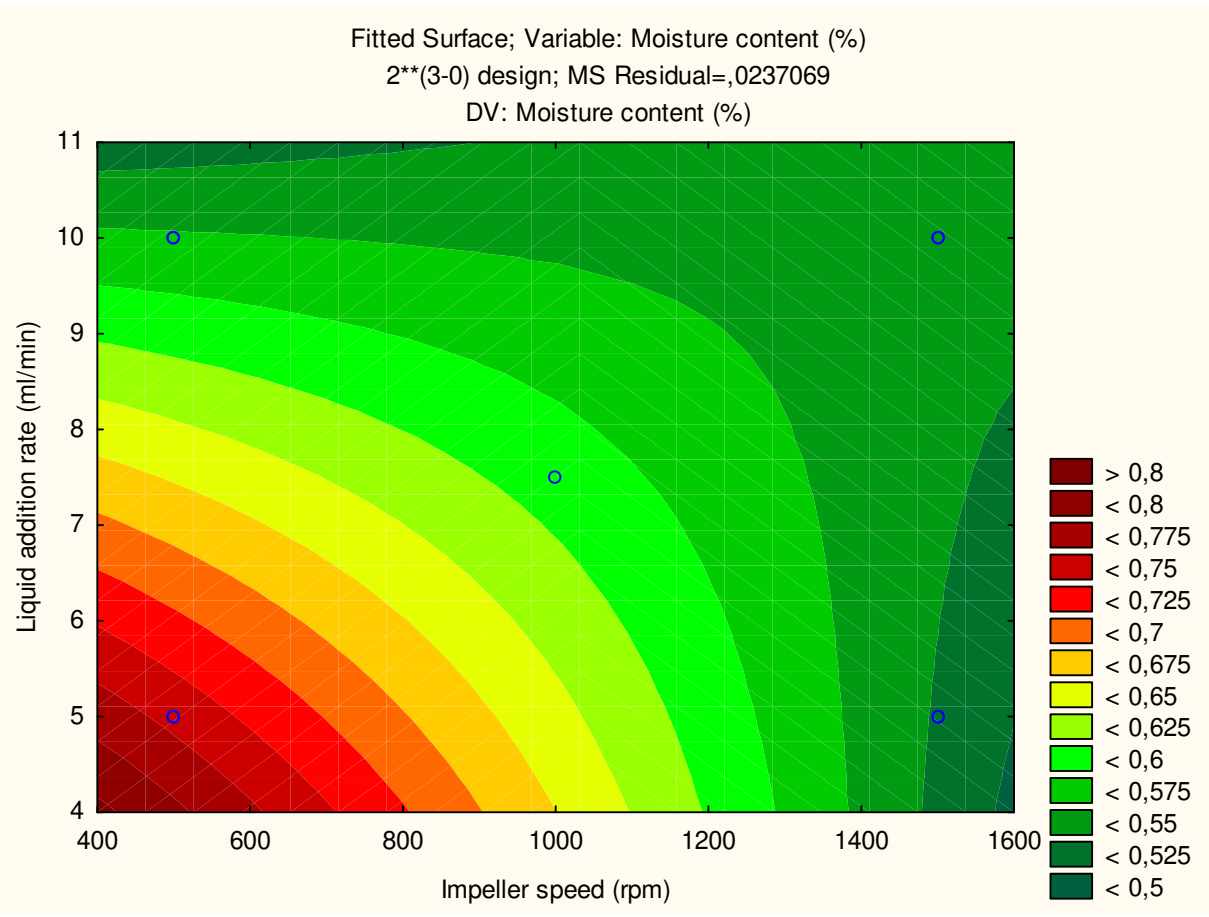

Fig. S12 Contour plot of moisture content of C1 at an extruder speed of 95 rpm

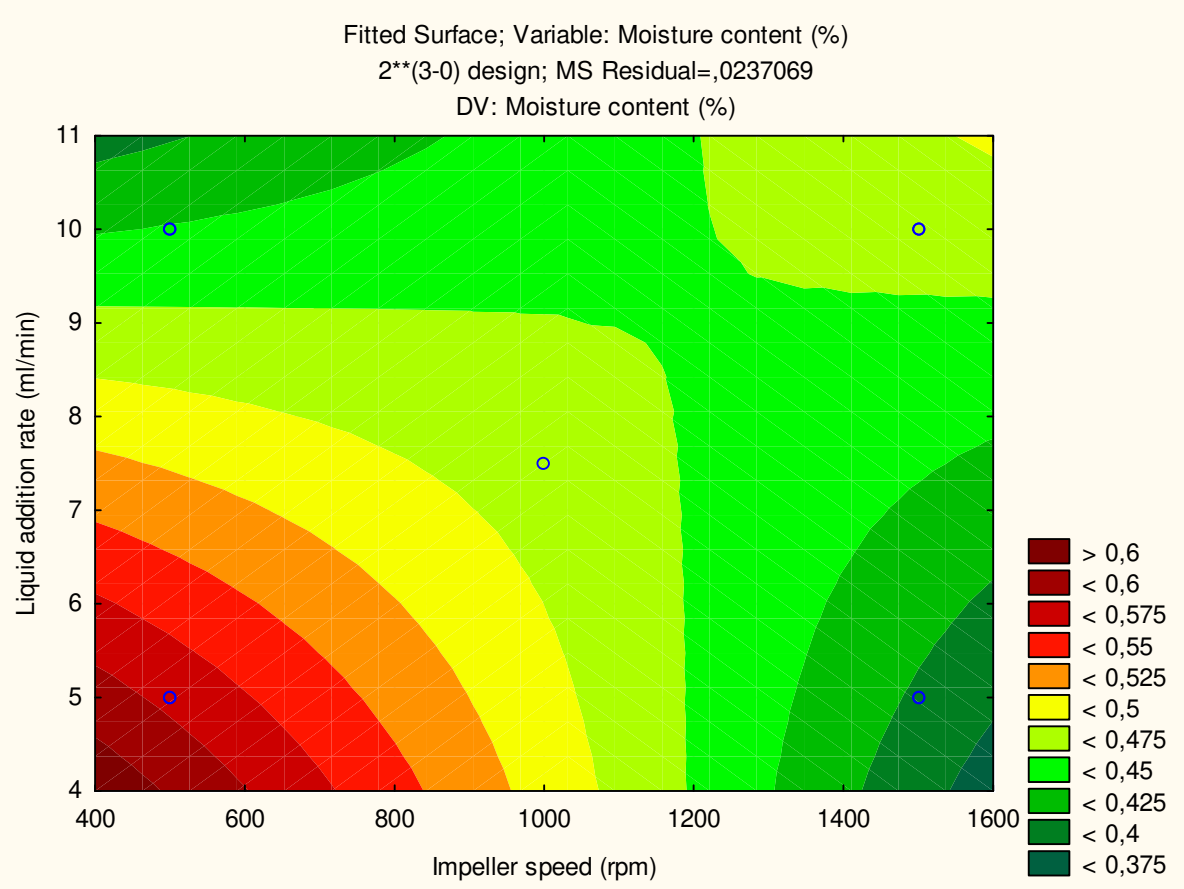

Fig. S13 Contour plot of moisture content of C1 at an extruder speed of 120 rpm

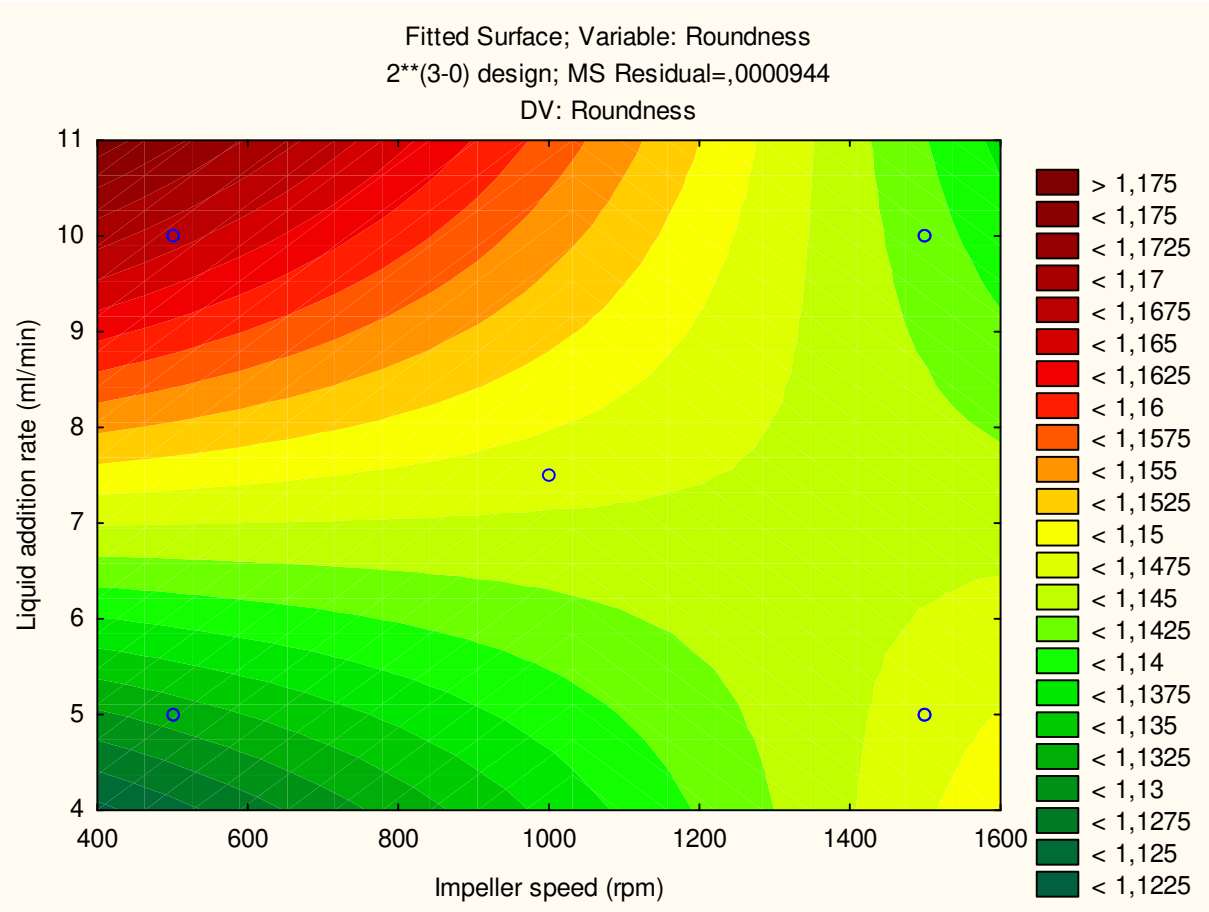

Fig. S14 Contour plot of roundness of C1 at an extruder speed of 70 rpm

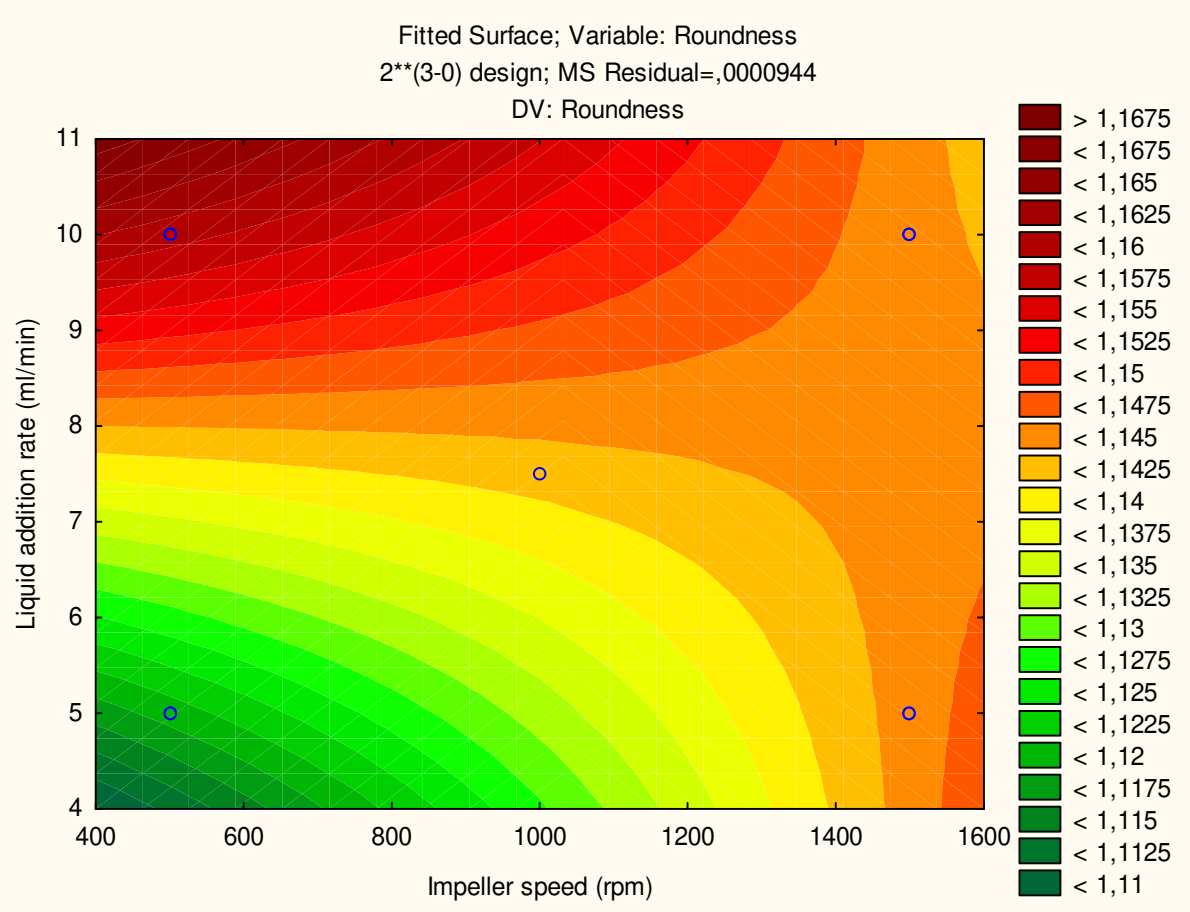

Fig. S15 Contour plot of roundness of C1 at an extruder speed of 95 rpm

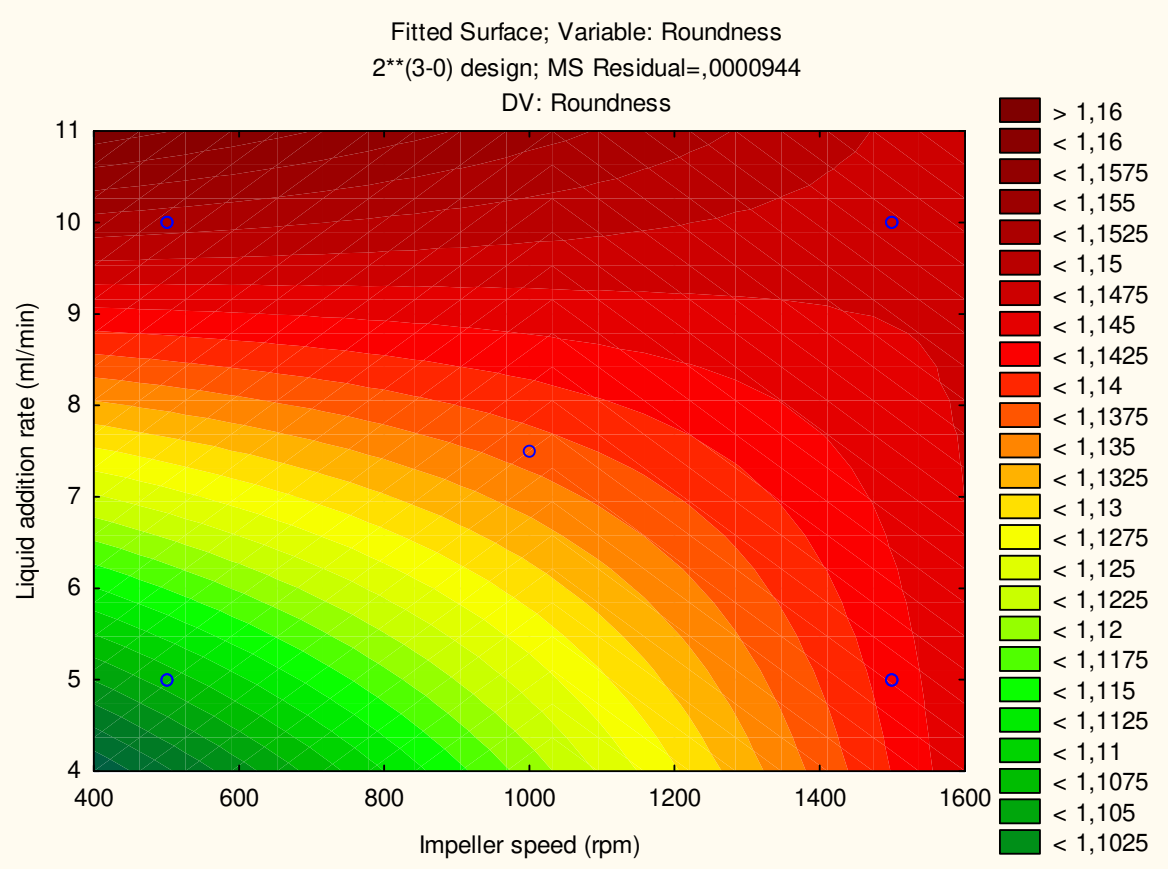

Fig. S16 Contour plot of roundness of C1 at an extruder speed of 120 rpm

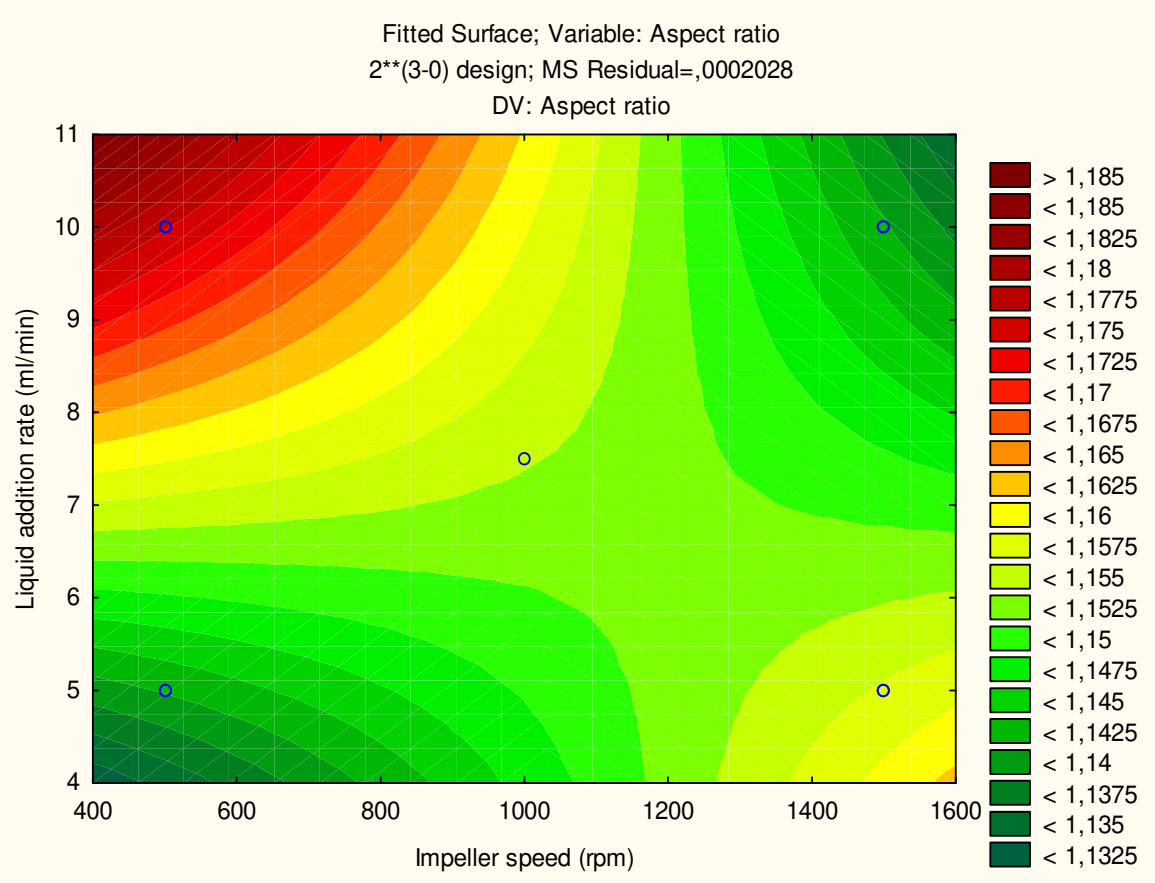

Fig. S17 Contour plot of aspect ratio of C1 at an extruder speed of 120 rpm

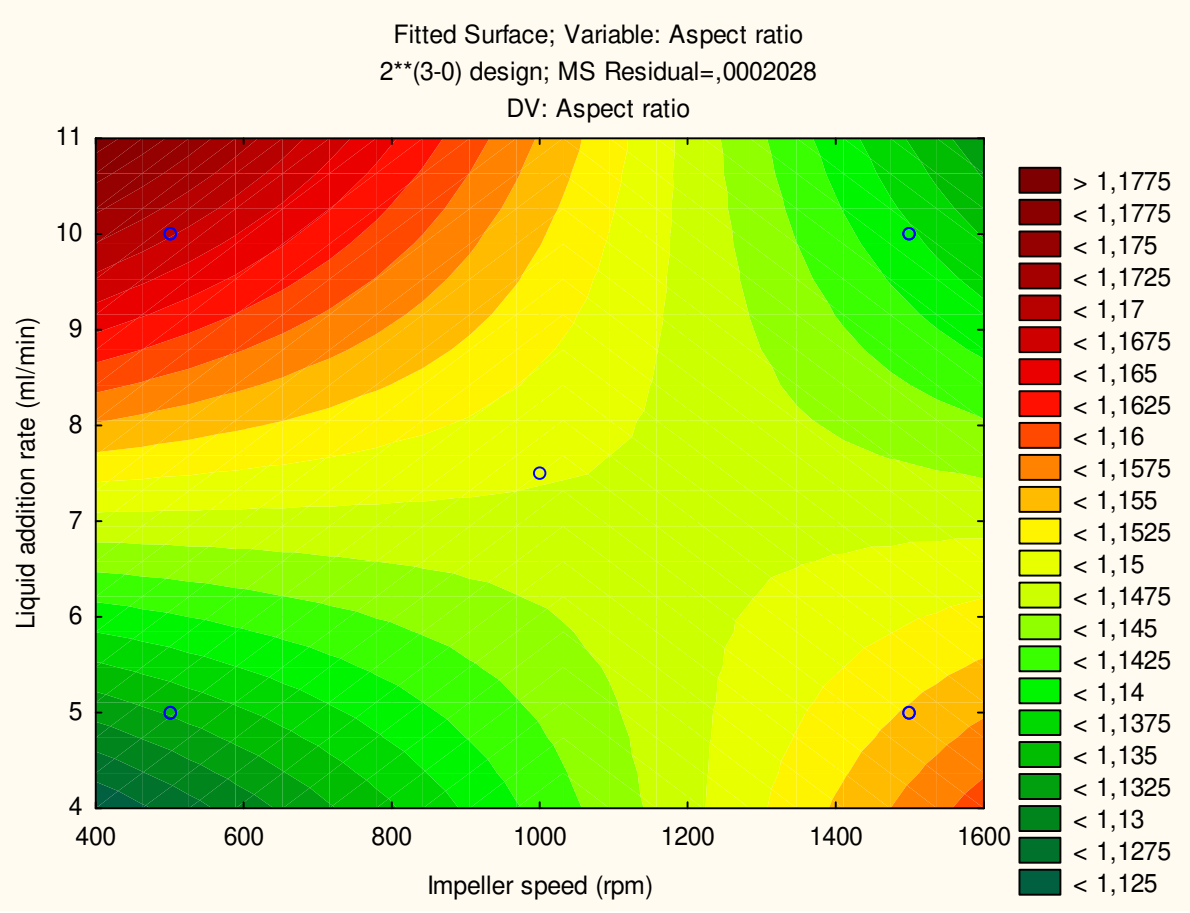

Fig. S18 Contour plot of aspect ratio of C1 at an extruder speed of 95 rpm

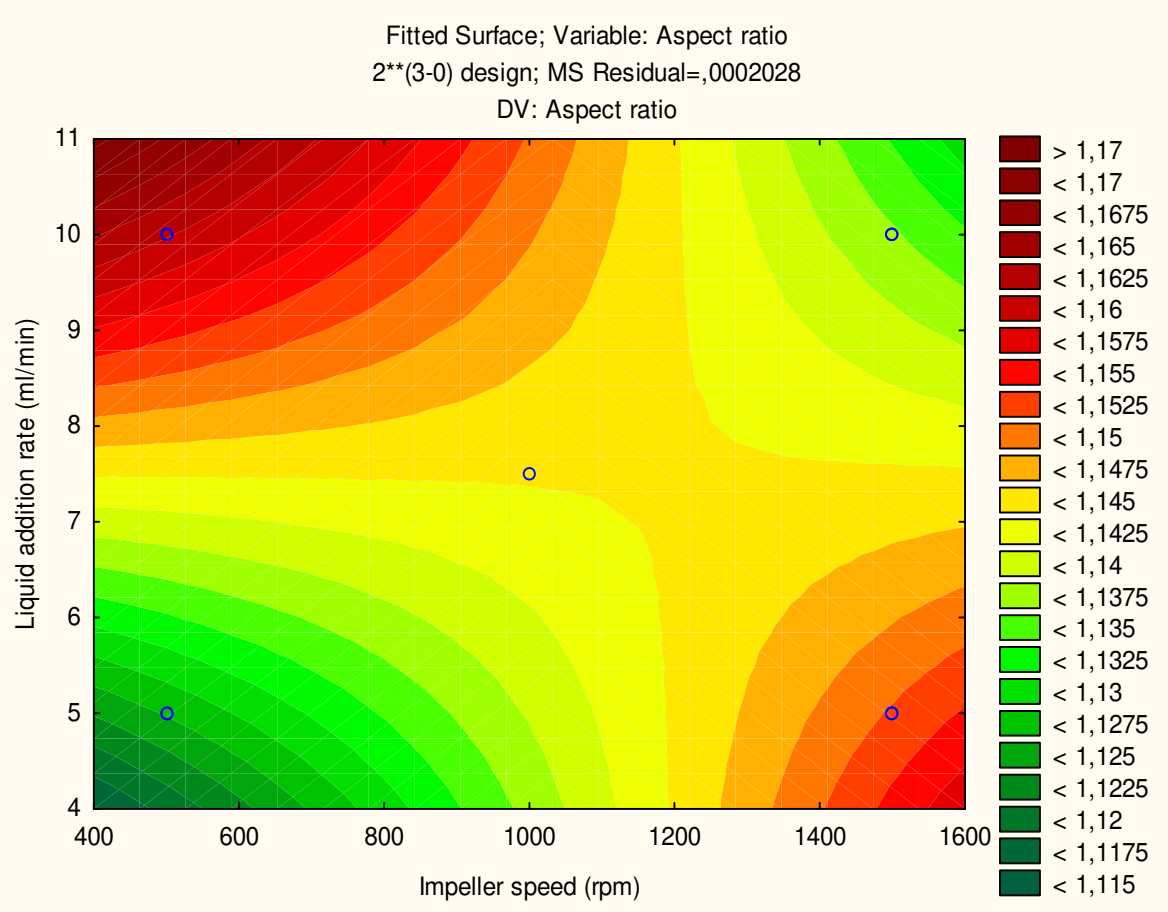

Fig. S19 Contour plot of aspect ratio of C1 at an extruder speed of 120 rpm

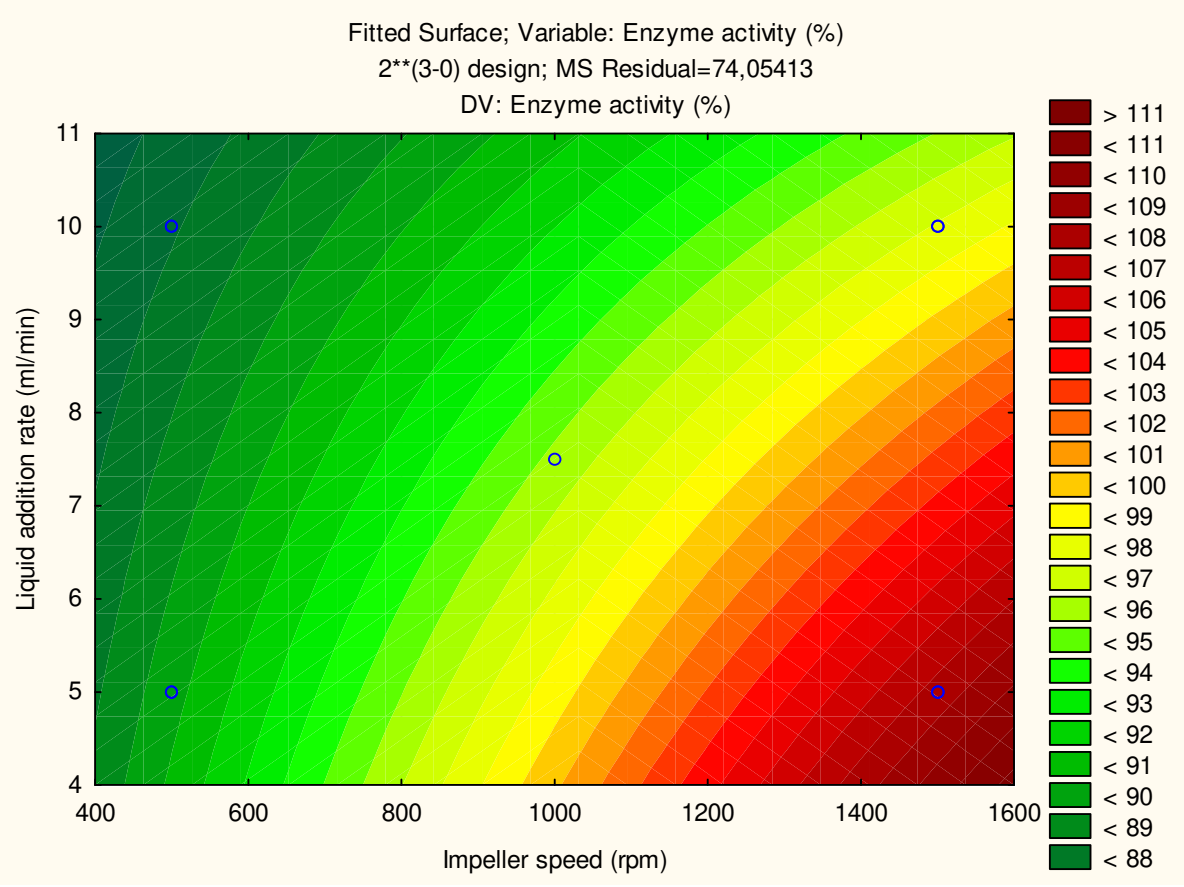

Fig. S20 Contour plot of the enzyme activity of C2 at an extruder speed of 70 rpm

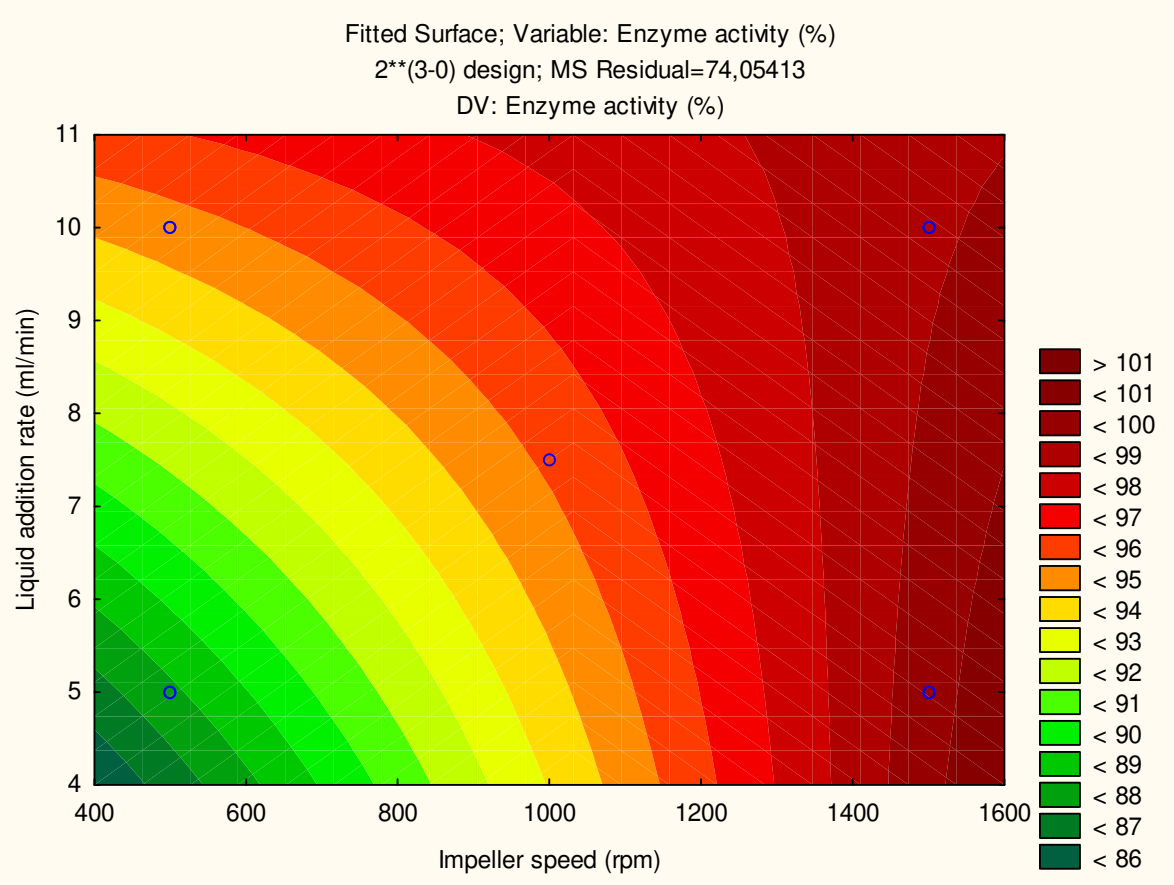

Fig. S21 Contour plot of the enzyme activity of C2 at an extruder speed of 95 rpm

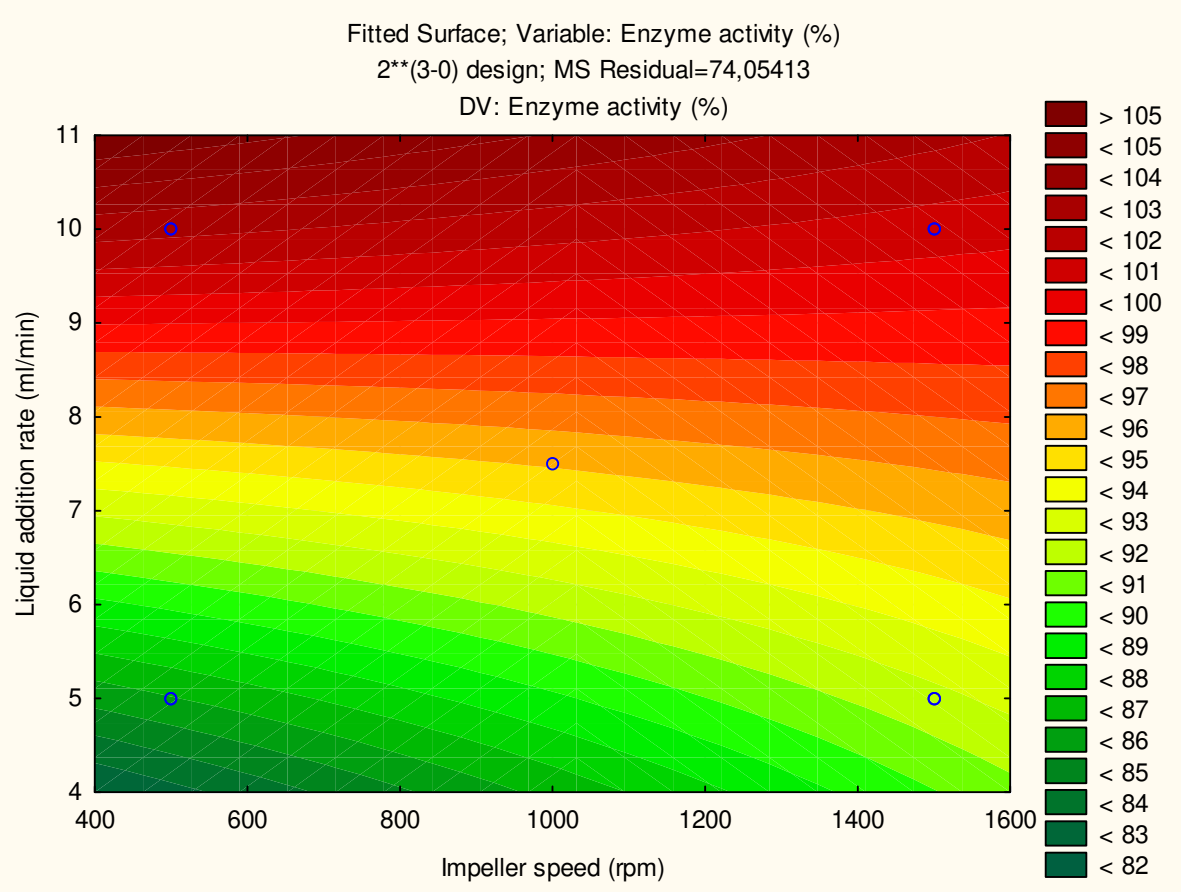

Fig. S22 Contour plot of the enzyme activity of C2 at an extruder speed of 120 rpm

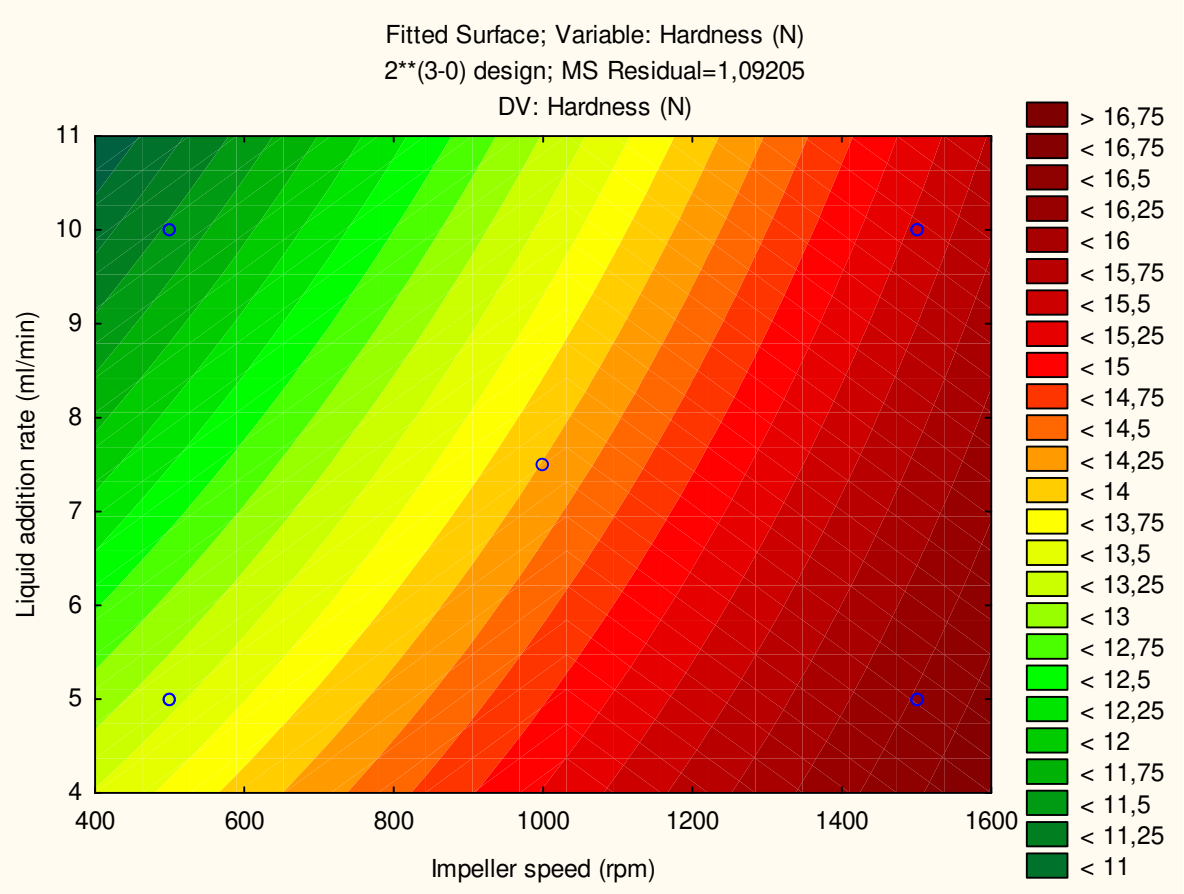

Fig. S23 Contour plot of the pellet hardness of C2 at an extruder speed of 70 rpm

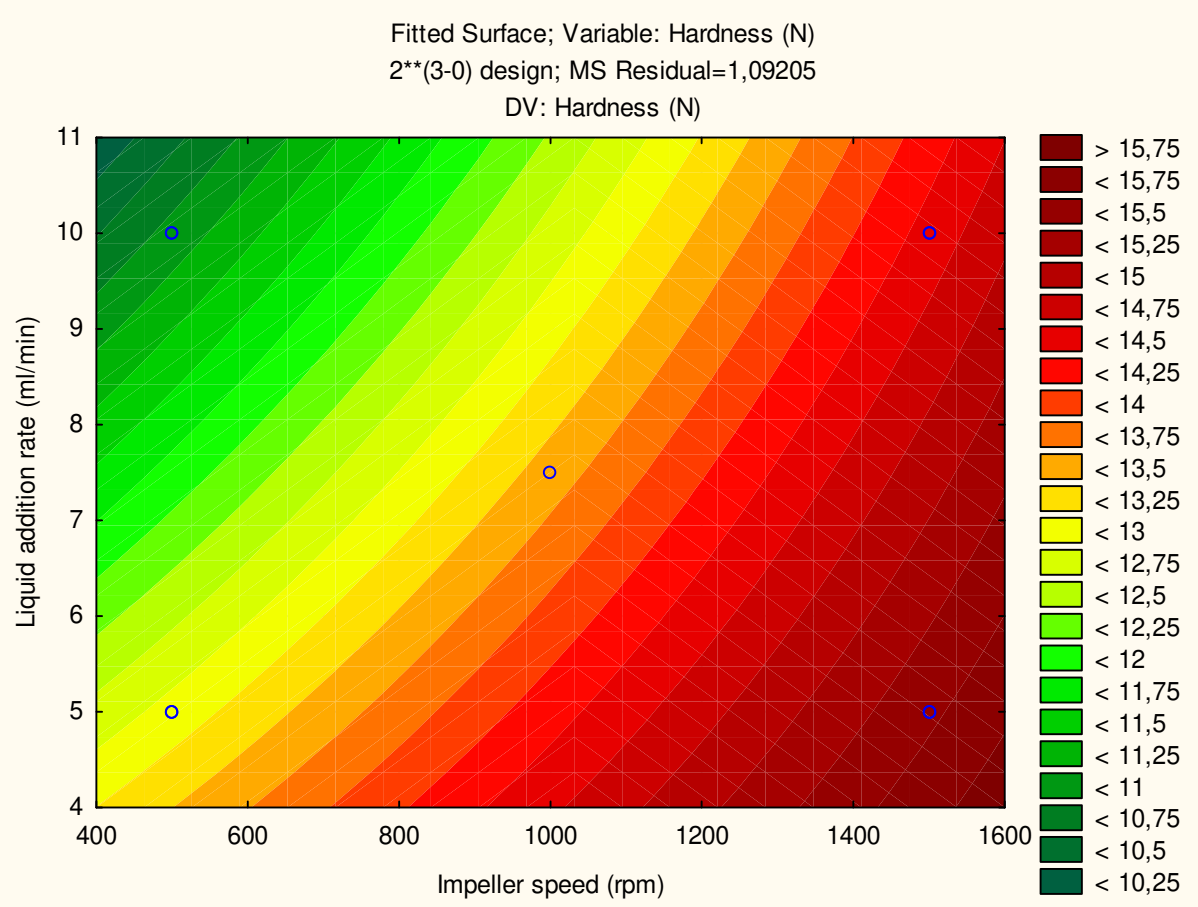

Fig. S24 Contour plot of the pellet hardness of C2 at an extruder speed of 95 rpm

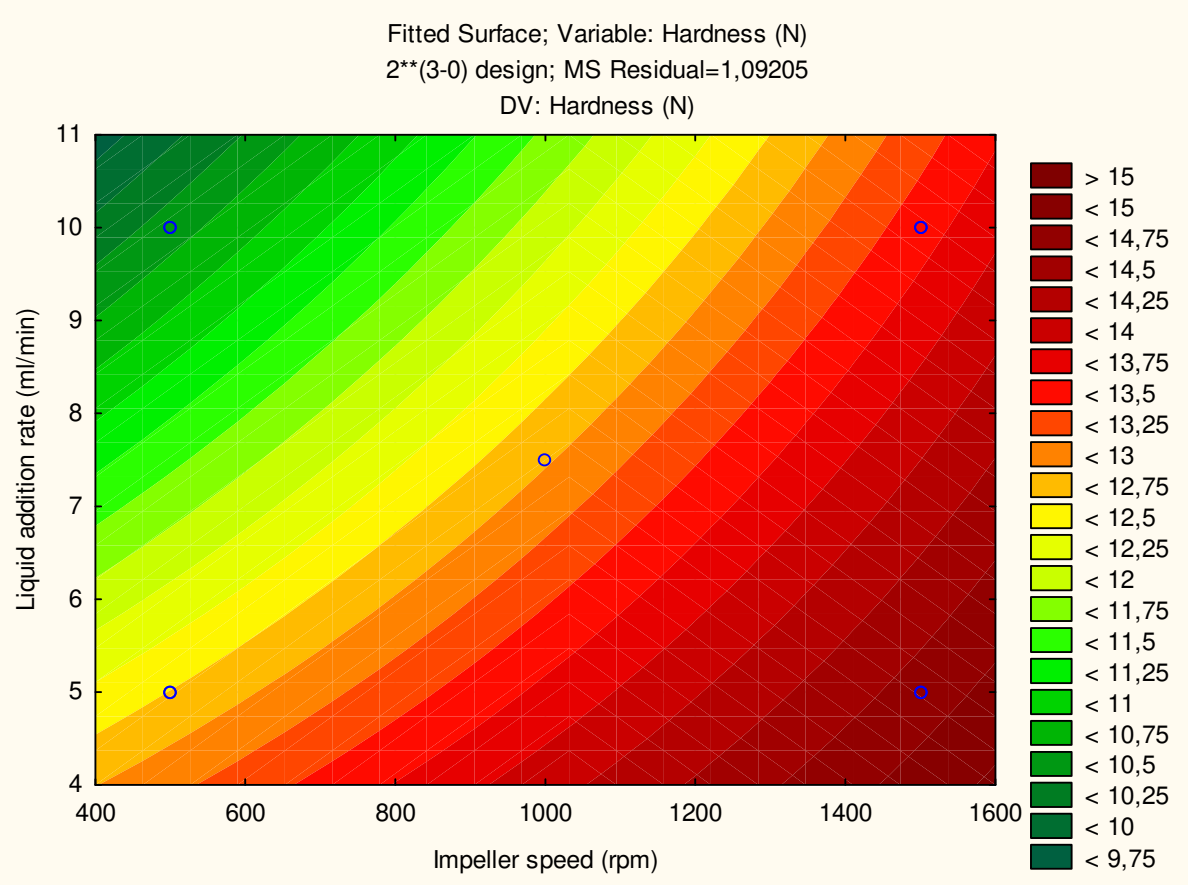

Fig. S25 Contour plot of the pellet hardness of C2 at an extruder speed of 120 rpm

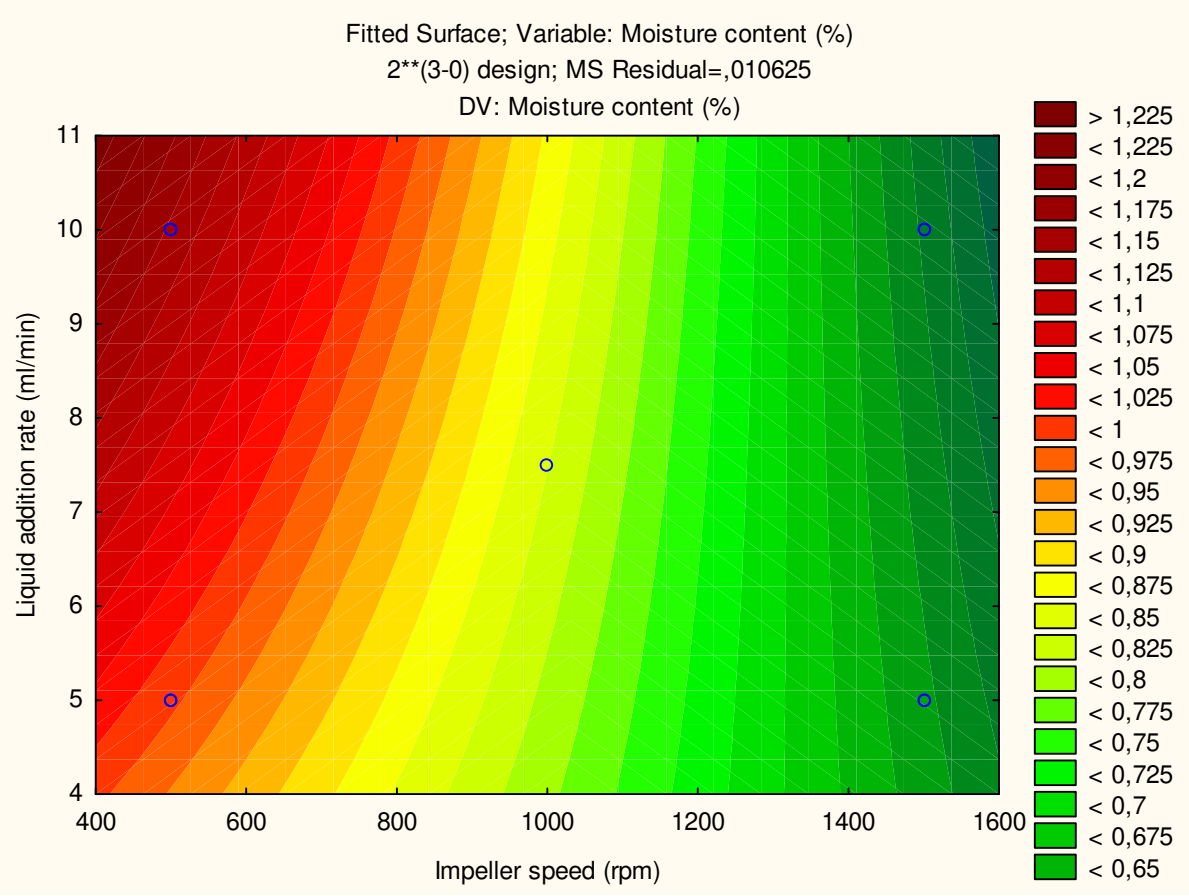

Fig. S26 Contour plot of the moisture content of C2 at an extruder speed of 70 rpm

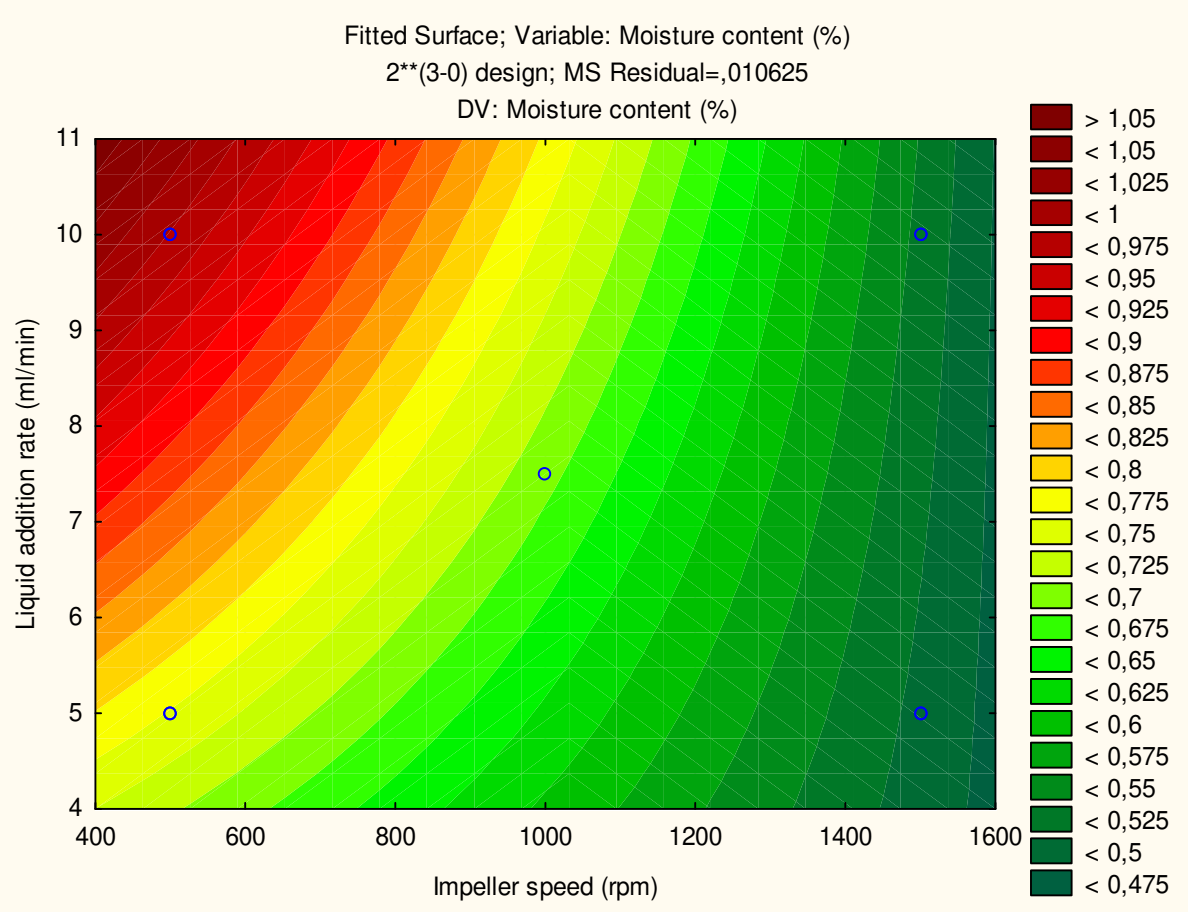

Fig. S27 Contour plot of the moisture content of C2 at an extruder speed of 95 rpm

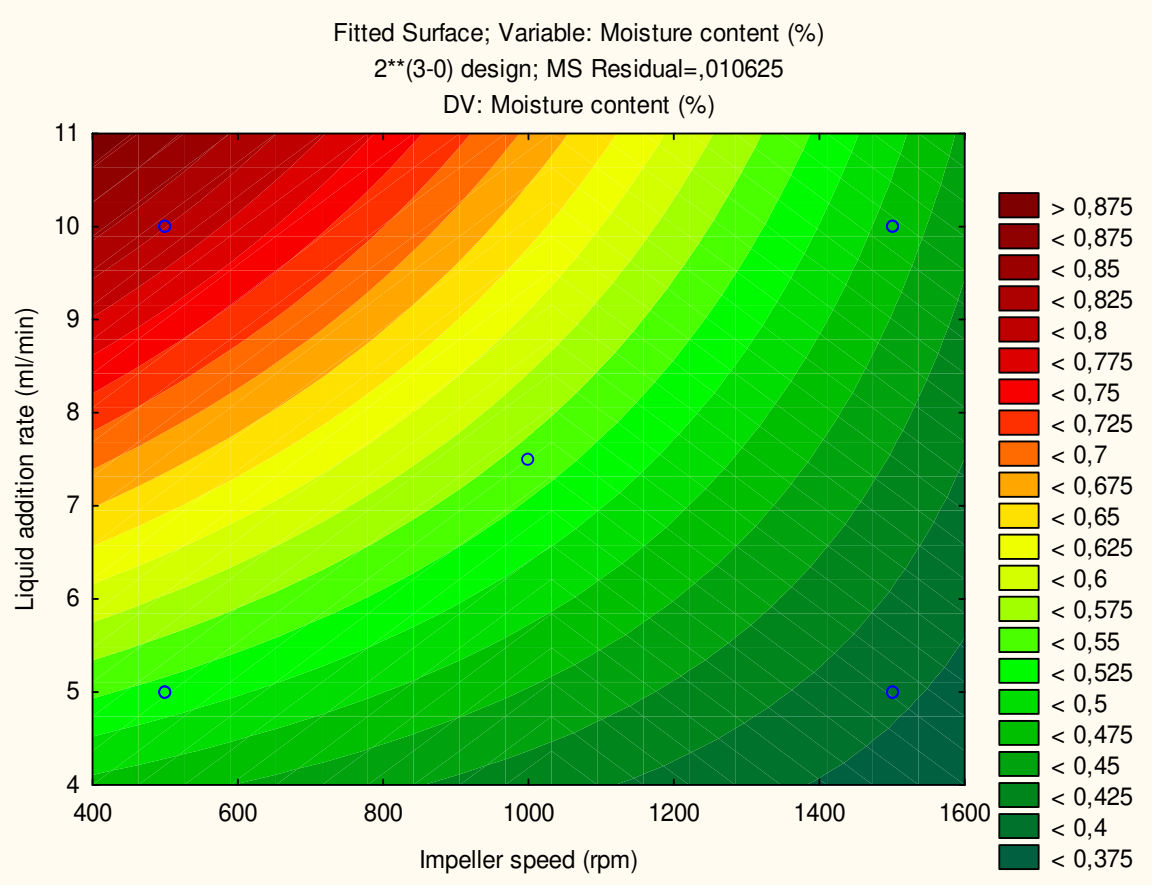

Fig. S28 Contour plot of the moisture content of C2 at an extruder speed of 120 rpm

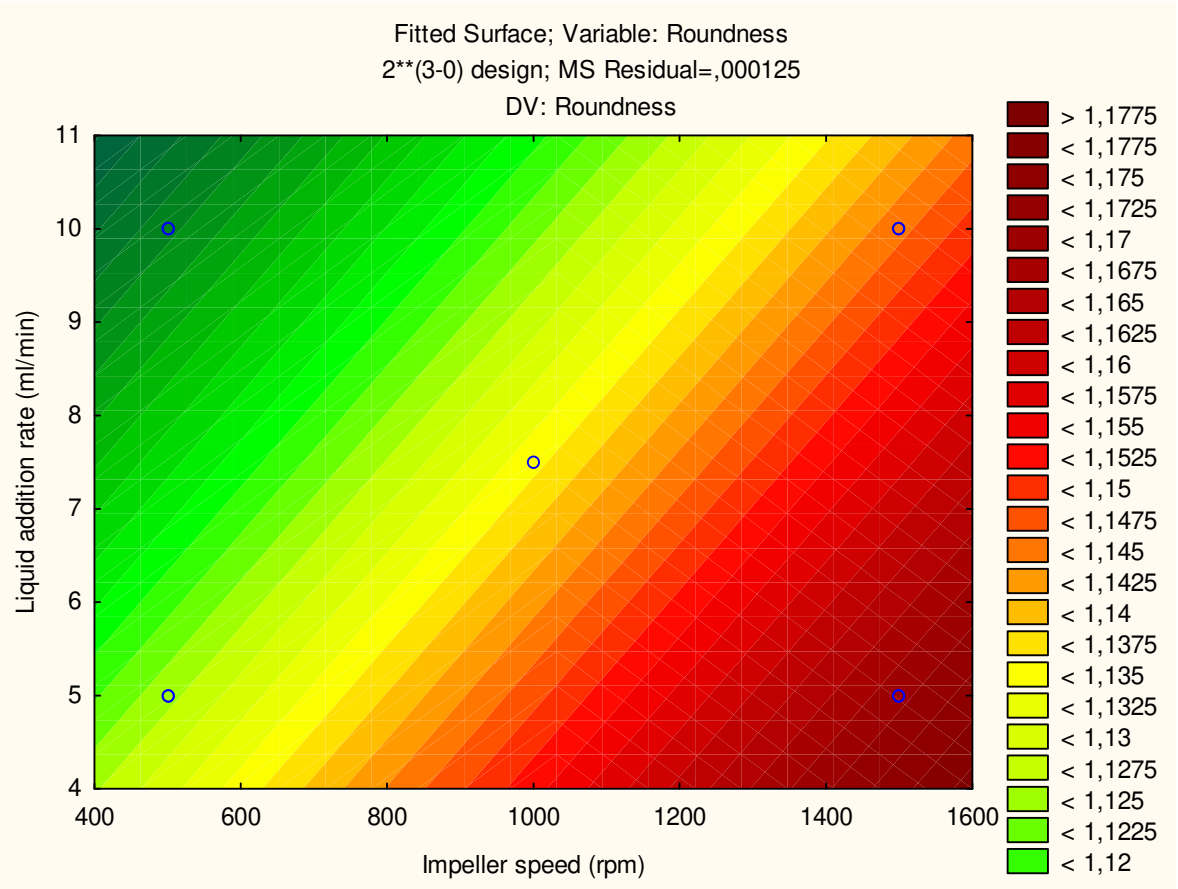

Fig. S29 Contour plot of the roundness of C2 at an extruder speed of 70 rpm

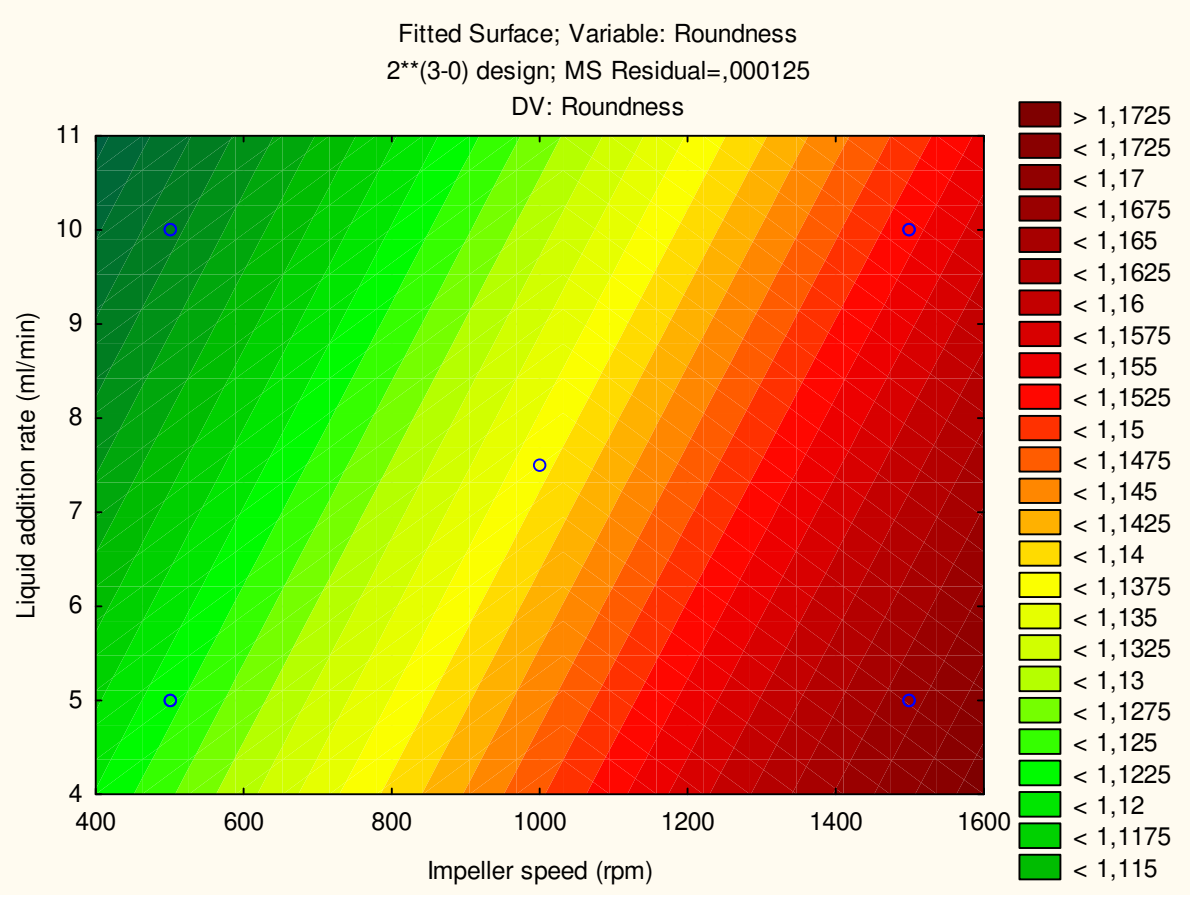

Fig. S30 Contour plot of the roundness of C2 at an extruder speed of 95 rpm

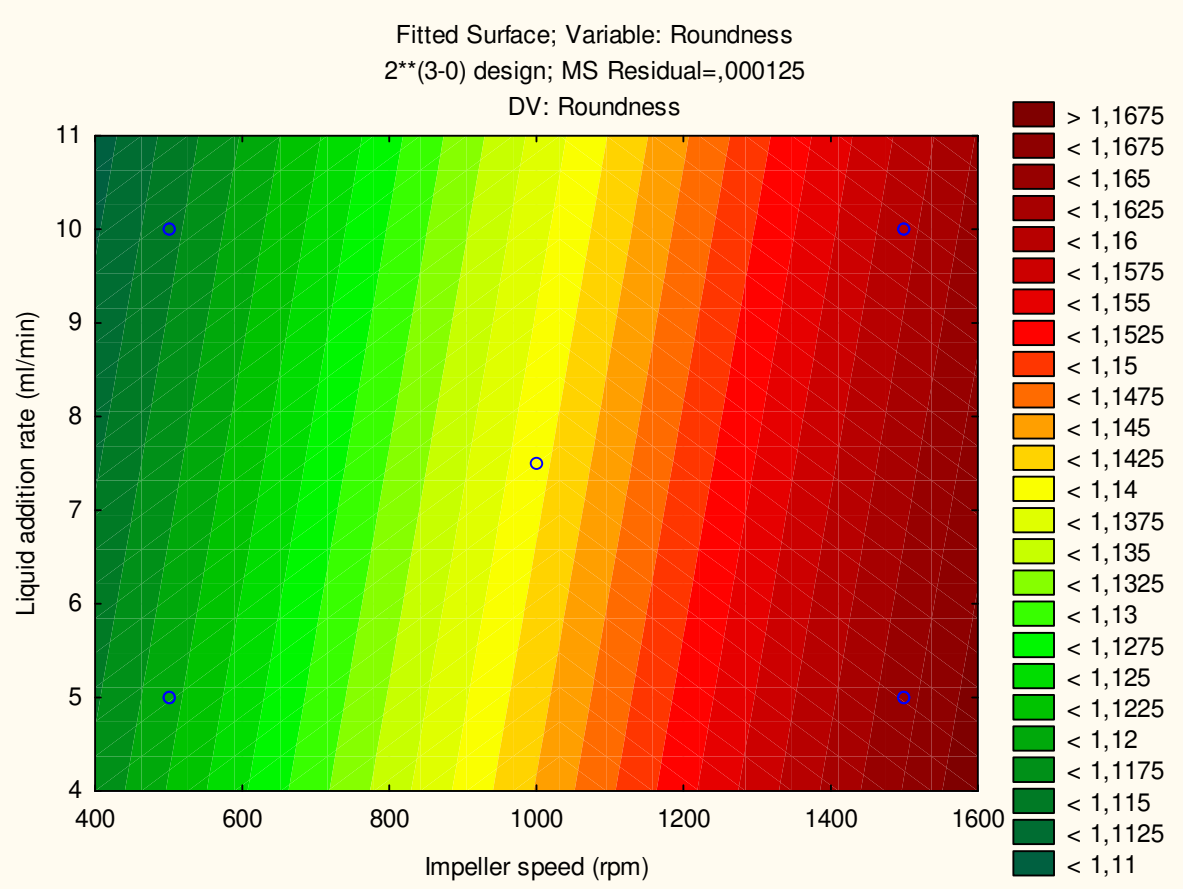

Fig. S31 Contour plot of the roundness of C2 at an extruder speed of 120 rpm

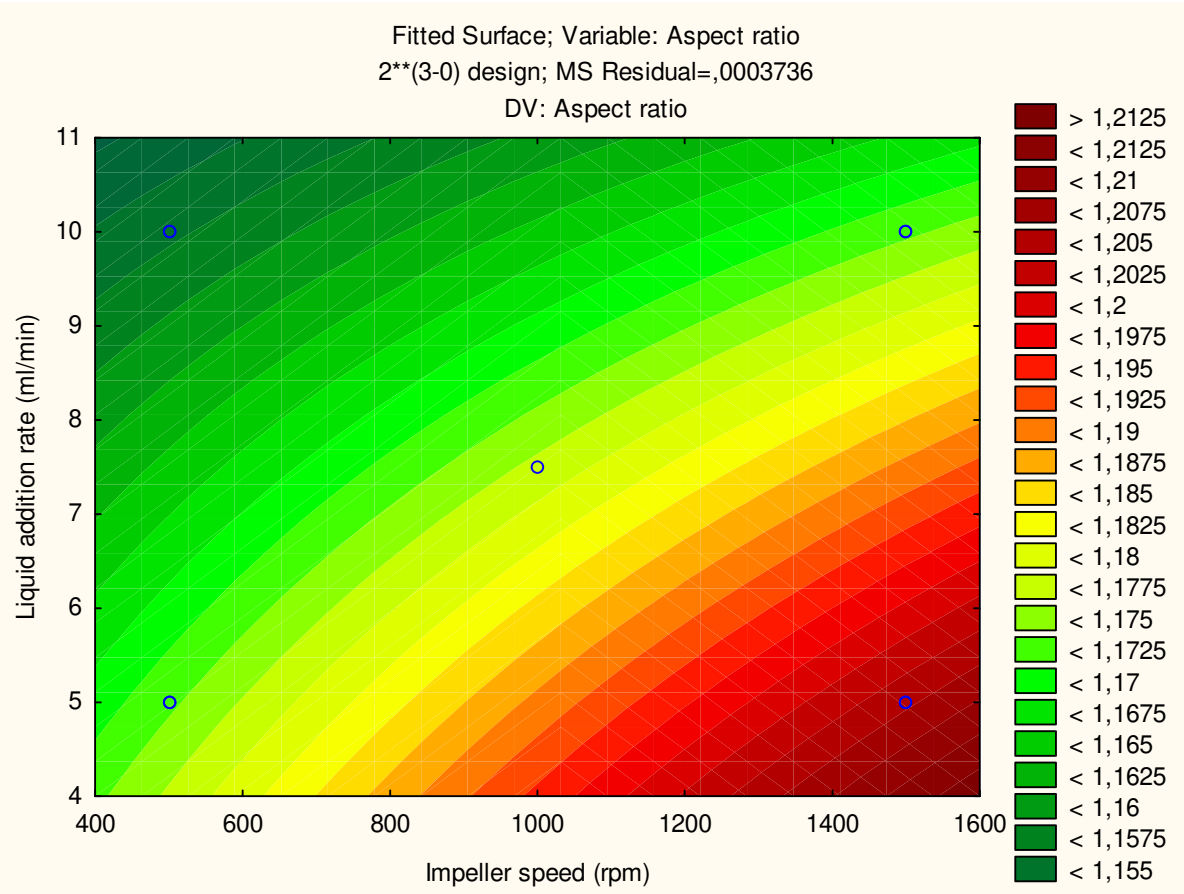

Fig. S32 Contour plot of the aspect ratio of C2 at an extruder speed of 70 rpm

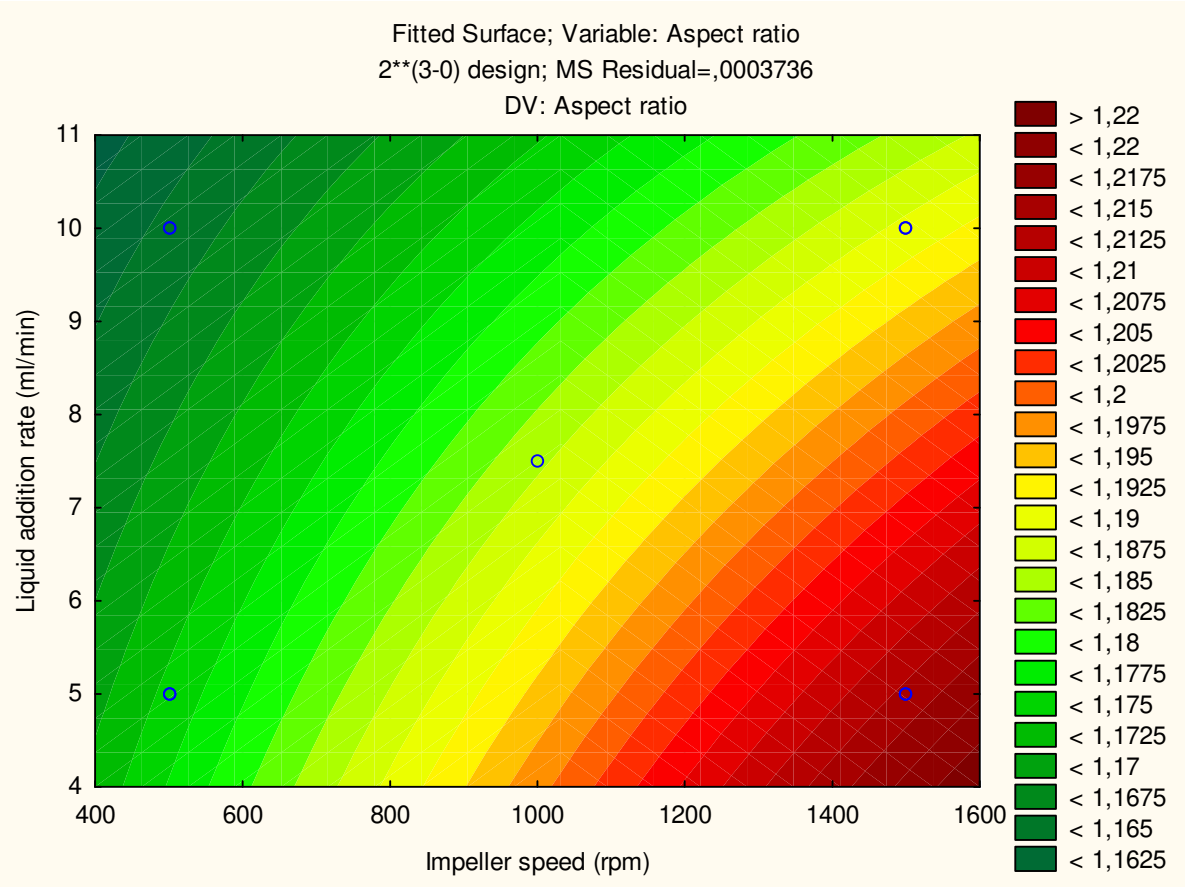

Fig. S33 Contour plot of the aspect ratio of C2 at an extruder speed of 95 rpm

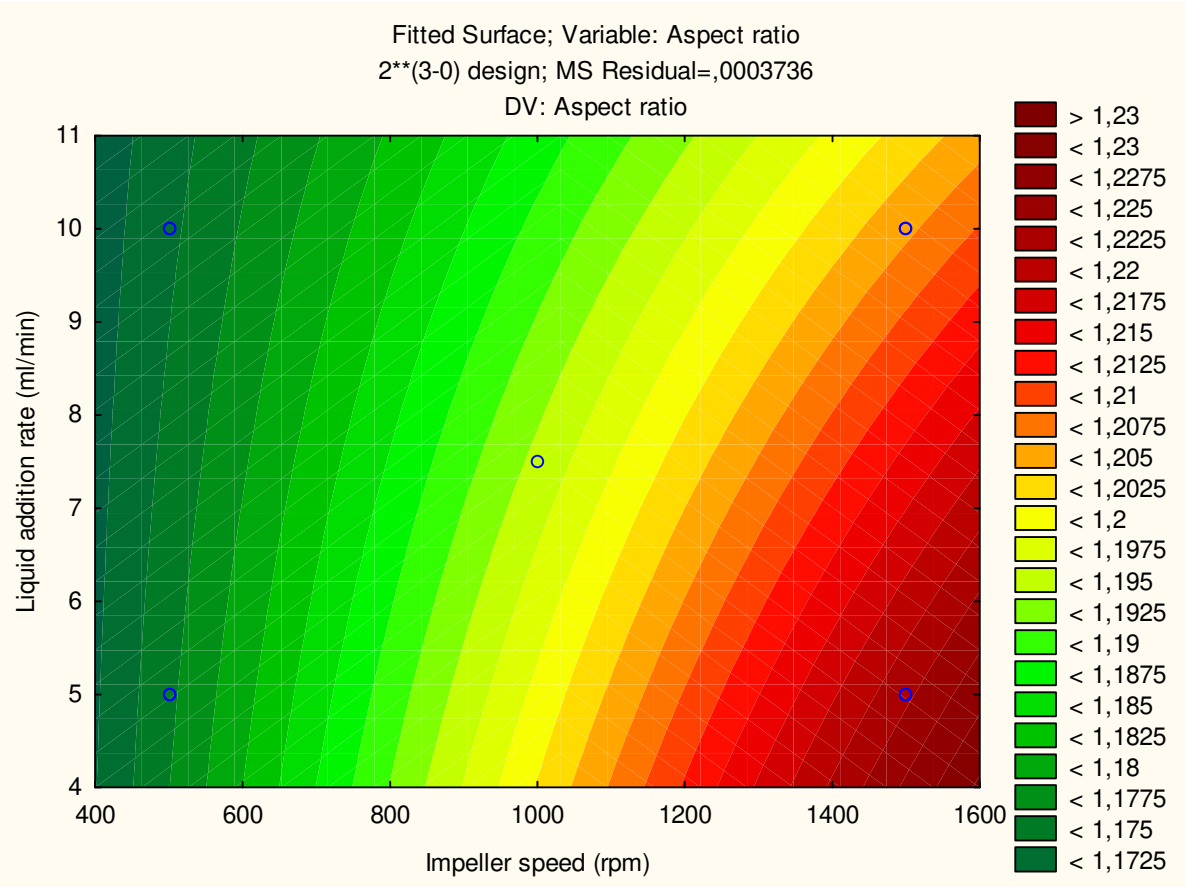

Fig. S34 Contour plot of the aspect ratio of C2 at an extruder speed of 120 rpm

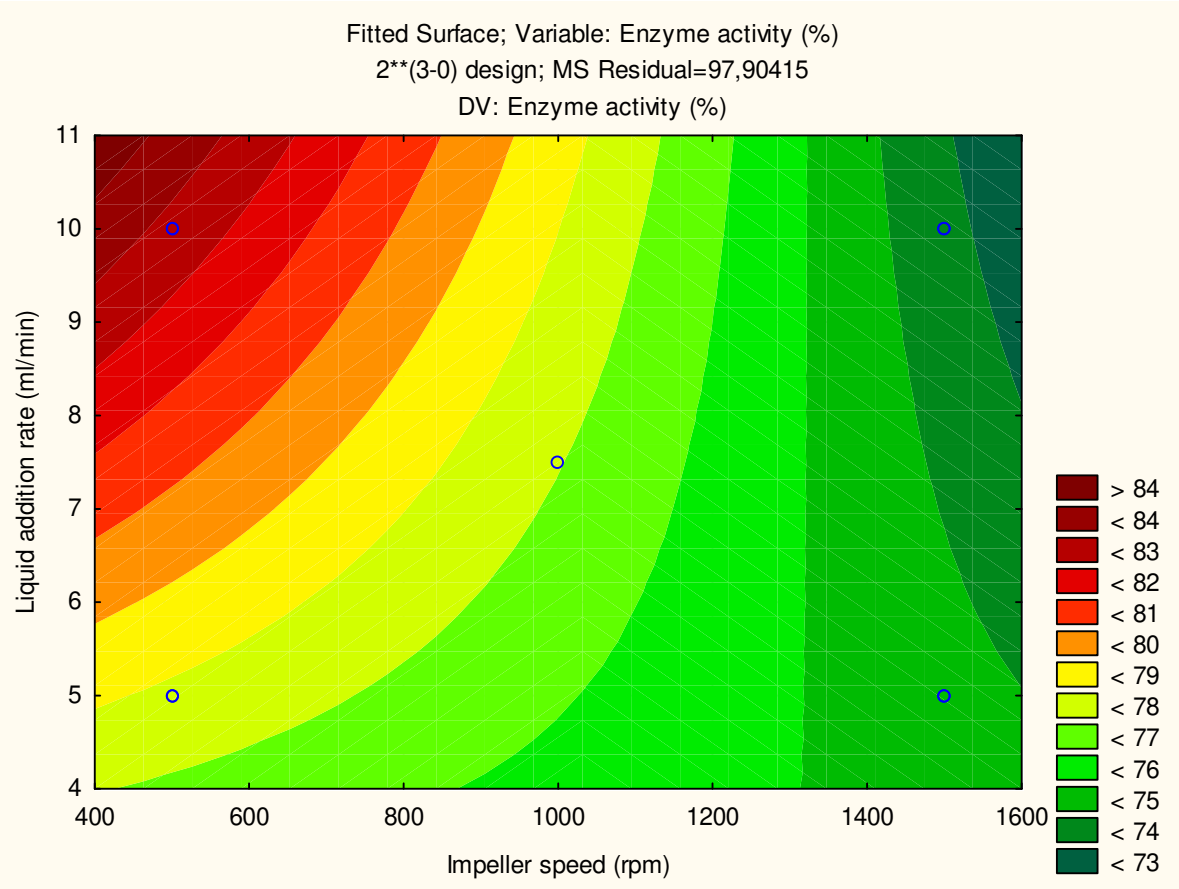

Fig. S35 Contour plot of the enzyme activity of C3 at an extruder speed of 70 rpm

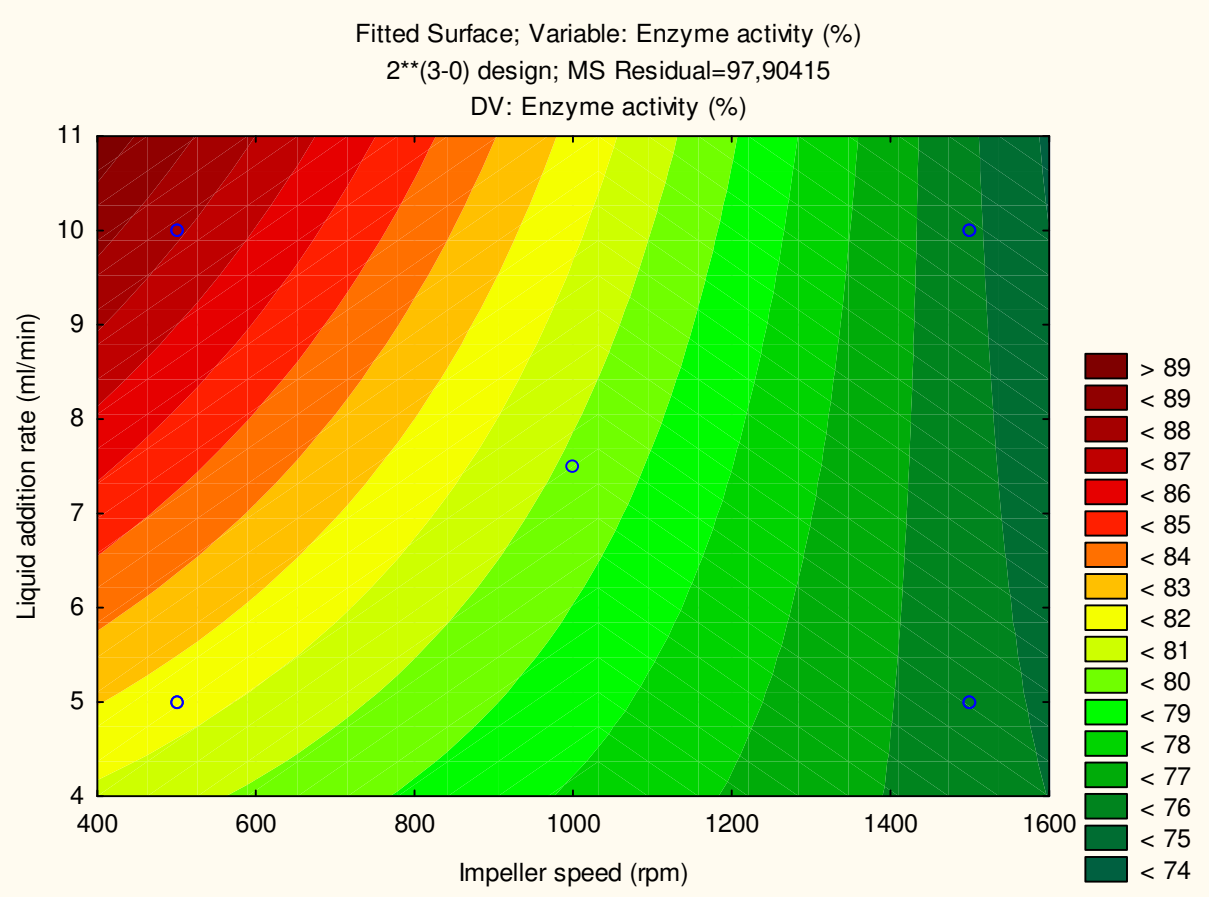

Fig. S36 Contour plot of the enzyme activity of C3 at an extruder speed of 95 rpm

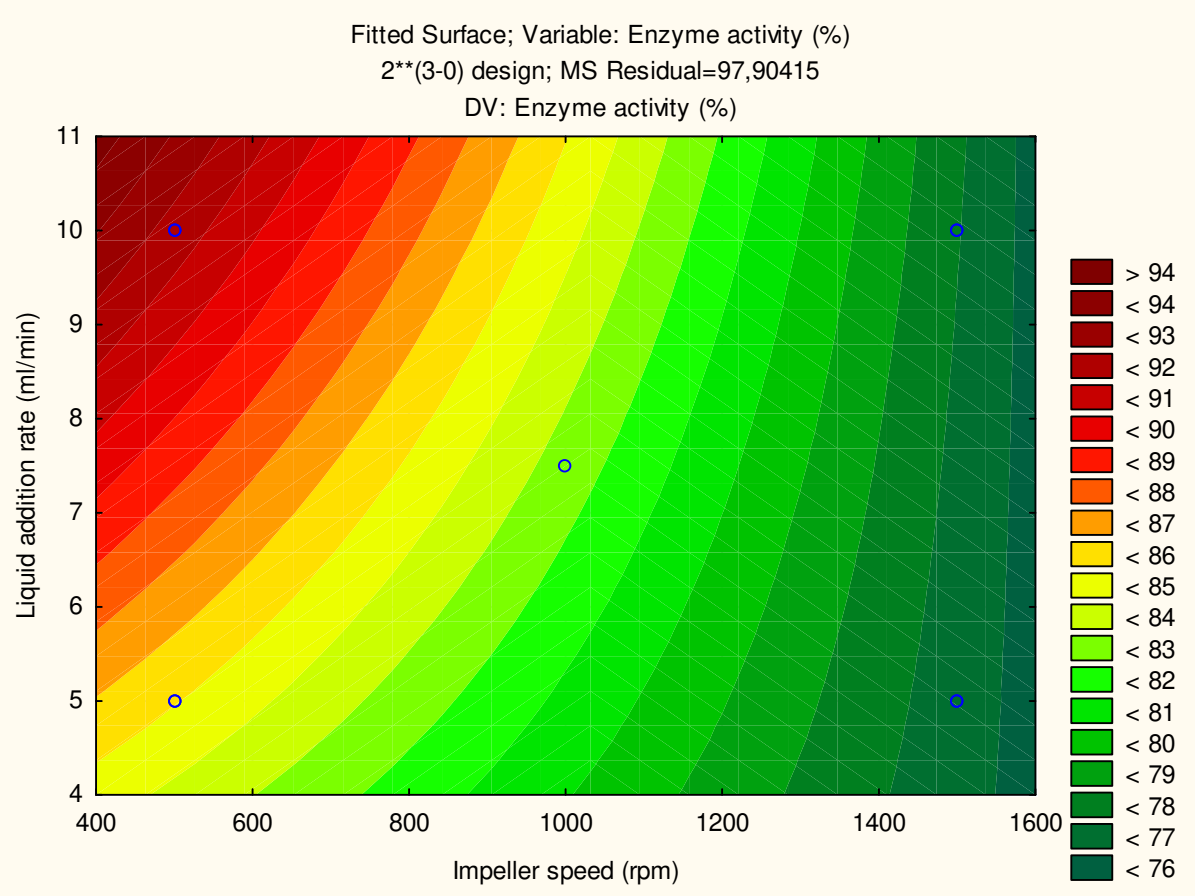

Fig. S37 Contour plot of the enzyme activity of C3 at an extruder speed of 120 rpm

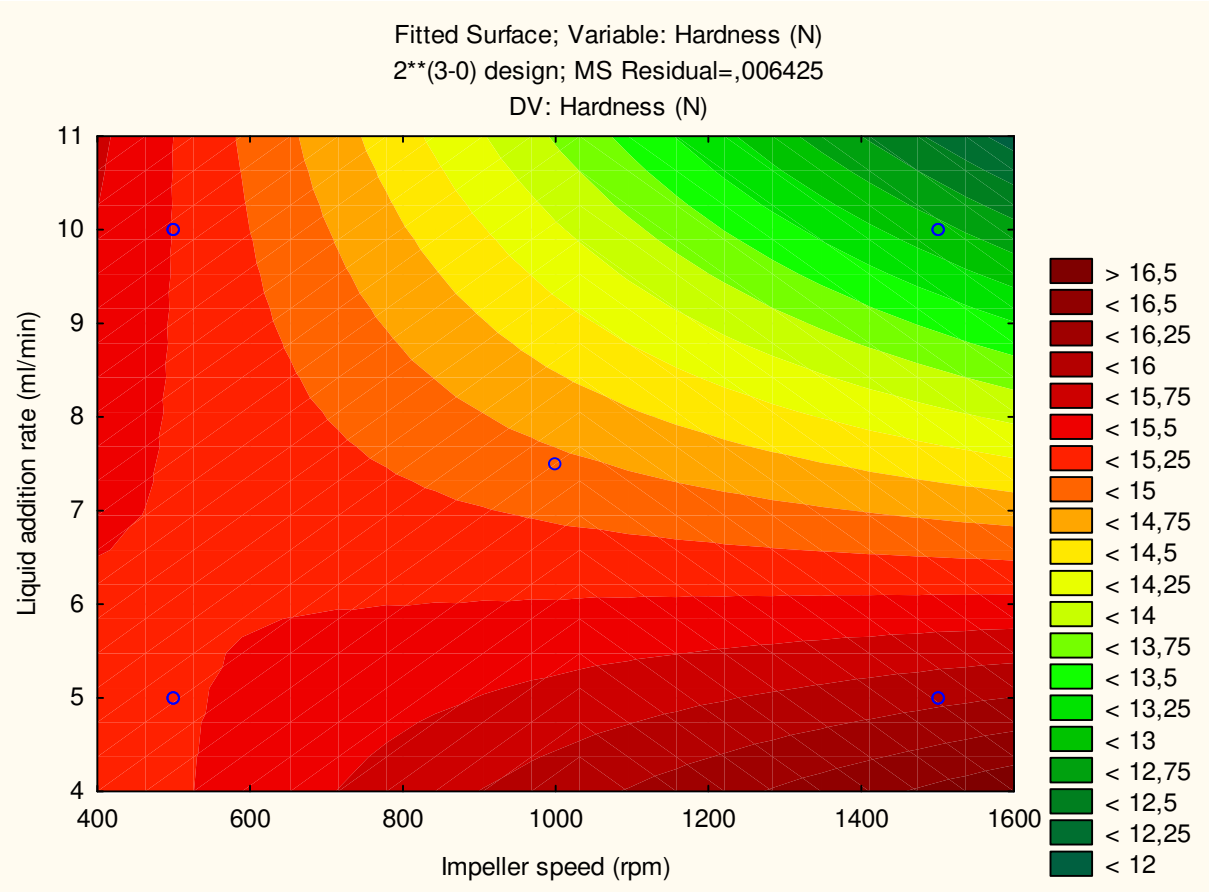

Fig. S38 Contour plot of the hardness of C3 at an extruder speed of 70 rpm

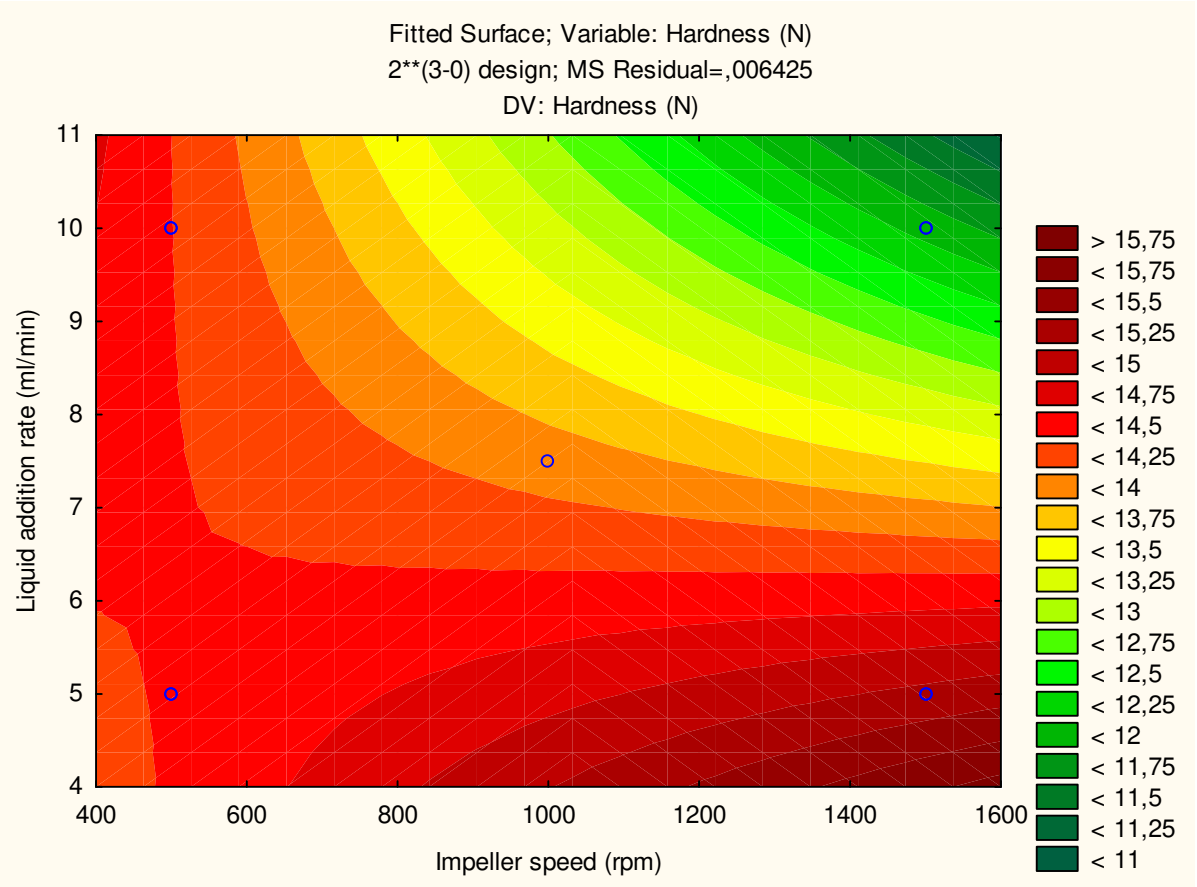

Fig. S39 Contour plot of the hardness of C3 at an extruder speed of 95 rpm

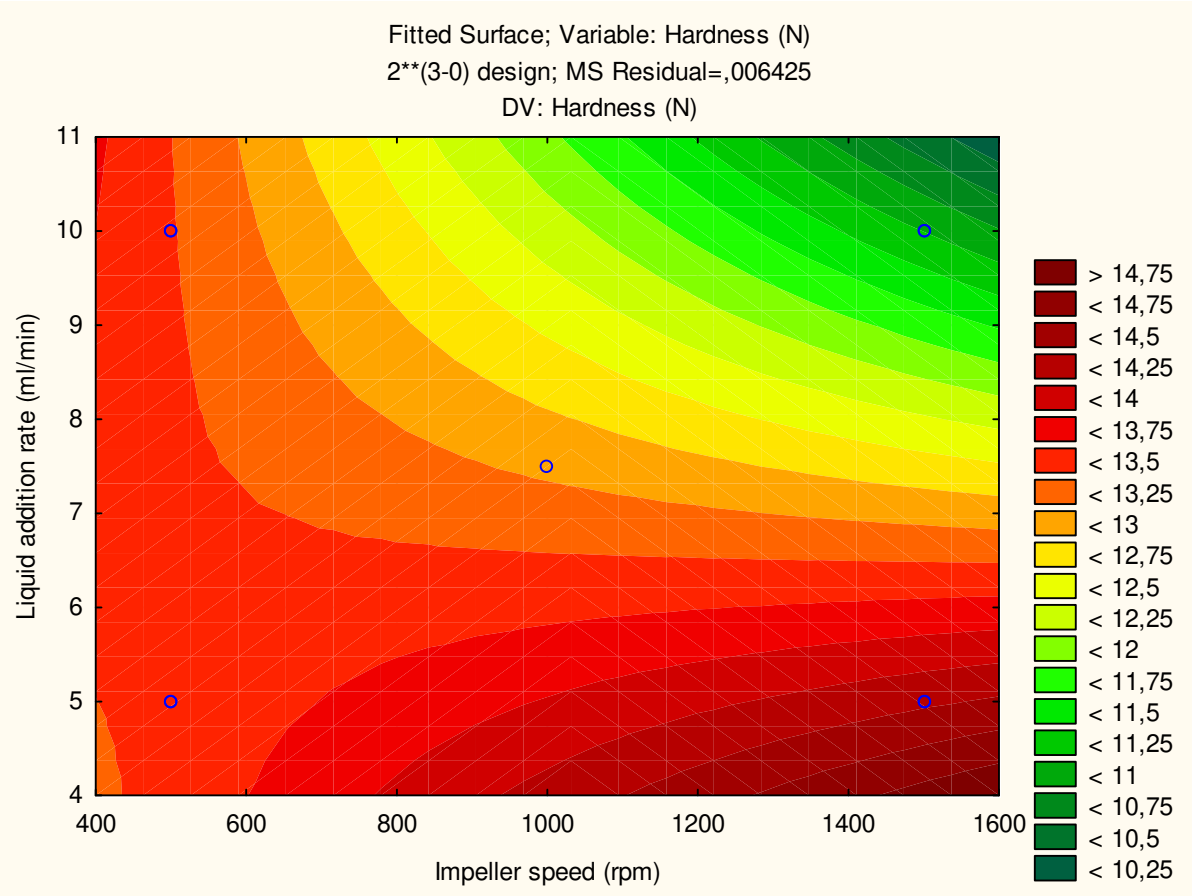

Fig. S40 Contour plot of the hardness of C3 at an extruder speed of 120 rpm

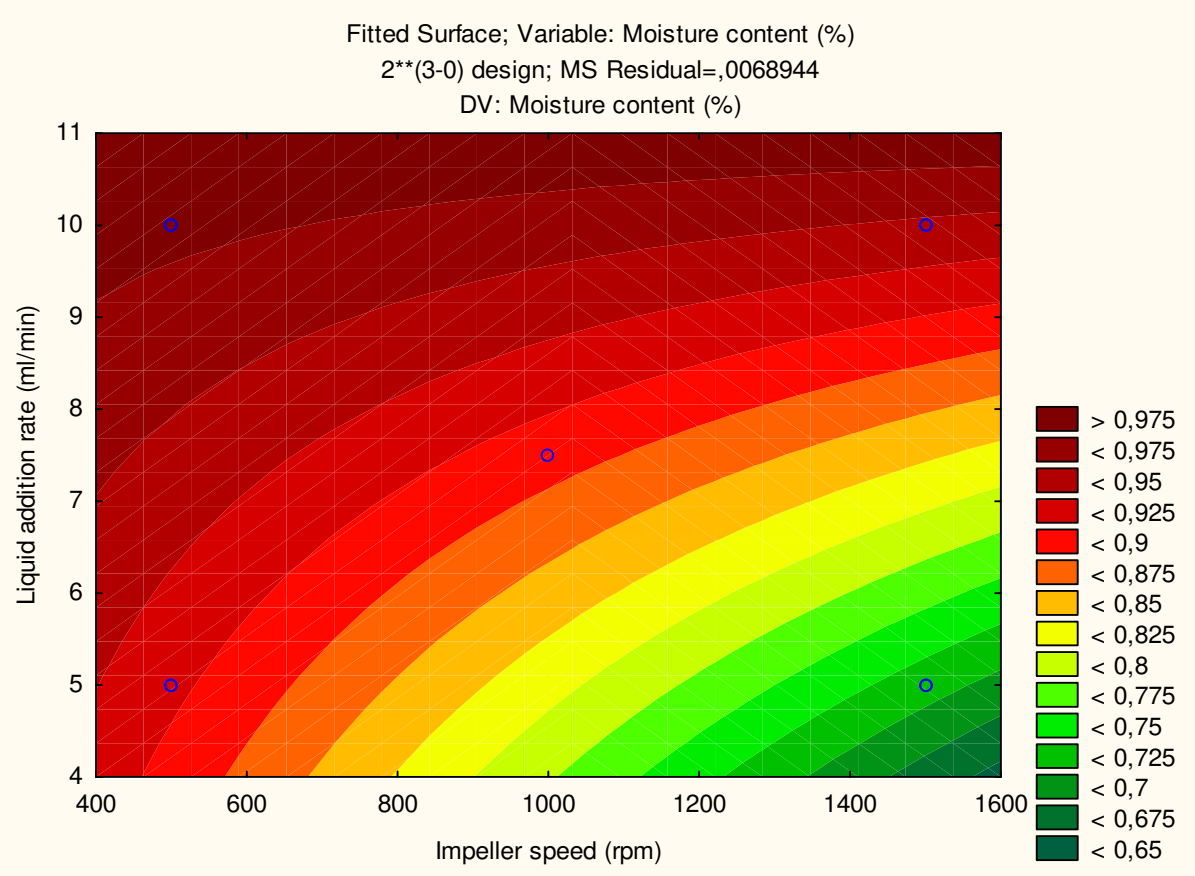

Fig. S41 Contour plot of the moisture content of C3 at an extruder speed of 70 rpm

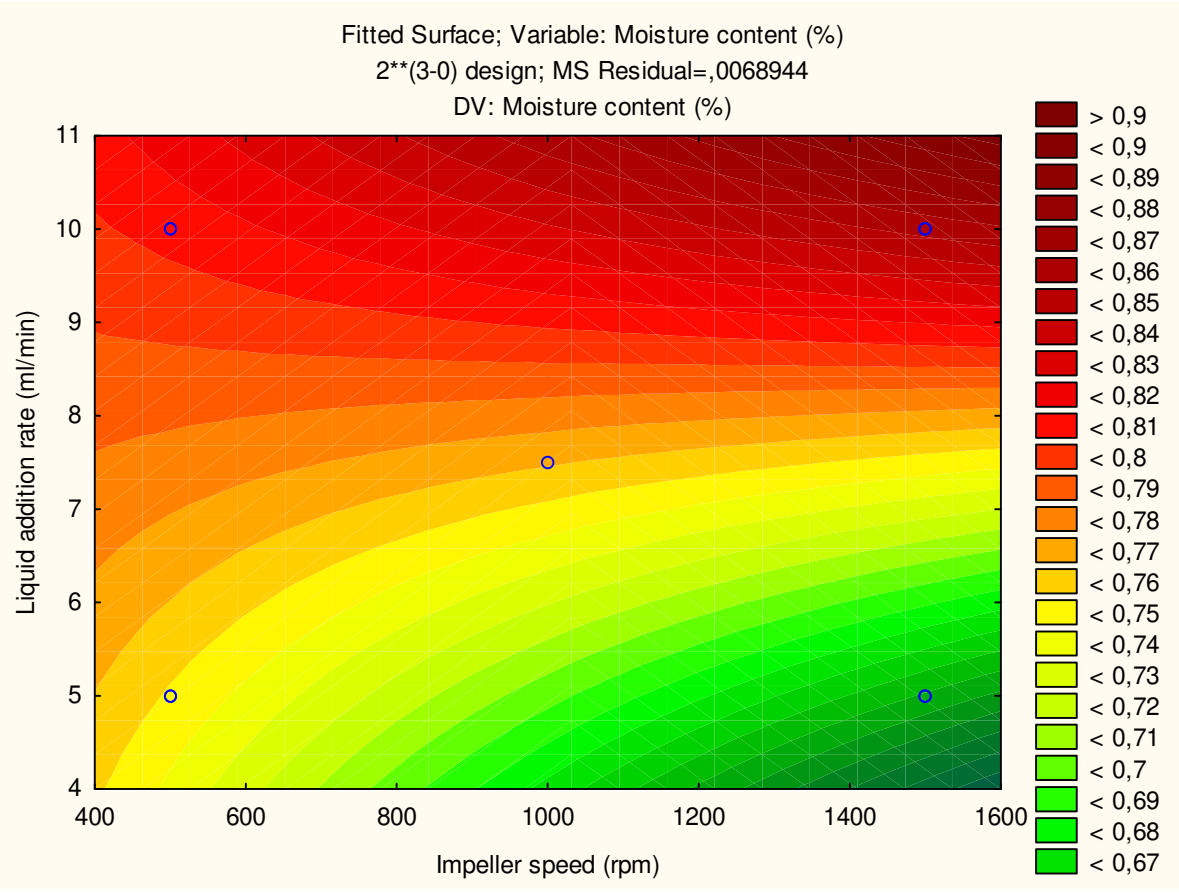

Fig. S42 Contour plot of the moisture content of C3 at an extruder speed of 95 rpm

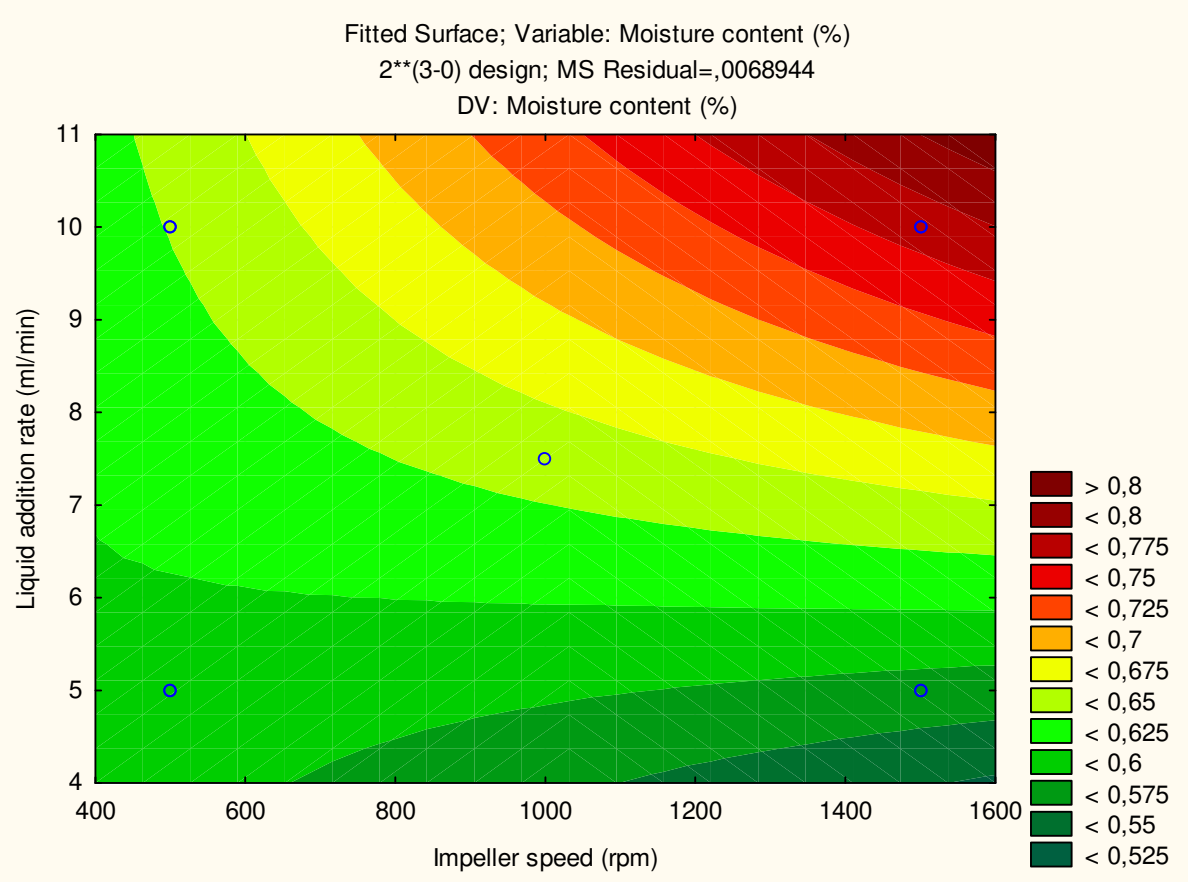

Fig. S43 Contour plot of the moisture content of C3 at an extruder speed of 120 rpm

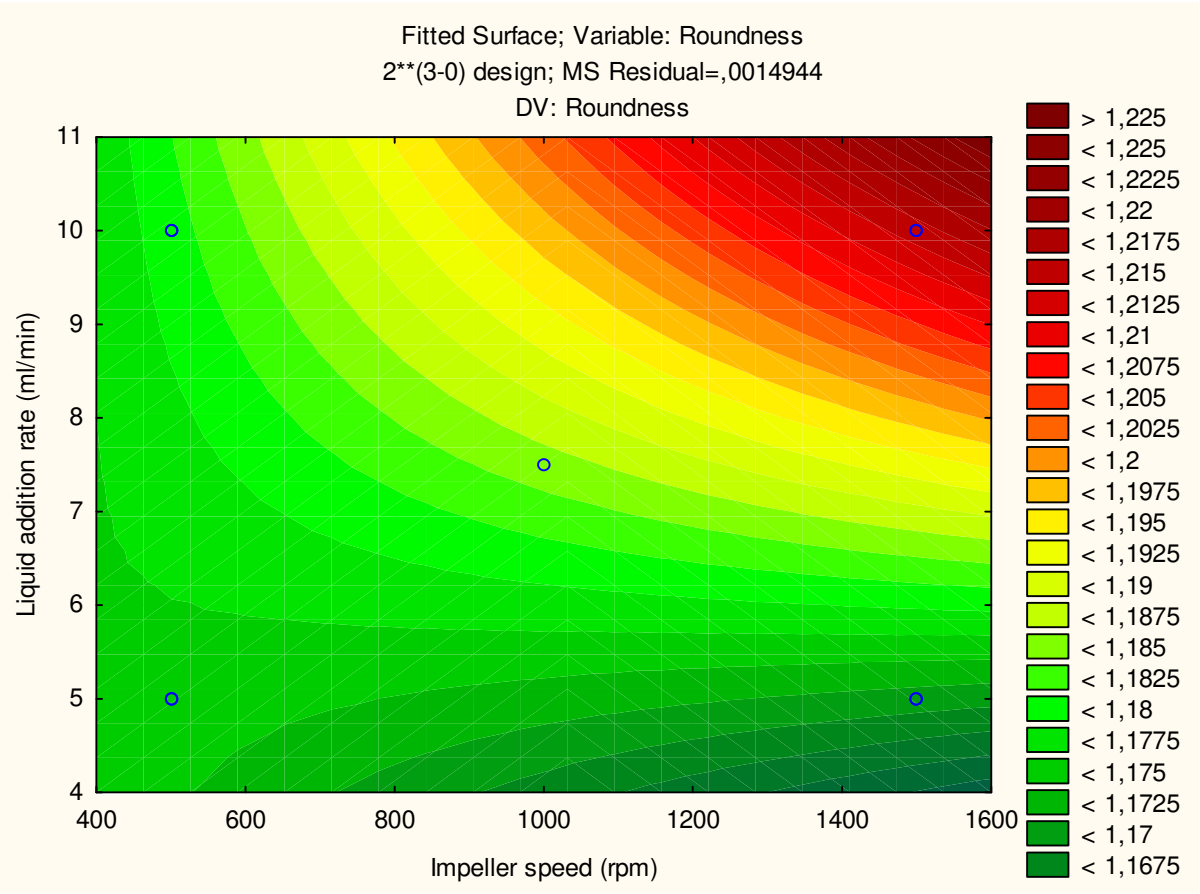

Fig. S44 Contour plot of the roundness of C3 at an extruder speed of 70 rpm

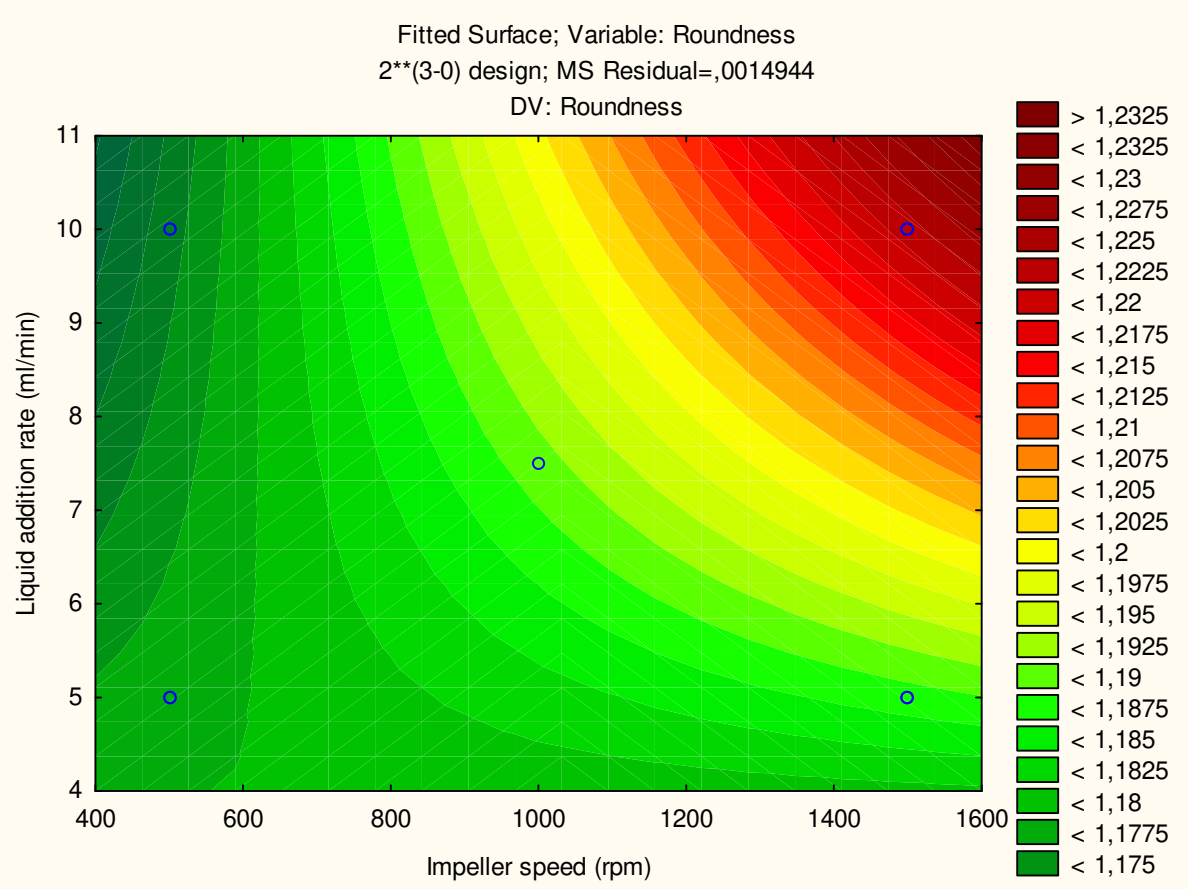

Fig. S45 Contour plot of the roundness of C3 at an extruder speed of 95 rpm

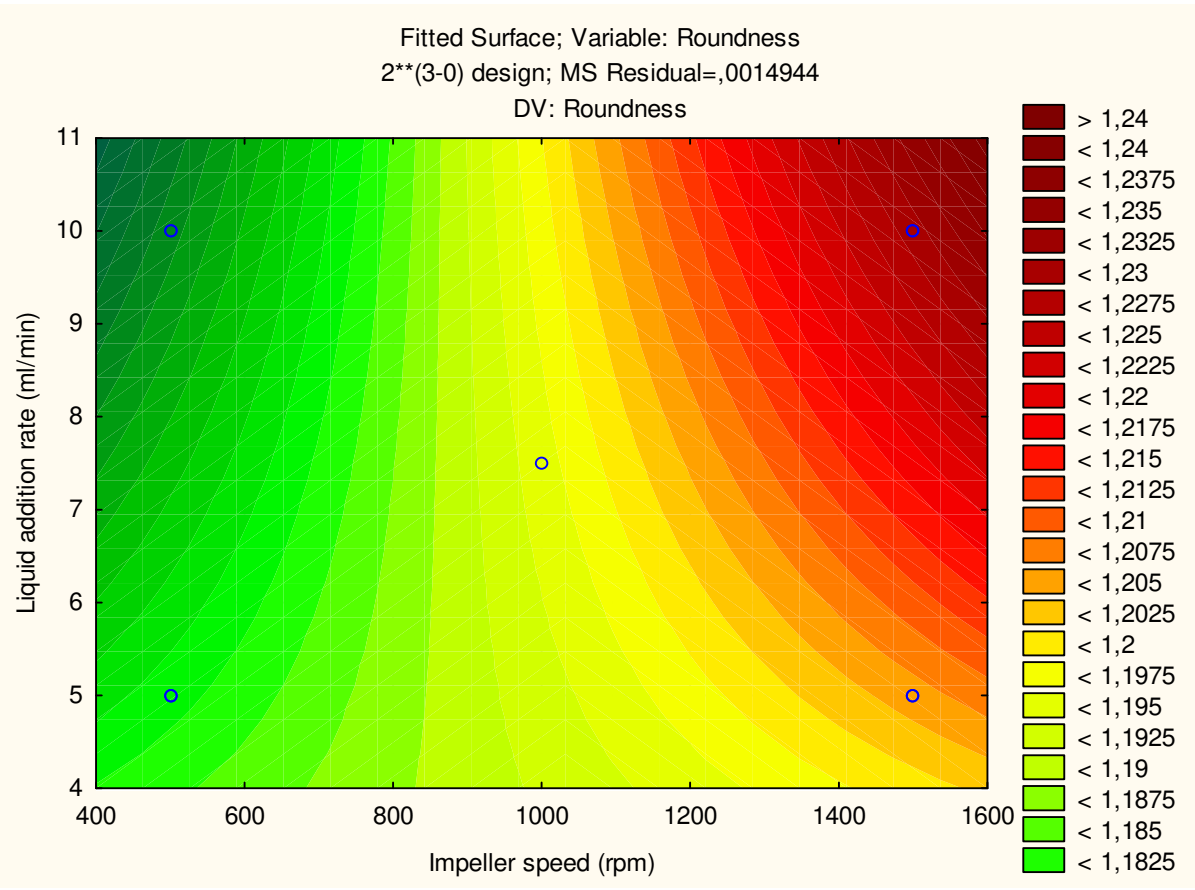

Fig. S46 Contour plot of the roundness of C3 at an extruder speed of 120 rpm

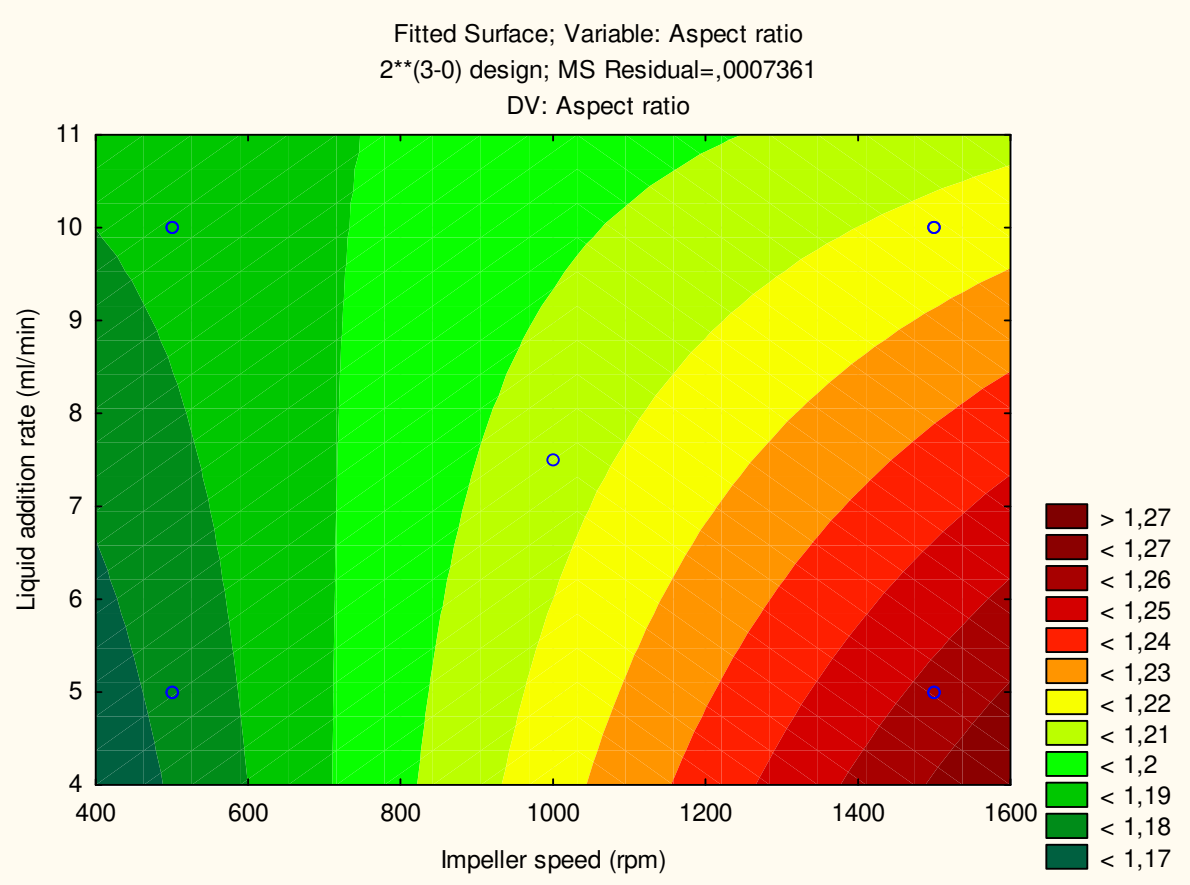

Fig. S47 Contour plot of the aspect ratio of C3 at an extruder speed of 70 rpm

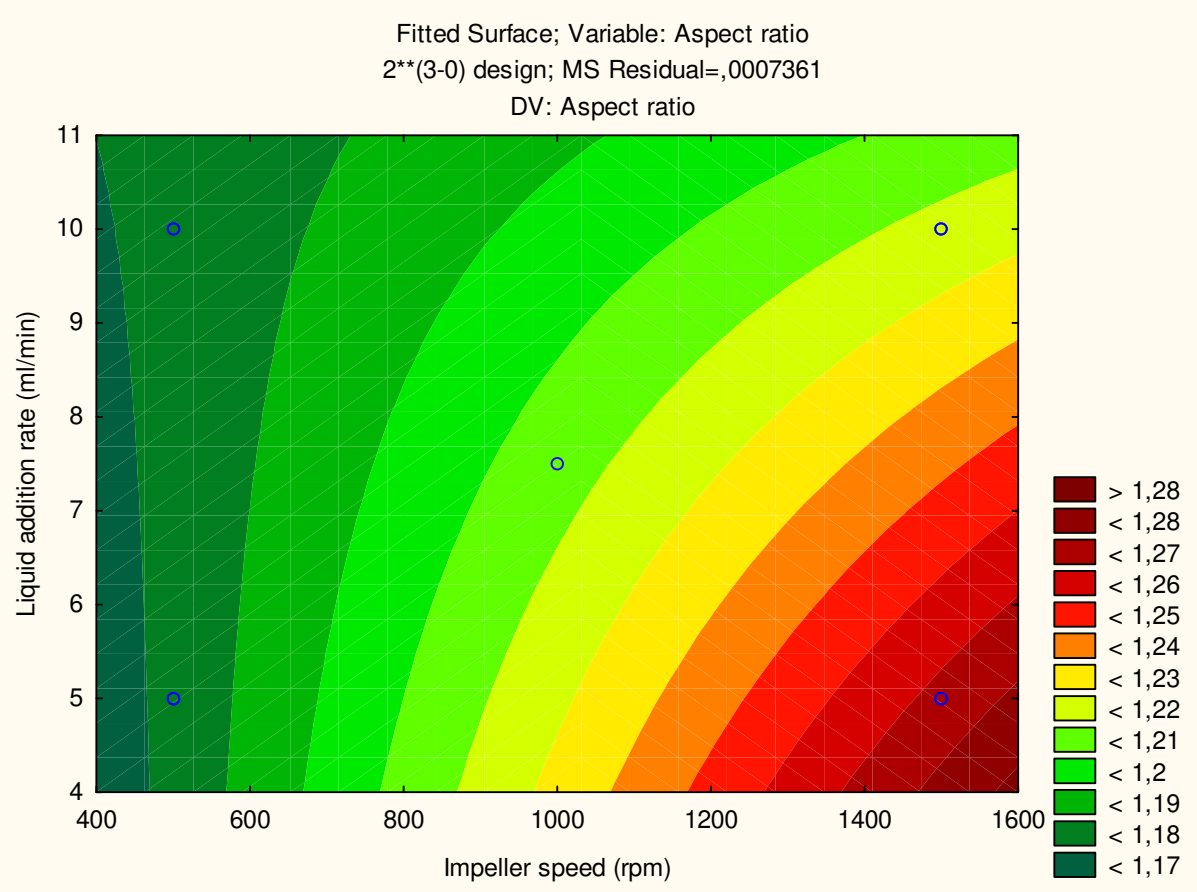

Fig. S48 Contour plot of the roundness of C3 at an extruder speed of 95 rpm

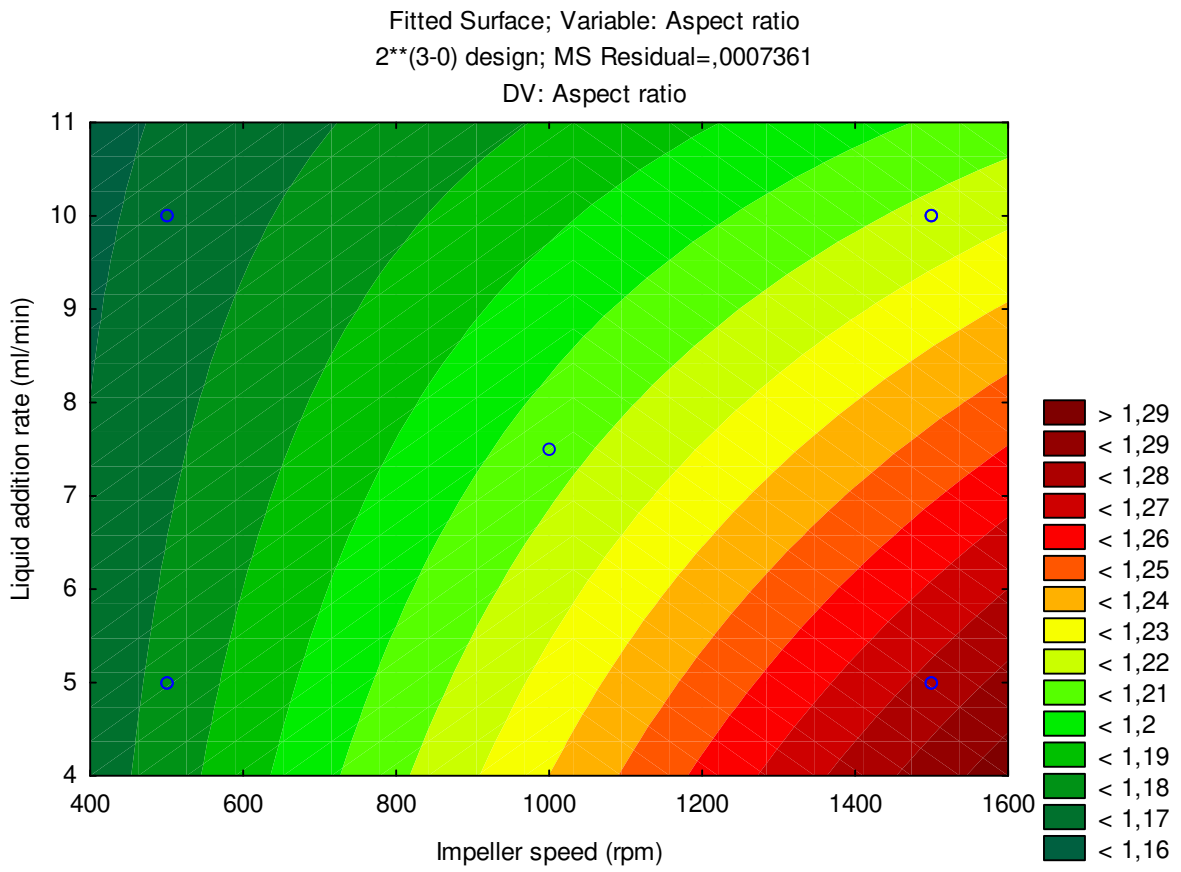

Fig. S49 Contour plot of the roundness of C3 at an extruder speed of 120 rpm

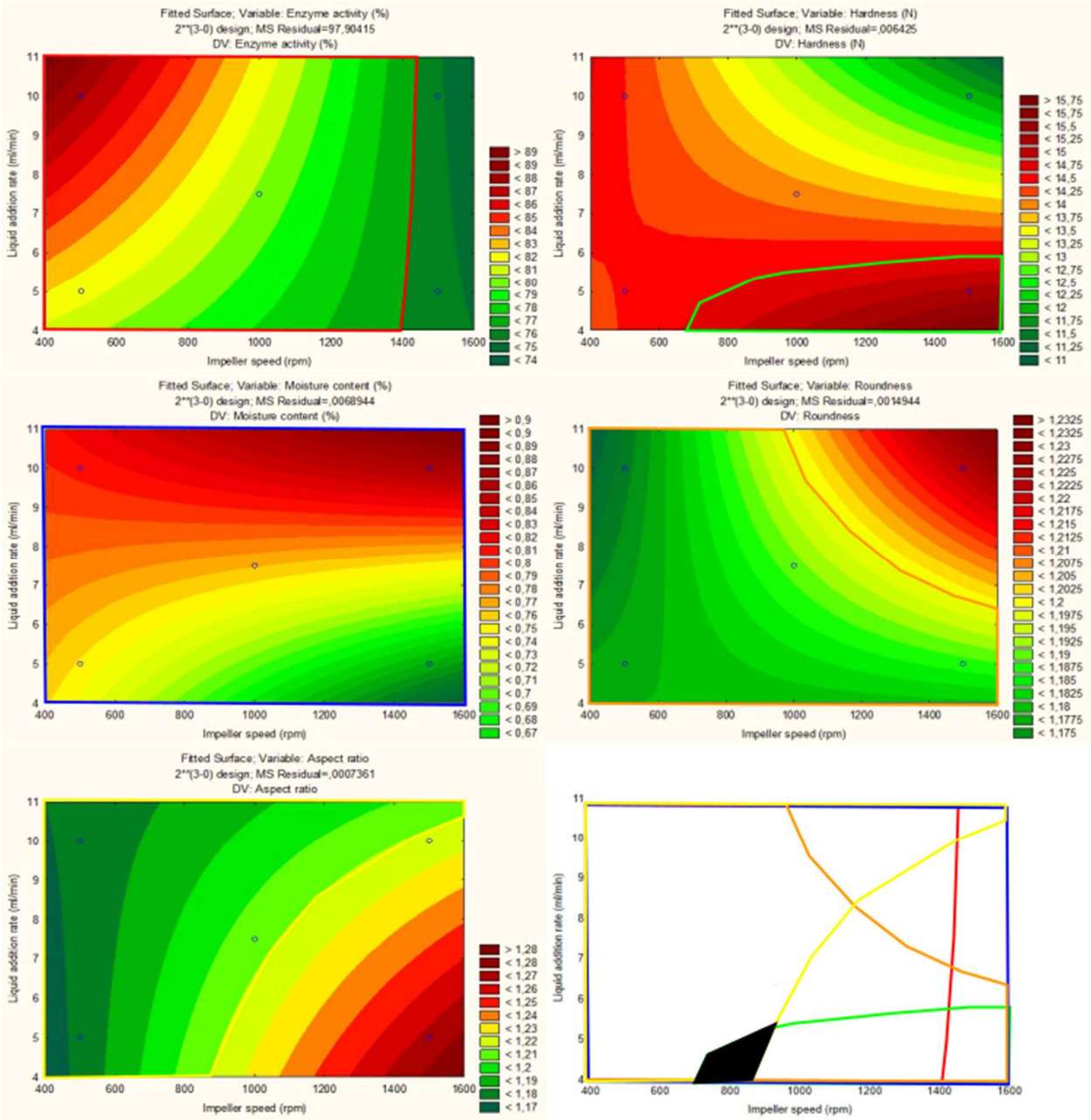

Fig. S50 Scheme of the determination of DS as an example of C3 95 rpm extruder speed

The areas fit to the acceptance criteria of various CQAs were merged into one graph, and the overlapping area (black), where all CQA fits to requirements was selected as nonlinear representation of DS.

ANNEX - 4

European Journal of Pharmaceutical Sciences 146 (2020) 105270

Contents lists available at ScienceDirect

European Journal of Pharmaceutical Sciences

journal homepage: www.elsevier.com/locate/ejps

Design and characterization of chitosan/citrate films as carrier for oral macromolecule delivery

Yousif H-E.Y. Ibrahim[a,b], Géza Regdon jr.[a], Katalin Kristó[a], András Kelemen[b], Mohamed E. Adam[c], Elnazeer I. Hamedelniel[d], Tamás Sovány[a,*]

[a] University of Szeged Institute of Pharmaceutical Technology and Regulatory Affairs, Eötvös u. 6. H-6720, Szeged, Hungary
[b] University of Szeged, Department of Applied Informatics, Boldogasszony sgt. 6. H-6725, Szeged, Hungary
[c] Medicinal Chemistry Department, University of Khartoum, Khartoum, Sudan
[d] Pharmaceutics Department, Omdurman Islamic University, Omdurman, Sudan

ARTICLE INFO

Keywords:
Chitosan
Citric acid
FT-IR
Mucoadhesion
Mechanical properties
Plasticizer
Surface characteristics

ABSTRACT

The oral delivery of biopharmaceuticals requires the including of absorption enhancer, protease inhibitor and a suitable carrier system. The aim of the present work was to formulate and characterize chitosan solutions/films incorporating citric acid (CA) as potential excipient in comparison to the well-known acetic acid (AA)-based films as a reference. Films were made by the solvent casting method with/without glycerol (G), propylene glycol (PG) and polyethylene glycol (PEG-400) as plasticizers. The minimum film forming temperature (MFFT) of the prepared solutions, film thickness, hardness/deformation, mucoadhesivity, moisture content, FT-IR spectra and surface free energy (SFE) were investigated. Chitosan has been reported as a safe and effective paracellular absorption enhancer for hydrophilic macromolecules, therefore there would be more rationale for incorporating CA as a solubility enhancer, a permeation enhancer and an enzyme inhibitor. CA shows good cross-linking, an ideal plasticizing property and increases both tensile strength and mucoadhesivity, thus its incorporation simplifies the formulation while improving effectiveness. We concluded that CA (3.5, 4 and 5 w/v %)-based chitosan solution could be used as a novel coating/subcoating polymer for oral macromolecule delivery, or as oral mucoadhesive films.

1. Introduction

Generally, numerous bioactive proteins and peptides are going through the clinical trials or have already been approved by the Food and Drug Administration (FDA) for marketing (Batista et al., 2018). This attracts and encourages researchers to develop less costly, reproducible and more applicable oral delivery systems because currently biopharmaceuticals are restricted as injectable dosages for therapy since they cannot be delivered orally (Goldberg and Gomez-Orellana, 2003). Therefore, the commercial success of protein/peptide drugs remains limited as their successful delivery requires the accomplishment of three key tasks: protection from degradation in the gastrointestinal tract (GIT), permeation through the intestinal barriers and the absorption of molecules into the systemic circulation (Brown, 2005, Choonara et al., 2014). The bioavailability of these molecules is dependent on their molecular mass since bioavailability sharply decreases if the molecular mass increases above 500-700 Da. (Muheem et al., 2016). Therefore, the development of oral macromolecular drugs requires a thorough understanding of the physicochemical properties of drugs, such as molecular weight, hydrophilicity, ionization constants and pH stability as well as knowledge about the barriers that act as obstacles for absorption, like enzymatic degradation, membrane efflux and pH variability (Mahato et al., 2003). Recently, Sovány et al. (2016) investigated the possibility of the successful formulation of pellets containing lysozyme using the quality by design approach (QbD) and process analytical technology (PAT). They succeeded in recognizing and specifying the design space for the pelletization process while preserving the lysozyme activity . This study opens the field for the production of solid dosage forms containing biopharmaceuticals. However, it is still necessary to introduce helpful formulation excipients that protect the labile drug against enzymatic activity and at the same time enhance and control release through the GIT.

Chitosan is a linear polysaccharide composed of randomly distributed ß (1, 4) - linked *D*-glucosamine and *N*-acetyl-*D*-glucosamine units, where the amount of *D*-glucosamine is greater than 50%. It is mainly obtained by the partial deacetylation of chitin (Shah et al.,

* Corresponding author.
E-mail address: t.sovany@pharm.u-szeged.hu (T. Sovány).

https://doi.org/10.1016/j.ejps.2020.105270
Received 21 June 2019; Received in revised form 31 January 2020; Accepted 16 February 2020
Available online 19 February 2020
0928-0987/

2018; Li et al., 2017; Liu and Li, 2018), which makes a natural and sustainable pharmaceutical excipient. The most known source for chitosan is the exoskeleton of marine organisms like squids and crustacean shells, and in recent years it has been derived from insects and fungi as well (Perinelli et al., 2018). This versatility of the sources together with its unique properties, e.g. biocompatibility, biodegradability, non-toxicity and low immunogenicity, makes chitosan the second most abundant natural polymer in the world (Cao et al., 2018, Rotta et al., 2009). Chitosan is a weak base, which is soluble in an aqueous acidic media and produces highly viscous solutions suitable for the preparation of free films and coatings (Rahmouni et al., 2018). Chitosan exhibits excellent mucoadhesive properties due to presence of reactive hydroxyl and amino groups providing excessive hydrogen bonding as well as a positive charge, resulting in a unique linear polycation with a high charge density (Agarwal et al., 2018). It was found that the ionic bonds between the sialic acid residues of the mucosa and the amino groups of chitosan play an important role in the mucoadhesion process (Phanindra et al., 2013). Bioadhesion is the adhesion of a natural, semi-synthetic or synthetic substance to a biological surface, whilst mucoadhesion is the adherence of a substance to mucus or an epithelial surface (Rajaram and Laxman, 2016). Mucoadhesive drug delivery may include gastrointestinal, oral cavity, nasal, ocular, vaginal and rectal drug delivery systems (Rajput et al., 2010).

Moreover, chitosan, when protonated below pH 6.5, is able to increase the paracellular permeability of macromolecules across the mucosal epithelium by opening the tight junctions (TJs) and allowing the penetration of macromolecular compounds like peptide drugs (Hombach and Bernkop-Schnürch, 2009, Thanou et al., 2001). The reversible TJs opening has been approved as a safe approach for permeation enhancement, therefore chitosan is regarded as a safe and efficient absorption enhancer for therapeutic macromolecules (Sonaje et al., 2011, Fan et al., 2016). Furthermore, the use of chitosan as a drug delivery system may enable the controlled release of the incorporated macromolecule, permeation enhancer and protease inhibitor at the absorption site and thus may prolong the drug action, and due to its mucoadhesivity it can form a special microenvironment at the mucosal membrane (Jiang et al., 2017).

During matrix preparation chitosan is usually dissolved in diluted organic acids, usually in acetic acid (AA). However, its replacement with citric acid (CA) would be advantageous, since it was reported that CA can be used effectively to suppress the luminal serine proteases, and recently it has been used to deliver some oral peptides. The rationale behind this strategy is that incorporating a pH modifier can result in an acidic microenvironment, which decreases protease activity (Aguirre et al., 2016). Moreover, CA has been described to increase the absorption of peptides by different mechanisms, such as permeation enhancement by calcium chelation and protease inhibition (Devendra et al., 2013; Welling et al., 2014). Recently, the absorption enhancing effect of chitosan-citrate was confirmed by administering chitosan-citrate gel vaginally to deliver poorly absorbable drugs such as acyclovir, ciprofloxacin and high molecular weight hydrophilic molecules such as FD4 (Bonferoni et al., 2008). The multicarboxylic structure of CA is responsible for its use as a compatibilizer, cross-linker and plasticizer (Garcia et al., 2011). Citrate cross-linked chitosan films were examined by Shu et al. (Shu, 2001). The swelling ratio of the chitosan/citrate film and the drug release profile using brilliant blue and riboflavin as model drugs were studied, and it was concluded the citrate/chitosan film was valuable in drug delivery like targeted drug controlled release in the stomach (Shu, 2001). Nevertheless, this study achieved cross-linking of chitosan by the dipping of ready films into sodium-citrate solution and not by direct dissolution of chitosan in citric acid solution.

In conclusion, it could be a logical approach when macromolecules (like peptides/proteins) are suitably incorporated in a multifunctional mucoadhesive polymer (e.g. chitosan/citrate), which will enhance bioavailability by the different ways discussed above, and by the control of the release of the incorporated drug through forming a gel-matrix, which is essential for macromolecules that have a short circulating time due to the initiation of the immune response.

The main objective of this work was to formulate and characterize chitosan/citrate films with the direct dissolution of chitosan in citric acid solution and evaluate their applicability as functional mucoadhesive subcoating of a controlled release multiparticulate drug delivery system in comparison to chitosan/acetate films as a reference. As secondary objective the applicability of films as mucoadhesive oral carrier film (MOF) is also tested as MOF is one of the most hopeful approaches to deliver macromolecules sticking to the oral mucosa, providing rapid absorption, bypassing the hepatic first-pass effect and offering ease of handling (Rajaram and Laxman, 2016). As tertiary objective, the effect of a high-amount plasticizers on the properties of chitosan solutionsfilms was also studied. The obtained solutions were physically characterized for minimum film forming temperature (MFFT) a crucial property of coating formulations, while the prepared films were characterized for their thickness, hardness/deformation behaviour, mucoadhesivity, moisture content and surface free energy (SFE).

2. Materials and Methods

2.1. Materials

Chitosan 80/1000 (Heppe Medical Chitosan GmbH., Germany) (MW = 300000–350000 Da) was used as a film-forming polymer, acetic acid 99.8% (Sigma-Aldrich, Germany) and citric acid monohydrate (CA) (Molar Chemicals Ltd., Hungary) were used as solubility enhancers for chitosan, glycerol (G), propylene glycol (PG) (Hungopharma Plc., Hungary) and polyethylene glycol 400 (PEG-400) (Sigma-Aldrich, Germany) were used as plasticizers, mucin 75–95 % (Roth, Germany) was used as a reagent for the mucoadhesivity investigation and diiodomethane (VWR Prolabo, USA) was used as non-polar liquid for the SFE investigation, all were of analytical grade.

2.2. Methods

2.2.1. Preparation of the Films

Chitosan films were prepared by the solvent casting method, by dissolving the polymer (2 w/v%) in aqueous acetic acid (AA) solution (2 v/v%) as prescribed by Liu et al. (Liu et al., 2013) as a reference, and with the use of CA (2.5, 3, 3.5, 4, 5 and 7 w/v %). Plasticizers were added to AA, CA 2.5% and CA 7%-based solutions in approx. five to ten times excess (5 w/v% and 10 w/v%) compared to polymer, to obtain significant modification of the surface characteristics, which could be crucial if the obtained films are applied as subcoating. Films plasticized with 5 or 10% of glycerol, propylene glycol or polyethylene glycol are referred later as G 5%, G 10%, PG 5%, PG 10%, PEG 5% and PEG 10%, respectively. The exact compositions of the prepared solutions/films are shown below in Table 1, while the molar ratios may be found in Table

Table 1
Composition of prepared citric acid (CA)- and acetic acid (AA)-based solutions/films, G = glycerol, PG = propylene glycol, PEG = polyethylene glycol.

Plasticizer	w/v%	Chitosan w/v%	CA w/v %	CA w/v %	CA w/v %	CA w/v %	CA w/v %	CA w/v %	AA v/v %
-	0	2	2.5	3	3.5	4	5	7	2
G	5	2	2.5	-	-	-	-	7	2
	10	2	2.5	-	-	-	-	7	2
PG	5	2	2.5	-	-	-	-	7	2
	10	2	2.5	-	-	-	-	7	2
PEG-400	5	2	2.5	-	-	-	-	7	2
	10	2	2.5	-	-	-	-	7	2

S1. A magnetic stirrer was used to obtain 100 mL homogeneous solutions. Heating to 50–58 °C for two hours was required to dissolve chitosan containing a low amount of CA (2.5 and 3 w/v %), as the pH of CA (2.5–3 w/v%) was around pH 4, which is higher compared to the pH of the AA-based solution (pH of ~2.75). For AA and CA (3.5–7 w/v %) heating was not required. After the whole polymer dissolved, the obtained solutions were left to stand for 3 h to enable the entrapped air bubbles to evolve. A portion (~ 25 mL) of each solution was taken for MFFT testing, while the remaining amount was cast into gasket rings (19.635 cm^2 x 0.5 cm) as 10 g/ring. The rings were fixed onto Teflon surface by applying a thin layer of the polymer solution at the bottom to prevent any leakage. The cast solutions were dried under ambient condition (25.5 ± 1 °C and 28 ± 1 RH%) for 48 h, the dried films were carefully released from the plates and preserved in tightly closed containers for further investigations.

2.2.2. Minimum film forming temperature (MFFT) investigation

MFFT was investigated with a Rhopoint MFFT-60 Bar tester (Rhopoint, UK), the temperature bar consisted of a platen with an electronically imposed temperature gradient, and the MFFT was investigated in the temperature range of 15–60 ºC. After temperature equilibrium had been established, a cube applicator was used to make 5 parallel films of 75 µm thickness over the temperature bar. The hinged Perspex cover was returned down to provide atmospheric and thermal equilibrium whilst enabling the visual inspection of the applied films. The films (n = 5) were then let completely dried and the result was recorded manually by inspecting the cracked regions on the applied films form on the graduating scale of the equipment.

2.2.3. FT-IR spectra

Infrared spectra for the films and the other excipients were obtained by using an FT-IR (Avatar 330 FT-IR ThermoScientific, USA) apparatus coupled with a Zn/Se HATR (horizontal attenuated total reflectance) accessory. Each film was directly placed on an ethanol-cleaned crystal of the equipment, the scanning was run in the wavelength range of 600–4000 cm^{-1}, the spectra were collected from 128 scans to obtain smooth spectra, at the spectral resolution of 4 cm^{-1} and applying CO_2 and H_2O corrections.

2.2.4. Film thickness

The thickness of films was measured at 10 randomly selected points on each film (n = 10) by using a screw micrometre (Mitutoyo Co. Ltd, Japan) with sensitivity of 0.001 mm, and the means and SDs were calculated.

2.2.5. Hardness and mucoadhesion investigations

Hardness and mucoadhesive forces were investigated by a laboratory constructed texture analyser. The equipment and software were developed at the Institute of Pharmaceutical Technology and Regulatory Affairs, University of Szeged. The equipment is designed to assemble different sample holders as well as different stainless-steel moving probes depending on the test to be conducted, with a controllable force, moving speed and direction.

2.2.5.1. Hardness and deformation process investigation. For the hardness test, a needle-like probe with a half-sphere end was fixed at the top movable part of the assembly and set to move downward with a controllable speed toward the tested film, which was tightly fixed on a sample holder enabling the moving probe to pass through the fixed film until the film cracked. This test was repeated ten times for each film (n = 10), and the means and SDs were calculated.

2.2.5.2. Mucoadhesion force measurement. The same texture analyser with different setting and assembling parameters was used to investigate mucoadhesion. A rod-like probe with an outer diameter of 9 mm represented the sample holder. A double-faced adhesive tape was used to fix the polymer film with equivalent area on its surface. At the equipment bottom, a circular flat disc with an outer diameter of 35 mm was fixed, on which a few drops of freshly prepared 1 mg/mL mucin solution were spread. The equipment was adjusted to move downward to press the film with 50 ± 1 N force for 30 s to the mucin, which may be followed as a steady state part in the related force-time curve (Fig. 3). The probe then moves upwards, which is resulted in the drop down of the force curve until the fixed film starts to detach from the mucin, which is represented as a sharp peak on the force-time curve, where the peak maximum represents the mucoadhesive force. This test was repeated five times (n = 5), and the means and SDs were calculated.

2.2.6. Moisture content measurement

The moisture content of the prepared films was measured by using a Mettler–Toledo HR73 (Mettler–Toledo, Hungary) halogen moisture analyzer. The moisture content of approximately 0.5 g of the films was measured three times (n = 3) at a drying temperature of 105 °C until a constant weight was obtained, and the means and SDs were calculated.

2.2.7. Calculation of SFE

SFE is one of the most essential parameters that could be used to characterize the surface properties of the prepared films, especially if it is involved in a coating process (Kristó et al., 2016). Therefore, by measuring SFE the wetting behaviour and the applicability of the tested polymer for the coating process can be evaluated. The SFE of a mucoadhesive polymer should be adequate to enable the wetting with the mucosal surface (Andrews et al., 2009).

SFEs were calculated indirectly from the means of the contact angles (Θ) of two liquids (Schuster et al., 2015), with known surface tension, dispersive and polar components by using the optical contact angle-measuring apparatus (OCA20-DataPhysics Instrument GmbH, Filderstadt, Germany), via the application of the sessile drop method. Distilled water (γ^{tot} = 72.8 mN/m, γ^{d} = 21.8 mN/m, γ^{p} = 51.0 mN/m) and diiodomethane ($\gamma^{tot.}$ = 50.8 mN/m, γ^{d} = 50.8 mN/m, γ^{p} = 0 mN/m) were used as polar and non-polar reagents, respectively. One drop of each liquid (10 µL of distilled water and 5 µL of diiodomethane) was applied via a motor-driven micro-syringe on the prepared thin, plain and smooth film of chitosan and the angles were measured automatically for 30 s. The starting (0 s) and equilibrium (30 s) contact angles (n = 10 of each liquid) were recorded, and the means and SDs were calculated separately. The results were introduced into OCA-20 SFE-calculating-program by introducing the means and SDs of first and equilibrium contact angles in every combination by applying the method of Wu. (Eq. 1):

$$(1 + \cos\theta)\gamma = \frac{4(\gamma_s^d \cdot \gamma_l^d)}{\gamma_s^d + \gamma_l^d} + \frac{(\gamma_s^p \cdot \gamma_l^p)}{\gamma_s^p + \gamma_l^p} \quad (1)$$

where Θ is the contact angle, γ_l is the liquid surface tension; γ_s is the solid surface energy, and the superscripts indicate their polar (γ^p) and dispersive components (γ^d). As the surface free energy of the film is the sum of the dispersive part and the polar part, the polarity (percent of hydrophilic groups formed during film formation) of the prepared films could be calculated by the following formula (Eq. 2):

$$Polarity\% = (Polar part / Surface energy) \times 100 \quad (2)$$

2.2.8. Statistical analysis

The gathered data were analysed with according to a factorial ANOVA method using Tibco Statistica v13.1 (Statsoft, Tulsa, OK, USA) software.

3. Results and Discussion

3.1. Visual Appearance of Prepared Solutions and Films

The pH of the obtained AA-based solutions (Table S2) was varied in the 2.75 ± 0.25 range and all solutions were transparent. The addition of plasticizers slightly increased the pH, but G 10% solution showed pH was comparable to a plasticizer-free solution. The appearance of the films was similar, smooth and transparent in colour, except for films made with the addition of PEG-400, which had white, opalescent colour, which may be attributed mainly to elevated light scattering as result of the increased film thickness caused by the intercalation of long plasticizer chains between chitosan backbone. The pH values of the obtained CA 2.5%-based solutions were in a relatively higher range (pH 4.12-5.37) (Table S3), which explains why heating was necessary to dissolve the polymer. Nevertheless, the visual appearance of solutions and films with and without different plasticizers was totally comparable with that of AA-based ones. The PEG-400-containing films were also translucent and had a smooth waxy texture. To eliminate the problems of the elevated pH, a series of CA-based solutions was made in the range of 2.5–7 w/v% (Table S4). The pH of the solutions was decreased from 4.25 to 2.58 with the increment of the CA concentration, which was comparable with the pH of AA-based solutions and enabled the dissolution of the polymer without heating. The visual appearance of the films was also similar to the AA-based ones.

The effect of plasticizers on the properties of CA 7w/v%-based chitosan films (Table S5) was comparable with that of AA-based ones, the obtained films were of smooth texture and transparent colour, except for the one made with PEG-400, which showed the same white, opalescent colour and transparency degree as PEG-400 plasticized CA 2.5w/v%- and AA-based films.

3.2. Physical Properties of the Prepared Films

The minimum film forming temperature (MFFT) was less than 15 ºC for all investigated compositions as shown below in Table 2. All films applied on the temperature bar were dried as smooth, transparent and continuous films, i.e. no cracking or other failures were observed, which confirms the applicability of the compositions for the coating/subcoating of protein-containing solid dosage forms, since the low MFFT enables to perform a failureless coating process under gentle temperature conditions (between 30–45 ºC), which may generally decrease the risk of temperature-induced misfolding of the processed polymers. Furthermore, the low MFFT enabled the drying of the cast films under ambient conditions.

The thicknesses of the prepared films are shown in Table 2. The plasticizer-free AA-based chitosan films showed the least thickness (0.07 mm), in accordance with the literature (Bhuvaneshwari et al., 2011). The thickness of CA-based chitosan films was minimum the double and proved to be directly proportional to the CA concentration (0.13–0.27 mm), indicating dilatation in the polymer backbone as a result of cross-linking by CA. A similar direct relation between lactic acid quantity and the thickness of chitosan film was also reported by Bujang et al. (Bujang et al., 2013). The addition of a plasticizer also increases the film thickness up to a certain limit in the order of G < PG < < PEG-400 in all cases (Table 2).

The increment in film thickness upon the addition of the plasticizer is attributed to a good distribution of these plasticizers within the chitosan backbone. The significantly ($p < 0.001$) higher thickness obtained with PEG-400 may be due to the bigger molecular weight, and higher chain length of this plasticizer, which was resulted in bigger distance between chitosan chains and higher water retention capacity. Generally, the film thickness of the chitosan film may be manipulated and optimized by the amount of the plasticizer and the amount of chitosan itself, as was also shown by Nady and Kandil (Nady and Kandil, 2018).

The results also support that differences in film thickness may also contribute in the difference of the moisture content (MC) of the various samples as a weak positive correlation was revealed between these two parameters. The MC of plasticizer-free chitosan films showed no significant difference and was approximately 1% up to 5% CA content. However, after a certain threshold, MC increases and may reach 9.15%, as recorded for the CA 7%-based film. This may also be explained by the cross-linking between CA and chitosan, which may result in the entrapment of water molecules within the polymer backbone. The addition of plasticizers significantly ($p < 0.0001$) increased MC in all cases as a result of physical interactions enabling the solvent to be entrapped within the polymer skeleton and also due to their hygroscopic and

Table 2
Physical properties of the various chitosan films (MFFT = minimum film forming temperature, MC = moisture content).

AA (v/v%)	CA (w/v%)	Plasticizer	Plasticizer content (w/v%)	MFFT (°C)	Thickness (mm)	Hardness (N)	Mucoadhesion (N)	MC (w/w%)
2	-	-	0	<15	0.07 ± 0.02	44.63 ± 3.4	42.30 ± 3.60	01.20 ± 1.70
2	-	G	5	<15	0.21 ± 0.04	2.39 ± 0.9	9.00 ± 4.62	13.83 ± 3.64
2	-		10	<15	0.32 ± 0.10	2.91 ± 1.1	8.34 ± 1.63	11.15 ± 0.54
2	-	PG	5	<15	0.33 ± 0.01	6.66 ± 0.71	19.49 ± 3.20	06.41 ± 2.34
2	-		10	<15	0.13 ± 0.02	6.81 ± 0.72	10.37 ± 2.27	07.80 ± 1.90
2	-	PEG 400	5	<15	0.21 ± 0.01	20.88 ± 1.7	13.68 ± 3.40	7.92 ± 2.71
2	-		10	<15	0.43 ± 0.03	18.48 ± 1.7	8.69 ± 2.89	13.27 ± 3.96
-	2.5	-	0	<15	0.13 ± 0.01	36.01 ± 3.70	47.57 ± 3.03	0.75 ± 1. 26
-	3	-	0	<15	0.15 ± 0.10	35.65 ± 3.36	35.41 ± 2.22	0.86 ± 2.54
-	3.5	-	0	<15	0.14 ± 0.01	48.52 ± 0.50	42.68 ± 3.10	1.14 ± 3.34
-	4	-	0	<15	0.16 ± 0.04	32.83 ± 4.78	41.10 ± 2.93	1.99 ± 2.82
-	5	-	0	<15	0.23 ± 0.02	39.20 ± 5.40	30.32 ± 1.84	1.05 ± 2.46
-	7	-	0	<15	0.27 ± 0.02	8.40 ± 1.98	25.65 ± 3.90	9.15 ± 3.84
-	2.5	G	5	<15	0.17 ± 0.02	1.04 ± 0.27	14.52 ± 1.28	0.86 ± 3.43
-	2.5		10	<15	0.20 ± 0.01	1.93 ± 0.89	13.71 ± 0.46	1.14 ± 3.03
-	2.5	PG	5	<15	0.21 ± 0.01	1.39 ± 0.43	13.77 ± 1.78	1.99 ± 2.50
-	2.5		10	<15	0.22 ± 0.01	4.95 ± 0.68	9.91 ± 2.18	1.05 ± 0.92
-	2.5	PEG 400	5	<15	0.26 ± 0.02	8.12 ± 3.95	8.67 ± 2.10	2.15 ± 1.56
-	2.5		10	<15	0.34 ± 0.01	6..22 ± 1.92	7.86 ± 3.86	2.75 ± 2.01
-	7	G	5	<15	0.10 ± 0.01	0.58 ± 0.64	11.07 ± 2.76	11.83 ± 4.52
-	7		10	<15	0.14 ± 0.01	0.64 ± 0.64	13.24 ± 1.10	17.36 ± 3.67
-	7	PG	5	<15	0.16 ± 0.01	1.33 ± 0.14	15.80 ± 0.84	8.33 ± 1.80
-	7		10	<15	0.18 ± 0.01	1.27 ± 0.25	12.20 ± 1.22	10.46 ± 2.67
-	7	PEG 400	5	<15	0.23 ± 0.02	2.75 ± 1.10	18.13 ± 2.57	4.55 ± 0.73
-	7		10	<15	0.33 ± 0.02	6.22 ± 1.80	16.79 ± 1.35	3.25 ± 2.22

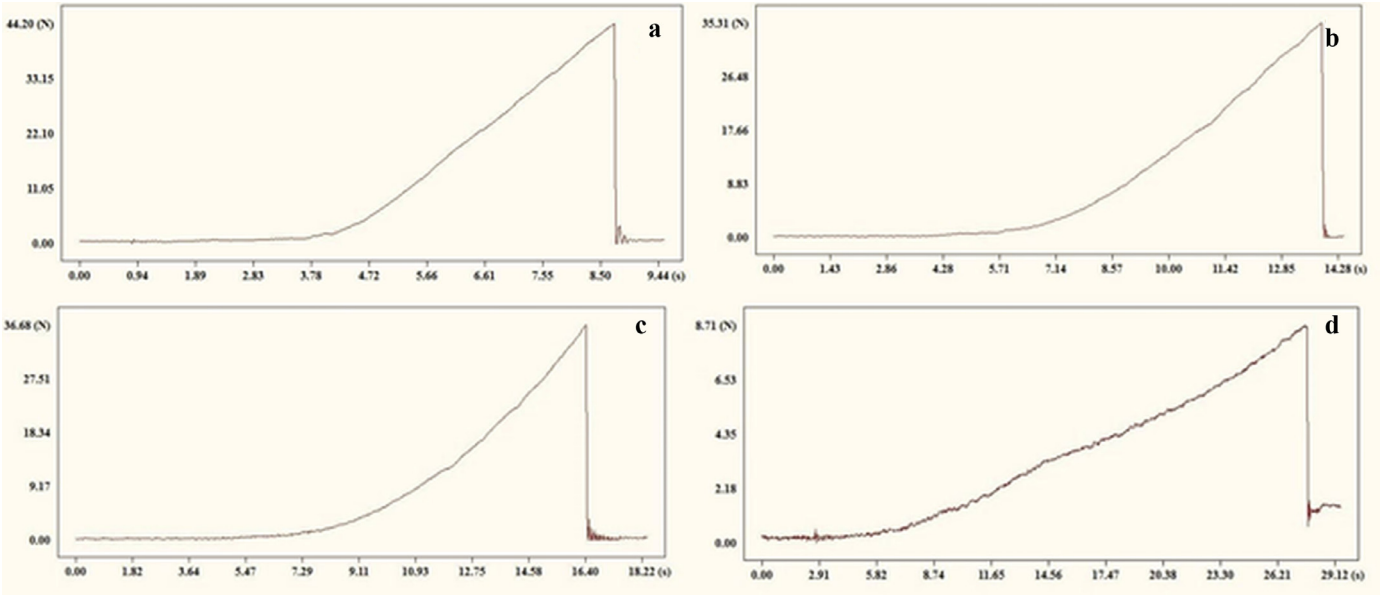

Fig. 1. Breaking curves of CA 2.5% (a), CA 4% (b), CA 5% (c) and CA 7%-based chitosan films.

moisture retentive behaviour. From this aspect, G exhibited significantly higher MC ($p < 0.01$) than PG or PEG, which may be connected to the presence of unbounded OH groups. It is also notable that MC showed considerable pH dependency since the CA 2.5%-based samples exhibited significantly lower MC ($p < 0.0001$) than others, which may be due to a lower degree of ionization.

Plasticizer-free films made with CA in different quantities (2.5, 3, 3.5, 4, and 5 w/v %) showed a high breaking force in the range of 32.83–48.52 N, which was comparable with AA-based chitosan films. Nevertheless, a dramatic increase was observed in the time of elongation (Fig. 1) due to a viscoelastic change in the texture of films, found to be proportional to the amount of CA. However, when CA reaches 7 w/v %, a sharp reduction of hardness may be observed with a marked increase in elasticity. In conclusion, CA may be a good plasticizer for chitosan and the ideal mechanical property may be achieved when it is used in the 3.5–5 w/v % range. Wan et al. (Wan et al., 1993) prepared CA-based hydroxypropyl-methylcellulose (HPMC) and CA-based sodium carboxymethylcellulose (NaCMC) films containing theophylline, and they concluded that the films made with 10% of CA were brittle and CA should be beyond 30% to obtain a good plasticizing effect (Wan et al., 1993). Shi et al. (2008) stated that CA used in a concentration of 5 wt% increases the tensile strength of polyvinyl alcohol/starch films, and above this concentration (5–30 wt%) the excess of CA acts as plasticizer and hence reduces tensile strength (Shi et al., 2008). In present study CA exerts the plasticizing effect above 3 w/v% but results in a significant decrease of hardness only above 7 w/v%, which equals 150% and 350% CA content compared to the polymer, respectively, which is higher compared to the above. Nevertheless, the different behaviour may attribute, to the weak alkaline nature of chitosan forming stronger interactions and requiring much more CA than needed by HPMC, NaCMC and polyvinyl alcohol/starch.

Independently from the original hardness, the addition of plasticizers significantly ($p < 0.0001$) decreased the hardness of all investigated films (Table 2), in the order of PEG-400 < < PG < G. Nevertheless, despite the significant decrease in hardness, a notable viscoelastic deformation was observed, which resulted in an increase of the required time of elongation (Figs. 2 a,b). A comparable finding for chitosan/G was obtained by Zaini et al. (Ziani et al., 2008).

As regards the hardness of films made with PEG-400, it was significantly ($p < 0.0001$) better compared to the other plasticizers. However, it is notable that the addition of PEG-400 affects hardness inversely compared to PG or G, and a further decrease in hardness was observed when the added quantity of PEG-400 was increased. In contrast, the increasing amount of PG and G resulted in a slight, but not significant increase in hardness.

Regarding mucoadhesion, the plasticizer-free AA-based chitosan films exhibited a high force of detachment (42.30 N) (Table 2), whereas plasticizer-free CA 2.5 w/v%-based films showed even higher values (47.57 N), possibly due to the lower degree of ionization, which enables the formation of strong ionic interactions between the unionized amino groups of chitosan and the sialic acid parts of mucin molecules (Bravo-Osuna et al., 2007, Peppas and Huang, 2004). In contrast, the increment of CA content or the addition of a plasticizer significantly ($p < 0.0001$) reduced mucoadhesive force (Figure 3). This could be attributed to the interactions between chitosan and the plasticizers, which decrease the number of free functional groups, or to the covering of the pores at the film surface and retarding the wetting process. Compared to the other films, CA 3.5, 4 and 5 w/v%-based films are the most applicable depending on their tensile strength and mucoadhesion in these concentration ranges, as CA showed an ideal plasticizing effect as well as a good cross-linking effect on the chitosan molecule.

The obtained SFEs of the prepared films are shown in Table 3. The plasticizer-free AA-based film exhibited moderate SFE (~27 mN/m), while CA-based films showed significantly higher SFE around 40 mN/m without any considerable difference regarding the CA content. The polarity of CA-based films was also higher than that of the AA-based one, however, the increasing CA content significantly decreased polarity, which may be related to the pH of the solution. The addition of PEG-400 increased SFE as well as polarity, in both 5 and 10 w/v% concentrations, which may be due to presence of polar oxygens in the PEG backbone, which will be presented on the film surface after cross-linking of the chitosan chains, or in a manner enabling the polymer to dissolve in a relatively high amount of CA, resulting in ester formation and at the same time saving some polar functional groups (OH groups) at the surfaces when the films got dry. Despite these, the mucoadhesivity of PEG-containing samples was relatively low, since the presence of PEG may decrease surface porosity and the polar oxygens are weak proton acceptors and therefore may poorly interact with mucin.

On the other hand, films made with the addition of G and PG demonstrated a strong decrease in both SFE and polarity. This may be attributed to the inclusion of the polar groups of these plasticizers with the carboxyl group of the acid, or involvement in hydrogen bonding

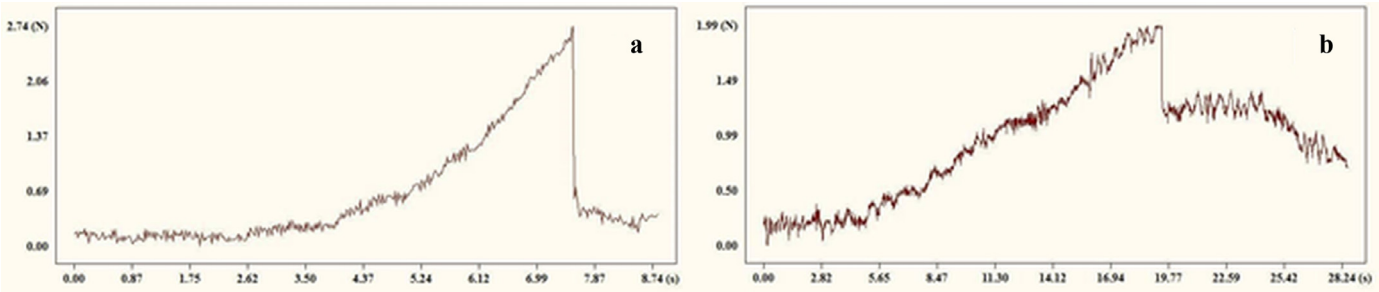

Fig. 2. Hardness of CA 2.5%-based chitosan film plasticized with 10 w/v% PG (a) or G (b).

with chitosan and hydrocarbon backbone on the surface decreases polarity, surface porosity and therefore reduces wettability. All of these events also participate in the reduction of the mucoadhesivity of these films. As wetting is the first step of the mucoadhesion process, Casariego et al. (Casariego et al., 2008) reported that the addition of a hydrophilic plasticizer such as glycerol and sorbitol reduces the wettability and adhesion coefficient of chitosan films (Casariego et al., 2008). Overall, a plasticizer-free CA-based film may be chosen as an oral film to deliver a macromolecule, as the values of hardness and SFE were relatively adequate, while the good wetting and high mucoadhesivity enables the films to tightly adhere to the mucosal surface. However, if the film would be utilized as the subcoating of an intestinosolvent coat, the PEG plasticized film seems to be best solution due to its higher hardness and higher surface free energy, which will enable better spreading and adhesion of the intestinosolvent coat on the substrate surface.

3.3. Investigation of the Chemical Structure and Interactions

The FT-IR spectrum of chitosan biopolymer is shown in Fig. 4, which reveals the fundamental absorption bands. The stretching vibrations of the –OH and N-H groups of chitosan are shown by a broad band between 3800–3400 cm^{-1} and 3300 3000 cm^{-1}, respectively. The peak around 2870 cm^{-1} belongs to the symmetric stretching of the CH_3 group in the acetyl side chain, while that of 2715 cm^{-1} to the symmetric CH_2 stretching in the ring. The strong absorption band at 1660 cm^{-1} belongs to the C=O stretching of the acetylated carbon amide group. The absorption bands around 1592 cm^{-1}, at 1423 cm^{-1} and 1377 cm^{-1} belong to the presence of N–H, C—H and O—H bending vibrations, respectively. The peak at 1170 cm^{-1} is attributed to the asymmetric stretching of the (C–O–C) bridge.

Chitosan was dissolved in AA 2 v/v% due to the ionization of the non-acetylated amide groups as it is shown by the right shift of the N—H stretching and the left shift of the N—H bending absorption bands. The appearance of a new band at 1750 cm^{-1} indicates the esterificaion and hydrogen bonding of some hydroxyl groups, similarly to the right shift of the broad O—H stretching peak at 3600–3000 cm^{-1} and the left shift of the OH bending. The addition of plasticizers resulted in no considerable change in the texture, but some signs of weak hydrogen bonds were noticed in the order of G > PEG-400 > PG, which may be due to the number of free hydroxyl groups on the plasticizers.

The FT-IR spectra of CA-based chitosan films made with variable amounts of CA (Fig. 5) indicates the presence of strong H-bonds between the OH groups of the polymer and the carboxyl groups of the acid by right shift of OH stretching peak between 3600–3300 cm^{-1}. The more intensive right shift of the N—H stretching signal between 3300–3000 cm^{-1}, the stronger left shift of the NH bending at 1590 cm^{-1} and the increasing intensity of the new broad peak at 2000 cm^{-1} indicate the stronger ionization of the amino groups with the increasing CA content. In all the shown film spectra, the presence of peak around 1400 cm^{-1} was due to carboxylate anion absorption ($–COO^-$), indicating citrate salt formation. According to Llanos et al. (Llanos et al., 2015), the peak around 1588 cm^{-1} is due to the protonation of amine group NH_3^+ and its intensity can be used to estimate the degree of protonation, while according to Lusiana et al. (Lusiana et al., 2018), the appearance of a peak around 1580–1590 cm^{-1} indicates the

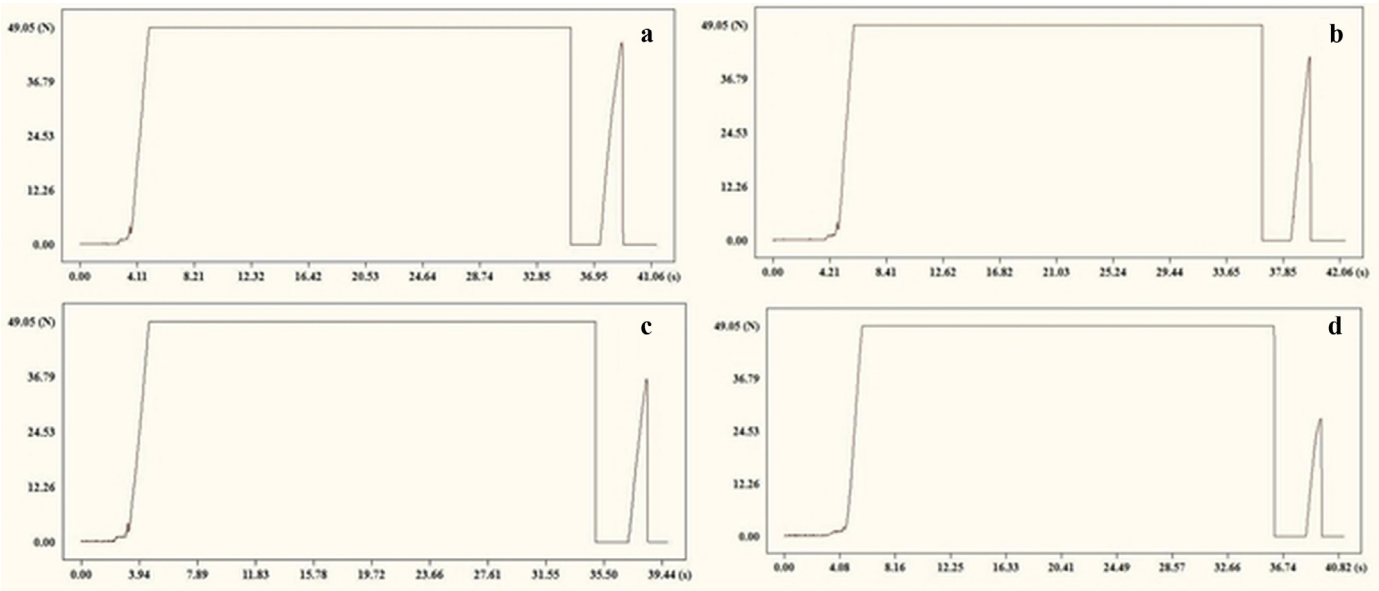

Fig. 3. Mucoadhesion curves of CA 2.5% (a), CA 4% (b), CA 5% (c) and CA 7%-based chitosan films.

Table 3
SFE (γ^{total}), its dispersive (γ^{d}) and polar (γ^{p}) components and polarity of the prepared films.

AA (w/v%)	CA (w/v%)	Plasticizer	Plasticizer content (w/v%)	γ^{total} (mN/m)	γ^{d} (mN/m)	γ^{p} (mN/m)	Polarity (%)
2	-	-	0	26.58 ± 2.25	14.82 ± 0.65	11.80 ± 2.15	44.40
2	-	G	5	15.55 ± 1.94	9.22 ± 0.78	6.33 ± 1.80	40.71
2	-		10	13.21 ± 1.85	8.21 ± 0.78	5.00 ± 1.70	37.85
2	-	PG	5	14.95 ± 2.12	8.12 ± 0.94	7.33 ± 1.90	49.03
2	-		10	15.75 ± 1.84	12.39 ± 0.86	3.40 ± 1.38	21.61
2	-	PEG 400	5	44.71 ± 2.74	22.38 ± 0.90	22.20 ± 2.60	49.65
2	-		10	47.30 ± 3.00	25.66 ± 1.50	22.10 ± 2.56	46.72
-	2.5	-	0	41.50 ± 1.90	18.33 ± 0.90	23.13 ± 1.70	55.73
-	3	-	0	44.31 ± 1.65	24.44 ± 0.70	19.87 ± 1.50	44.84
-	3.5	-	0	37.97 ± 1.80	17.12 ± 0.68	20.90 ± 1.63	55.04
-	4	-	0	43.34 ± 1.72	17.12 ± 0.74	20.76 ± 1.55	48.00
-	5	-	0	42.54 ± 1.71	23.98 ± 0.86	18.31 ± 1.50	43.04
-	7	-	0	39.40 ± 2.65	22.80 ± 2.01	16.59 ± 1.64	41.40
-	2.5	G	5	29.60 ± 2.02	16.54 ± 1.33	13.05 ± 1.50	44.10
-	2.5		10	27.23 ± 2.72	16.69 ± 2.01	10.54 ± 1.70	38.71
-	2.5	PG	5	47.66 ± 1.84	29.38 ± 1.12	18.30 ± 1.50	38.40
-	2.5		10	36.85 ± 1.80	19.15 ± 0.90	17.82 ± 1.54	48.40
-	2.5	PEG 400	5	57.40 ± 1.73	35.73 ± 1.00	21.70 ± 1.42	37.80
-	2.5		10	54.14 ± 1.60	35.16 ± 0.82	19.00 ± 1.33	35.10
-	7	G	5	40.10 ± 1.85	27.58 ± 1.27	12.50 ± 1.64	31.20
-	7		10	38.57 ± 1.52	24.98 ± 0.72	13.60 ± 1.33	35.30
-	7	PG	5	37.30 ± 2.04	26.78 ± 1.58	10.25 ± 1.31	27.50
-	7		10	36.63 ± 1.72	26.84 ± 1.15	9.80 ± 1.25	26.80
-	7	PEG 400	5	65.77 ± 2.11	34.37 ± 1.55	31.40 ± 1.43	47.74
-	7		10	68.11 ± 1.81	36.77 ± 1.23	31.35 ± 1.32	46.03

modification of the amine groups in chitosan from primary amine to secondary amine upon the addition of acid. However, according to our knowledge, the secondary amine did not show N—H absorption in this range. On the other hand, He et al. reported the characteristic peak around 1588 cm^{-1} due to the N-H bending vibration of primary amine -NH_2 (He et al., 2011), which opinion corresponds with our point of view.

When chitosan was dissolved in CA (Figs. 6 and 7), the addition of plasticizers also resulted in the formation of weak H bonds, but in this case in the order of PG > G > PEG-400, which also confirms the differences in the texture formation and interactions of AA- and CA-based films. However, no considerable difference was observed between CA 2.5% and CA 7% films in this manner, which indicates that the polymer-plasticizer interactions may be related mostly to the bonding of -OH groups, and therefore the increasing ionization grade of chitosan does not considerably affect the strength of these interactions.

Generally, it could be concluded that the addition of polyhydroxy alcohols like G, PG and PEG-400 will result in the formation of weak H bonds with the hydroxyl groups of chitosan, and the white opalescent colour of chitosan/PEG-400-based films was only due to physical interactions and may be not connected more intensive chemical change (Thuran et al., 2001).

4. Conclusions

In the present study it was successfully proven that chitosan films may be successfully prepared with the direct dissolution of the polymer in CA solution, and the obtained films exhibited comparable properties as AA-based ones. However, the achievable wider pH range enables the tailoring of the ionization grade of chitosan which provides advantages from the aspect to achieve an ideal mucoadhesivity. The lower degree of ionization resulting from the higher pH of the solutions with a low CA content increased mucoadhesivity compared to AA-based films. The MFFT and SFE of chitosan citrate films, which are essential to be investigated before the coating process but had never been reported in the literature before, were also investigated. Both AA and CA-based films

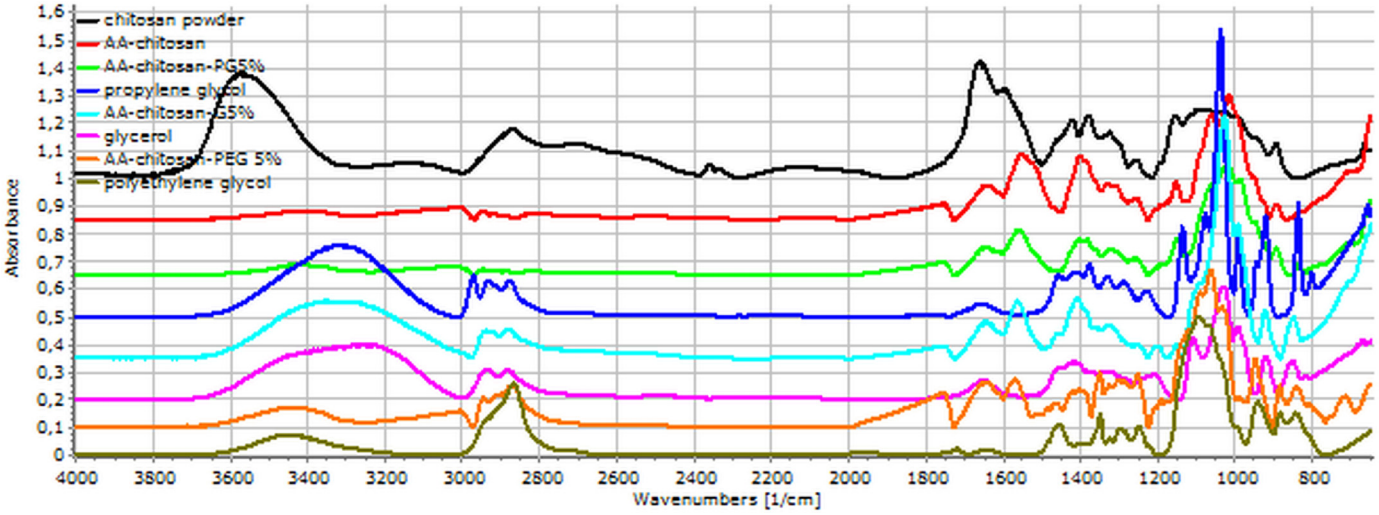

Fig. 4. FT-IR spectra of raw materials and AA-based films.

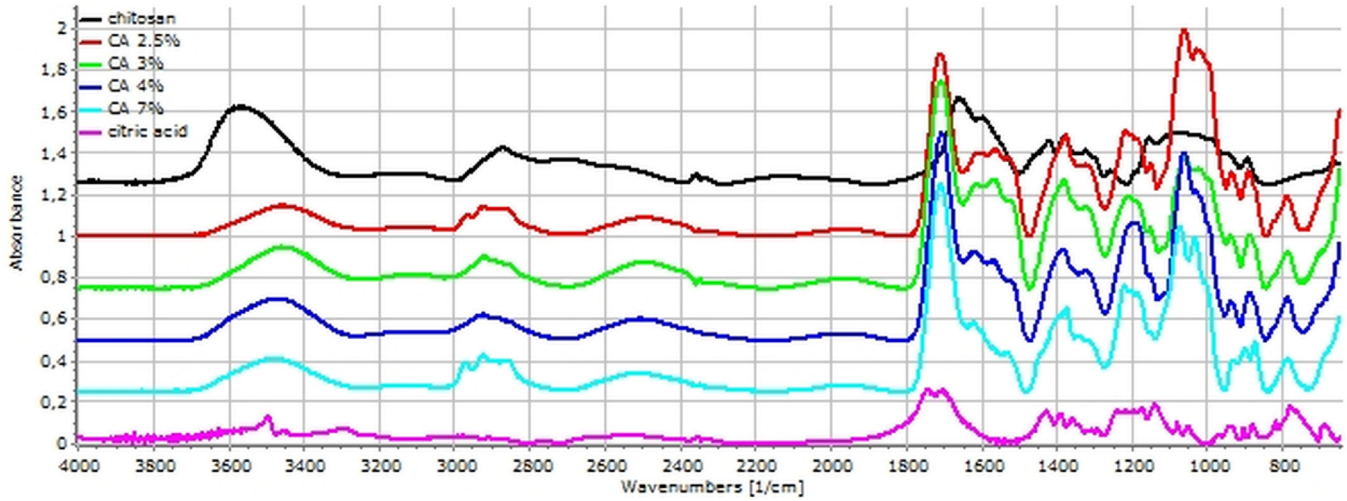

Fig. 5. FT-IR spectra for 2.5, 3, 4, and 7 w/v% CA-based chitosan films.

showed MFFT less than 15 °C, which is quite good for the coating process and ensures the required integrity of the coat even at low drying temperatures, while the slightly higher SFE of CA-based formulations enables the better tuneability to achieve the required properties of the subcoating layer. However, the increasing CA content decreased hardness but increased elasticity, which was directly proportional to the CA quantity. It could be concluded that CA 3.5–5% w/v-based chitosan solutions (without a plasticizer) represent novel solutions for the coating process or for developing novel oral mucoadhesive films for macromolecule delivery as at these concentrations they showed an excellent cross-linking, plasticizing effect, MFFT, film thickness, higher force of both deformation and mucoadhesion and suitable moisture content, thus simplifying the formulation, and they seem to be satisfactory to make an acidic microenvironment sufficient to inhibit the peptidases.

The addition of high amounts of various additional plasticizers, e.g. G, PG and PEG, dramatically reduces the force of deformation, wettability and mucoadhesivity for both CA- and AA-based films, while enhancing elasticity; therefore, these films can be utilized as impermeable coats for site-specific drug delivery or even for food preservation. Furthermore, high-dose plasticizers were effective in the modification of the surface free energy of the films, which may be essential to optimize film properties if they are used for the coating/subcoating of various substrates. The addition of plasticizers affects film thickness up to a certain limit in a manner proportional to the plasticizer quantity and type. Also, CA quantity affects the film thickness in a direct proportional manner, but to an acceptable extent. The addition of PEG-400 results in an unsatisfactory appearance of the films made with both CA and AA due to some opalescence but brings smaller decrease in hardness or mucoadhesivity of both AA- and CA-based films a G or PG. It also seems the magnitude of SFE has no relation to wettability in the presence of G, PG and PEG for both AA- and CA-based films, as the variation in SFE and just minimally affect mucoadhesivity, which mainly depends on the wetting process.

Overall, it may be concluded that chitosan-citrate based formulations may provide ideal platform in applications for oral macromolecule delivery.

Declaration of Competing Interest

None.

Acknowledgement

This research was supported by the EU-funded Hungarian grant EFOP-3.6.1-16-2016-00008.

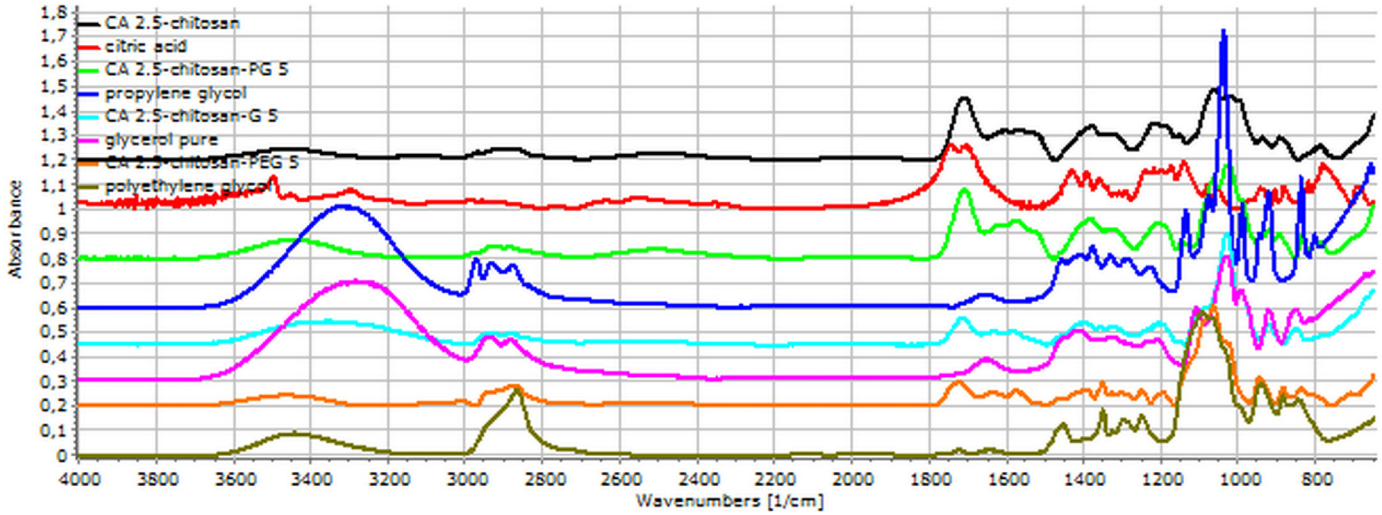

Fig. 6. FT-IR spectra of raw materials and CA 2.5%w/v-based chitosan films.

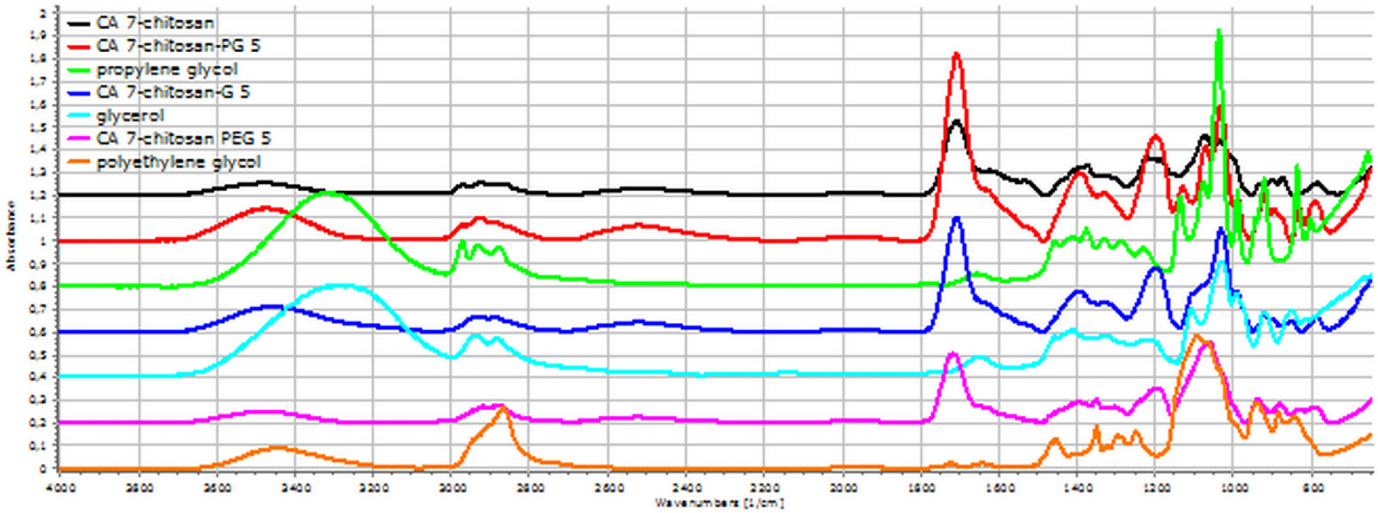

Fig. 7. FT-IR spectra of raw materials and CA 7%w/v-based CH films.

Supplementary materials

Supplementary material associated with this article can be found, in the online version, at doi:10.1016/j.ejps.2020.105270.

References

Batista, P., Castro, P.M., Madureira, A.R., Sarmento, B., Pintado, M., 2018. Recent insights in the use of nanocarriers for the oral delivery of bioactive proteins and peptides. Peptides 101, 112–123. https://doi.org/10.1016/j.peptides.2018.01.002.

Goldberg, M., Gomez-Orellana, I., 2003. Challenges for the oral delivery of macromolecules. Nat. Rev. Drug Discovery 2, 289–295. https://doi.org/10.1038/nrd1067.

Brown, LR., 2005. Commercial challenges of protein drug delivery. Expert Opin. Drug Deliv. 2, 29–42. https://doi.org/10.1517/17425247.2.1.29.

Choonara, B.F., Choonara, Y.E., Kumar, P., Bijukumar, D., du Toit, L.C., Pillay, V., 2014. A review of advanced oral drug delivery technologies facilitating the protection and absorption of protein and peptide molecules. Biotechnol. Adv. 32, 1269–1282. https://doi.org/10.1016/j.biotechadv.2014.07.006.

Muheem, A., Shakeel, F., Jahangir, M.A., Anwar, M., Mallick, N., Jain, G.K., et al., 2016. A review on the strategies for oral delivery of proteins and peptides and their clinical perspectives. Saudi Pharm. J. 24, 413–428. https://doi.org/10.1016/j.jsps.2014.06.004.

Mahato, R.I., Narang, A.S., Thoma, L., Miller, D.D., 2003. Emerging trends in oral delivery of peptide and protein drugs. Crit. Rev. Ther. Drug Carrier Syst. 20, 153–214. https://doi.org/10.1615/CritRevTherDrugCarrierSyst.v20.i23.30.

Sovány, T., Csordás, K., Kelemen, A., Regdon, G., Pintye-Hódi, K., 2016. Development of pellets for oral lysozyme delivery by using a quality by design approach. Chem. Eng. Res. Des. 106, 92–100. https://doi.org/10.1016/j.cherd.2015.11.022.

Shah, A., Hussain, I., Murtaza, G., 2018. Chemical synthesis and characterization of chitosan/silver nanocomposites films and their potential antibacterial activity. Int. J. Biol. Macromol. https://doi.org/10.1016/j.ijbiomac.2018.05.057.

Li, P., Zhao, J., Chen, Y., Cheng, B., Yu, Z., Zhao, Y., et al., 2017. Preparation and characterization of chitosan physical hydrogels with enhanced mechanical and antibacterial properties. Carbohydr. Polym. 157, 1383–1392. https://doi.org/10.1016/j.carbpol.2016.11.016.

Liu, S., Li, L., 2018. Unique gelation of chitosan in an alkali/urea aqueous solution. Polymer 141, 124–131. https://doi.org/10.1016/j.polymer.2018.03.012.

Perinelli, D.R., Fagioli, L., Campana, R., Lam, J.K.W., Baffone, W., Palmieri, G.F., et al., 2018. Chitosan-based nanosystems and their exploited antimicrobial activity. Eur. J. Pharm. Sci. 117, 8–20. https://doi.org/10.1016/j.ejps.2018.01.046.

Cao, J., You, J., Zhang, L., Zhou, J., 2018. Homogeneous synthesis and characterization of chitosan ethers prepared in aqueous alkali/urea solutions. Carbohydr. Polym. 185, 138–144. https://doi.org/10.1016/j.carbpol.2018.01.010.

Rotta, J., Ozório, R.Á., Kehrwald, A.M., de Oliveira Barra, G.M., de Melo Castanho Amboni, R.D., Barreto, P.L.M., 2009. Parameters of color, transparency, water solubility, wettability and surface free energy of chitosan/hydroxypropylmethylcellulose (HPMC) films plasticized with sorbitol. Mater. Sci. Eng. 29, 619–623. https://doi.org/10.1016/j.msec.2008.10.032.

Rahmouni, N., Tahri, W., Sbihi, H.M., Nehdi, I.A., Desbrieres, J., Besbes-Hentati, S., 2018. Improvement of chitosan solubility and bactericidity by synthesis of N -benzimidazole- O -acetyl-chitosan and its electrodeposition. Int. J. Biol. Macromol. 113, 623–630. https://doi.org/10.1016/j.ijbiomac.2018.02.121.

Agarwal, M., Agarwal, M.K., Shrivastav, N., Pandey, S., Gaur, P., 2018. A simple and effective method for preparation of chitosan from chitin. Int. J. Life-Sci. Sci. Res. 4, 1721–1728. https://doi.org/10.21276/ijlssr.2018.4.2.18.

Phanindra B., Moorthy B.K., Muthukumaran M.. Recent advances in mucoadhesive/ bioadhesive drug delivery system: a review2013.

Rajaram, D.M., Laxman, S.D., 2016. Buccal Mucoadhesive Films: A Review. Syst. Rev. Pharm. 8, 31–38. https://doi.org/10.5530/srp.2017.1.7.

Rajput, G.C., Majmudar, F.D., Patel, J.K., Patel, K.N., Thakor, R.S., Patel, B.P., et al., 2010. Stomach specific mucoadhesive tablets as controlled drug delivery system–a review work. Int. J. Pharm. Biol. Res. 1, 30–41.

Hombach, J., Bernkop-Schnürch, A., 2009. Chitosan solutions and particles: evaluation of their permeation enhancing potential on MDCK cells used as blood brain barrier model. Int. J. Pharm. 376, 104–109. https://doi.org/10.1016/j.ijpharm.2009.04.027.

Thanou, M., Verhoef, J.C., Junginger, H.E., 2001. Oral drug absorption enhancement by chitosan and its derivatives. Adv. Drug. Deliv. Rev. 52, 117–126. https://doi.org/10.1016/S0169-409X(01)00231-9.

Sonaje, K., Lin, K.-J., Tseng, M.T., Wey, S.-P., Su, F.-Y., Chuang, E.-Y., et al., 2011. Effects of chitosan-nanoparticle-mediated tight junction opening on the oral absorption of endotoxins. Biomaterials 32, 8712–8721.

Fan, B., Xing, Y., Zheng, Y., Sun, C., Liang, G., 2016. pH-responsive thiolated chitosan nanoparticles for oral low-molecular weight heparin delivery: in vitro and in vivo evaluation. Drug Deliv. 23, 238–247.

Jiang, W.-Z., Cai, Y., Li, H.-Y., 2017. Chitosan-based spray-dried mucoadhesive microspheres for sustained oromucosal drug delivery. Powder Technol. 312, 124–132. https://doi.org/10.1016/j.powtec.2017.02.021.

Aguirre, T.A.S., Teijeiro-Osorio, D., Rosa, M., Coulter, I.S., Alonso, M.J., Brayden, D.J., 2016. Current status of selected oral peptide technologies in advanced preclinical development and in clinical trials. Adv. Drug. Deliv. Rev. 106, 223–241. https://doi.org/10.1016/j.addr.2016.02.004.

Devendra, S., Pankaj, K.S., Udai, V.S.S., 2013. Enhancement of intestinal absorption of poorly absorbed drugs by using various permeation enhancers: an overview. World J. Pharma. Pharm. Sci. 2, 17998.

Welling, S.H., Hubálek, F., Jacobsen, J., Brayden, D.J., Rahbek, U.L., Buckley, S.T., 2014. The role of citric acid in oral peptide and protein formulations: Relationship between calcium chelation and proteolysis inhibition. Eur. J. Pharm. Biopharm. 86, 544–551. https://doi.org/10.1016/j.ejpb.2013.12.017.

Bonferoni, M.C., Sandri, G., Rossi, S., Ferrari, F., Gibin, S., Caramella, C., 2008. Chitosan citrate as multifunctional polymer for vaginal delivery. Eur. J. Pharm. Sci. 33, 166–176. https://doi.org/10.1016/j.ejps.2007.11.004.

Garcia, P.S., Grossmann, M.V.E., Yamashita, F., Mali, S., Dall'Antonia, L.H., Barreto, W.J., 2011. Citric acid as multifunctional agent in blowing films of starch/PBAT. Química Nova 34, 1507–1510. https://doi.org/10.1590/S0100-40422011000900005.

Shu, X., 2001. Novel pH-sensitive citrate cross-linked chitosan film for drug controlled release. Int. J. Pharm. 212, 19–28. https://doi.org/10.1016/S0378-5173(00)00582-2.

Liu, M., Zhou, Y., Zhang, Y., Yu, C., Cao, S., 2013. Preparation and structural analysis of chitosan films with and without sorbitol. Food Hydrocolloids. 33, 186–191.

Kristó, K., Kovács, O., Kelemen, A., Lajkó, F., Klivényi, G., Jancsik, B., et al., 2016. Process analytical technology (PAT) approach to the formulation of thermosensitive protein-loaded pellets: Multi-point monitoring of temperature in a high-shear pelletization. Eur. J. Pharm. Sci. 95, 62–71. https://doi.org/10.1016/j.ejps.2016.08.051.

Andrews, G.P., Laverty, T.P., Jones, D.S., 2009. Mucoadhesive polymeric platforms for controlled drug delivery. Eur. J. Pharm. Biopharm. 71, 505–518. https://doi.org/10.1016/j.ejpb.2008.09.028.

Schuster, J.M., Schvezov, C.E., Rosenberger, M.R., 2015. Analysis of the Results of Surface Free Energy Measurement of Ti6Al4V by Different Methods. Proc. Mater. Sci. 8, 732–741. https://doi.org/10.1016/j.mspro.2015.04.130.

Bhuvaneshwari, S., Sruthi, D., Sivasubramanian, V., Niranjana, K., Sugunabai, J., 2011. Development and characterization of chitosan films. Ijera 1, 292–299.

Bujang, A., Nur'Adila, S., Suyatma, N.E., 2013. Physical properties of chitosan films as affected by concentration of lactic acid and glycerol. 4th international conference on

biology. Environ. Chem. IPCBEE 58, 27–31.
Nady, N., Kandil, SH., 2018. Novel blend for producing porous chitosan-based films suitable for biomedical applications. Membranes 8, 2.
Wan, L.S.C., Heng, P.W.S., Chia, C.G.H., 1993. Citric acid as a plasticizer for spray-dried microcapsules. J. Microencapsul. 10, 11–23. https://doi.org/10.3109/02652049309015308.
Shi, R., Bi, J., Zhang, Z., Zhu, A., Chen, D., Zhou, X., et al., 2008. The effect of citric acid on the structural properties and cytotoxicity of the polyvinyl alcohol/starch films when molding at high temperature. Carbohydr. Polym. 74, 763–770. https://doi.org/10.1016/j.carbpol.2008.04.045.
Ziani, K., Oses, J., Coma, V., Maté, J.I., 2008. Effect of the presence of glycerol and Tween 20 on the chemical and physical properties of films based on chitosan with different degree of deacetylation. LWT - Food Sci. Technol. 41, 2159–2165. https://doi.org/10.1016/j.lwt.2007.11.023.
Bravo-Osuna, I., Vauthier, C., Farabollini, A., Palmieri, G.F., Ponchel, GMucoadhesion, 2007. Mechanism of chitosan and thiolated chitosan-poly(isobutyl cyanoacrylate) core-shell nanoparticles. Biomaterials 28, 2233–2243. https://doi.org/10.1016/j.biomaterials.2007.01.005.
Peppas, N.A., Huang, Y., 2004. Nanoscale technology of mucoadhesive interactions. Adv. Drug. Deliv. Rev. 56, 1675–1687. https://doi.org/10.1016/j.addr.2004.03.001.
Casariego, A., Souza, B.W.S., Vicente, A.A., Teixeira, J.A., Cruz, L., Díaz, R., 2008. Chitosan coating surface properties as affected by plasticizer, surfactant and polymer concentrations in relation to the surface properties of tomato and carrot. Food Hydrocolloids. 22, 1452–1459. https://doi.org/10.1016/j.foodhyd.2007.09.010.
Llanos, J.H.R., Vercik, L.C., de, O., Vercik, A., 2015. Physical properties of chitosan films obtained after neutralization of polycation by slow drip method. J. Biomater. Nanobiotechnol. 06, 276–291. https://doi.org/10.4236/jbnb.2015.64026.
Lusiana, R.A., Siswanta, D., Mudasir, M., 2018. Preparation of citric acid crosslinked Chitosan/Poly(Vinyl Alcohol) blend membranes for creatinine transport. Indonesian J. Chem. 16, 144–150. https://doi.org/10.22146/ijc.21157.
He, Q., Ao, Q., Gong, Y., Zhang, X., 2011. Preparation of chitosan films using different neutralizing solutions to improve endothelial cell compatibility. J. Mater. Sci. Mater. Med. 22, 2791–2802. https://doi.org/10.1007/s10856-011-4444-y.
Thuran, K.N., Shabaz, F., Güner, A., 2001. A spectrophotometric study of hydrogen bonding in methylcellulose-based edible films plasticized by polyethylene glycol. J. Food Sci. 66, 59–62.

ANNEX - 5

Material	MW (Da)	Concentration		No. of monomers	Molar ratio	Molar ratio (in relation of monomers)
		(g/100 ml)	(mol/100ml)			
Chitosan	300000-350000	2	0,00000571-0,00000667	1595-1860	1	1
Citric acid	192,12	2,5	0,013	1	1950-2276	1,04-1,43
		7	0,036		5398-6305	2,90-3,95
Propylene glycol	76,09	5	0,066	1	9895-11559	5,32-7,25
		10	0,132		19790-23118	10,64-14,50
Glycerol	92,09	5	0,054	1	8096-9457	4,35-5,93
		10	0,108		16192-18914	8,70-11,86
PEG-400	380-420	5	0,011-0,013	6-8	1799-2102	6,77-9,23
		10	0,024-0,026		3598-4204	13,44-18,46

Table S1: Molar ratios of raw materials in various formulations

Chitosan (w/v%)	Plasticizer	Plasticizer content (w/v%)	Obtained Sol.	pH	Film's appearance
2	-	0	transparent	2.75	transparent
2	G	5	transparent	2.82	transparent
2	G	10	transparent	2.70	transparent
2	PG	5	transparent	2.81	transparent
2	PEG 400	5	transparent	2.92	opalescent
2	PEG 400	10	transparent	2.95	opalescent

Table S2: The pH and visual appearance of prepared chitosan/AA-based solutions and films, G=glycerol, PG= propylene glycol, PEG=polyethylene glycol

Chitosan (w/v %)	Plasticizer	Plasticizer content (w/v %)	Obtained Sol.	pH	Film's appearance
2	G	5	transparent	4.47	transparent
2	G	10	transparent	4.12	transparent
2	PG	5	transparent	4.86	transparent
2	PG	10	transparent	4.92	transparent
2	PEG 400	5	transparent	5.21	opalescent
2	PEG 400	10	transparent	5.37	opalescent

Table S3: The pH and visual appearance of solutions and films made with CA 2.5w/v% and different plasticizers

Chitosan (w/v %)	CA (w/v%)	pH	Obtained solution	Obtained film
2	7	2.40	transparent	transparent
2	5	2.56	transparent	transparent
2	4	2.63	transparent	transparent
2	3.5	2.99	transparent	transparent
2	3	3.45	transparent	transparent
2	2.5	4.25	transparent	transparent

Table S4: The pH and visual appearance of solutions and films prepared by different CA quantities

Chitosan (w/v %)	Plasticizer	Plasticizer content (w/v %)	Obtained Sol.	pH	Film's appearance
2	G	5	transparent	2.58	transparent
2	G	10	transparent	2.72	transparent
2	PG	5	transparent	2.76	transparent
2	PG	10	transparent	2.81	transparent
2	PEG 400	5	transparent	2.79	opalescent
2	PEG 400	10	transparent	2.89	opalescent

Table S5: The pH and visual appearance of solutions and films made with CA7w/v% and different plasticizers